| 1. Report No. UMTA-MA-06-0100-81-1 | 2. Government Accession No. | 3. Recipient's Catalog No. |
|---|---|---|
| 4. Title and Subtitle Pilot Study for Definition of Track Component Load Environments | | 5. Report Date February 1981 |
| | | 6. Performing Organization Code DTS-741 |
| 7. Author's) Thomas R. Stagliano[1], Lawrence J. Mentel[1], Edward C. Gadden, Jr.[2], Bob W. Baxter[2], Warren K. Hale[3], Russell W. Maccabe, Jr.[3] | | 8. Performing Organization Report No. DOT-TSC-UMTA-81-8 |
| 9. Performing Organization Name and Address [1]Kaman AviDyne, 83 Second Ave., Burlington MA* [2]Kaman Sciences Corporation, Colorado Springs CO (Subcon) [3]Thomas K. Dyer, Inc. Lexington MA (Subcontractor) | | 10. Work Unit No. (TRAIS) UM148/R1711 |
| | | 11. Contract or Grant No. DOT-TSC-1605 |
| | | 13. Type of Report and Period Covered Final Report October 1978–May 1980 |
| 12. Sponsoring Agency Name and Address U.S. Department of Transportation Urban Mass Transportation Administration Office of Technology Development and Deployment Washington DC 20590 | | |
| | | 14. Sponsoring Agency Code UTD-30 |
| 15. Supplementary Notes *Under contract to: | U.S. Department of Transportation Research and Special Programs Administration Transportation Systems Center Cambridge MA 02142 | |

16. Abstract

This report describes the results of an experimental and analytical effort to define the vehicle induced load environment in an at-grade, concrete tie/ballast transit track structure. The experiment was performed on the UMTA transit track oval at TTC in Pueblo, Colorado in order to establish an initial data baseline which could be extended to include data from tests conducted on various transit track structural systems. Standard experimental techniques generally were used to measure the pressures, strains and applied wheel/rail loads in the various track structure components; however, innovations were effectively introduced for measuring pressures on the bottom of the concrete tie and in the ballast. Track design methods and analytical computer techniques for predicting the load environment in the various track components were evaluated through comparisons with the experimental data. Design conservatism in the tie/ballast transit track systems was evaluated from the aspect of stress criteria versus other design factors based on experience and initial capital costs versus maintenance costs for transit systems. It was indicated from these tests, performed on a well constructed and maintained track structure, that there exists significant conservatism based on stress criteria, but the transit industry believes that the savings on construction costs for a more optimal stress design would be overshadowed by anticipated increases in maintenance costs. It is indicated by the results of this effort that many of the design stress methods currently being used should be improved, especially in the prediction of the load environment in the ballast and subgrade. It is anticipated that the experience gained in this pilot study can be applied in defining the load environment for other transit track configurations.

| 17. Key Words Load Environment Track Components Transit Track Design Track Instrumentation Transit Track Testing — Track Costs | 18. Distribution Statement DOCUMENT IS AVAILABLE TO THE PUBLIC THROUGH THE NATIONAL TECHNICAL INFORMATION SERVICE, SPRINGFIELD, VIRGINIA 22161 | | |
|---|---|---|---|
| 19. Security Classif. (of this report) Unclassified | 20. Security Classif. (of this page) Unclassified | 21. No. of Pages 218 | 22. Price |

Form DOT F 1700.7 (8-72)    Reproduction of completed page authorized

# PREFACE

# METRIC CONVERSION FACTORS

## Approximate Conversions to Metric Measures

| Symbol | When You Know | Multiply by | To Find | Symbol |
|--------|---------------|-------------|---------|--------|
| | | **LENGTH** | | |
| in | inches | 2.5 | centimeters | cm |
| ft | feet | 30 | centimeters | cm |
| yd | yards | 0.9 | meters | m |
| mi | miles | 1.6 | kilometers | km |
| | | **AREA** | | |
| in$^2$ | square inches | 6.5 | square centimeters | cm$^2$ |
| ft$^2$ | square feet | 0.09 | square meters | m$^2$ |
| yd$^2$ | square yards | 0.8 | square meters | m$^2$ |
| mi$^2$ | square miles | 2.6 | square kilometers | km$^2$ |
| | acres | 0.4 | hectares | ha |
| | | **MASS (weight)** | | |
| oz | ounces | 28 | grams | g |
| lb | pounds | 0.45 | kilograms | kg |
| | short tons (2000 lb) | 0.9 | tonnes | t |
| | | **VOLUME** | | |
| tsp | teaspoons | 5 | milliliters | ml |
| Tbsp | tablespoons | 15 | milliliters | ml |
| fl oz | fluid ounces | 30 | milliliters | ml |
| c | cups | 0.24 | liters | l |
| pt | pints | 0.47 | liters | l |
| qt | quarts | 0.95 | liters | l |
| gal | gallons | 3.8 | liters | l |
| ft$^3$ | cubic feet | 0.03 | cubic meters | m$^3$ |
| yd$^3$ | cubic yards | 0.76 | cubic meters | m$^3$ |
| | | **TEMPERATURE (exact)** | | |
| °F | Fahrenheit temperature | 5/9 (after subtracting 32) | Celsius temperature | °C |

## Approximate Conversions from Metric Measures

| Symbol | When You Know | Multiply by | To Find | Symbol |
|--------|---------------|-------------|---------|--------|
| | | **LENGTH** | | |
| mm | millimeters | 0.04 | inches | in |
| cm | centimeters | 0.4 | inches | in |
| m | meters | 3.3 | feet | ft |
| m | meters | 1.1 | yards | yd |
| km | kilometers | 0.6 | miles | mi |
| | | **AREA** | | |
| cm$^2$ | square centimeters | 0.16 | square inches | in$^2$ |
| m$^2$ | square meters | 1.2 | square yards | yd$^2$ |
| km$^2$ | square kilometers | 0.4 | square miles | mi$^2$ |
| ha | hectares (10,000 m$^2$) | 2.5 | acres | |
| | | **MASS (weight)** | | |
| g | grams | 0.035 | ounces | oz |
| kg | kilograms | 2.2 | pounds | lb |
| t | tonnes (1000 kg) | 1.1 | short tons | |
| | | **VOLUME** | | |
| ml | milliliters | 0.03 | fluid ounces | fl oz |
| l | liters | 2.1 | pints | pt |
| l | liters | 1.06 | quarts | qt |
| l | liters | 0.26 | gallons | gal |
| m$^3$ | cubic meters | 35 | cubic feet | ft$^3$ |
| m$^3$ | cubic meters | 1.3 | cubic yards | yd$^3$ |
| | | **TEMPERATURE (exact)** | | |
| °C | Celsius temperature | 9/5 (then add 32) | Fahrenheit temperature | °F |

# TABLE OF CONTENTS

# TABLE OF CONTENTS (CONTINUED)

# TABLE OF CONTENTS (CONCLUDED)

# LIST OF ILLUSTRATIONS

# LIST OF ILLUSTRATIONS (CONTINUED)

# LIST OF ILLUSTRATION (CONTINUED)

# LIST OF ILLUSTRATIONS (CONCLUDED)·

# LIST OF TABLES

# LIST OF TABLES (CONTINUED)

# LIST OF TABLES (CONCLUDED)

# LIST OF ABBREVIATIONS

AAR       American Association of Railroads

APTA      American Public Transit Association

AREA      American Railway Engineering Association

cwr       continuous welded rail

FAST      Facility for Accelerated Service Testing

kips      thousands pounds (force)

KSC       Kaman Sciences Corporation

MBTA      Massachusetts Bay Transit Authority

mph       miles per hour

NYCTA     New York City Transit Authority

TSC       Transportation Systems Center, Cambridge MA

TTC       Transportation Test Center, Pueblo CO

TTT       Transit Test Track, at TTC

UMTA      Urban Mass Transportation Administration, Washington DC

# 1. INTRODUCTION

The determination of vehicle induced forces on various transit track configurations should enhance the understanding of the load environment within each component of the track system and aid in the ongoing effort to improve design methods and system maintainability. Currently, the design standards are governed by the materials presently used in the track system, by the history of construction methods and practices used in the industry and by the general experience of acceptable limits for safety, ride quality, reliability and, probably most important, economics. Track design practices may be categorized as approaches primarily relying on the designer's experiences and on some handbook specifications and/or recommendations. The design criteria used are related to the strength of individual components, material availability and cost considerations.

Operational rail systems are expected to achieve certain performance levels based upon safety, ride quality, noise and ground vibration and maintainability (and thus also long term costs). Many design procedures do not consider performance aspects per se; but they do try to meet the strength criteria which are indirectly related to performance. A reliance upon basic strength calculations tempered with a tremendous amount of past experience tends to be the design method used by present day designers to achieve the required track system performance criteria.

Current transit design practices are spinoffs from established railroad track technology and, therefore, may result in conservatism in track system design for the lighter transit vehicles. There are major considerations that should be taken into account when evaluating transit versus railroad track systems. Railroad tracks are almost all at-grade tie-ballast construction, while transit tracks have different segments: at-grade, elevated and underground, which can involve tie-ballast or concrete slab construction with direct fixation fasteners. Ballasted track construction for both railroad and transit systems use either wood or prestressed concrete ties, but in transit track systems, curves have shorter radii of curvature, maintenance is constrained due to short operational headways and short periods of night closings, and operation

is within the confines of densely populated areas. If improved and economical transit track systems are to be achieved for urban areas it is necessary that the transit track design community be provided with a better understanding of the load environment in all of their transit track components. This better defined load environment should also result in improved design tools for the designers, and may influence general maintenance procedures.

To improve the design techniques, it is necessary to evaluate load environment predictions obtained with the current design methodologies for the various track components. This can be accomplished by comparing the load environment obtained from current practices with experimental data from well controlled field tests. If it turns out from these assessments that the presently used load prediction techniques for transit track design are unsatisfactory in certain aspects, then the prediction and utilization techniques should be improved. Such improvements must be in "practical terms" and economically justifiable if they are to be understood, accepted and used by the designers.

This pilot study is an initial effort to define the track component load environment for a selected transit track system. Thus, the limited objective of this initial program is to define the load environment in a transit track system of at-grade concrete tie-ballast type of construction from vehicle induced forces. The experiment for determining the load environment in the ties, fasteners and ballast/subgrade components of this track configuration provides data for comparisons with the analytical tools currently being used in the industry. The current track design methods are to be evaluated and the degree of conservatism existing in current practice is to be identified for the tested transit track configuration.

The UMTA transit test track (TTT) at the Transportation Test Center (TTC) at Pueblo, Colorado was selected by DOT/TSC as the test site to perform the experimental determination of the vehicle induced forces. It was felt that the initial test effort should be at the controlled environment provided by this UMTA facility. A test plan for measurement

2

of track component loads using current state-of-the-art instrumentation techniques was developed and implemented at tangent and curved sites selected along the TTT. In this effort the available computer analyses and design methods used to predict the load environment for tie-ballast track configurations are reviewed and applied to the selected track configuration at TTC. The uncertainties existing in the load prediction techniques are evaluated and compared with experimental results. The degree of conservatism implied by the specific load environment obtained in this pilot study is assessed considering the initial construction costs and the eventual maintenance cost for a transit track system.

A program summary is given in Section 2 which gives the reader an overall view of what was accomplished during the study. The description of the load environment experiment conducted at TTC is given in Section 3. In Section 4 the test results are presented and evaluated, and load environment comparisons with analysis and design values are made. In Section 5 transit track design techniques are presented and current numerical computer models of the track structure are generated and discussed. An assessment of the degree of conservatism in track design is made in Section 6. The conclusions and recommendations are presented in Section 7 and various appendices which support the main sections of the report are presented after this section.

# 2. PROGRAM SUMMARY

## 2.1 BACKGROUND

This pilot study represents the start of a program to examine the vehicle induced force environment on various transit track systems. This initial effort is directed towards an at-grade tie-ballast transit track configuration selected on the UMTA transit test track at TTC Pueblo, Colorado. The purpose of the study is to provide data defining the load environments in the ties, fasteners and ballast/subgrade components of the transit track structure selected. These data are then used to compare with results from existing computer code models and design methods. Based on the results from the track configuration tested, an assessment of the degree of conservatism in present transit designs is made from the structural aspect and a first cut evaluation of initial cost versus maintenance costs is made relative to this assessment.

The UMTA transit test track at Pueblo is illustrated in Figure 2.1. The test track is divided into six sections, and each section is of a different type of track construction as indicated in Figure 2.1. A tangent and a curved site on the concrete tie with welded rail section (Section IV) were selected for track structure measurement locations. The locations of the old existing wayside test stations are designated as TTC-4A (near station 365) and TTC-4B (near station 428). New instrumented stations were established very near the existing stations and are designated as KSC-1 and KSC-2. The new instrumented stations were the primary data acquisition source while the old existing stations (installed in 1971) provided very little useful data due to degradation of transducers and the lack of recorded calibration information. This track section consists of 119 lb welded rail with Gerwick RT-7 Mark 38 prestressed concrete ties spaced at 30 inches on tangent and 27 inches on curved track. The rails are attached to the concrete ties by the Rails Company "Flexiclip" fasteners. The depth of the ballast is 12 inches and consists of crushed stone AREA No. 4 gradation. The subballast is 6 inches of ungraded stone. The subgrade in the region of the test stations can be categorized generally as silty sand.

5

SECTION V
119# WELDED RAIL
CONCRETE TIES
(23" O.C.)

SECTION VI
119# WELDED RAIL
CONCRETE TIES
(33" O.C.)

N

SECTION I
119# WELDED RAIL
WOOD TIES (24" ON
TANGENT:
23" ON CURVE)

SECTION IV
119# WELDED RAIL
CONCRETE TIES
(30" ON TANGENT
27" ON CURVE)

UMTA
TEST TRACK
(9.123 MILES)

○ OLD TEST STATIONS (1972)
□ NEW TEST STATIONS (1979)

KSC-2

KSC-1

SECTION III
100# JOINTED RAIL
WOOD TIES (24" ON
TANGENT
23" ON CURVE)

SECTION II
100# WELDED RAIL
WOOD TIES (23" O.C.)

FIGURE 2.1.  UMTA TRANSIT TRACK TEST SITE

6

The types of measurements made at these wayside test stations include wheel/rail loads, bending strains on concrete ties, strains in fastener clips, and pressure and strains in roadbed structure (ballast, subballast and subgrade). Figure 2.2 shows the cross section of the track structure and the general instrumentation locations at the KSC test stations. In addition to this instrumentation profile at KSC-1 and KSC-2, 12 other ties at each site were strain gaged for bending at three positions on the tie. At the tangent site 10 additional wheel/ rail load measurement locations were instrumented on the outside rail. They were spaced so as to record loads for the entire circumference of the transit vehicle wheel. These measurements were made during the passage of transit vehicles at prescribed speeds. In particular, six test-vehicle configurations were used, namely: two NYCTA R-42 cars in tandem at two weight conditions (crush and empty) and at two speeds (30 and 50 mph), and two MBTA cars (Blue line) at crush weight and two speeds (30 and 50 mph).

## 2.2 RESULTS AND CONCLUSIONS

The experimental data is examined by track system component type: wheel to rail vertical and lateral load transfer, tie bending moments, ballast and subgrade pressure and strain distribution, rail-tie fastener strains, and soil material definition. The experimental data is compared to itself for different vehicle configurations, compared to other known applicable experimental data and used as a basis for an analytical correlation study. In parallel with this experimental and analytical study of a transit track load environment, the cost of at-grade transit track construction is parametrically examined by component cost and by anticipated effects on maintenance cost.

The wheel to rail loads data is compiled from both the loads measured during the gathering of tie and roadbed data with variable vehicle configurations at the tangent and curve sites and from the specific wheel to rail loads study conducted at the tangent site with a crush loaded R-42 vehicle traveling at either thirty or fifty miles per hour passing through a special instrumentation layout. The specific wheel to rail

7
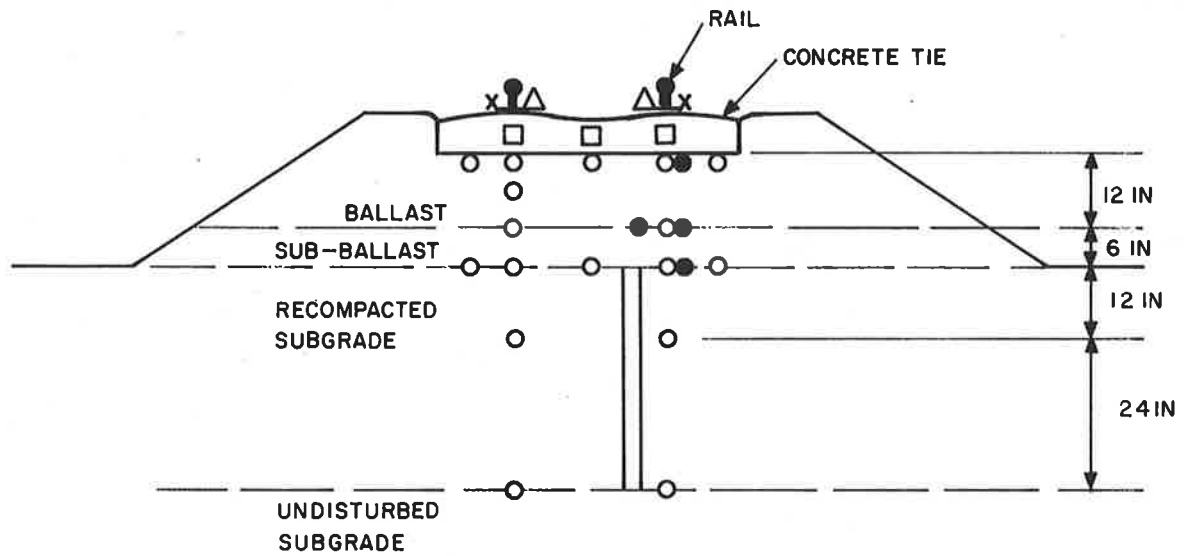
| MEASUREMENT | SYMBOL |
|---|---|
| W/R LOADS | X |
| TIE BENDING STRAINS | □ |
| FASTENER STRAINS | △ |
| PRESSURES | ○ |
| SOIL STRAINS | ● |
| EXTENSOMETER (STRAIN) | \|\| |

FIGURE 2.2.  INSTRUMENTATION LOCATIONS AT KSC TEST STATIONS

loads study conducted at the tangent site with the crush loaded R-42
vehicle indicates no statistically significant differences among
vertical or lateral applied wheel laods at either thirty or fifty miles
per hour.  One of the parameters that affects the magnitude of the load
transferred from the wheel to the track structure is the wheel flats.
This study includes the effects of wheel flats but the track geometry
is without any measured perturbations.  The additional wheel to rail
loads data gathered at both the curve and tangent sites for the six test-
vehicle configurations show negligible differences in applied vertical
load between the tangent and the curve (3820 foot radius, 1°30') and
indicate that the lateral loads are two to three times larger at the curve
for each vehicle configuration.  The statistical study at the tangent
site indicates a design laod factor defined as the load that is exceeded
only five percent of the time with a ninety-five percent confidence level.
For the tangent site and the crush loaded R-42 at either velocity these
design loads are 18 kips vertical and 4 kips lateral.

At each site (tangent and curve) thirteen ties were instrumented
for tie bending moment measurements.  For the crush loaded R-42 vehicle
all the ties responded similarly, there were no unbalanced bending
moments at the curve and the maximum bending moments measured were
approximately one-half the design value.  The present design formulations,
both numerical and analytical, provide excellent correlations between
the predicted and the measured bending moments.

The ballast and subgrade pressures were measured at sixteen locations
at both the tangent and curve sites.  Differences in pressures measured
under the inner or outer rail seat at either site appear to be due more
to roadbed construction and ballast tamping than to vehicle configuration
or track curvature.  The present eighteen inch ballast and subballast
depth provides a reasonably even pressure distribution at the top of
the subgrade, regardless of the pressure distribution measured at the
tie/ballast interface.  The maximum pressures measured at the top of
the subgrade or the tie/ballast interface are all below design standards

9

by at least a factor of three, and all of the pressures measured in the recompacted subgrade are negligible and should not influence the untreated subgrade. The presently used design formulae could not predict accurately the pressures at the top of the subgrade and there was a 100 percent scatter in predictions among AREA recommended design formulas. The numerical predictions provided by the ILLITRACK and MULTA computer codes showed fair to reasonable correlation with the experimental data, once the appropriate material description for the ballast and subgrade was determined.

The roadbed strains and deflections were all small and measurably elastic. These deformations compared reasonably well with measurements conducted at the nearby FAST facility - with similiar vehicle truck loads and similar roadbed geometry. The main usefulness of the strain and deflection instrumentation is for the long term examination of the settling and "aging" of the track roadbed. This information can then be used to follow the history of track component load levels.

Four fasteners were measured for dynamic strain levels at each site. This data shows that the maximum stress levels experienced by the fasteners are below the yield level by an approximate factor of two. The measured dynamic stress increment placed on the fasteners during vehicle passage was determined to be sufficiently small that the fastener should be able to complete its design life without a bending fatigue failure. This fastener study did not examine the tie down bolts or the bolt to concrete tie fixture, and the study did not include track perturbations which would lead to significantly different fastener stress levels.

The subgrade soil was sampled at the tangent site, and six soil samples representing three soil depths were triaxially tested. Six different stress paths were used in the triaxial tests to examine the effects stress paths (especially "dynamic" stress paths induced by a rolling wheel) have on the soil material properties. More samples and more varied stress paths are needed to provide statistically signifi-cant results, but these preliminary tests indicate some response dif-ferences among the various stress paths. All the stress path data from

the two samples representing the top of the subgrade soil were used to determine the material constants to be used in the ILLITRACK and MULTA numerical analyses. These material constants appeared to be a reasonable representation of the soil and showed good correlation with material constants determined at the nearby FAST facility.

A parametric study was carried out examining the relative effects that changes in rail size, tie size, tie spacing, and ballast depth have upon the initial construction cost of a transit track system. The loads study (experimental and analytical) showed that, based upon stress criteria, the applied industrial design standards had overdesigned the UMTA transit test track. Indeed, thirty-three inch tie spacing is employed in the adjoining curve (Section VI) of the TTT (see Figure 2.1) which exceeds design practice by six inches; there have been no unusual maintenance problems here during the seven year existence. The parametric study indicates that significant construction cost savings can be made by varying the appropriate component designs. It was found that varying tie size and spacing and varying ballast depth have the most significant effect upon the construction cost, and based upon design stress criteria these three variables could be changed without exceeding design stress maximums. However, other design criteria have not been accounted for totally nor have the effects upon maintenance costs been fully evaluated. It is concluded that life cycle loads and therefore maintenance costs must be examined carefully before design procedures could be altered.

Overall, a reasonably complete description of the track component single cycle load environment has been determined and found to be conservative. The design practices are enumerated, and examples carried out, and comparisons are made with newly developed numerical computer codes. A parametric study of the effect of individual component design upon construction costs is examined, and potential construction cost savings are indicated, but the effects upon maintenance costs are indeterminable from this pilot study.

11/12

# 3. TRANSIT TRACK LOAD ENVIRONMENT EXPERIMENT

A primary task of this program effort was to determine the load environment of a transit track system by experimental measurements at a representative transit site. An extensive set of measurements was therefore made in transit track ties, ballast, subballast and subgrade in order to form a data base for use in evaluating current transit design methods and current numerical analysis techniques.

## 3.1 SITE SELECTION

TSC determined that the UMTA transit test track (TTT) at the TTC facility in Pueblo, Colorado, would provide a representative sample of well built transit track designed by the current state-of-the-art techniques. The TTT shown in Figure 2.1 is configured with several combinations of ties, rail and tie spacing. TSC selected the concrete ties and continuously welded rail section of the test loop for the experiment, since this section is representative of new at-grade transit track construction. Two sites along the TTT were chosen for instrumentation, and both sites are located in close proximity to existing instruments that were installed during the construction of the TTT. There is a tangent and a curved site with identical rail, ties, fasteners, ballast, subballast and subgrade materials leaving only the tie spacing and track curvature as variables. The curved site has a 1.5 degree curvature (radius equal to 3820 feet) which is substantially more gradual than typical transit curves but is the maximum curvature existing along the TTT. The test site includes a 0.69 percent grade clockwise from the tangent site to the curved site. The tangent site is designated KSC-1 and is located near track station 365 and approximately twenty eight feet from instrument site TTC-4A. The curved site is designated KSC-2 and is located near track station 428 and approximately twenty seven feet from instrument site TTC-4B.

## 3.2 TRACK MATERIALS

Both test locations are configured as follows:

| | |
|---|---|
| Rail | 119 lb Welded Rail |
| Tie | Gerwick RT-7 Mark 38 |
| | Prestressed Concrete Tie |

| Fastener | The Rail Co. "Flexiclip" |
|---|---|
| Tie Spacing | 30 in. on tangent track |
| | 27 in. on curved track |
| Ballast | 12 in. of Crushed Stone AREA No. 4 Gradation |
| Subballast | 6 in. of ungraded stone |
| Subgrade | Silty Sand |

The subgrade consists of a thirty inch depth of recompacted soil above the undisturbed subgrade. The track materials and tie spacing are similiar to those used in present day construction of at-grade transit track.

## 3.3 REQUIRED MEASUREMENTS

The experimental task of this study was to determine the loads induced in the transit track system from the rails down into the undisturbed subgrade by the passage of transit vehicles. There have been no previous comprehensive measurements of this type performed on transit track systems. The types of measurements of primary interest to be obtained are as follows:

a)   wheel-to-rail vertical and lateral loads

b)   rail seat loads

c)   tie bending moments

d)   tie-ballast pressure

e)   ballast-subballast pressure

f)   pressure distribution in subballast

g)   tie settlement

h)   ballast and subgrade strains

## 3.4 EXISTING INSTRUMENTATION

The selection of the locations for instrumentation sites KSC-1 and KSC-2 included the desire of close proximity to existing instrumentation sites as mentioned in Section 3.1 and illustrated in Figure 2.1. Instrumentation sites TTC-4A and TTC-4B were installed during the construction of the TTT in 1972. The instrumentation consisted mainly

of Bison soil strain measurement systems and soil pressure gages (Gentran and Carlson types). All of this instrumentation was installed in the track ballast as shown in Figure 3.1, and there were no instruments placed into the recompacted subgrade. Upon examination of these previously installed instruments it became apparent that many transducers had degraded, and calibrations were no longer available for others. Very limited data were obtained from those transducers that were still operating for comparison with the newly-installed transducers.

3.5 TRANSDUCER SELECTION

Transducer selections for the experimental activities were based on one or more of the following considerations: cost, availability, commonality with existing TTT transducers and/or contractual direction. The following paragraphs describe selection of the various transducers and transducer applications employed in instrumentation of the curved and tangent test areas of the TTT.

3.5.1 Crosstie Strain Gages

KSC consulted with personnel of the Waterways Experiment Station (WES), Corps of Engineers in Vicksburg, Mississippi, regarding strain gage instrumentation and calibration of concrete crossties. The WES had previously been involved in similar efforts with concrete crossties utilized in the TTC Facility for Accelerated Service Testing (FAST) track, and this experience was deemed directly applicable. Recommendations received and utilized included use of full-bridge strain gage circuits for maximum signal output, isolation of the inactive strain gages from rail seat stress gradients, and methods of detection and filling of subsurface voids in the strain gage areas. In addition, the WES load calibration testing experience to determine rail seat strains was considered by KSC in specification of laboratory test procedures.

3.5.2 Rail Clip Strain Gages

Strain gages were selected as the method for assessment of the stress condition in the rail clips in view of time and cost constraints. A small gage length was selected because of the varying stress field in

15
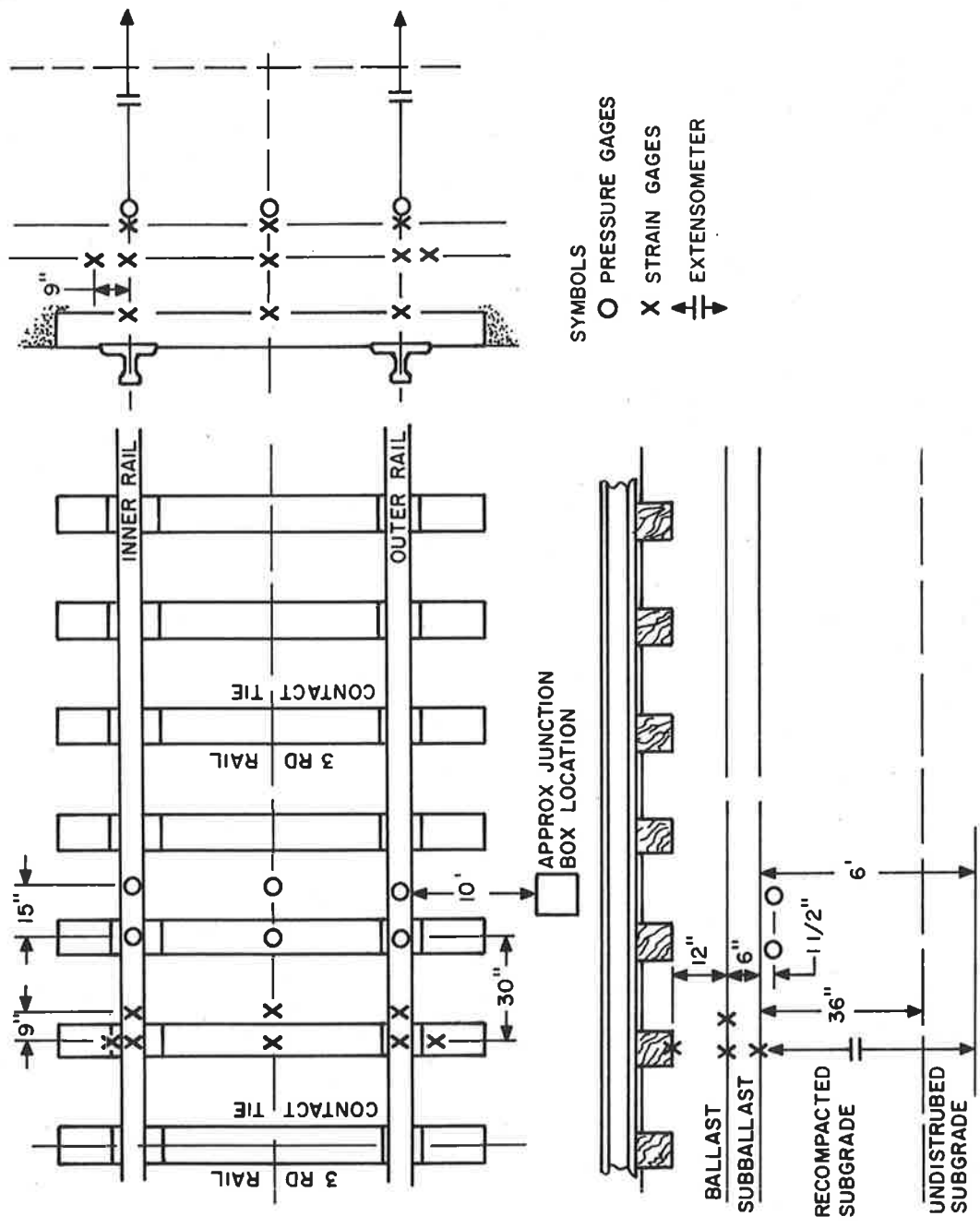
FIGURE 3.1.  INSTRUMENTATION LOCATIONS AT TTC-4A & B TEST STATIONS

16

the only accessible gaging surface.  These strain gages provide an indication of the load environment of the fastener clips and their susceptibility to fatigue.  The use of these strain gages for measuring the rail seat loading was also considered (see Section 3.5.7.).

### 3.5.3  Lateral/Vertical Wheel Rail Load Circuits

KSC opted to employ the web and base chevron strain gage circuits for measurement of vertical and lateral wheel-rail loads.  This method is the generally accepted one, and the TTC had available locating fixtures and templates to assure accurate gage placements.  Hitec weldable strain gages were selected because of favorable TTC experience in this application.  The lateral circuits were load calibrated while subjected to constant vertical loads encompassing the expected range thereof to account for the known effects of vertical load on lateral circuit sensitivity.

### 3.5.4  Sensotec Soil Pressure Gages

Several alternative soil pressure transducers were considered for use in this effort.  The selection of Sensotec gages was made primarily on availability and cost.  These gages were implanted directly in the soil, encapsulated between bearing plates in both the soil and in the ballast, and imbedded in crosstie bottom surfaces.  Encapsulated and imbedded Sensotec gages were subjected to laboratory load calibration to determine output characteristics when loaded by planar surfaces.

### 3.5.5  Bison Soil Strain Measurement System

Bison instrumentation and transducers were employed to measure roadbed strains and deflections in the TTT at Stations 4A and 4B.  The TTC had available the calibration fixture and the electonics unique to these transducers.  KSC was aware of the cumbersome aspects of these gages for dynamic response applications and the effects of large bodies of metal, such as a transit vehicle, upon both the zero reference and sensitivity.  Because of the inherent limitations, only one Bison array was employed to measure ballast strains at each test area.

### 3.5.6  Soil Extensometer

Carlson stress meters were among the transducers originally installed in the TTT roadbed at Stations 4A and 4B, while soil extensometers there operated on the Bison principle.  In view of the known limitations of Bison measurement systems for this application, KSC opted for extensometers employing Carlson joint meters.  The company responsible for fabrication and installation of the Carlson stress meters at Stations 4A and 4B was selected to design and fabricate two Carlson joint meter extensometers for installation at Stations KSC-1 and KSC-2.

### 3.5.7  Rail Seat Loads

As pointed out in Section 3.5.2, strain gages were installed on the fastener clips in order to measure the stress in the fasteners.  This method was discovered to be unreliable for the alternate use of accurately determining the rail seat loads.  However, other methods that have been previously used in the measurement of rail seat loads, such as load cell transducers placed under the rail, are known to alter the normal response of the rail-tie system to the induced vehicle load.  Use of transducers such as load washers beneath the attachment bolt heads or instrumented bolts was rejected because of the variable surface of the rail clip inter-face and the eccentric loading that such transducers would experience.  Therefore, these methods were not used to measure rail seat load, and this load detail was left undetermined in this experimental effort.

### 3.5.8  Miscellaneous Transducers

The remaining transducers including the moisture density meter, thermocouple arrays, and optical speed indicator were TTC equipment operated by the TTC O&M contractor.

### 3.6  PREPARATION/CALIBRATION ACTIVITIES

Various preparatory activities preceded excavation and installation of transducers and instrumented track structure components in the Transit Test Track.  These included instrumentation and laboratory load calibration of concrete crossties, encapsulation and load calibration of ballast Sensotec soil pressure gages, installation of strain gages on rail clips, and evaluation of and compensation for the effects of large metallic objects on Bison soil strain coils.  These activities are discussed in detail in the following paragraphs.

### 3.6.1 Concrete Crossties

Four used Gerwick RT-7, Mark 38 crossties identical to those existing at the two test areas were obtained from TTC inventory for special instrumentation and laboratory load calibration prior to installation in the Transit Test Track for testing. Instrumentation consisted of five full bridge strain gage circuits installed on each crosstie and five Sensotec soil pressure gages interfacing with steel ballast bearing plates recessed flush into the bottom surfaces of two of these crossties as shown in Figures 3.2 and 3.3.

A fixture for locating strain gage positions at the rail seat and midspan areas was designed and fabricated for use on this program. As shown in place in Figures 3.4 and 3.5, this fixture indexed off the gage side rail clips and fasteners and permitted accurate and repeatable marking of the strain gage locations. By measuring strains at the same points on all crossties, the need for performing laboratory load calibrations on the eleven crossties strain gaged in situ at each test area was partially obviated.

Each four arm strain gage circuit was comprised on one BLH FAE2-300-35-S6L two-arm active gage (3-inch length) and one BLH FAE2-25-35-S6L two-arm inactive gage (1/4-inch length). The 3-inch gage length was selected to average out effects of internal aggregates on the surface strain. Availability considerations precluded use of a longer gage, such as 5-inches, which would have been preferable for strain averaging.

Surface preparation of the concrete for installation of the active gages consisted of light tapping to reveal any internal voids followed by surface grinding. Small voids and imperfactions were filled by successive applications of epoxy followed by light sanding. The final strain gage application surface was smooth and flat and was essentially the concrete surface with all voids filled. Gages were applied using manufacturer's specifications and recommendations.

Each inactive gage was bonded to a small piece of phenolic which in turn was cemented with RTV to the crosstie adjacent to the active gage. The phenolic was selected to provide approximately the same
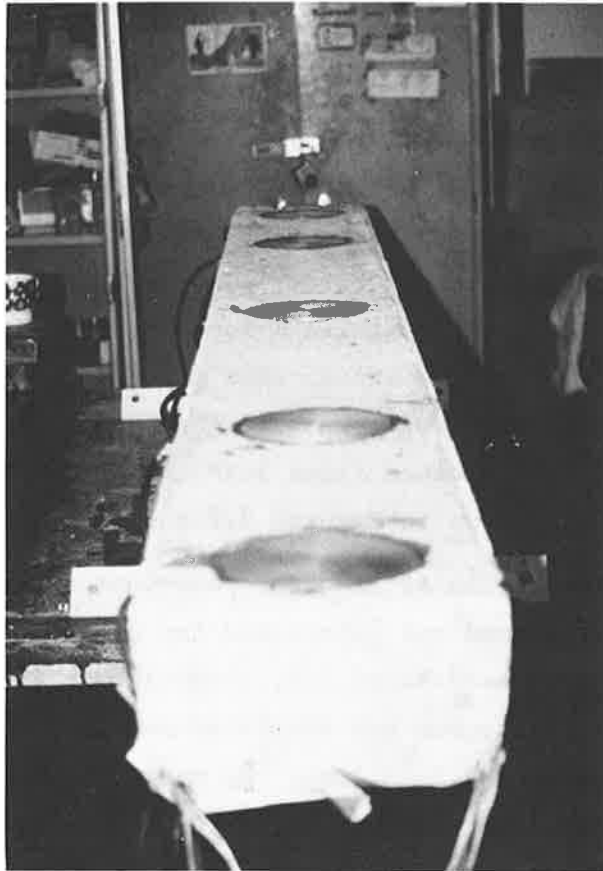
FIGURE 3.2. SOIL PRESSURE GAGES AND BEARING PLATES INSTALLED IN CROSSTIE BOTTOM SURFACE
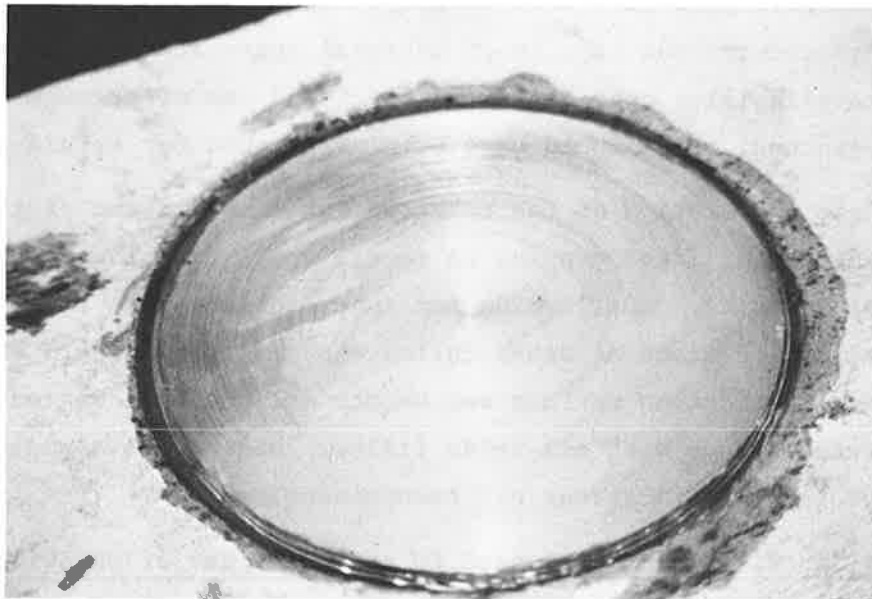


FIGURE 3.3. BEARING PLATE INSTALLED FLUSH WITH CROSSTIE BOTTOM SURFACE
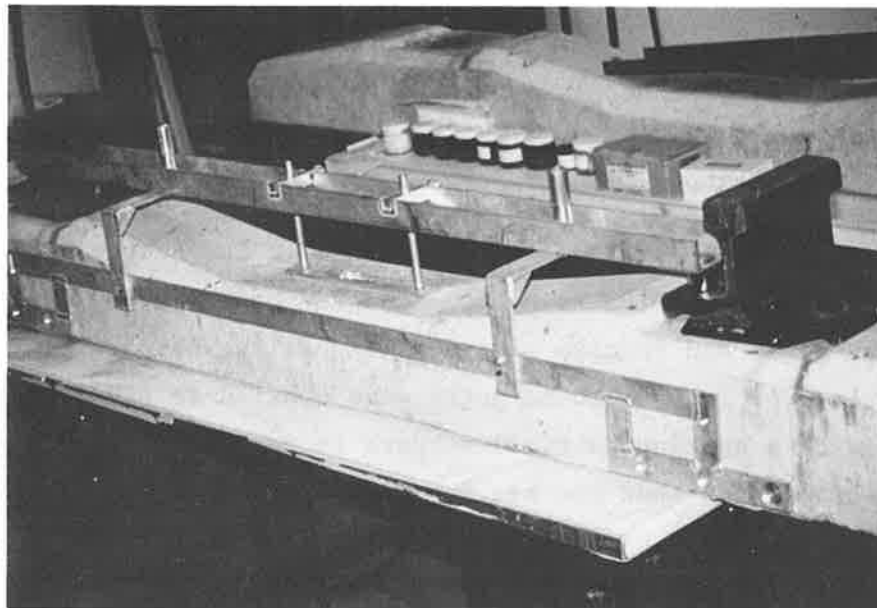
FIGURE 3.4.   STRAIN GAGE LOCATING FIXTURE POSITIONED ON CONCRETE CROSSTIE
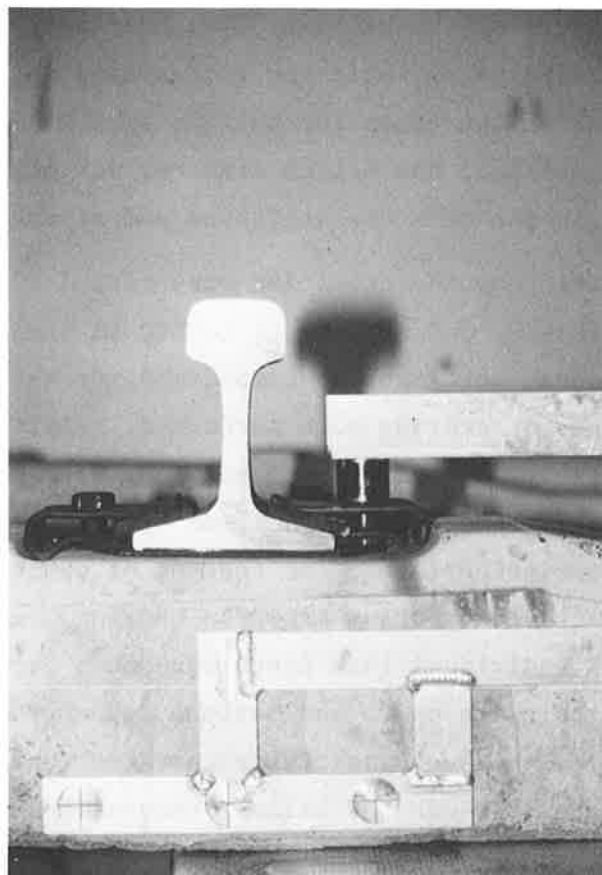


FIGURE 3.5.   RAIL SEAT MARKING TEMPLATE DETAILS, STRAIN GAGE LOCATING FIXTURE

thermal expansion characteristics as the concrete, although no long-term temperature compensation was required for this effort. The RTV provided isolation from strains induced in the concrete by transit vehicle passage.

Five two-step recesses were machined in the bottom surfaces of two of these used crossties to accept Sensotec Model SA-E, 0-750 psi soil pressure gages and cadmium plated steel ballast bearing plates as shown in Figure 3.6. The Sensotec gages were epoxied in place to prevent motion and provide a continuous rigid support to the back surfaces. The gages were located such that the bearing plates could be set flush with the bottom surface of the crosstie and maintained in place by a bead of RTV around the circumference.

The function of the bearing plate was to distribute uniformly the point loadings from the underlying ballast to the strain gaged diaphragm of the Sensotec gage. These gages, which were designed for use in a fluid or fluid-like medium, would give meaningless readings or be damaged by direct contact with the ballast. The bearing plate diameter was limited by a desire to minimize the recess size in the crosstie. Ideally, a plate diameter of ten times the ballast size is needed to average the loading irregularities; the 6-inch diameter was selected to avoid significant changes in the crosstie stiffness and strength characteristics.

The four instrumented crossties were tested by Hauser Laboratories in Boulder, Colorado, under contract to KSC in accordance with the test plan and procedures set forth in Appendix B, Crosstie Load Calibration Tests. Two types of testing were performed. Positive moment rail seat bending and negative moment midspan bending tests were performed on each crosstie, utilizing the set-up specified by the American Railway Engineering Association (AREA) for testing of concrete crossties. From these tests, the strain versus crosstie bending moment relationships were obtained. Individual load tests were then performed on each of the imbedded Sensotec gages up to the maximum capacity of the gage to ascertain the load versus sensitivity characteristics of these transducers when loaded through the ballast bearing plates.
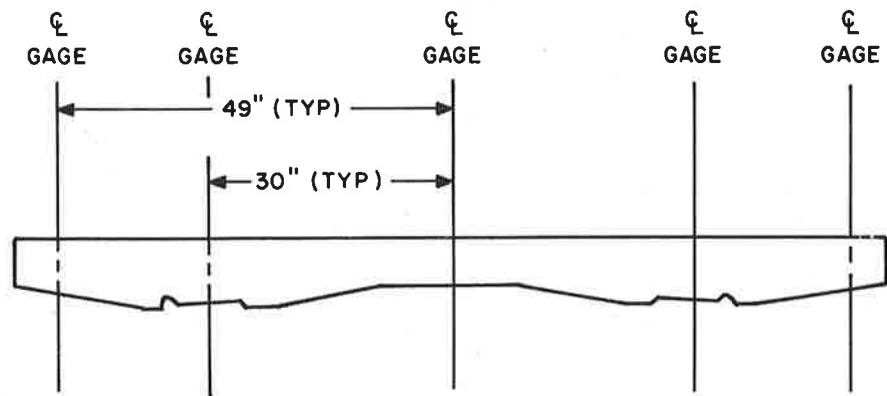
GERWICK RT-7, MARK 38 CONCRETE CROSSTIE
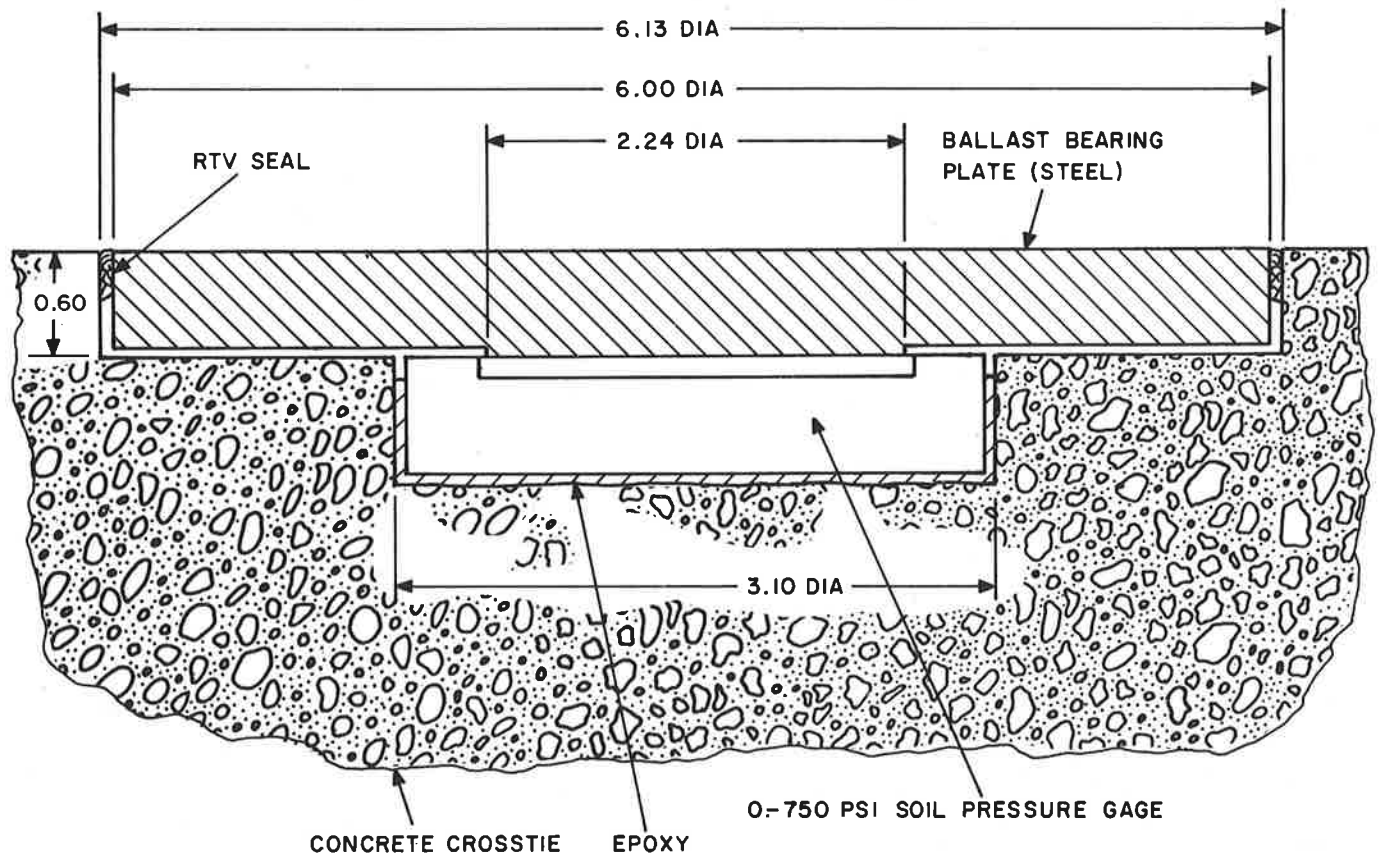


NOTE:  ALL DIMENSIONS IN INCHES

FIGURE 3.6.  DETAILS OF SOIL PRESSURE GAGE INSTALLATION IN CONCRETE CROSSTIES

### 3.6.2  Encapsulated Pressure Gages

Sensotec Model SA-E soil pressure gages of various pressure ratings to be implanted in the ballast were first encapsulated between flat circular cadmium plated steel bearing plates as shown in Figure 3.7. These plates served the same function as the bearing plates imbedded in the crossties by distributing uniformly the point loadings from the surrounding ballast to the strain gaged diaphragm of the Sensotec gage. Bearing plate diameters were selected in accordance with the gage pressure rating and the expected ballast pressure levels. Four different diameters (4-, 5-, 7-, and 10-inch) were required because of the limited availability of gages having common pressure ratings. Before implantation, all encapsulated Sensotec gages were load tested to the maximum capacity of the gage to ascertain the load versus sensitivity characteristics when loaded through the encapsulation plates.

### 3.6.3  Soil Strain Gages

The Bison Model 4101A soil strain measurement system employing 4-inch sensors was employed to measure vertical and lateral ballast strain. In operation, receiver sensors are located at known distances from a common sender sensor. The separation of the sensors is related to the electromagnetic coupling between the receivers and senders. By means of an inductance bridge contained in the 4101A instrument package, an output voltage as a function of sensor displacement may be obtained since a change in spacing from the initial position produces a bridge unbalance. It was determined during preliminary calibrations that both the null indications and output sensitivities of the Bison system were affected by the presence of metallic bodies. To account for the effects induced by passage of the transit vehicles, a Bison field compensator was constructed as shown in Figure 3.8. This device consisted of one sender sensor situated between two receiver sensors with the same spacing as that employed in the active array. These sensors were supported in a plastic tube which isolates the array from ballast strain. The effects of transit vehicle passage can therefore be determined independently and used to correct the signals obtained from the active array.

24
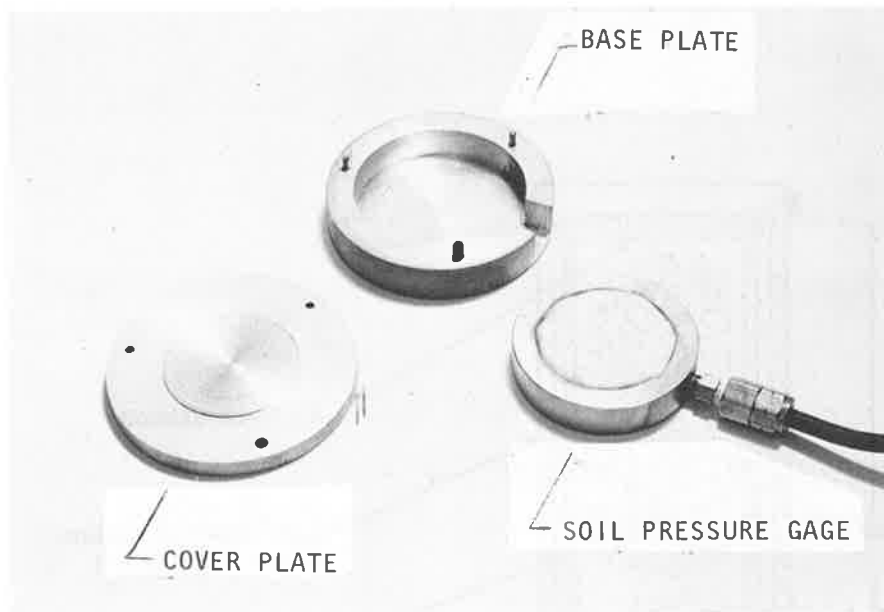
| "A" DIAMETER (INCHES) | GAGE PRESSURE RATINGS (PSI) |
|---|---|
| 4.00 | 0-100 |
| 5.00 | 0-100 & 0-600 |
| 7.00 | 0-600 |
| 10.00 | 0-600 |

ALL DIMENSIONS IN INCHES
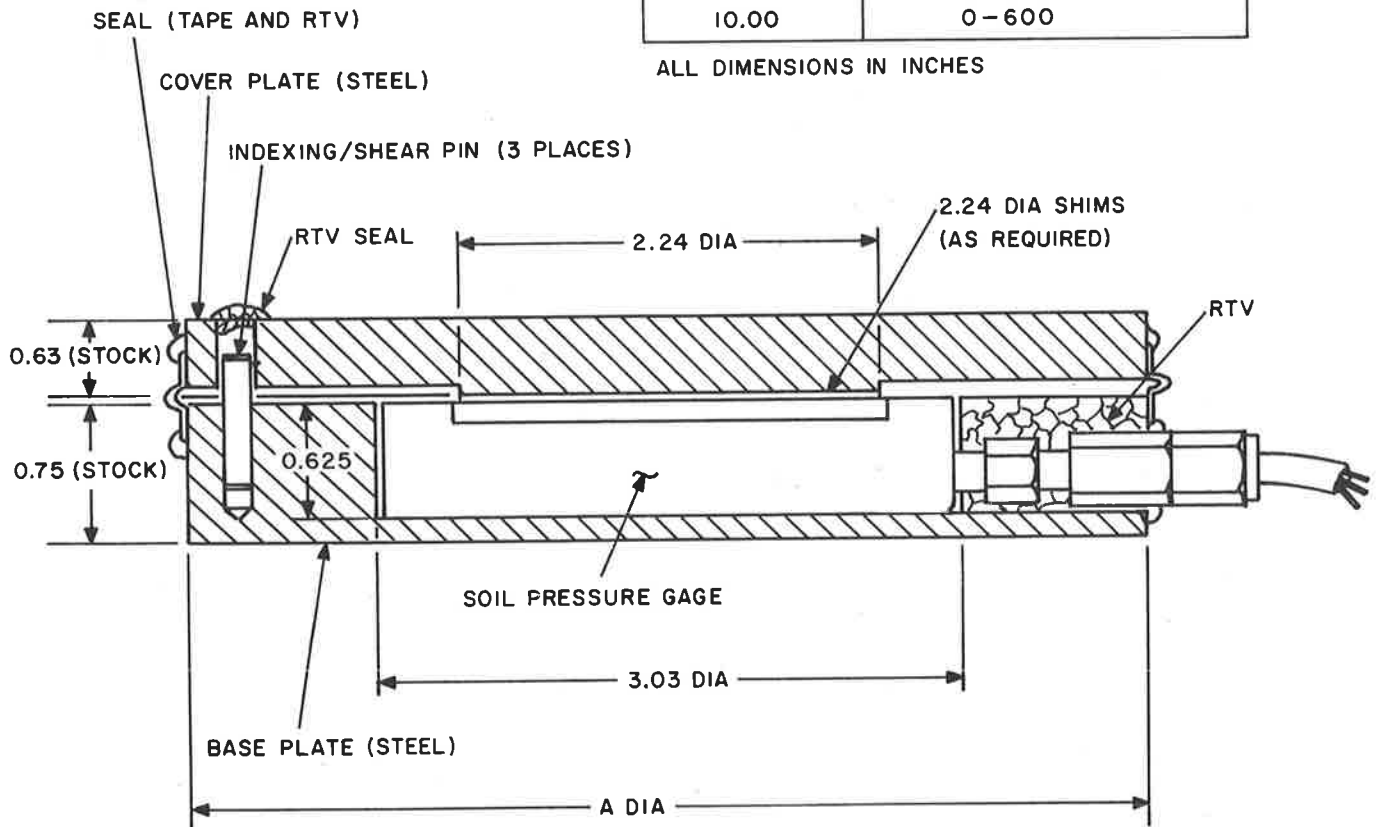
FIGURE 3.7. SOIL PRESSURE GAGE ENCAPSULATION DETAILS
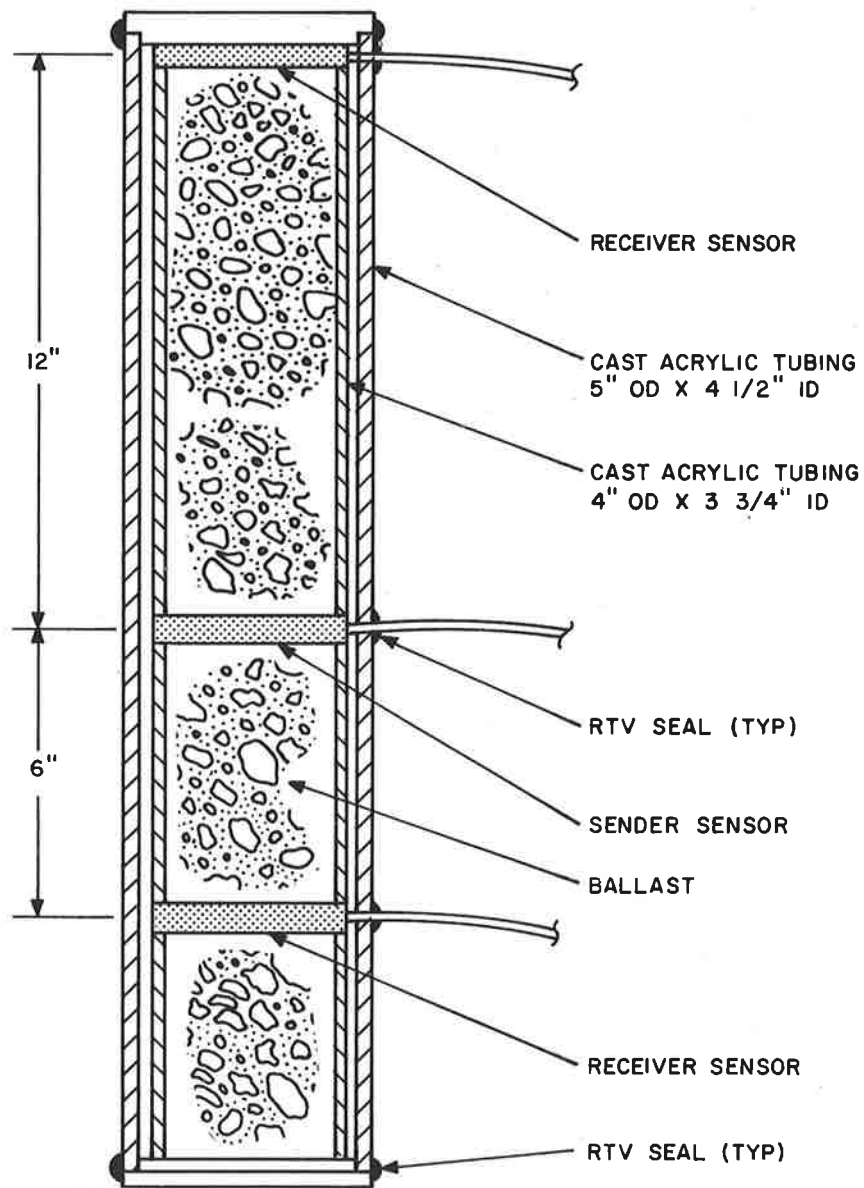
FIGURE 3.8.  BISON FIELD COMPENSATOR CONFIGURATION

RECEIVER SENSOR

CAST ACRYLIC TUBING
5" OD X 4 1/2" ID

CAST ACRYLIC TUBING
4" OD X 3 3/4" ID

RTV SEAL (TYP)

SENDER SENSOR

BALLAST

RECEIVER SENSOR

RTV SEAL (TYP)

12"

6"

### 3.6.4. Instrumented Rail Clips

Eight Flexiclip rail fasteners, manufactured by The Rails Company, were obtained from TTC inventory and instrumented with full bridge strain gage circuits as shown in Figure 3.9. Strain gages employed were Micro-Measurements EA-13-250-BF-350 (1/4-inch gage length) for both active and inactive arms. Original plans called for laboratory load calibrations of these instrumented rail clips to determine the load versus sensitivity characteristics of each. Upon closer consideration, it was decided that the many variables in the interfacing components would render invalid any laboratory calibrations when reassembled in the field. In situ load calibration was therefore performed on the instrumented rail clips after installation in the TTT to determine the output sensitivities.

### 3.7 SITE INSTALLATION

The same types and quantities of transducers were installed at both the curved and tangent test areas of the Transit Test Track. As shown in Figures 3.10 and 3.11, the transducer orientation at the two test areas was identical except for being symmetrically opposite. The TTC O&M contractor, under the direction of KSC personnel, supplied much of the labor and equipment for the actual transducer installation. The following paragraphs describe in detail the installation processes. Since essentially the same procedures were employed for installations at both sites, this discussion will be based upon that at the curved test area with any differences noted. For orientation purposes, corresponding crosstie identification numbers at the tangent test area will be noted in parentheses.

### 3.7.1 Primary Transducer Arrays

The largest concentration of transducers was included within, between, and beneath crosstie numbers 428 -13 and -14 (365 +8 and +9) with a lesser number included beneath crosstie 428 -15 (365 +10). These transducer arrays are identified as #1, #2, and #3 Array on Figures 3.10 and 3.11 and the transducer orientations of each are shown in Figures 3.12, 3.13 and 3.14.
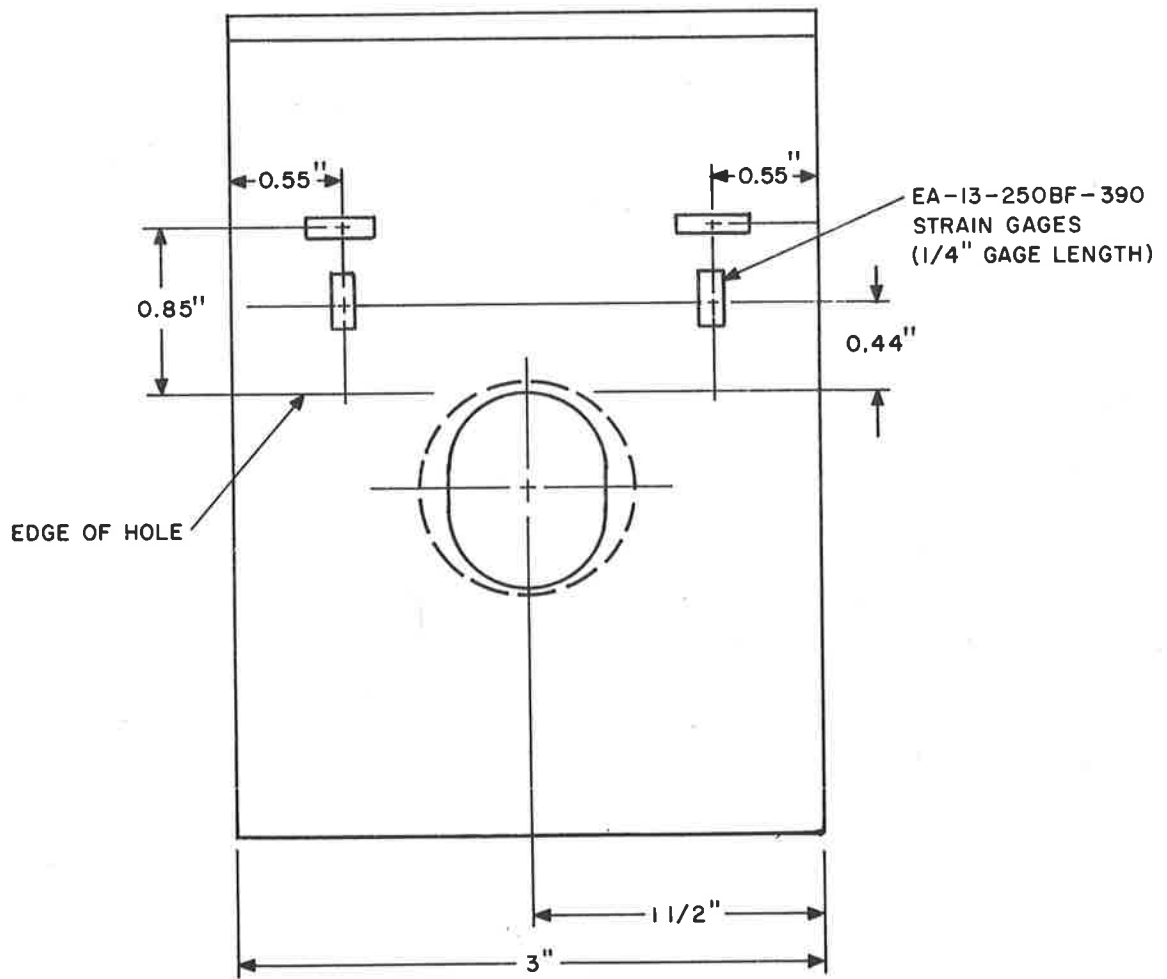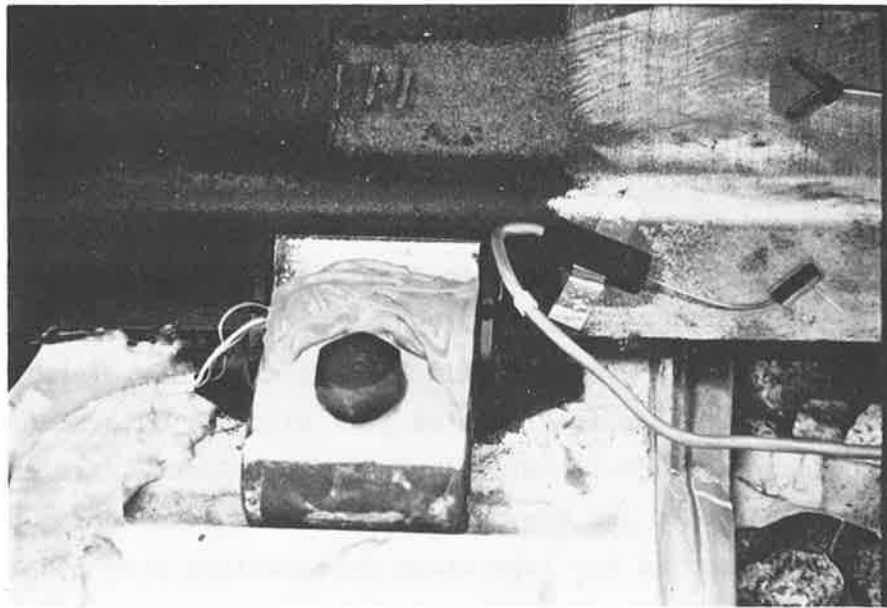
FIGURE 3.9.  STRAIN GAGE INSTRUMENTATION OF RAIL CLIP
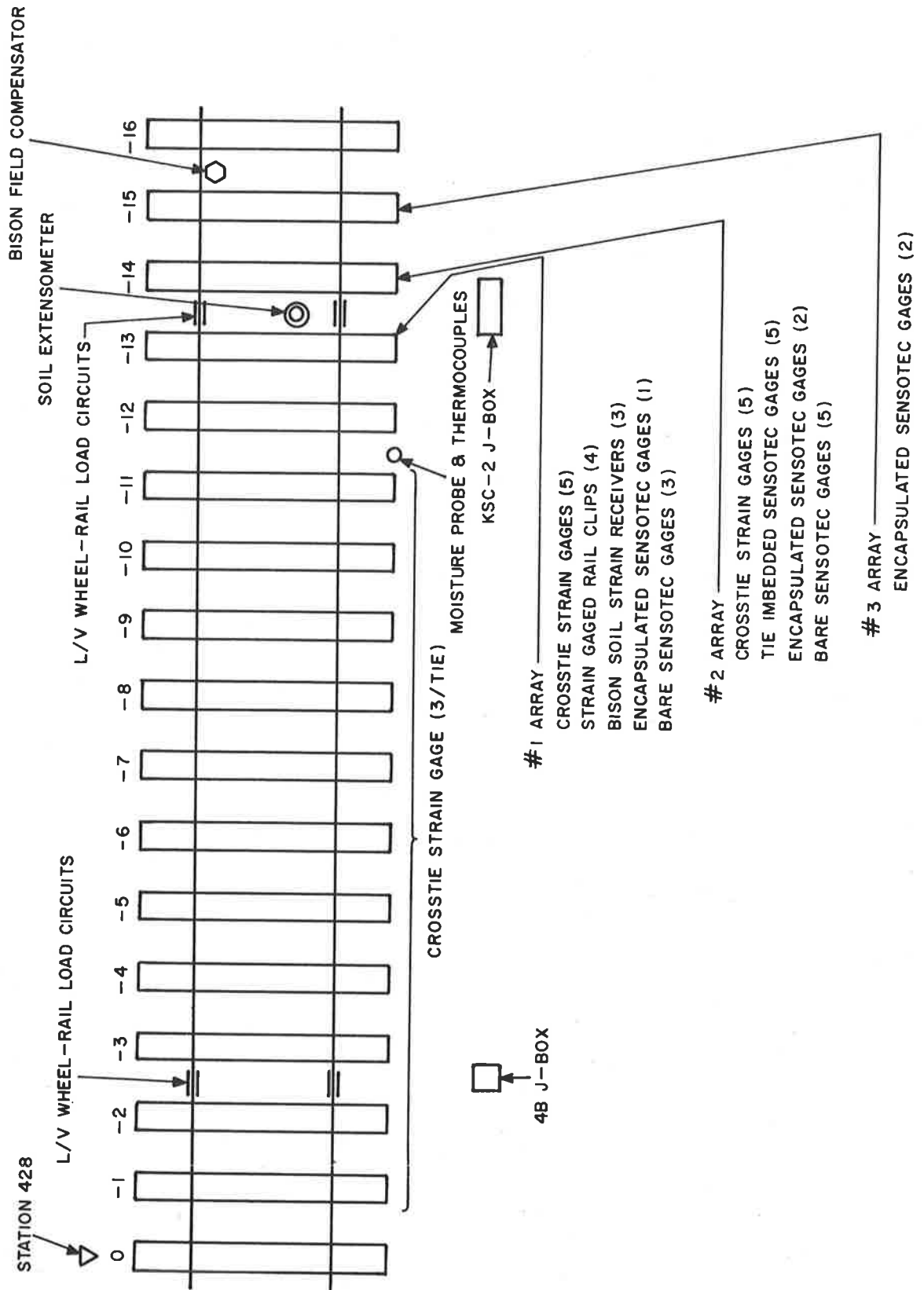
FIGURE 3.10. TRANSDUCER ORIENTATION AT CURVED TEST AREA

STATION 428

L/V WHEEL-RAIL LOAD CIRCUITS

L/V WHEEL-RAIL LOAD CIRCUITS

BISON FIELD COMPENSATOR

SOIL EXTENSOMETER

MOISTURE PROBE & THERMOCOUPLES

KSC-2 J-BOX

CROSSTIE STRAIN GAGE (3/TIE)

#1 ARRAY
CROSSTIE STRAIN GAGES (5)
STRAIN GAGED RAIL CLIPS (4)
BISON SOIL STRAIN RECEIVERS (3)
ENCAPSULATED SENSOTEC GAGES (1)
BARE SENSOTEC GAGES (3)

#2 ARRAY
CROSSTIE STRAIN GAGES (5)
TIE IMBEDDED SENSOTEC GAGES (5)
ENCAPSULATED SENSOTEC GAGES (2)
BARE SENSOTEC GAGES (5)

#3 ARRAY
ENCAPSULATED SENSOTEC GAGES (2)

4B J-BOX

29

FIGURE 3.11. TRANSDUCER ORIENTATION AT TANGENT TEST AREA

KEY
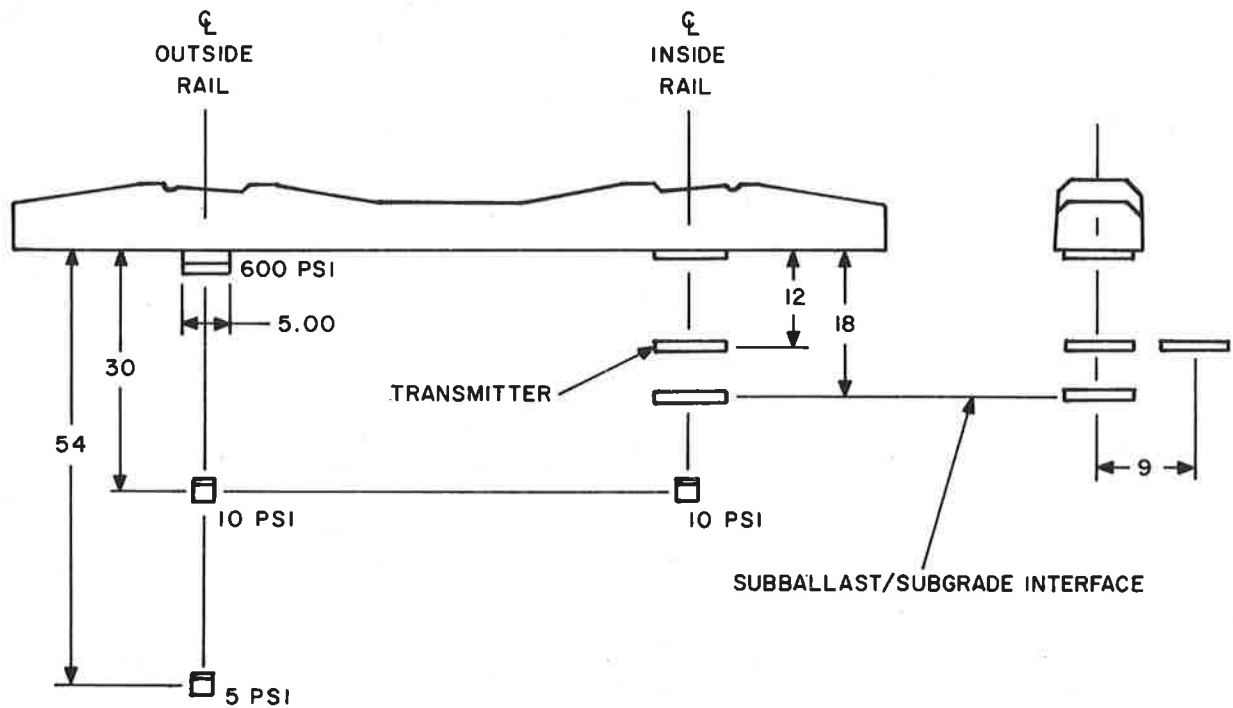
⬜ = ENCAPSULATED SENSOTEC GAGE

|←——→| XXX (ENCAPSULATION DIAMETER)

◻ = BASIC 2.25 DIA SENSOTEC GAGE

▭ = BISON SOIL STRAIN COILS

ALL DIMENSIONS IN INCHES

FIGURE 3.12.   TRANSDUCER ORIENTATION – NO. 1 ARRAY
(CURVED AND TANGENT TEST AREAS)

31
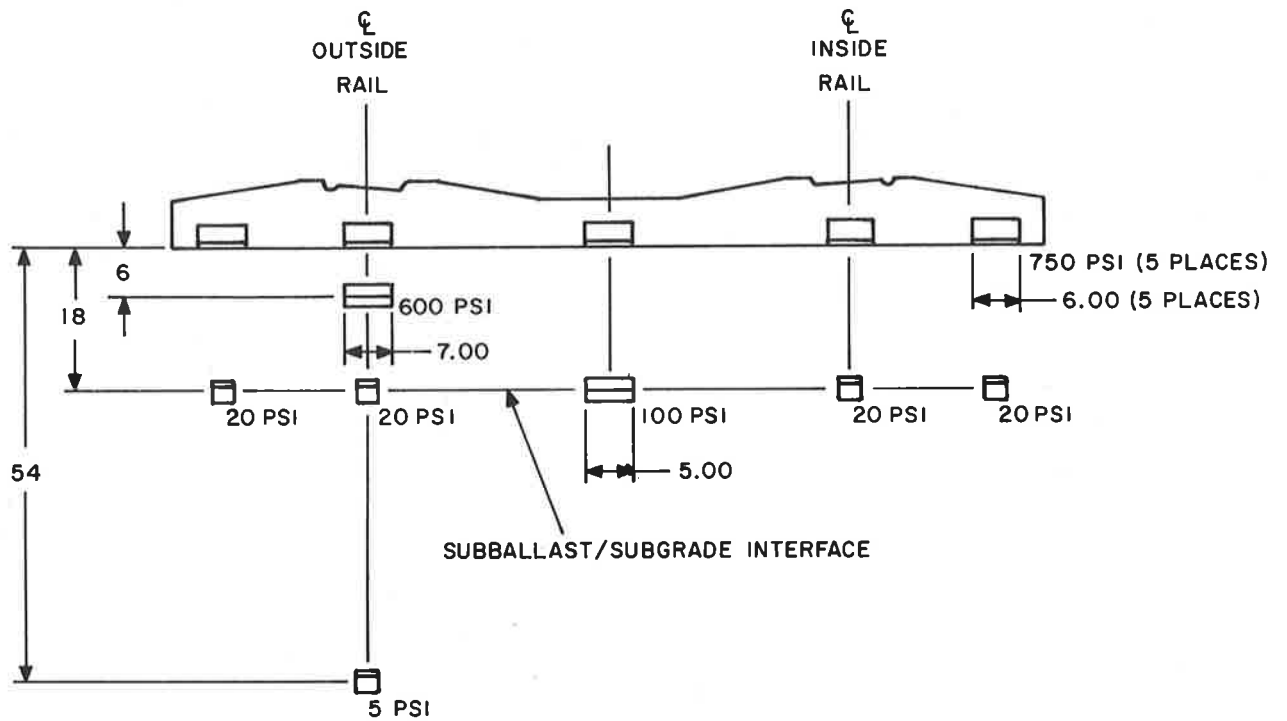
KEY

◫ = IMBEDDED SENSOTEC GAGE

|←→| XXX (PRESSURE PLATE DIAMETER)

▤ = ENCAPSULATED SENSOTEC GAGE

|←→| XXX (ENCAPSULATION DIAMETER)

▢ = BASIC 2.25 DIA SENSOTIC GAGE

ALL DIMENSIONS IN INCHES

FIGURE 3.13.    TRANSDUCER ORIENTATION – NO. 2 ARRAY
(CURVED AND TANGENT TEST AREAS)

32

KEY

☰ = ENCAPSULATED SENSOTEC GAGE

|← →| XXX (ENCAPSULATION DIAMETER)
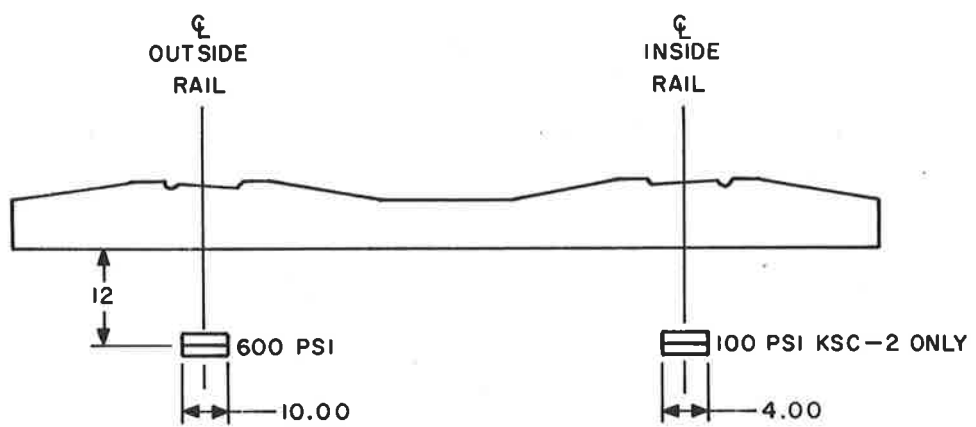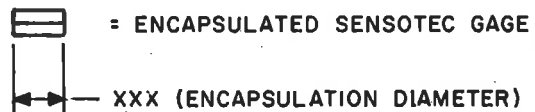
ALL DIMENSIONS IN INCHES

FIGURE 3.14. TRANSDUCER ORIENTATION – NO. 3 ARRAY
(CURVED AND TANGENT TEST AREAS)

33

To begin the transducer installation, ballast beneath crosstie numbers 428 -13 and -14 (365 +8 and +9) was scraped away, and these crossties were removed. Ballast was further removed to the subballast-subgrade interface. Using hand tools, the subgrade soil was trenched as shown in Figure 3.15 to provide for transducer implantation and lead wire routing.

Survey techniques were employed as shown in Figure 3.16 to insure transducer placement to within $\pm 1/4$-inch of the desired position both vertically and laterally. At the curved test area, all instrumentation lead wires were routed through interconnected PVC piping, the termini of which were located immediately adjacent to each transducer. At the tangent test area, PVC piping was employed only within the ballast and subballast to protect instrumentation lead wires; those located below the ballast/subballast interface were routed directly through the sandy subgrade soil. This was done to minimize subgrade disturbances that resulted from additional trenching requirements solely for the PVC pipe that were observed at the curved test area. After each transducer was implaced, the respective holes were filled with subgrade soil which was hand-tamped to approximate the prevailing compaction as closely as possible without disturbing the transducer location or orientation.

After installation of the subgrade transducers in the #1 and #2 Arrays, the Terrametrics Model 1-RC single position borehole extenso-meter was installed in the hole provided. The integral 2-inch soil auger was screwed to the proper depth in the subgrade at the hole bottom using the setting tool provided. Attachment of the Carlson joint meter and upper portion of the extensometer were straight-forward and in accordance with the manufacturer's instructions.

Next, the previously instrumented and laboratory load calibrated crossties were inserted and secured in place to the rails with the Flexiclip rail fasteners at locations 428 -14 and -15 (365 +8 and +9) as shown in Figures 3.17 and 3.18. The strain gaged Flexiclip rail fasteners were employed to attach crosstie 428 -13 (365 +8).
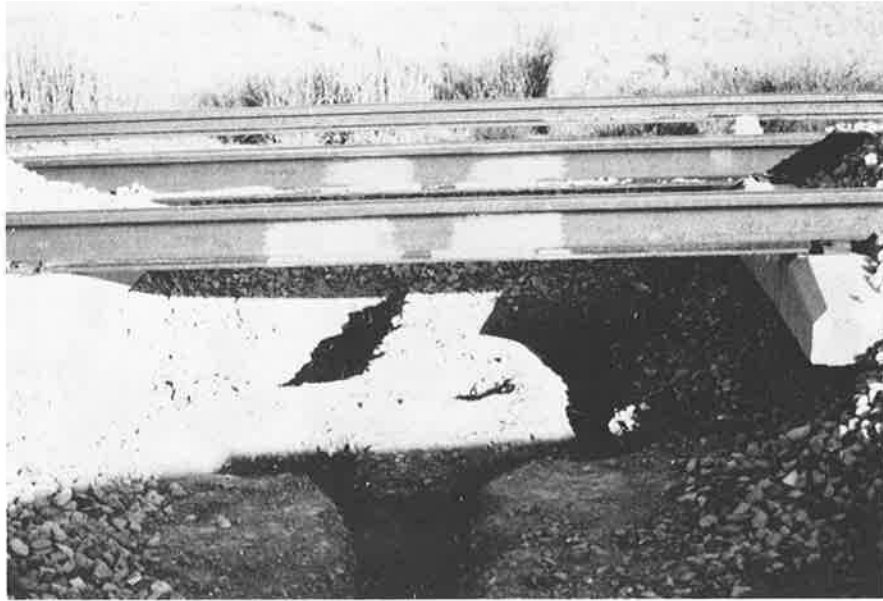
FIGURE 3.15.   ROADBED TRENCHING PRIOR TO TRANSDUCER INSTALLATION
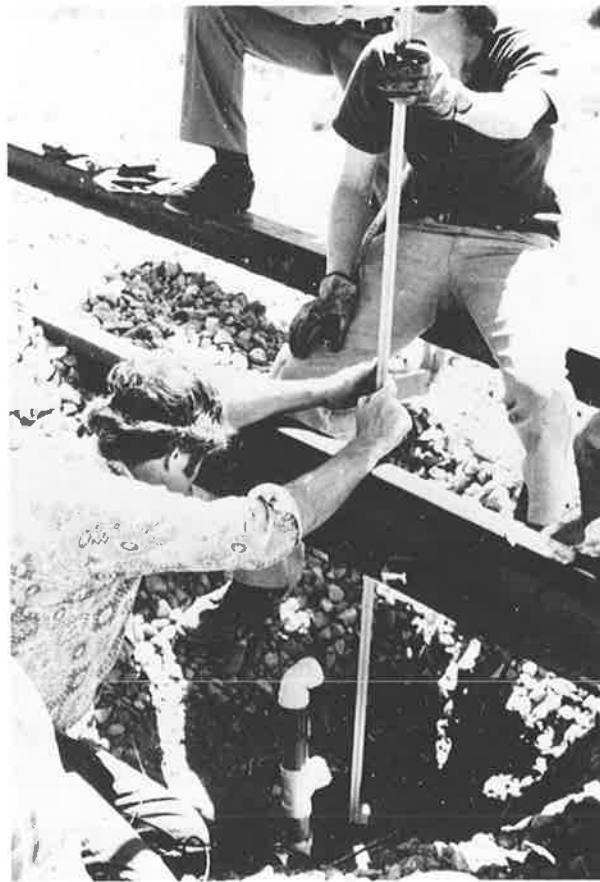


FIGURE 3.16.   PLACEMENT OF TRANSDUCERS USING SURVEY TECHNIQUES

FIGURE 3.17.   INSTALLATION OF INSTRUMENTED CROSSTIE
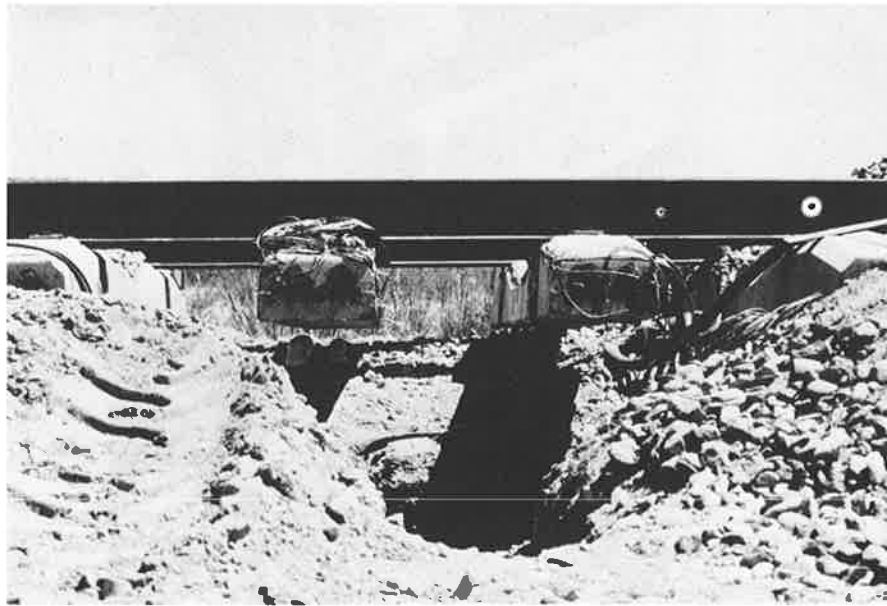


FIGURE 3.18.   INSTRUMENTED CROSSTIES SECURED TO RAILS

The remainder of the subballast and ballast transducers in the #1, #2, and #3 Arrays were installed as the ballast was backfilled beneath the crossties and in the crib areas. One encapsulated Sensotic 0-100 psi soil pressure gage was found to be inoperative and therefore was not installed in the #3 array at the tangent test area. To consolidate the ballast in the excavated areas, a mechanical tamper was employed as shown in Figure 3.19. Close supervision was provided to guard against damage to the rail seat strain gages and disturbance of the ballast transducers.

### 3.7.2 Strain Gaged Crossties

As indicated in Figures 3.10 and 3.11, eleven crossties at each test area were instrumented with three strain gages each. These strain gages were installed by KSC personnel on the in situ crossties. Gage types, connections, and installation procedures matched those employed for the two instrumented and laboratory load calibrated crossties at each test area. The strain gage locating fixture was utilized to insure accurate and repeatable positioning of the rail seat and midspan strain gages identical to that of the calibrated crossties. Installation of the rail seat strain gages necessitated temporary removal of the crib ballast adjacent to each rail seat. Clamps were fabricated for use as shown in Figure 3.20 to apply the required bonding pressure. Formed stainless steel protective covers were bonded in place over each rail seat strain gage installation prior to backfilling of the ballast. Lead ingots were employed to apply vertical bonding pressure for the midspan strain gages. Formed stainless steel protective covers were also bonded in place over all midspan strain gage installations.

### 3.7.3 Miscellaneous Transducers

The Bison field compensator (Figure 3.21) was installed between crossties 428 -15 and -16 (365 +10 and +11) by removing the crib positioning the array at the proper elevation with the top receiver sensor located at the crosstie bottom plane, and backfilling the ballast.
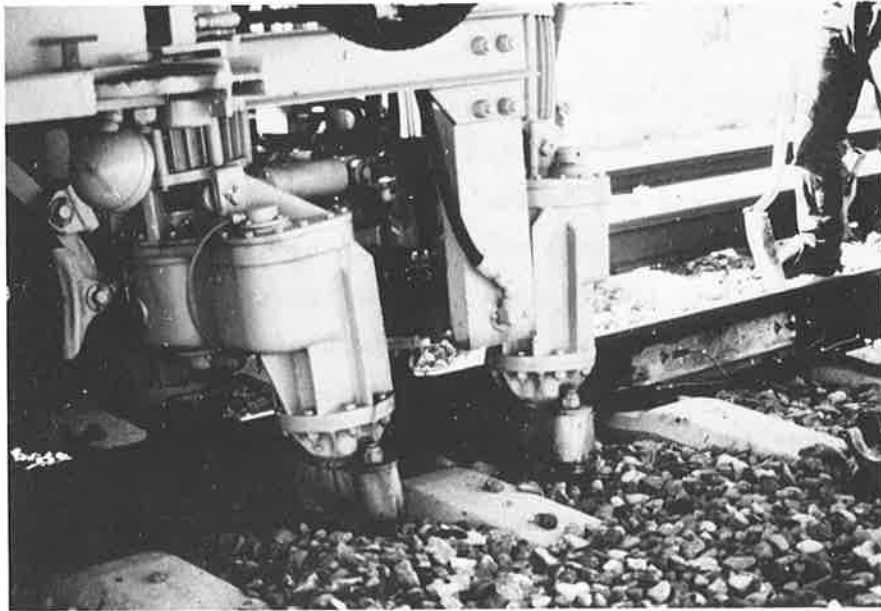
FIGURE 3.19. BALLAST TAMPING OPERATIONS IN EXCAVATED AREA
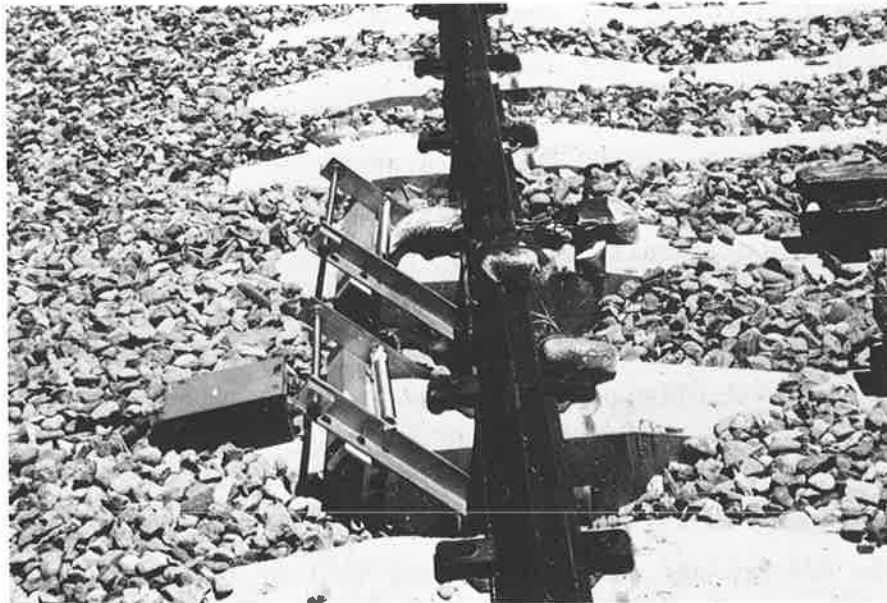


FIGURE 3.20. CLAMPS PROVIDE BONDING PRESSURE FOR RAIL SEAT STRAIN GAGES

FIGURE 3.21. BISON FIELD COMPENSATOR PRIOR TO INSTALLATION
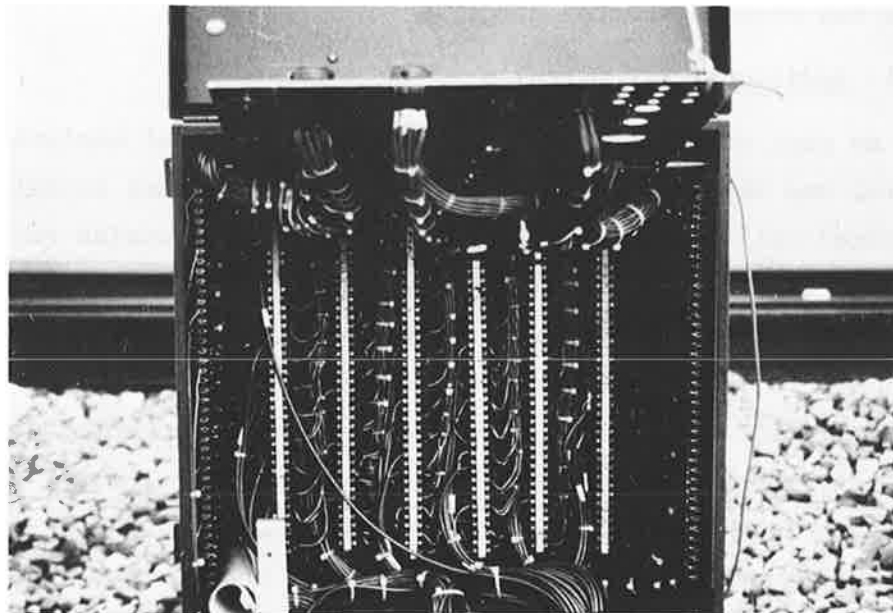


FIGURE 3.22. INTERNAL WIRING OF KSC J-BOX

All instrumentation lead wires were routed below ground to the respective KSC J-box at each test area where terminations were made to terminal strips as shown in Figure 3.22. The J-box hinged front connector panel provided the primary instrumentation interfaces to the TTC data van.

The TTC O&M contractor installed web and base chevron strain gage circuits on both rails between crossties 428 -2 and -3 (365 -3 and -4) and between crossties 428 -13 and -14 (365 +8 and +9) for measurement of lateral and vertical (L/V) wheel-rail loads. Strain gages employed were Hitec HBW-35-125-6-10GP (1/8 inch gage length) uniaxial gages welded to the rail base flange for lateral load measurement and Hitec HBWC-35-1256-10GP-TR (1/8-inch gage length) 90-degree chevron dual gages welded to the rail web at the neutral axis for vertical load measurement. Gage locations and circuit connections were as shown in Figure 3.23. Instrumentation lead wires for all L/V wheel-rail load circuits were routed along one of the two crossties immediately adjacent to bracket-mounted connectors located on the crosstie end.

The TTC O&M contractor also installed a vertical tube between crossties 428 -11 and -12 (365 +7 and +8) to accept the Soiltest NIC-5 nuclear moisture density meter. In the same area, the O&M contractor installed a vertical array of eight copper-constantan Type T thermo-couples at depths of 0-, 12-, 18-, 24-, 30-, 36-, 42-, and 54-inches below the crosstie bottom plane.

3.7.4 Additional L/V Circuits

As part of the effort to determine statistical variations in lateral and vertical wheel-rail loads, KSC personnel installed ten L/V wheel-rail load measurement circuits on the outside rail of the TTT oval in the vicinity of the tangent test area as shown in Figure 3.24. Installation, connection and instrumentation lead wire routing were identical to those of the corresponding circuits installed by the TTC O&M contractor. The measurement locations were selected so that during a single passage of the NYCTA R-42 transit vehicle, every point on the circumference of each 34-inch diameter wheel would be encompassed by at least one of the 10-inch measurement zones. The location of the

40

VERTICAL GAGES:
HBWC-35-125-6-10GP-TR
(4 PLACES)

2 21/32"

6 13/16"

3.124"

5 1/2"

119 RE RAIL

VIEW B-B

1.0 (4 PLACES)

45° (4 PLACES)

LATERAL GAGES:
HBW-35-125-
6-10GP (4 PLACES

VERTICAL CIRCUIT

LATERAL CIRCUIT

NEUTRAL AXIS

( ) = FARSIDE

1.0

1.0

VIEW A-A
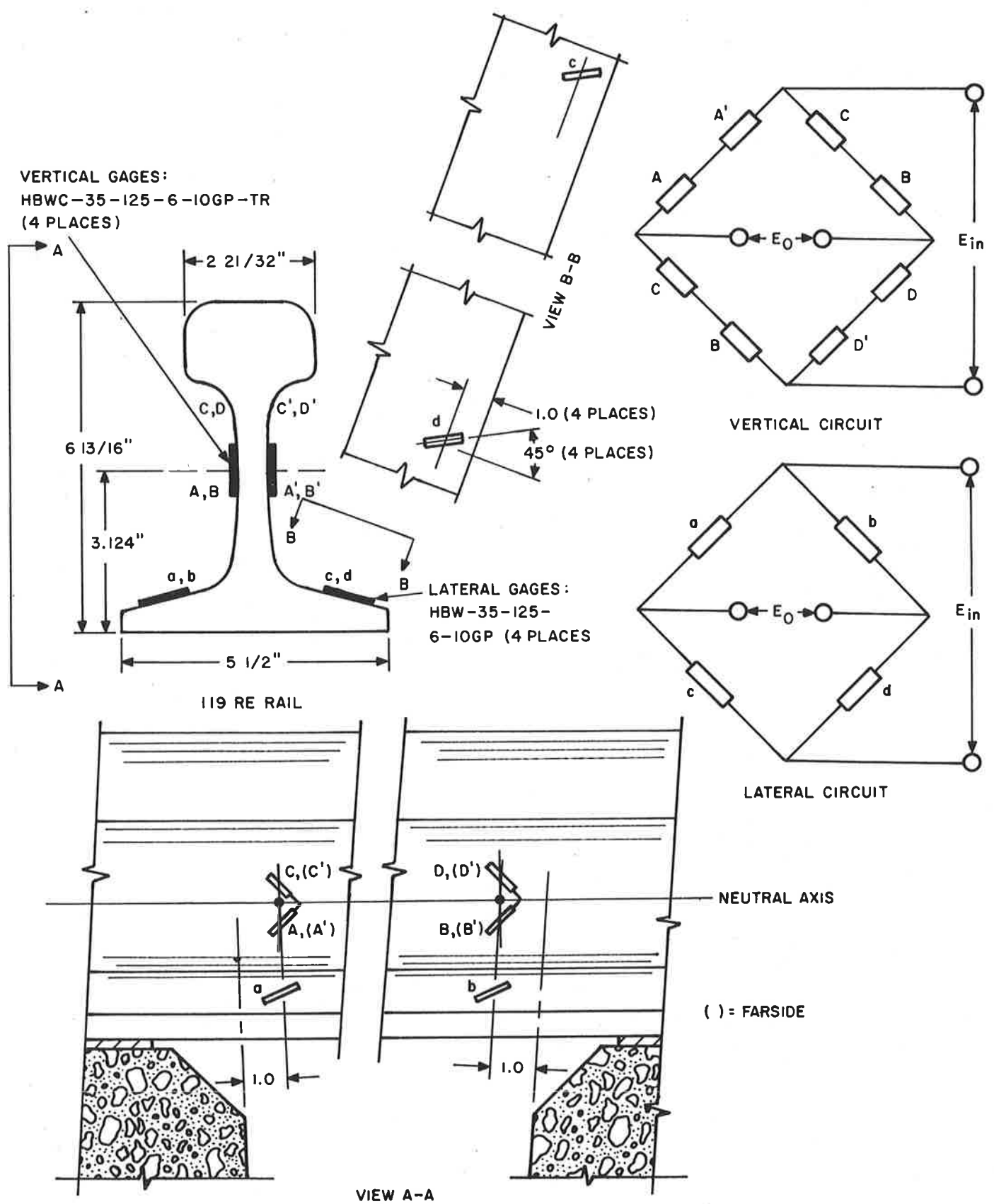
FIGURE 3.23. L/V WHEEL-RAIL LOAD STRAIN GAGE LOCATIONS
AND CIRCUIT CONNECTION
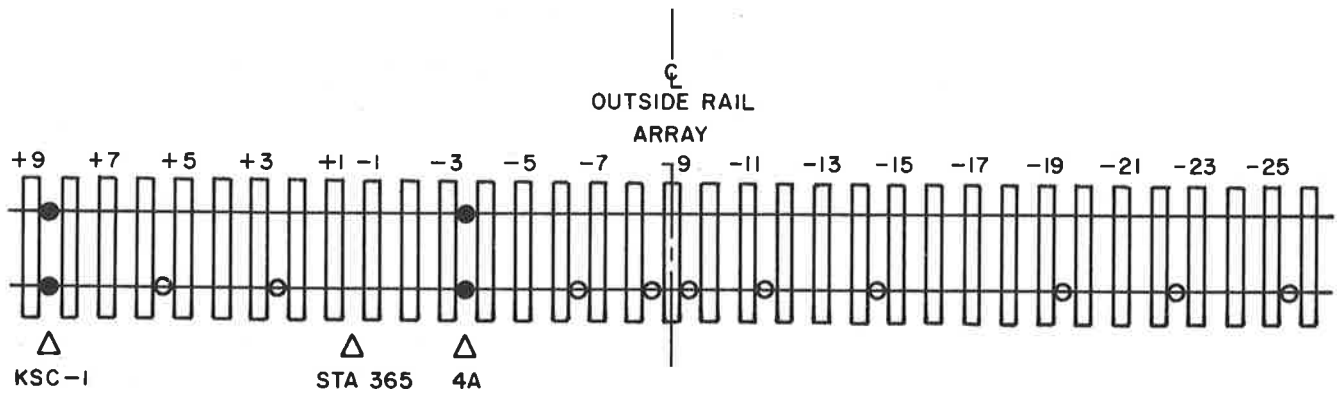
41

FIGURE 3.24. L/V WHEEL-RAIL LOAD MEASUREMENT
CIRCUITS IN TANGENT TEST AREA

42

overall array was chosen to accommodate future efforts to measure wheel-rail loads induced by lateral and/or vertical track perturbations; perturbation lengths of up to 80-feet, symmetrical about crosstie 365 -9, can be incorporated without disturbing the instrumentation arrays at KSC-1.

## 3.8 SITE DATA ACQUISITION AND RECORDING

The TTC O&M contractor was responsible for integration, operation, and maintenance of all test-related equipment including the transit vehicles, the TTC No. 54 Calibration Car, the TTC No. 408 Data Van and ancillary items such as the diesel power supply and specialized transducer/instrumentation items. KSC personnel assisted in the set-up and data acquisition effort wherever appropriate.

The block diagram for data acquisition and recording using the TTC No. 408 Data Van is given in Figure 3.25. All data except for soil temperature and moisture density were FM multiplexed and recorded on analog tape. Resistive calibration techniques were employed for most transducers to obtain the comparative signal strengths for scaling of the output data.

## 3.9 PRE TEST CALIBRATIONS

A series of load calibration tests was performed on each L/V wheel-rail load measurement circuit to determine load versus output characteristics of both the lateral and vertical circuits and the influence of vertical load on lateral circuit sensitivity. Load calibration testing was also performed on the strain gaged Flexiclip rail fasteners to determine the load sensitivities. The L/V circuits installed by the TTC O&M contractor and KSC and the strain gaged rail fasteners were load calibrated in accordance with the test plan set forth in Appendix C, Calibration Loading Test Plan for L/V rail circuits and Instrumented Crossties.

All calibration loading was applied using the TTC No. 54 Calibration Car, a loaded 100-ton bottom-dump hopper car incorporating a hydraulic loading apparatus mounted between the hopper chutes. This apparatus has

43
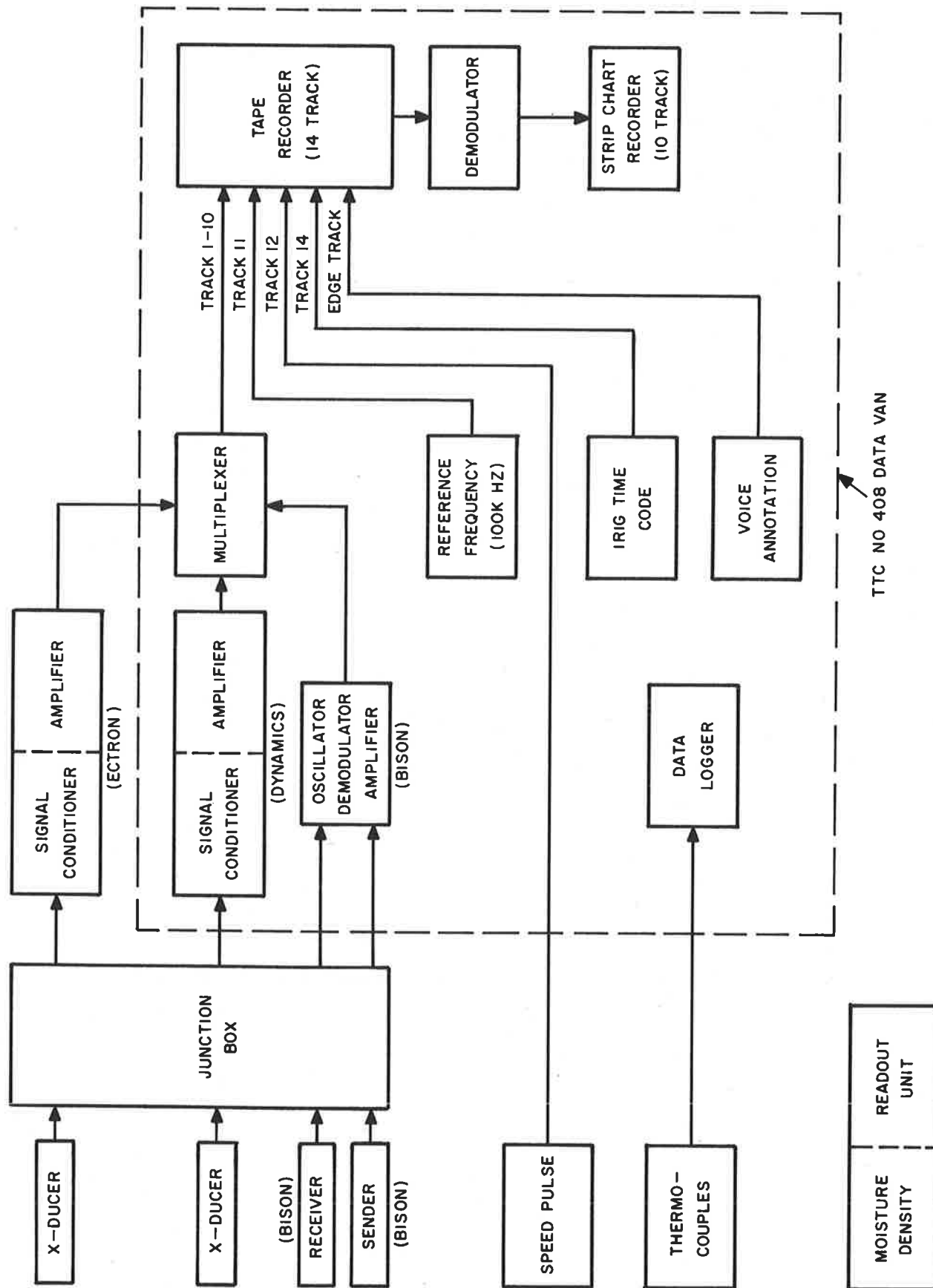
FIGURE 3.25. DATA ACQUISITION AND RECORDING SYSTEM BLOCK DIAGRAM

44

the capability of applying simultaneous loads of up to 40,000 pounds vertically and 20,000 pounds laterally to both rails. Loading is transmitted to each rail through a section removed from a "partially worn" wheel. Load cells in series with the vertical and lateral hydraulic cylinders monitor the applied load. Details of the loading apparatus are shown in Figures 3.26 and 3.27.

The TTC O&M contractor operated the calibration car and provided data acquisition, recording and plotting. For the strain gaged rail clips, plots were obtained showing output sensitivity versus vertical load to 20,000 pounds. For each L/V wheel-rail load measurement circuit, a calibration plot was obtained for the loading sequences given in Appendix C.

## 3.10 TRANSIT VEHICLE TEST OPERATIONS

Two types of transit vehicles, each type operating as married pairs, were employed to induce forces in the transit track structure. The NYCTA R-42 transit vehicles on loan to the TTC, were used in both the crush loaded and light configuration for data acquisition passes at both the curved and tangent test areas. In addition, the MBTA Blue Line transit vehicles, then undergoing testing at the TTC, were similarly employed in the crush loaded configuration only, for data acquisition passes at both test areas. Finally, the crush loaded R42 transit vehicles were again used for data acquisition passes at the tangent test area, this time to allow measurement and recording of wheel-rail loads from the fourteen L/V wheel-rail load measurement circuits installed in this area shown in Figure 3.24.

As shown in Table 3.1, a total of sixty-eight transit vehicle data passes was made between September 19 and December 10, 1979, during which data was recorded from the stations indicated. This seemingly large number of data passes was necessitated in part by the data acquisition and recording limitations of the TTC No. 408 data van and ancillary equipment. Repeated data acquisition passes at the curved and tangent test areas were required in an attempt to obtain data from transducers either excluded previously or that had produced data of doubtful quality.
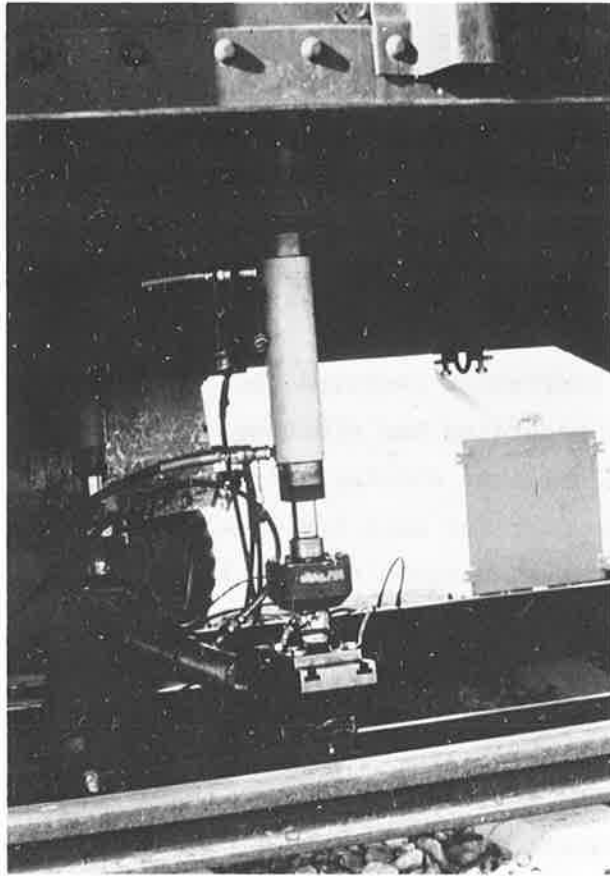
FIGURE 3.26.   VERTICAL LOADING STRUT ON TTC CALIBRATION LOADING CAR
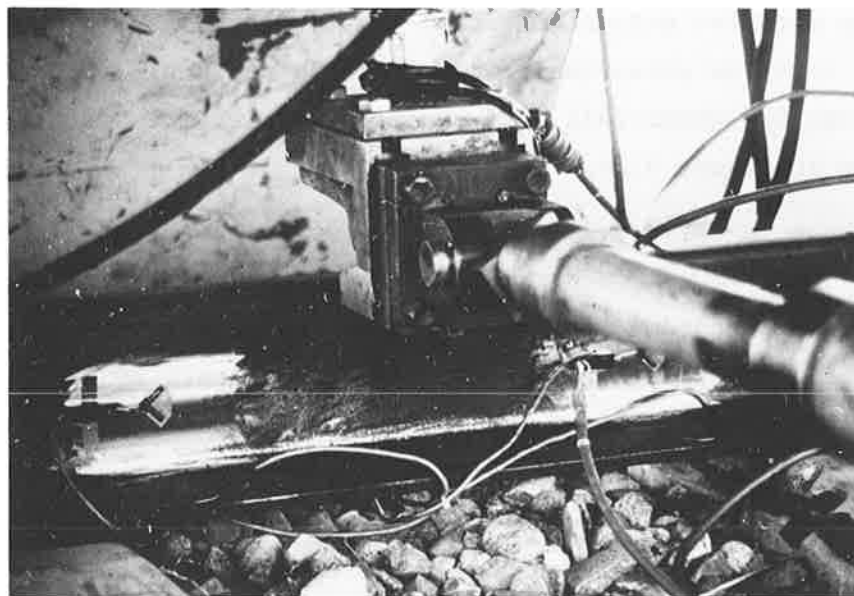


FIGURE 3.27.   LATERAL LOADING STRUT ON TTC CALIBRATION LOADING CAR

TABLE 3.1

## VEHICLE INDUCED FORCES DATA ACQUISITION PASSES

| Date | Transit Vehicles | Loading Condition | Velocity (mph) | Direction | Run Number | Event Number | Recording Station | Weight Distribution (CCW→) B | A | A | B |
|------|------|------|------|------|------|------|------|------|------|------|------|
| 9/19/79 | R42 | Crush | 30.3 | CCW | 1 | 1a | KSC-2 | | | | |
| 9/19/79 | R42 | Crush | 30.5 | CW | 2 | 2 | KSC-2 | | | | |
| 9/19/79 | R42 | Crush | 30.4 | CCW | 3 | 1b | KSC-2 | | | | |
| 9/19/79 | R42 | Crush | 35.5 | CW | 4 | 5 | KSC-2 | 52520 | 52500 | 52500 | 52500 |
| 9/19/79 | R42 | Crush | 49.9 | CCW | 5 | 4a | KSC-2 | | | | |
| 9/19/79 | R42 | Crush | 50.8 | CCW | 6 | 4b | KSC-2 | | | | |
| 9/19/79 | R42 | Crush | 30.5 | CCW | 7 | 3 | 4B | | | | |
| 9/19/79 | R42 | Crush | 49.5 | CCW | 8 | 6 | 4B | | | | |
| 9/20/79 | R42 | Light | 30.4 | CCW | 9 | 7a | KSC-2 | | | | |
| 9/20/79 | R42 | Light | 30.1 | CW | 10 | 8 | KSC-2 | | | | |
| 9/20/79 | R42 | Light | 30.6 | CCW | 11 | 7b | KSC-2 | | | | |
| 9/20/79 | R42 | Light | 40.4 | CW | 12 | 11 | KSC-2 | 43100 | 43040 | 43160 | 43020 |
| 9/20/79 | R42 | Light | 50.3 | CCW | 13 | 10a | KSC-2 | | | | |
| 9/20/79 | R42 | Light | 49.0 | CCW | 14 | 10b | KSC-2 | | | | |
| 9/20/79 | R42 | Light | 31.0 | CCW | 15 | 9 | 4B | | | | |
| 9/20/79 | R42 | Light | 50.4 | CCW | 16 | 12 | 4B | | | | |
| 9/25/79 | R42 | Crush | 30.81 | CCW | 17 | 13a | KSC-1 | | | | |
| 9/25/79 | R42 | Crush | 30.54 | CW | 18 | 14 | KSC-1 | | | | |
| 9/25/79 | R42 | Crush | 30.7 | CCW | 19 | 13b/15 | KSC-1/4A | 52500 | 52560 | 52460 | 52520 |
| 9/25/79 | R42 | Crush | 50.5 | CCW | 20 | 16a | KSC-1 | | | | |
| 9/25/79 | R42 | Crush | 39.86 | CW | 21 | 17 | KSC-1 | | | | |
| 9/25/79 | R42 | Crush | 50.2 | CCW | 22 | 16b/18 | KSC-1/4A | | | | |
| 9/26/79 | R42 | Light | 30.2 | CCW | 23 | 19a | KSC-1 | | | | |
| 9/26/79 | R42 | Light | 30.18 | CW | 24 | 20 | KSC-1 | | | | |
| 9/26/79 | R42 | Light | 30.2 | CCW | 25 | 19b/21 | KSC-1/4A | 43280 | 42140 | 43120 | 42800 |
| 9/26/79 | R42 | Light | 50.08 | CCW | 26 | 22a | KSC-1 | | | | |
| 9/26/79 | R42 | Light | 44.92 | CW | 27 | 23 | KSC-1 | | | | |
| 9/26/79 | R42 | Light | 50.2 | CCW | 28 | 22b/24 | KSC-1/4A | | | | |
| 10/01/79 | MBTA | Crush | 30.96 | CCW | 1 | 13a | KSC-1 | | | | |
| 10/01/79 | MBTA | Crush | 30.0 | CW | 2 | 14 | KSC-1 | | | | |
| 10/01/79 | MBTA | Crush | 31.43 | CCW | 3 | 13b | KSC-1 | | | | |
| 10/01/79 | MBTA | Crush | 52.27 | CCW | 4 | 16a | KSC-1 | 37500 | 37080 | 39260 | 36520 |
| 10/01/79 | MBTA | Crush | 50.0 | CW | 5 | 17 | KSC-1 | | | | |
| 10/01/79 | MBTA | Crush | 50.0 | CCW | 6 | 16b | KSC-1 | | | | |
| 10/01/79 | MBTA | Crush | 30.0 | CCW | 7 | 15 | 4A | | | | |
| 10/01/79 | MBTA | Crush | 52.36 | CCW | 8 | 18 | 4A | | | | |
| 10/03/79 | MBTA | Crush | 30.0 | CCW | 9 | 1a | KSC-2 | | | | |
| 10/03/79 | MBTA | Crush | 30.0 | CW | 10 | 2 | KSC-2 | | | | |
| 10/03/79 | MBTA | Crush | 32.03 | CCW | 11 | 1b | KSC-2 | | | | |
| 10/03/79 | MBTA | Crush | 52.72 | CCW | 12 | 4a | KSC-2 | | | | |
| 10/03/79 | MBTA | Crush | 50.0 | CW | 13 | 5 | KSC-2 | 37500 | 37080 | 39260 | 36520 |
| 10/03/79 | MBTA | Crush | 50.0 | CCW | 14 | 4b | KSC-2 | | | | |
| 10/03/79 | MBTA | Crush | 32.06 | CCW | 15 | 3 | 4B | | | | |
| 10/03/79 | MBTA | Crush | 54.21 | CCW | 16 | 6 | 4B | | | | |
| 10/03/79 | MBTA | Crush | 31.76 | CCW | 17 | 3a | KSC-2 | | | | |
| 10/03/79 | MBTA | Crush | 53.92 | CCW | 18 | 6a | KSC-2 | | | | |
| 10/04/79 | R42 | Light | 29.2 | CCW | 1 | 3 | KSC-2/4B | | | | |
| 10/04/79 | R42 | Light | 50.2 | CCW | 2 | 6 | KSC-2/4B | 43280 | 42140 | 43120 | 42800 |
| 10/04/79 | R42 | Light | 30.7 | CCW | 3 | 3a | KSC-2/4B | | | | |
| 10/04/79 | R42 | Light | 50.4 | CCW | 4 | 6a | KSC-2/4B | | | | |
| 10/05/79 | R42 | Crush | 31.79 | CCW | 5 | 9 | KSC-2/4B | | | | |
| 10/05/79 | R42 | Crush | 51.22 | CCW | 6 | 12 | KSC-2/4B | 52600 | 52500 | 52540 | 52320 |
| 10/05/79 | R42 | Crush | 33.13 | CCW | 7 | 9a | KSC-2/4B | | | | |
| 10/05/79 | R42 | Crush | 51.57 | CCW | 8 | 12a | KSC-2/4B | | | | |
| 10/10/79 | R42 | Crush | 30.2 | CCW | 1 | 15 | KSC-1/4A | | | | |
| 10/10/79 | R42 | Crush | 50.4 | CCW | 2 | 18 | KSC-1/4A | 52600 | 52500 | 52540 | 52320 |
| 10/10/79 | R42 | Crush | 29.7 | CCW | 3 | 15a | KSC-1/4A | | | | |
| 10/10/79 | R42 | Crush | 50.2 | CCW | 4 | 18a | KSC-1/4A | | | | |
| 10/11/79 | R42 | Light | 30.4 | CCW | 5 | 21 | KSC-1/4A | | | | |
| 10/11/79 | R42 | Light | 50.4 | CCW | 6 | 24 | KSC-1/4A | 43440 | 43600 | 44200 | 43300 |
| 10/11/79 | R42 | Light | 30.3 | CCW | 7 | 21a | KSC-1/4A | | | | |
| 10/11/79 | R42 | Light | 50.6 | CCW | 8 | 24a | KSC-1/4A | | | | |
| 12/10/79 | R42 | Crush | 50.96 | CCW | M1 | —— | L/V+KSC-1 | | | | |
| 12/10/79 | R42 | Crush | 51.00 | CCW | M2 | —— | L/V+KSC-1 | | | | |
| 12/10/79 | R42 | Crush | 50.51 | CCW | M3 | —— | L/V+KSC-1 | 52510 | 52480 | 52500 | 52540 |
| 12/10/79 | R42 | Crush | 30.48 | CCW | M4 | —— | L/V+KSC-1 | | | | |
| 12/10/79 | R42 | Crush | 31.33 | CCW | M5 | —— | L/V+KSC-1 | | | | |
| 12/10/79 | R42 | Crush | 31.25 | CCW | M6 | —— | L/V+KSC-1 | | | | |

The testing to obtain data from the various transducers at the curved and tangent test areas using the R-42 and MBTA transit vehicles was done in accordance with Appendix D, Data Collection Test Plan. Additional testing using the R-42 transit vehicle to obtain data on wheel-rail loads was done in accordance with procedures set forth in Appendix D.

Ballasting of the transit vehicles to the crush loaded configurations was accomplished by the addition of lead ingots. This ballast was distributed within the vehicles to equalize the weight between the four trucks. Because of data recording equipment permanently contained in the R-42 transit vehicles, some ballast was required for weight equalization in the light configuration. After each reballasting, the vehicles were weighed truckwise on the TTC scales and the weight tickets provided to KSC; these weights are indicated on the test matrix (Table 3.1). Where employed, data acquisition passes with the light configuration transit vehicles followed the crush loaded ones except for the repeated R-42 testing at the curved test area where the opposite was true.

Prior to each series of crush loaded data acquisition passes, the track structure and roadbed transducers were subjected to static cal- ibration using the transit vehicle as loading stimulus. While proceeding in a counter-clockwise direction around the TTC oval, the leading wheel- set of the leading vehicle was parked in turn over each transducer array, L/V wheel-rail load measurement circuit, and strain gaged crosstie, and the resulting changes in output sensitivity measured and recorded. This was done to assure transducer operation and instrumentation lead wire continuity and to permit any adjustments to amplifier gain required.

After completion of any static calibrations, data acquisition passes were made in the order indicated in Table 3.1. Original plans specified the two vehicle speeds to be 30 and 50 miles per hour. How- ever, the crush loaded R-42 transit vehicles proved incapable of attaining the higher speed in the clockwise direction due to the prevailing grade. In most of the testing, the transit vehicles were cycled back and forth over the appropriate test area. In order to obtain a more random dis- tribution of the wheel positions for the L/V wheel-rail load measurements, the R-42 vehicles were continued counterclockwise around the TTT oval between data passes.

Three different methods were employed at various times to measure transit vehicle speed. The primary system used returns from reflective targets spaced at known distances on the side of each vehicle to generate data pulses which were recorded on tape. When the target spacing was divided by the time interval between the data pulses, an accurate determination of the vehicle speed was obtained. Transit vehicle speeds thus obtained are given to two decimal places in Table 3.1. Operational difficulties and an unexplained absence of the speed pulses on some of the data tapes prevented use of this method for all data acquisition passes. Those velocity values in Table 3.1 given to one decimal place were obtained from the speedometer in the MBTA transit vehicles or from a radar speed indicator mounted in the R-42 transit vehicles.

Soil temperature readings were obtained at one-minute intervals from the thermocouple array at each test area during most of the data acquisition passes. Soil moisture density readings were obtained during the period of major test activity at each test area by the TTC O&M contractor.

KSC personnel obtained samples of the subgrade soil from the tangent test area for analysis to determine the physical characteristics. Three samples were obtained, each to a depth of 5 feet, from between crossties 365 +11 and +12 (Figure 3.11). Each sample was obtained by driving three 2.120-inch diameter, 24-inch steel tube segments to successively greater depths using equipment fabricated by KSC expressly for this purpose.

Samples were transported to the University of Colorado, Boulder, Colorado, where triaxial testing was performed under contract to KSC in accordance with procedures set forth in Appendix E, Soil Sample Testing Procedure. Parameters were determined to allow calculation of resilient modulus, bulk modulus, and shear modulus values for two of these samples at three depths.

3.11  TRANSDUCER PERFORMANCE

With few exceptions, all transducers and instrumented components installed at the two test areas of the TTT performed satisfactorily and provided repeatable data throughout the data acquisition effort. The

few instances of missing or anomalous data can be attributed primarily to instrumentation limitations inherent in the TTC data van and to procedural errors in part due to the severe time constraints imposed on this effort by concurrent testing of the MBTA transit vehicles on the TTT. This latter dictated that installation of the primary transducer arrays at both test areas be accomplished in a single weekend and relegated most of the remaining installations and the load calibration and data acquisition activities to weekend or extended shift time periods. The following paragraphs detail the significant performance aspects of the various transducers employed in this effort.

### 3.11.1  Sensotec Soil Pressure Gages

Besides direct implantation in the subgrade soil, these gages were also employed encapsulated between bearing plates which were located in the ballast and soil, and imbedded in crosstie bottom surfaces utilizing bearing plates which acted directly upon the ballast. In most cases, these transducers responded satisfactorily, producing repeatable signals relatively free from noise.

### 3.11.2  Soil Strain Gages

Less than satisfactory results were obtained from the Bison soil strain arrays at both test areas. It was found that insufficient Bison electronics units were available at the TTC to enable simultaneous acquisition of data from all the coils at either test area. This necessitated multiple data acquisition passes and substitution of the Bison electronics units. The limited ballast strain data did appear consistent as is discussed in Section 4.4; however, future measurements should include an even closer scrutiny of the effects on the Bison coils of the vehicle presence.

### 3.11.3  Soil Extensometers

The Carlson joint meters employed in the extensometers are designed for continuous voltage of 0.5V and momentary peak voltage of 3.0V. At the curved test area, 10.0V excitation was inadvertently applied, which destroyed the transducer. The tangent area extensometer appeared to function satisfactorily, and the resulting deflections are discussed in Section 4.4.

50

### 3.11.4  Instrumented Rail Clips, Crossties

Strain gages installed on the rail clips and concrete crossties in nearly all cases produced good signals with low accompanying noise in spite of the low levels of strain involved.  Because of non-linearities introduced by shifting of the load application point during loading and also by the varying strain field in the location of the strain gages, this type of rail fastener is not ideally suited to application as a load transducer.  The measured strains were used, however, to compute stress levels as is discussed in Section 4.5.

### 3.11.5  L/V Wheel-Rail Load Circuits

No problems were experienced with the web and base chevron rail strain gage circuits.  Interpretation of the lateral load magnitudes was laborious but possible because of the extensive lateral load calibrations previously performed at various levels of accompanying vertical load.

### 3.12  TRANSDUCER IMPROVEMENTS

As previously discussed, transducer selection for this effort was influenced significantly by funding and schedule constraints and by a desire to duplicate existing instrumentation previously installed in the TTT.  Although most transducer types performed adequately during this experiment, it is appropriate to consider alternatives which could enhance the results in future activities of this type.

Perhaps the greatest potential for improvement exists in refining the functions performed by the Bison soil strain gages and the Carlson soil extensometers.  In both instances, devices utilizing linear variable differential transformers (LVDT's) would have provided better dynamic response, had extremely linear output characteristics, and, as opposed to the Bison transducers, been unaffected by the presence or absence of the transit vehicle metallic structure.  Direct current LVDT's are available which are compatible with commonly used power supply and signal conditioning equipment.

A second area for transducer improvement is for measurement of pressure in the ballast and at the tie-ballast interface. In both cases, the bearing surface area should be as large as possible to average out the effects of ballast irregularities. Two parallel circular plates separated by three load measuring devices (load washers or strain gaged links) located near the periphery and spaced 120 degrees apart could be designed and fabricated. A design requirement should be to match the compliance to that of the surrounding medium (ballast or crosstie) to minimize the effects of the transducer on the measurement accuracy.

A need exists to measure the rail-to-crosstie load transfer accurately in order to determine, in conjunction with measured wheel-rail loads, the load distribution between the adjacent crossties and therefore allow assessment of overall track structure performance. Although some rail fastener configurations may be amenable to instrumentation and calibration for this purpose, it is believed that development of load measurement devices which would replace and duplicate the significant characteristics of the various rail fastener systems would offer better potential for success.

# 4. TEST RESULTS: EVALUATION AND COMPARISON WITH ANALYSIS

Section 3 of this report describes an extensive vehicle induced force experiment that was conducted on the UMTA transit test track (TTT) at TTC with NYCTA R-42 and MBTA Blue Line transit vehicles. A series of six vehicle configurations were tested at both a tangent and a curve (3820 foot radius) site. This test matrix consisted of crush and light loaded R-42 vehicles at 30 mph and 50 mph and crush loaded MBTA vehicles at both speeds as shown in Table 3.1. At each test site (tangent and curve) there were instruments available to measure ballast, subballast and subgrade pressures, ballast and subballast strain, subgrade deflection, vertical and lateral wheel loads, tie bending moments, fastener strains and rail and tie deflections. Some of this instrumentation was installed during the construction of the test facility (1972) but most of the recording instruments were inplaced about eight weeks before these current tests were conducted.

Test data similar to that obtained from this study were not available for transit track roadbeds. In 1979, a brief report was published by Yoo and Selig (Reference 4.1) concerning similar measurements at the TTC-FAST facility for conventional railroad track and vehicles. The instruments and techniques used in that study appear to be similar to those used in this study, except that this study includes pressure sensors inside the actual subgrade to a depth of thirty-six inches below the top of the subgrade. This study is therefore unique from the standpoint that internal subgrade pressures have been measured. The proper understanding of the loads and the response to these loads by the roadbed material is necessary in order to evaluate the design techniques for and the overall integrity of a transit roadbed system.

The new instrumentation (sixteen pressure gages and four soil strain gages) was installed beneath three adjacent ties at each site according to the description given in Section 3, Figures 3.12-3.14. It was assumed that the wheel loading and the roadbed geometry were sufficiently similar over a five foot length of track, and therefore the load

53

distribution could be considered representative of any one of the ties being studied. The instruments were so distributed in order to reduce the effects of the instruments' material and geometric presence on the response of the ballast and subgrade under any one tie.

4.1 WHEEL TO RAIL LOADS

The determination of the load dissipation capability of a transit roadbed is governed by the magnitude of the load that is transmitted by the transit vehicle to the track system. This study was limited to direct rolling wheel loads (vertical and lateral), but longitudinal braking and tractive forces were not measured or considered in the analysis. The longitudinal forces (braking and tractive) are of major importance to rail selection and rail life but do not radically influence the load field in the roadbed material, unless there is a significant amount of heeling by the vehicle during braking or acceleration, and this is unlikely for steel wheeled transit vehicles.

At both the curve and the tangent test sites the vertical and lateral wheel to rail loads were measured on both the inner and outer rail at both the old and new instrumentation locations 4A, 4B, KSC-1 and KSC-2 (see Figures 3.10 and 3.11). In addition, there were twelve vertical and lateral wheel to rail load measurements on the outer rail taken in a symmetric pattern at the tangent site (see Figure 3.24). The pattern for these measurements was established for two reasons. First, the R-42 test vehicle has a 34 inch wheel diameter or a 106 inch wheel circumference, and each measurement zone (as described in Section 3) covers a ten to eleven inch section of rail. The twelve stations plus the pattern of installation allows for the measurement of the load as transmitted from each portion of the wheel circumference to the rail during one pass of the vehicle. Secondly the eighty-five foot test section is centered away from the KSC-1 instrumentation station to allow track geometry perturbution tests to be performed at some future date without disturbing the recently embedded soil instrumentation.

A crush loaded R-42 vehicle was passed through this test site at either 30 or 50 mph in a counter clockwise direction. The R-42 vehicle made at least three passes at each velocity through the tangent site for the specific purpose of wheel to rail measurements, (refer to the test matrix in Table 3.1). The R-42 vehicle was dispatched completely around the oval between each wheel to rail load test pass, assuring that a different portion of each wheel passed through a test station in different test runs. This feature introduced a randomness to the test data and eliminated spurious results due to the failure of a single measurement station, or the presence of an unknown local track perturbation. This test will give an indication of the dynamic load factor for a wheel in an <u>unperturbed</u> <u>tangent</u> track section. However it is possible for the <u>wheel</u> to have geometric imperfections (wheel flats). Upon examination of the wheels, flat spots were found and measured on some of the R-42 wheels. The largest measured flat was a chord length of 1.5 inch resulting in a decrease in wheel radius of 0.01655 inch. These wheel flats should appear as load spikes in the measured data, to be discernible from the vertical overload due to the movement of the wheel along an "elastic" rail.

The test matrix in Table 3.1 shows that the crush wheel load was 13125 lbs for each wheel (within 0.04%) during the wheel to rail load tests. Overall the average wheel loads for each vehicle configuration are: R-42 crush 13125 lbs, R-42 light 10700 lbs, and MBTA crush 9400 lbs, these values were obtained within one percent for the R-42 vehicle and three percent for the MBTA vehicle. Table 4.1 presents the known geometry of these two test vehicles. It should be noted that both the R-42 and MBTA test vehicles were two car units. This provided eight wheel information points along each rail during each vehicle pass. In addition the two car unit is more indicative of a train response because the effect of the relative location of adjacent trucks between the two coupled cars is included in the measurements.

Figures 4.1 and 4.2 depict typical calibration curves and load versus time plots for both the vertical and lateral wheel to rail loads. The calibration curves were obtained by using the TTC loading hopper

TABLE 4.1

Vehicle Configurations

|  | NYCTA R42 Car | MBTA |
|---|---|---|
| Length over Couplers | 60'-6" | 69'-9 3/4" |
| Length over anti-climber | 60'-2 1/2" | − |
| Width of car body | 10'-0" | NA |
| Truck centers | 44'-7" | 51'-0" |
| Wheel base | 6'-10" | 6'-10" |
| Wheel diameter | 34" | 28" |
| Static wheel load  crush | 13125 lbs | 9400 lbs |
| light | 10700 lbs | − |
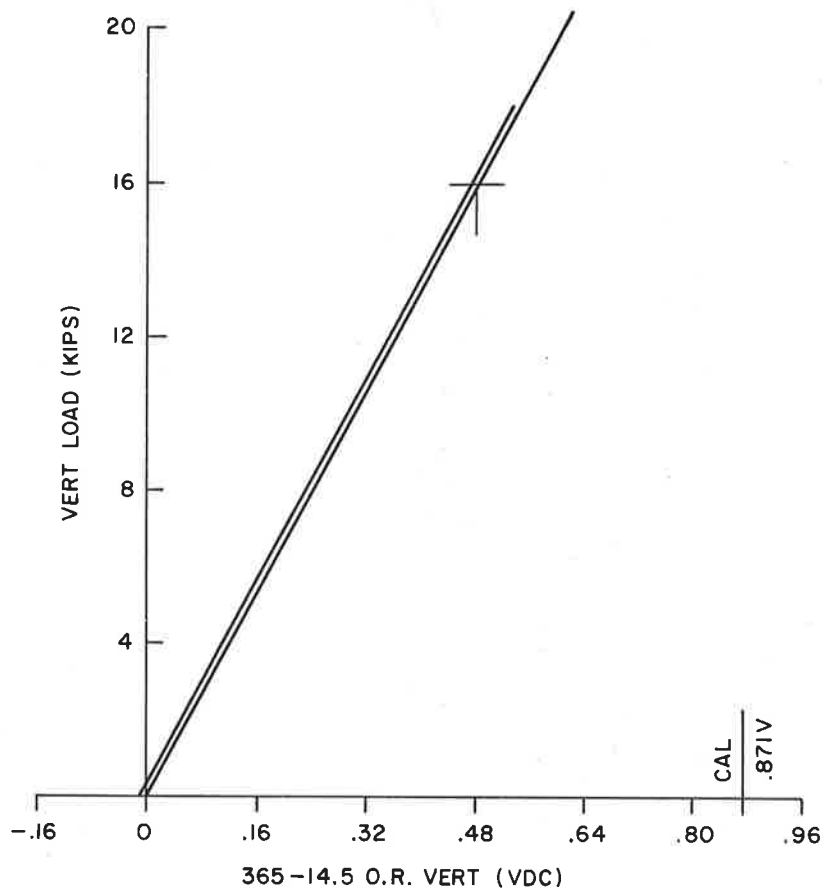
(a) Calibration Curve - Vertical Load Versus Output Voltage
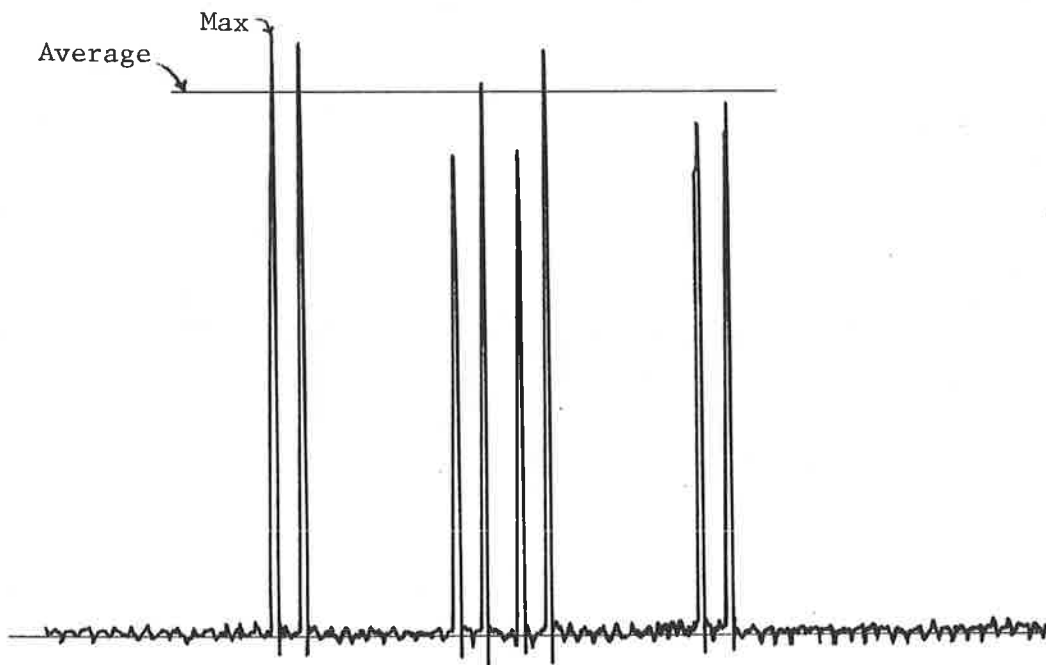


(b) Vertical Load Versus Time for Crush Loaded R-42 Vehicle Pass.

FIGURE 4.1. TYPICAL WHEEL TO RAIL VERTICAL LOADS CALIBRATION AND
LOAD-TIME HISTORY

57
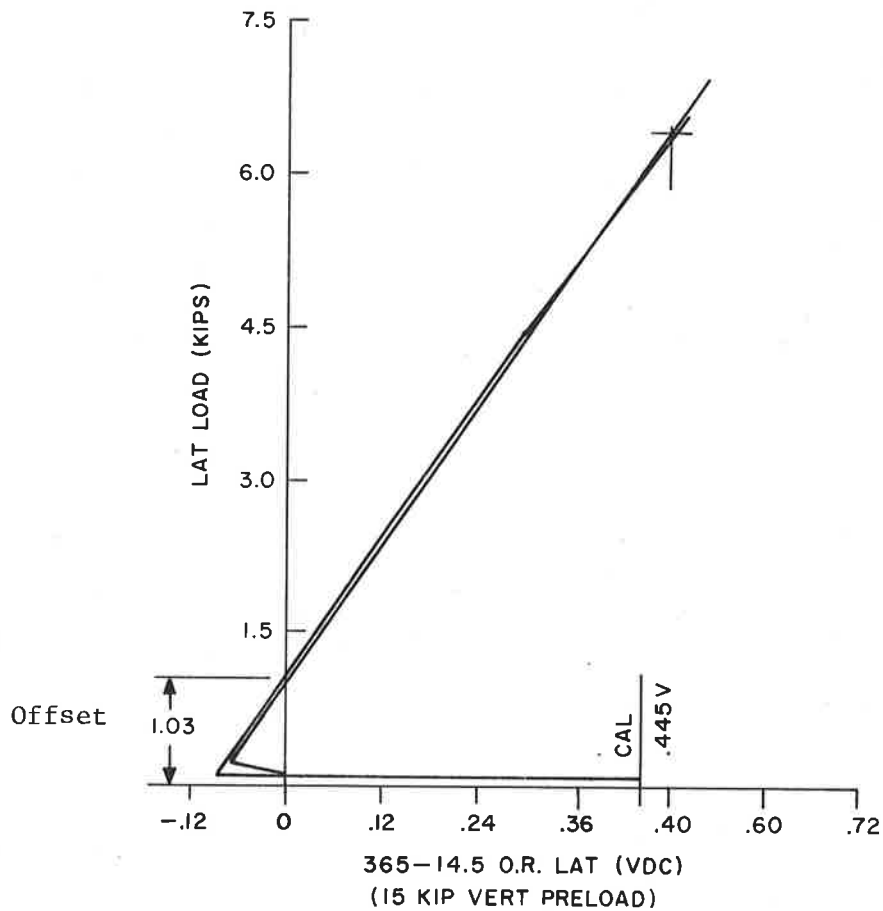
(a)   Calibration Curve - Lateral Load Versus Output Voltage
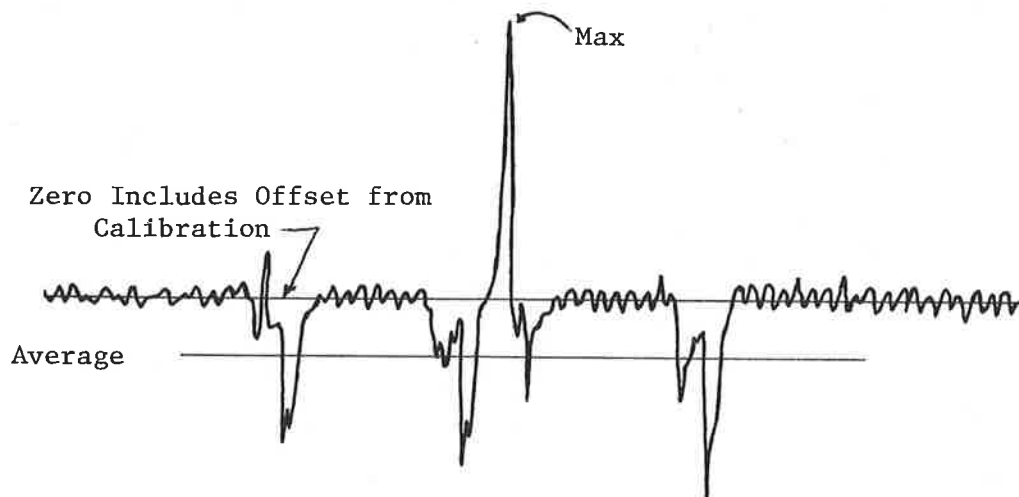


(b)   Lateral Load Versus Time for Crush Loaded R-42 Vehicle Pass.

FIGURE 4.2.   TYPICAL WHEEL TO RAIL LATERAL LOADS CALIBRATION AND
LOAD-TIME HISTORY

as described in Section 3.  The vertical load calibration (Figure 4.1a) is very linear and passes through zero; however, the lateral calibration (Figure 4.2a) has a 15 kip vertical preload and is linear but has a 1.03 kip load intercept.  These calibration curves are typical of all the hopper car calibrations obtained during this program.

Figures 4.1b and 4.2b show the typical timewise load response curve for a 50 mph CCW crush loaded R-42 vehicle pass.  It is noticed that the eight wheels are all easily distinguished.  There is no apparent over-lapping effect from one wheel to the next for the vertical load but there is for the lateral load.  In both the vertical and lateral load plots the maximum load and the average load is indicated in kips.  The vertical load plot (Figure 4.1b) has an average load slightly higher than the static wheel load, but the maximum load is about 15% higher, (both typical of all the wheel to rail vertical load measurements).  The maximum load spikes are due to both vehicle dynamics and wheel flats. The following analysis of wheel to rail loads uses only the maximum value from each vehicle pass at each station.  This then gives an indication of the maximum expected load that a tangent track roadbed will receive from a heavy transit vehicle.  The lateral load plot (Figure 4.2b) shows spikes that are positive and negative compared to the instrumentation zero.  However from Figure 4.2a it is noted that a lateral load of 1.03 kips is experienced due to the vertical preload. Figure 4.2b is typical of most of the lateral load measurements from either rail of the tangent or the outside rail of the curve site.  It appears that the transition from the first to the second car across the coupler of the R-42 vehicle creates a lateral movement of the second car and an ensuing large lateral load.  It is also possible that the outside wheel on the second car is out of true and causes a larger than expected lateral load.  There was no post-test vehicle inspection to confirm the reason why the large positive lateral load spikes exist.  A discussion of load differential between tangent and curve track will be given later in this subsection.

Table 4.2 presents a summary of the statistical analysis of the data gathered from the twelve vertical and lateral wheel to rail loads stations. A crush loaded R-42 vehicle was used with a 13.125 kip static wheel load making three passes at each velocity, and the train was positioned so a different portion of any wheel would be recorded at each measurement station for each vehicle pass. Only the maximum value of any one of the eight wheel loads at each station is used in the analysis presented in Table 4.2 (see examples in Figures 4.1b and 4.2b). The first point to be noted is the insignificant difference between the loads recorded at 30 mph and those recorded at 50 mph. Typical design standards apply a wheel dynamic factor that is linearly dependent upon the vehicle velocity, as depicted in Section 5.1. The average maximum loads are only twelve percent greater than the static wheel load and the 18 kip five percent exceedance vertical load is only thirty-seven percent greater than the static wheel load. However there are no track pertubations, and continuous welded rail is used in the track system so that no jointed rail sections are present. AAR guidelines presented in Section 5.1.5.5 of this report show design dynamic loads are from 30 to 48 percent greater than the static wheel load, while other design guides use a factor of two over the static wheel load for all dynamic design considerations. This experiment does not prove nor disprove any of these empirical design standards because typical track perturbations were not present.

Additional wheel to rail load data were gathered during the roadbed tests at the inner and outer rail of stations KSC-1, KSC-2, 4A and 4B. These data were obtained from crush and light loaded R-42 vehicles and the crush loaded MBTA vehicle at both thirty and fifty miles per hour.

A comparison of vertical and lateral wheel to rail loads that were measured at the roadbed instrumentation sites at the curve and tangent location for all test configurations of the R-42 and MBTA vehicles is made in Table 4.3. As was demonstrated from the extensive wheel to rail load study in Table 4.2, there is negligible difference between the loads recorded at 30 mph and 50 mph at each vehicle and track configuration, and Table 4.3 combines the data from both velocities. This may seem

TABLE 4.2

Statistical Summary of Maximum Wheel to Rail Loads Taken at Tangent Site
for Crush Loaded R-42 Vehicles

(Load measured in KIPS)

Vertical

30 mph

|  | |
|---|---|
| average | 14.71 |
| $\sigma$ | 1.30 |

50 mph

|  | |
|---|---|
| average | 14.67 |
| $\sigma$ | 1.88 |

Lateral

30 mph

|  | |
|---|---|
| average | 2.10 |
| $\sigma$ | 0.75 |

50 mph

|  | |
|---|---|
| average | 2.14 |
| $\sigma$ | 0.74 |

At the 95% confidence level only 5% of load greater than:

|  | |
|---|---|
| vertical | 18.0 |
| lateral | 4.0 |

TABLE 4.3

Comparison of Wheel to Rail Loads
Based on Vehicle and Track Configuration

|  |  | (Load Measured in KIPS) | | |
|  |  | R-42 Crush | R-42 Light | MBTA Crush |
|---|---|---|---|---|
| Tangent | Static Wheel Load | 13.1 | 10.7 | 9.4 |
| Vertical | Max | 19.8 | 21.6 | 13.3 |
|  | Avg | 15.3 | 12.8 | 10.8 |
| Lateral | Max | 2.2 | 3.2 | 1.1 |
|  | Avg | 0.5 | 0.0 | 0.2 |
| Curve |  |  |  |  |
| Vertical | Max | 21.4 | 15.6 | 14.0 |
|  | Avg | 15.2 | 11.9 | 10.9 |
| Lateral | Max | 5.4 | 4.1 | 3.0 |
|  | Avg | 1.9 | 2.1 | 1.7 |

Notes: 1. Neglible difference between 30 and 50 mph vehicle velocities, therefore this table includes averaged data from both velocities.

2. The vertical and lateral maximum loads are the single highest measured load at each site.

illogical at the curve site, but a comparison of average lateral loads
for the R-42 crush vehicle shows 1.88 kips at 30 mph and 1.89 kips at
50 mph, a difference that is well within measurement inaccuracies.  It
should be noted once again that the curve on the TTT has a 3820 foot
radius (1.5 degree curve) which is very gentle and therefore little
difference is expected (and measured) between 30 or 50 mph and inner or
outer rail load measurements.  The measurements presented in Table 4.3
are consistent with those shown in Table 4.2, given that there is at
least a ten percent measurement error in Table 4.3 due to the constraint
of two measurement stations for Table 4.3 compared to twelve measurement
stations for Table 4.2.

The maximum values reported in Table 4.3 are the single absolute
measured maximum at that site, and are largely due to wheel imperfections.
The MBTA vehicle did not show as many wheel imperfections as did the R-42
vehicle and for that reason the MBTA maximum loads are comparatively
small.  In Table 4.3, all the vertical average loads for each vehicle
and track configuration are within 12 to 19 percent greater than the
corresponding static wheel load.  There were no measured track perturbations
on the TTT (wheel flats did exist); however, a single vertical load
maximum for the R-42 light vehicle was twice as great as the static
value.

It is appropriate to comment from Tables 4.2 and 4.3 that there
appears to be a consistency among the load measurements for all the
vehicle and track configurations.  However, it is also apparent that no
justification for changing the dynamic multiplicative wheel load factor
of two (based on static load) for design purposes can be made based on
the limited data presented.  Indeed a multiplicative factor of two seems
to incorporate the wide span of measured load maximums as shown in
Table 4.3.  A question should be raised as to whether the absolute
maximum measured wheel to rail load should be used for design purposes
or, rather, should the 5% load exceedance value be used as described in
Table 4.2.  The 5% load exceedance level is that load value which is
expected to be exceeded only 5% of the time with a confidence of 95%.

This value gives a more realistic design load based on an expected load influence level acting on the track roadbed. However even this vertical load exceedance value (18 kips for the R-42 crush vehicle configuration) is forty percent greater than the static wheel load without track perturbation. Therefore the use of a multiplicative factor of two on the static wheel load for track design purposes can not be refuted from this study.

## 4.2 CONCRETE TIE BENDING MOMENTS

At each test site (tangent and curve) a series of thirteen ties was instrumented for bending moment measurements. The instrumentation is described in detail in Section 3.6, but briefly consisted of three 3-inch strain gages (temperature compensated), one mounted under each rail seat and one mounted at the tie center. At the rail seat the gage was mounted approximately 1.5 inches above the bottom of the tie along the side face. This location was the best measurement site of rail seat bending strain, allowing for gage isolation from the stress singularities (concentrations) at the actual rail seat and at the tie bottom resting on the ballast. At the tie center the gage was mounted on the upper surface which is completely isolated from stress concentrations.

Prior to the installation of gages at the test sites, four concrete ties (Gerwick RT-7 Mark 38) were laboratory tested (see Section 3.5.1 and Appendix B). Two of these ties were modified for pressure gage insertion (Section 3.6.1), and the laboratory bending tests were conducted to examine the change in bending stiffness of the instrumented ties, ties T+9 and C-14 (see Figures 3-10 and 3-11). All four ties are identical to those in place along the TTT in the tangent and curve test areas, and their properties are given in Table 4.4 along with the standard deviation recorded for strains measured at either the rail seat or the tie center due to a 70000 in.-lb applied moment. It is noted in Table 4.4 that there is little variation in the tie response due to the instrumentation that has been inserted. There is as much variation between the instrumented ties and the uninstrumented ties as there is between the two uninstrumented ties, a fact inherent in the nature of the tie construction.

64

TABLE 4.4

Concrete Tie Properties

Tie:              Gerwick RT-7 Mark 38
Length:           108 in.
Base Width:       11 in.
Cross Section:    Variable, see Figure B.1
Density:          145 pounds per cubic foot
E:                4600000 psi (Reference 5.2)
I:                Center:      202 $in^4$
                  Rail Seat:   339 $in^4$

For the four tested ties:

Standard Deviation in center strain for 70000 in-lb moment:  9 percent
Standard Deviation in rail seat strain for 70000 in-lb moment:  14 percent

### 4.2.1  Experimental Tie Bending Moment Measurements

Table 4.5 shows the experimental bending moments measured along several typical ties at either the curve or tangent sites. Four tie "types" are designated: normal refers to a tie near the old instrumentation sites (either 4A or 4B) that has a normal moment variation as shown in Section 5.1; "centerbound" is a tie between the old and new instrumentation locations that appears to be centerbound as defined in Section 5.1; a disturbed tie is one that is located next to the new instrumentation site but was not physically moved during soil instrument installation; a modified tie is either tie T+9 or C-14 that was physically modified for pressure gage insertion as described in Section 3.6. Figure 4.3 shows typical strain gage readings taken during the experimental runs. Figure 4.3a is the inner rail seat of tie T-4 located over 4A, and Figure 4.3b is the inner rail seat of tie T+9 located over KSC-1 (tie T+9 was modified for soil pressure gage insertion). The first conclusion that is drawn from both Table 4.5 and Figures 4.3a and b is the similiarity in bending moment response among all the ties measured. Table 4.6 shows the maximum bending moments that are allowed for either transit ties (Reference 4.3) or railroad ties (Reference 5.1). The second conclusion that can be drawn from these experimental data is that all of the experimentally measured tie bending moments are well below the allowables.

The maximum bending moments cited in Table 4.5 are for R-42 crush loaded vehicles at either 30 or 50 mph. These maximums or "spikes" as shown in Figure 4.3 are caused by perturbations in the vehicle wheels or wheel flats. These wheel flats were identified in Section 4.1 and have a large influence upon the observed track system response.

Table 4.7 gives a summary of experimental tie bending moment maximums as influenced by the type of vehicle and the track location (tangent or curve). Note that the maximum values shown in Table 4.7 for the crush loaded R-42 vehicle correspond to the cited maximums in Table 4.5 in which tie types within the tangent or the curve sites are examined.

66

# TABLE 4.5

## Typical[*] Tie Bending Moments
## (in–KIPS)

| Tie Type | Tie Outer Rail Seat | | Center | | Tie Inner Rail Seat | | |
|---|---|---|---|---|---|---|---|
| | Avg | Max | Avg | Max | Avg | Max | |
| Normal | 25 | 63 | 20 | 50 | 30 | 72 | |
| "Centerbound" | 15 | 50 | 50 | 60 | 20 | 50 | Tangent |
| Disturbed | 12 | 70 | 50 | 50 | 20 | 70 | |
| Modified | 20 | 55 | 17 | 40 | 18 | 60 | |
| Normal | 31 | 35 | 7 | 16 | 33 | 36 | Curve |
| Modified | 7 | 10 | 11 | 12 | 16 | 17 | |

[*]For R–42 crush loaded vehicles at either 30 or 50 mph.

Average    24.2 $\mu\epsilon$ *    Max    41.4 $\mu\epsilon$
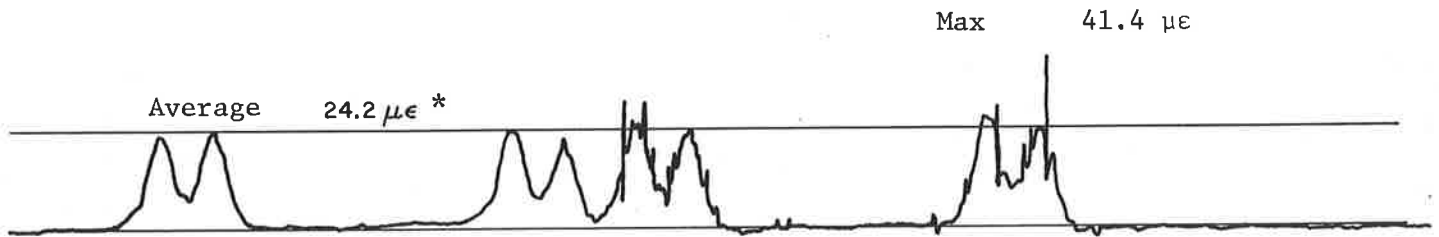
(a)   Tie T-4 Located Above Instrumentation Site TTC-4A



Average    19.1 $\mu\epsilon$    Max    54.2 $\mu\epsilon$
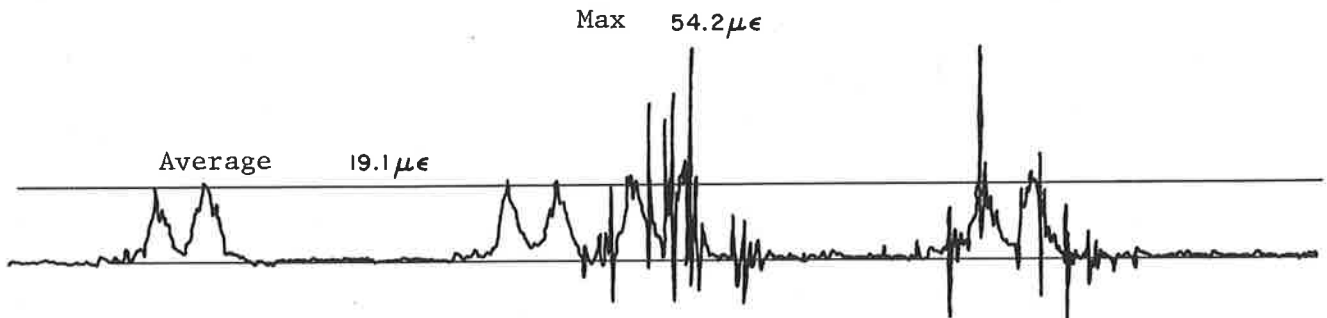
(b)   Modified Tie T+9 Located Above Instrumentation Site KSC-1.

*Output in micro in/in strain gage reading.

FIGURE 4.3.   TYPICAL INNER RAIL SEAT BENDING MOMENTS ALONG THE TANGENT

TABLE 4.6

Tie Flexural Strength Requirements

Monoblock Tie                                    (in-kips)

| Rail Seat Positive Moment | Transit[1] | Railroad[2] |
|---|---|---|
| Static | 154 | - |
| Dynamic | 114 | 350 |

Tie Center Negative Moment

| | | |
|---|---|---|
| Static | 131 | - |
| Dynamic | 102 | 200 |

(1)   See Reference 4.3

(2)   See Reference 5.1

TABLE 4.7

Tie Bending Moments versus Vehicle Configurations

| Tie Location | R-42 Crush | | R-42 Light | | MBTA (in-kips) | |
|---|---|---|---|---|---|---|
| | Avg | Max | Avg | Max | Avg | Max |
| Rail Seat – Tangent | 35.6 | 72.0 | 26.5 | 44.6 | 16.6 | 26.7 |
| Center – Tangent | 16.2 | 60.0 | 10.5 | 13.7 | 7.1 | 15.3 |
| Rail Seat – Curve | 25.8 | 47.0 | 23.4 | 45.0 | 13.9 | 27.4 |
| Center – Curve | 13.0 | 24.0 | 11.9 | 19.6 | 11.8 | 23.4 |

Note:  Only the maximum values from each vehicle run are used in this table.

There is a fairly consistent trend in Table 4.7; the vehicles with the greatest wheel loads induced the greatest bending moments, either on the average or considering the absolute maximum bending moments recorded. It is once again noted that all the maximum recorded values are well within the allowables cited in Table 4.6. There is little variation between bending moments recorded at the tangent and at the curve sites for the same vehicle that can't be explained by the closer tie spacing at the curve site. In addition it is obvious that, from a tie bending standpoint, the track is overdesigned for the MBTA vehicles, and excepting further track perturbation studies, appears to be overdesigned for the R-42 vehicle. It should be noted that overdesigned as used here is based on the stress criteria only.

4.2.2 Analytical Correlation with Tie Bending Moment Data

The analytical methods discussed in Section 5 for load response predictions of transit roadbeds include techniques for predicting the tie bending moments. The designer's analytical formulas given in Figure 5.2 are supplemented by the predictive capabilities of the numerical computer codes ILLITRACK and MULTA (see Section 5.2). Tables 5.1a and 5.2 give the general tie geometry used for the ILLITRACK and MULTA models respectively. For the crush loaded R-42 vehicle the following shows the analytical prediction for tie bending moments:

| Method | | Rail Seat (in-kips) | Tie Center |
|---|---|---|---|
| Figure 5.2 | | 58 | 15 |
| ILLITRACK | (with new | 53 | 12 |
| MULTA | soil models) | 54 | 8.5 |

These analytical predictions compare favorably with the experimental results given in Tables 4.5 and 4.7. The close agreement of the three analytical methods is due to the fact that a tie bending moment response is generally elastic and linear, and most of these numerical techniques are well formulated for this response range.

4.3 BALLAST/SUBGRADE PRESSURES

The previous two subsections have defined the load that is being transmitted to the transit test roadbed and the response of the transit concrete tie. As described in Section 5.1 once the rail has been

selected and the tie chosen, the next major stress design criteria is to satisfy stress distribution guidelines for the ballast and subballast. The only two stress criteria that are used for design of the ballast and subballast are the following AREA suggestions:

a)   Pressure at tie-ballast interface shall not exceed 65 psi

b)   Pressure at top of subgrade shall not exceed 20 psi

It is expected that if these two stress criteria are met, and if rail stress and deflection and tie bending moment are all within the design guidelines, then a reasonable transit roadbed has been designed.  This subsection will examine the pressure distribution measured in the ballast and subgrade of the tangent and curve sites.

Figure 2.2 is a composite drawing depicting the total distribution of soil pressure measurement equipment at both the tangent and curve sites.  These instruments are actually distributed beneath three adjacent ties, including the ties modified for tie-ballast pressure transfer measurements (T+9 and C-14).  Composite drawings will be used in this subsection to indicate the pressure distribution in the roadbed for the various vehicle configurations tested.

As shown in Table 3.1 several passes were made with each vehicle at each velocity and weight configuration.  The data presented here are taken from a representative data pass at each vehicle velocity and configuration.  A preliminary study of duplicate runs showed virtually no difference in wheel load, tie response or roadbed response.  It should be pointed out that the test vehicle was backed up through the test section between similar runs so that the same portion of each vehicle wheel would pass over the instrumented sections during each run. This is different from the wheel to rail load study in which an effort was made to change the wheel rolling pattern between each vehicle passage.

4.3.1  Experimental Pressure Measurements

Figures 4.4 and 4.5 show a composite view of the maximum and average pressures experienced in the roadbed for the R-42 crush loaded vehicle at both 30 and 50 mph at the tangent and curve sites respectively.  The crush
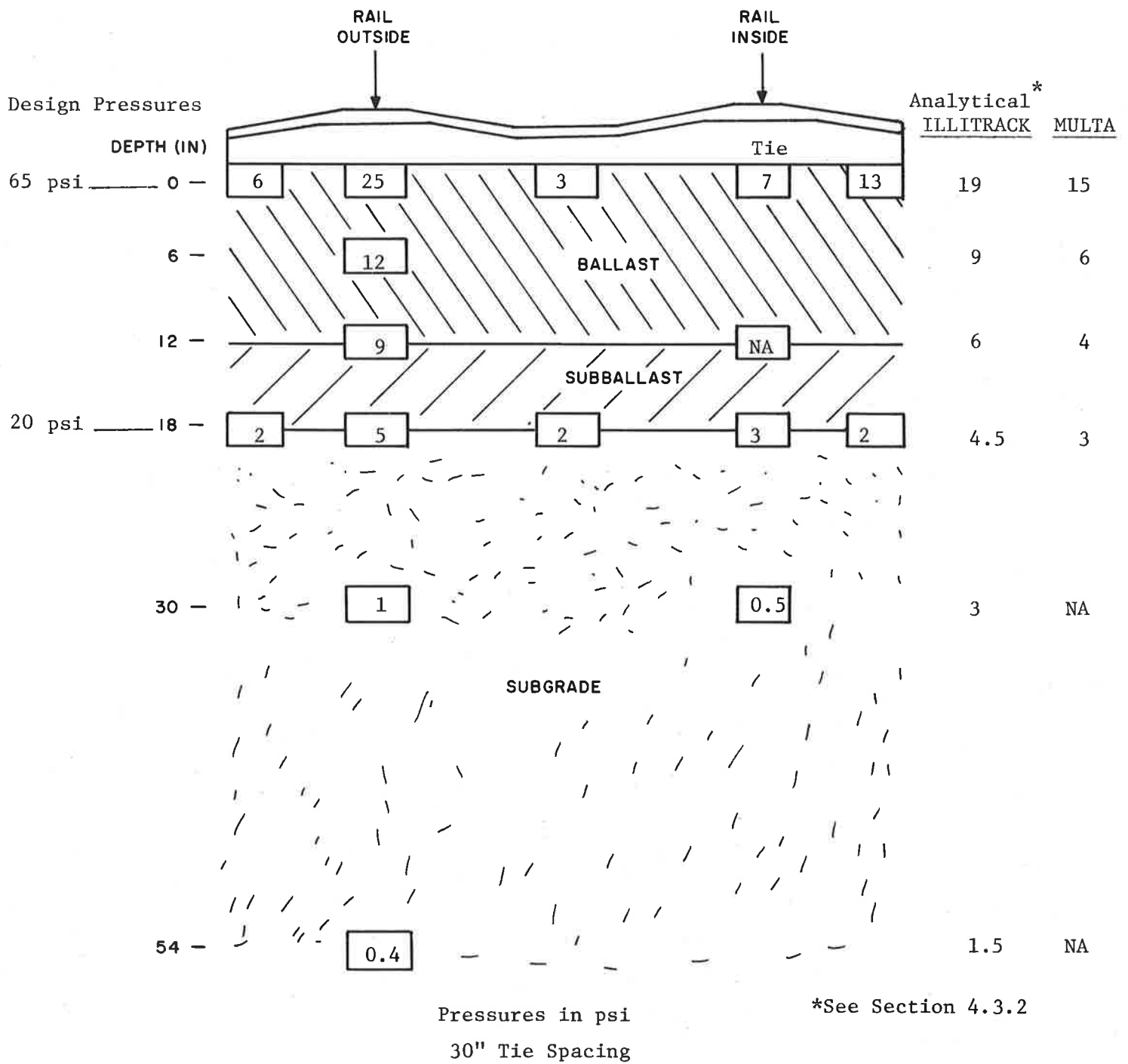
FIGURE 4.4a.  TYPICAL MAXIMUM PRESSURE DISTRIBUTION AT TANGENT
FOR CRUSH LOADED R-42 VEHICLE

Pressure in psi

30" Tie Spacing
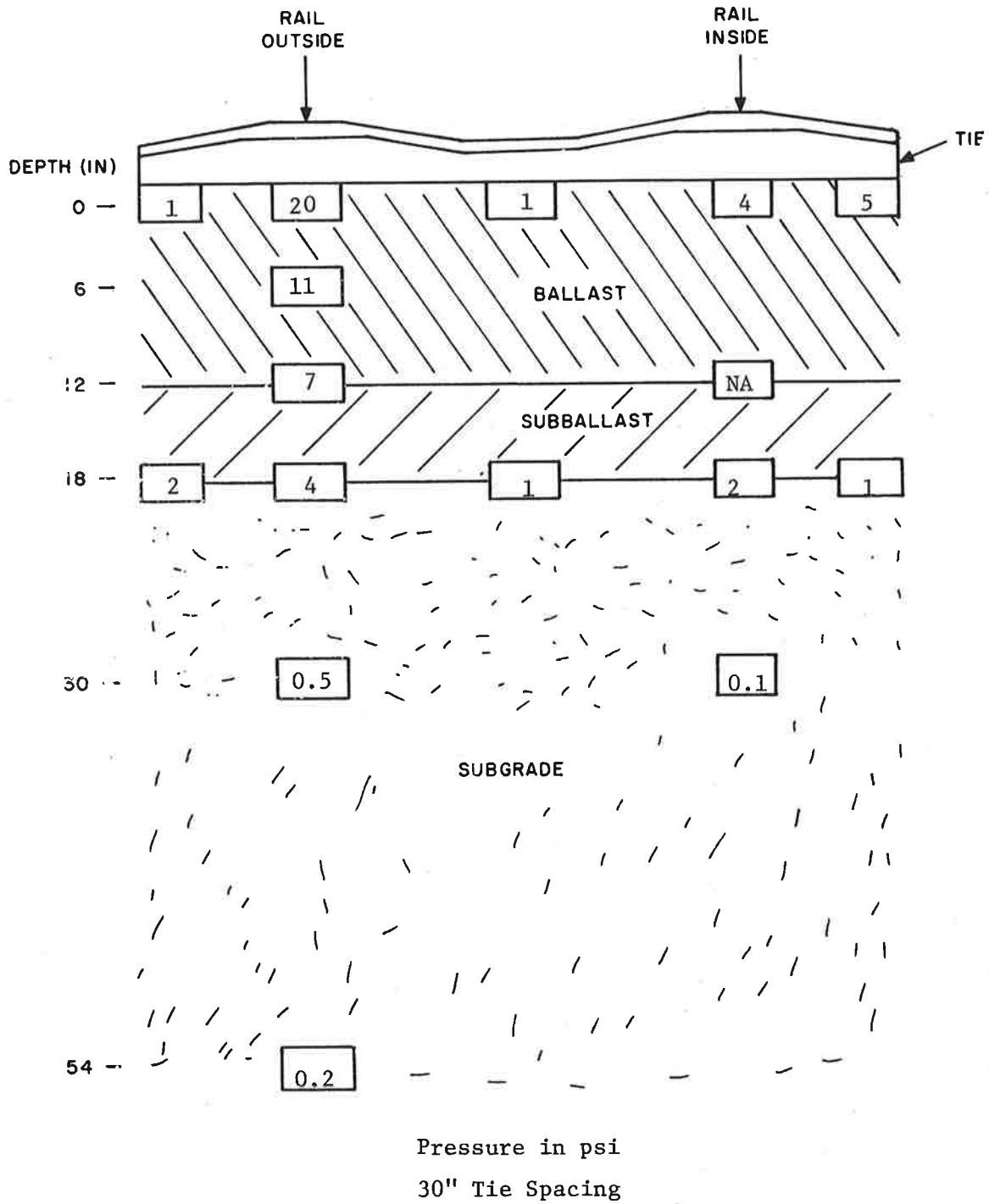
FIGURE 4.4b.   TYPICAL AVERAGE PRESSURE DISTRIBUTION AT TANGENT
FOR CRUSH LOADED R-42 VEHICLE
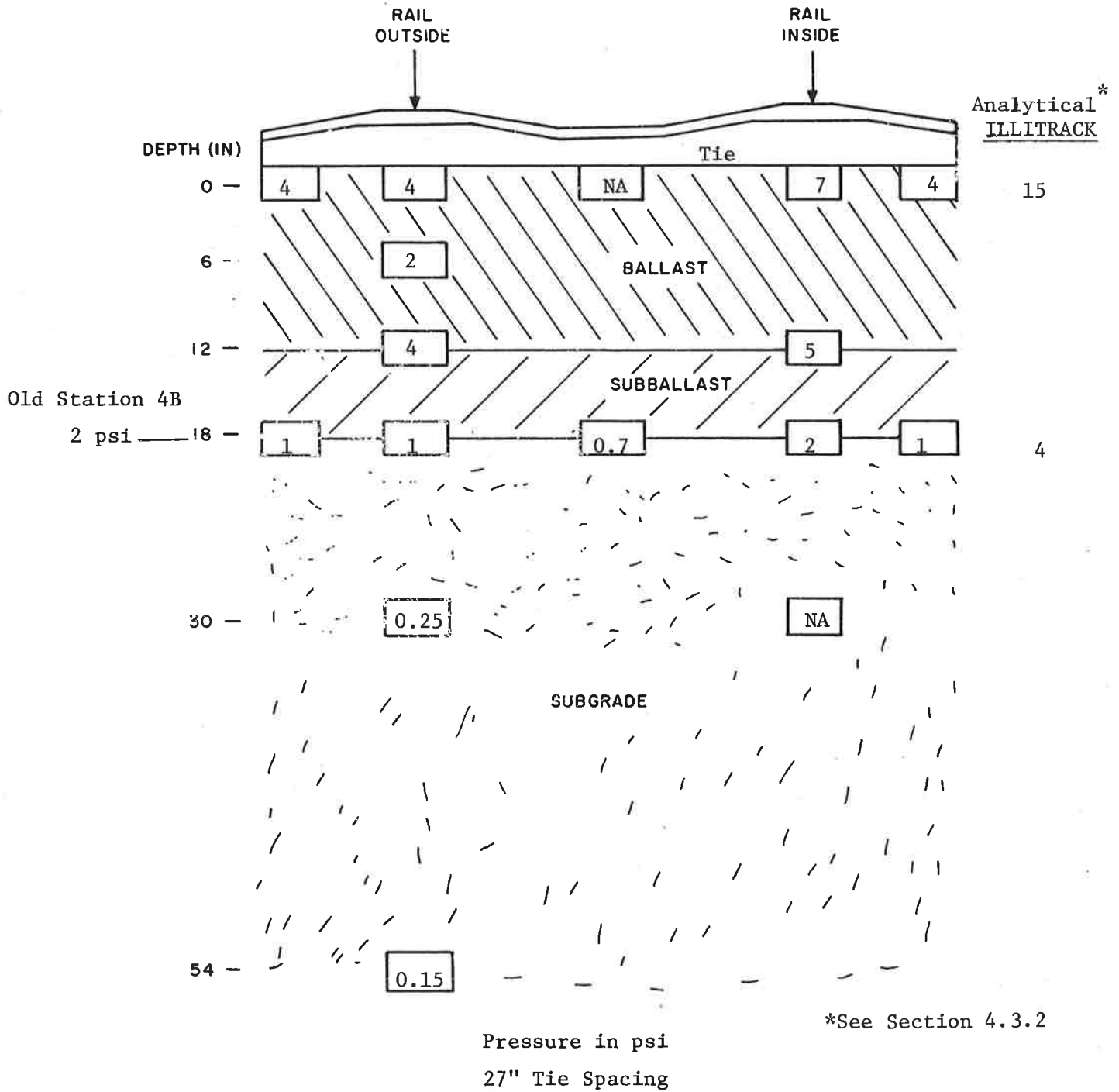
FIGURE 4.5a.  TYPICAL MAXIMUM PRESSURE DISTRIBUTION AT CURVE
FOR CRUSH LOADED R-42 VEHICLE

Pressure in psi

27" Tie Spacing
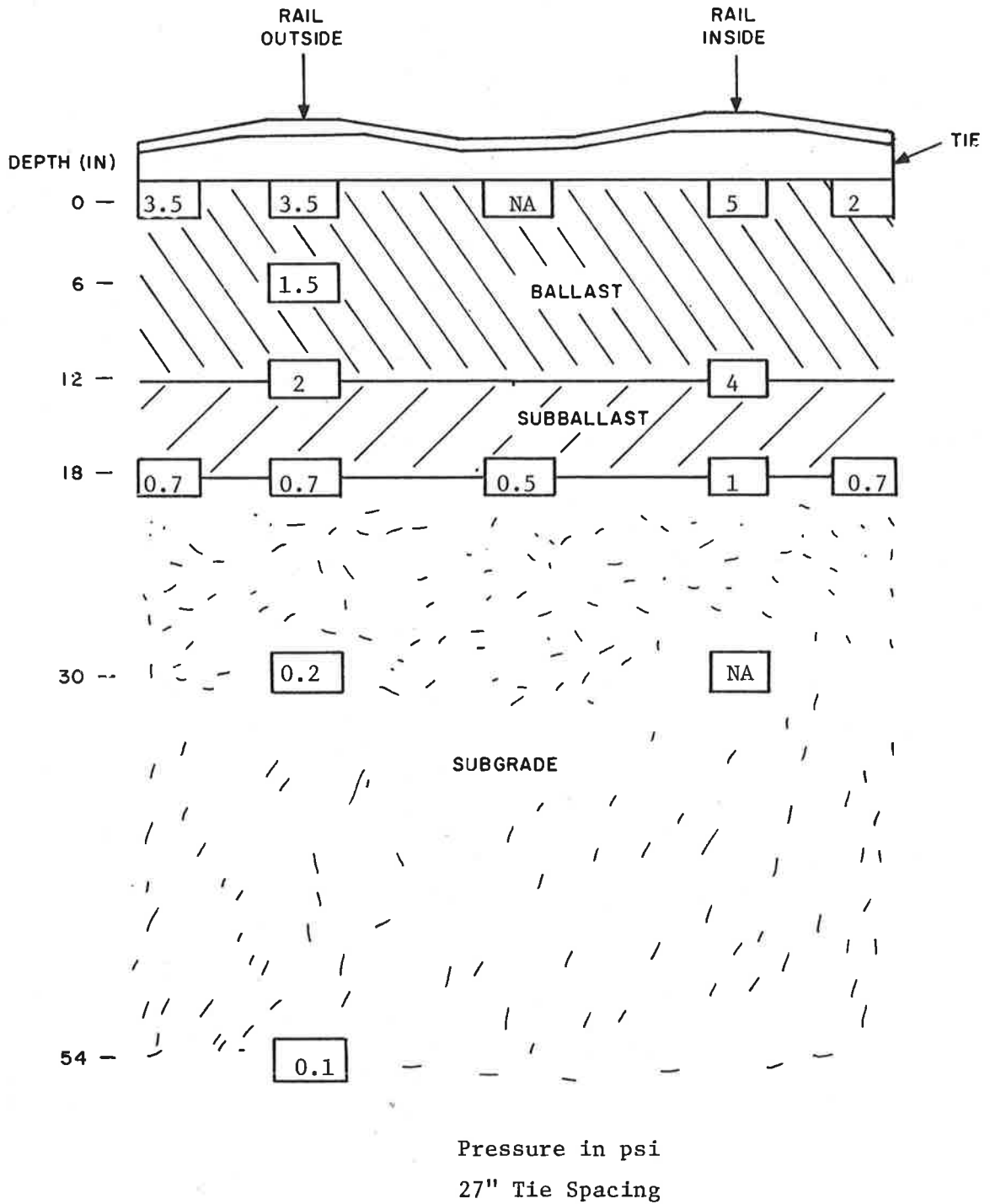
FIGURE 4.5b. TYPICAL AVERAGE PRESSURE DISTRIBUTION AT CURVE
FOR CRUSH LOADED R-42 VEHICLE

loaded R-42 vehicle (13.125 kips static or 15 kips dynamic wheel load) was the maximum loading condition for the track system (see example of tie bending moments in Section 4.2) and caused the highest pressures to occur in the roadbed.

Figures 4.4a and b show the maximum pressures and the average pressure distribution for the tangent section. The five pressures measured directly under the tie and the five pressures measured at the top of the subgrade are all under the same tie. It should be noted that the pressures consistently dissipate with depth, and there is an even application of pressure at the top of the subgrade (similarly noted for Figures 4.5a and b for the curve). The pressure distributions throughout both the tangent and curve sites appear to be consistent except for the gage at a depth of six inches in the curve ballast. It is possible that either the gage is malfunctioning or the ballast was unevenly tamped. After the gages were inserted into the subgrade and ballast an extensive tamping process was conducted to recompact the disturbed roadbed region as evidenced by track settling. This tamping process occurred periodically until the vehicle experimentation was begun.

Table 4.8 shows the results of a photographic study performed during the vehicle experimentation. The average deflections (measured from the film) of the ties at KSC-2 and KSC-1 (ties C-14 and C-13 and ties T+8 and T+9 respectively) and the middle of the rail connecting these two ties are indicated in Table 4.8. The camera was mounted on the inside of the oval and the targets were afixed to the tie ends and to the webs of the rail. While visual inspection during the experiments indicated consistent tie and rail deflections, the values shown in Table 4.8 are inconsistent. It is inconceivable that the lightest transit vehicle (MBTA Blue Line car) should cause the greatest deflection at the curve, and that the light loaded R-42 should cause almost negligible deflection. In addition, visual inspection indicated that the deflections at the tangent were less than at the curve, but the photographically reduced displacements indicate the opposite. Although the values in Table 4.8 are questionable, it is known that the deflections at KSC-1 and KSC-2 were greater than at the adjacent tie locations. The visual measurement of tie deflection at the new instrumentation sites

## TABLE 4.8

### Photographically Measured Rail and Tie Deflections
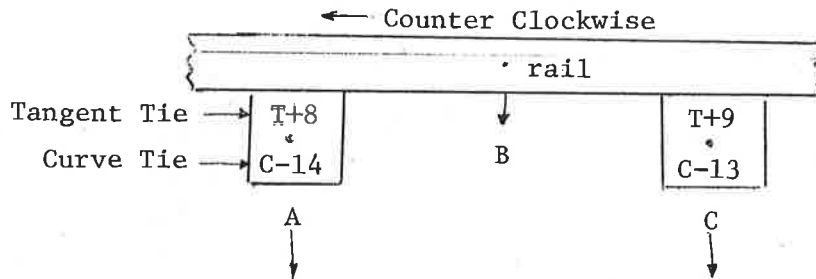


|  |  | Average Point Deflection (in) | | |
|---|---|---|---|---|
|  | Curve | A | B | C |
| R-42 | Crush | 0.13 | 0.09 | 0.13 |
|  | Light | 0 | 0.01 | 0.03 |
| MBTA | Crush | 0.15 | 0.16 | 0.13 |
|  | Tangent |  |  |  |
| R-42 | Crush | 0.18 | 0.26 | 0.18 |
|  | Light | 0.20 | 0.16 | 0.18 |

Note: Visual inspection noted tie and rail deflection during passage of vehicle but there are unresolved inconsistencies in the magnitude of this measured data.

indicates that the roadbed was moderately "soft" at these local tie positions but was within operational limits.

Figures 4.6 and 4.7 show typical pressure measurements taken at the tangent and curve sites respectively. Figures 4.6a-e show pressure versus time measurements for a gage directly under the inner rail seat at the top of the ballast and for gages located at varying depths under the outer rail seat or subjected to varying test vehicle configurations and located at the top of the subgrade. Figures 4.6a-c depict typical pressure distributions from the top of the ballast to a depth of 34" into the roadbed due to the passage of a 30 mph crush loaded R-42 test vehicle. Note the spikes that occur in all the pressure figures (similar to the spikes shown in Figure 4.1b) depict wheel flats passing over the instrumentation. It is interesting to note that these pressure spikes occur at all measured depths in the transit roadbed in response to the impact of a wheel flat. From each pressure-time plot it is evident that there is no coupling of roadbed response from the loading induced by the two trucks of the same transit car. However, for pressure measurements, there is a definite coupling of effects from one axle to the next on the same truck, and, as the depth increases, a coupling of the loads induced by the trucks of the two adjacent transit cars. These observations are valid also for the pressure measurements taken at the curve site, Figure 4.7. This demonstrated interdependence of loads from adjacent cars, but the independence of the loads generated by the two trucks of the same car, and the apparent elastic response for each test vehicle passage, justifies the utilization of a two car test vehicle for this experimental program.

Figures 4.6b, d, and e demonstrate the change in pressure response as a function of vehicle test configuration. All of these measurements were made at the top of the subgrade, which is a critical design point. It should be noted that there is very little difference in magnitude or shape between the pressure measurements taken at the different test vehicle velocities of thirty or fifty miles per hour. Figures 4.7a and b give further demonstration to this similiarity between pressure measurements at the two test velocities. The curve along the TTT

79

6.96 PSI

4.11 PSI

(a) Top of Ballast, Inner Rail Seat, 30 mph Crush Loaded

5.28 PSI

4.29 PSI

(b) Top of Subgrade, Outer Rail Seat, 30 mph, Crush Loaded

0.262 PSI

0.174 PSI

(c) 12 in. Below Top of Subgrade, Outer
    Rail seat, 30 mph, Crush Loaded

5.28 PSI

3.7 PSI

(d) Top of Subgrade, Outer Rail Seat, 50 mph, Crush Loaded

4.8 PSI

3.08 PSI

(e) Top of Subgrade, Outer Rail Seat, 30 mph, Light Load
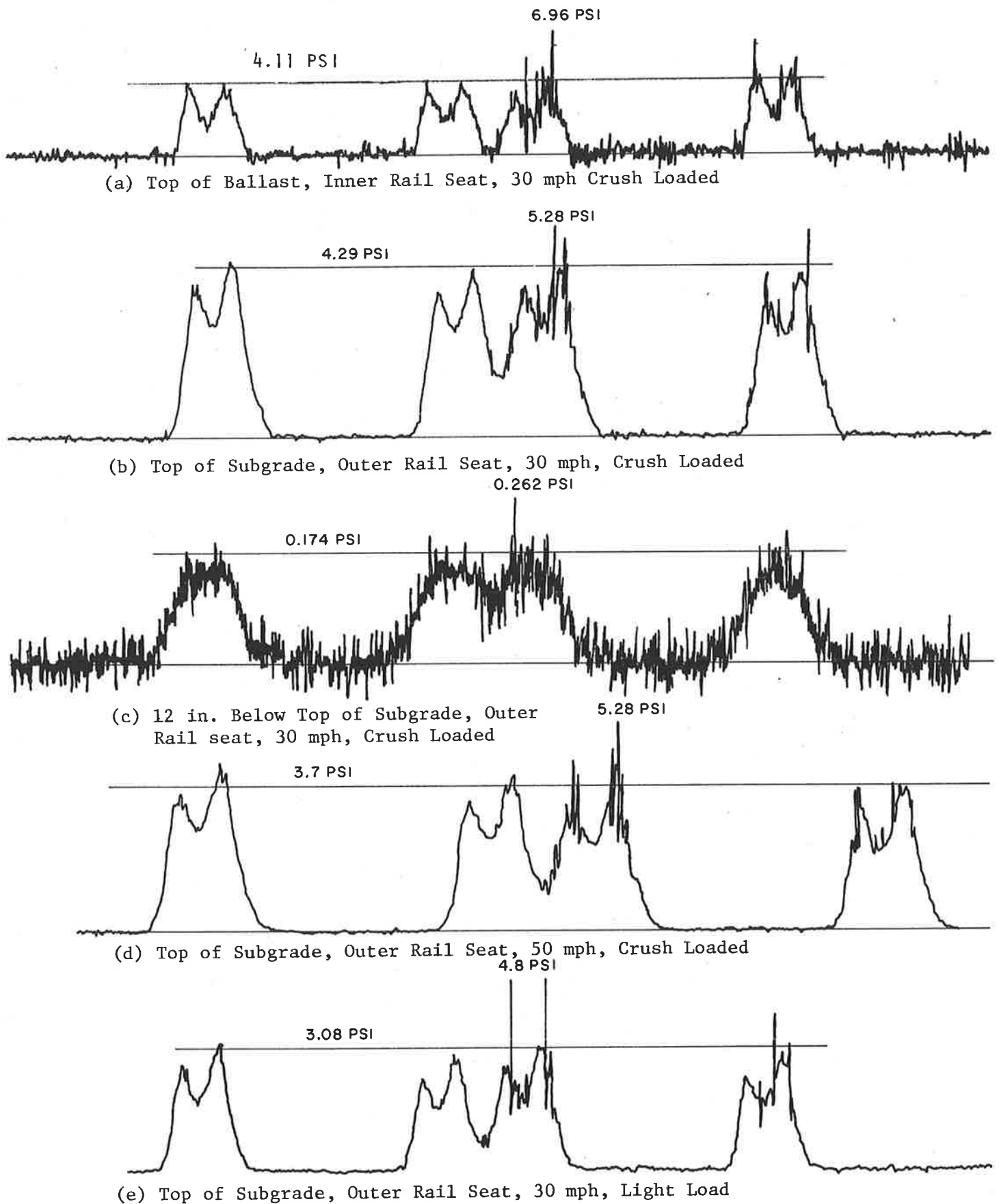
FIGURE 4.6.   PRESSURE VERSUS TIME PLOTS FOR R-42
VEHICLES AT THE TANGENT
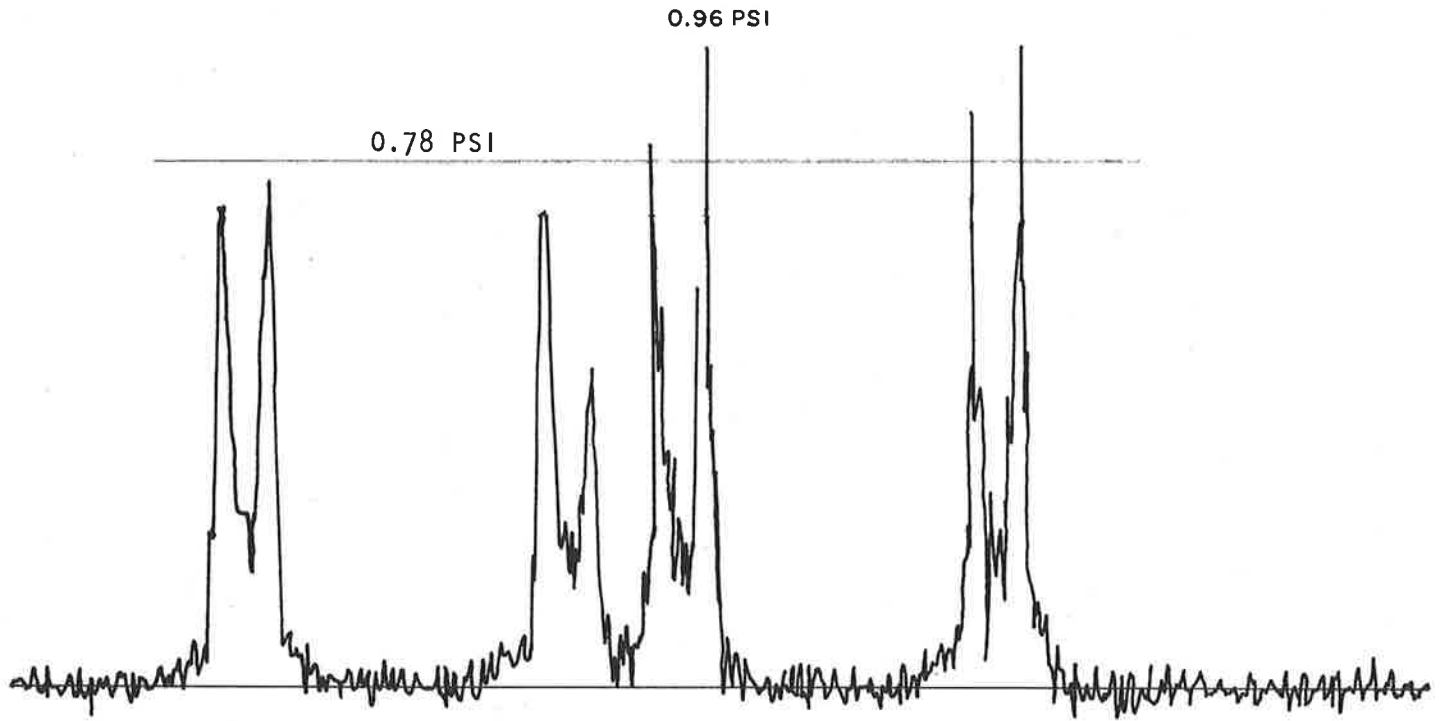
(a)  Top of Subgrade, 30 mph
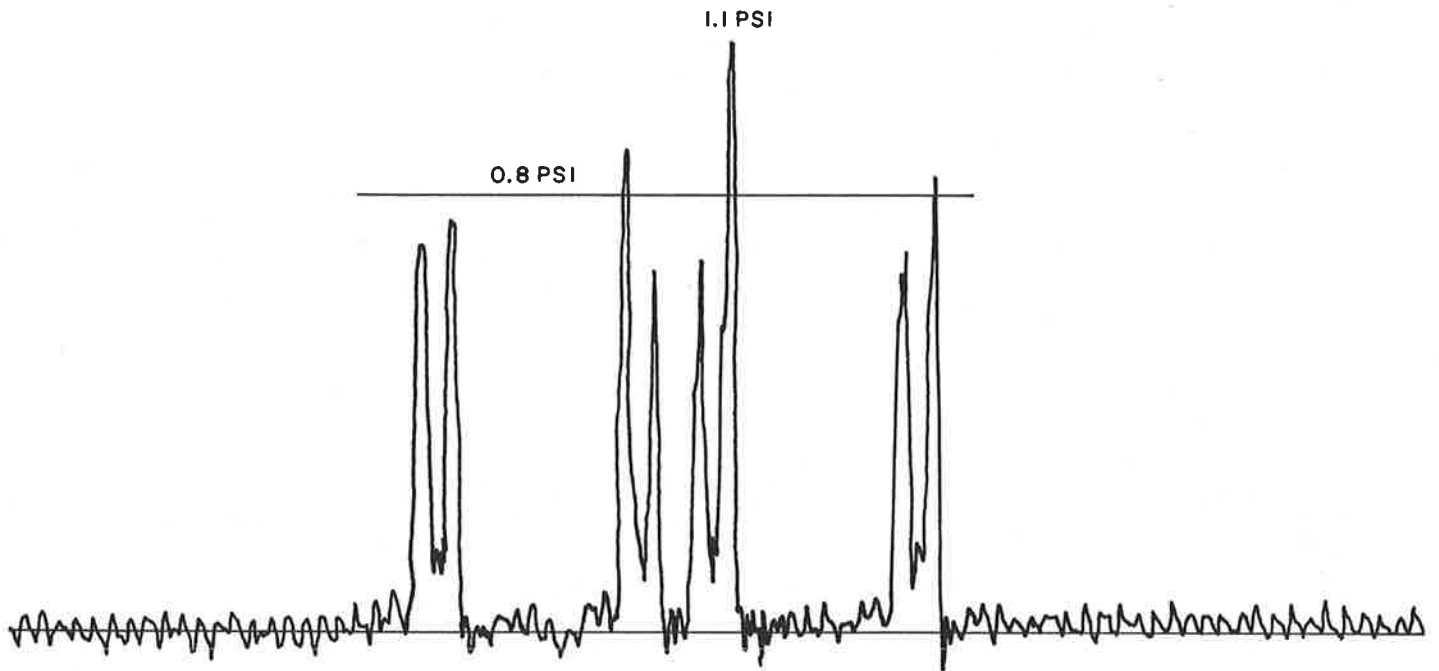
(b)  Top of Subgrade, 50 mph

FIGURE 4.7.  PRESSURE VERSUS TIME PLOTS FOR CRUSH LOADED R-42
VEHICLES AT OUTER RAIL OF CURVE

has a 3820 foot radius and a 4.5 inch superelevation. The maximum
additional force that can be transmitted vertically into the roadbed is
sixteen pounds, or about a 0.03 psi increase in top of ballast applied
pressure. This pressure increase for the fifty mile per hour run is
well within any measurement accuracy bounds for these same roadbed
pressure measurements. It is evident therefore that the curve site at
the TTT provides experimental data that is relevant more as an indication
of tie spacing effects than as a comparison between transit curve and
tangent sections. From the wheel to rail loads data and the tie bending
moment data shown earlier in this section and based on the pressure data
presented above there is little difference in roadbed response from
inner to outer rail, and little difference in roadbed response for
different vehicle velocities; wherein large differences would be anti-
cipated for actual transit sized curves (i.e., 300 to 500 foot radii).
The TTT curve is set for a balanced load at 67.5 mph (see Section 5.1.5.6),
but the unbalanced loads induced at 30 or 50 mph are negligible for this
gentle curve.

The maximum pressure readings shown in Figures 4.4 and 4.5 indicate
a few important observations from this study. First the maximum pressure
values correspond to loads induced by the measured wheel flats. The
"average" pressures, or those anticipated from the dynamic load of a
perfect wheel, are approximately thirty percent below those peak values
shown in Figures 4.4 and 4.5. Secondly, the pressures induced at
depths of one and three feet into the subgrade are influenced by the
spikes in the wheel to rail loads, but are sufficiently small, even in
their maximum values, to be ignored in this and probably in future
experimental studies. Finally, the pressures at the two "design points"
(top of ballast and top of subgrade) are all within the design guide-
lines of 65 and 20 psi, respectively, by a factor between two and three.

The pressure at the tie/ballast interface is first a function of
tie bearing area and secondly a function of tie spacing and the elastic
properties of the roadbed. However, the pressure at the top of the sub-
grade is equally dependent upon all the basic design parameters, and
additionally, the design load at this point in the roadbed is one of the

most significant criteria affecting roadbed life. Table 4.9 examines the change in top of subgrade pressure and tie/ballast interface pressure as a function of test vehicle configuration, for the tangent and curve sites.

As pointed out earlier in this section and in Section 3, both test sites (tangent and curve) were moderately soft but within operational limits during the experimental program. It is evident from visual inspection and an examination of Table 4.9 and Figures 4.4 and 4.5 that the curve site was softer than the tangent site. The wheel to rail load data presented in Section 4.1 show that there is negligible difference between wheel loads induced by thirty or fifty miles per hour test vehicle passages. However, Table 4.9 shows a decrease in pressure loading at the top of the subgrade for the 50 mph vehicle velocity at the curve site, whereas at the tangent site the pressure distributions are invarient with vehicle velocity. This fact implies a "bridging" phenomenon occurring at the curve site, in which some of the load is carried by adjacent ties and is bridged over the KSC-2 instrumentation. If this is indeed occurring then the 50 mph pressure distributions should be less than the 30 mph measurements because the time of load application becomes a factor if bridging is important. Table 4.9 does indicate a drop in subgrade pressure as the test vehicle weight is reduced. This is consistent with the measured wheel to rail loads shown in Section 4.1 and the measured tie bending moments shown in Section 4.2.

Referring to Figure 4.5a, the only measured pressure from the old instrumentation stations (4A and 4B) is presented for the top of sub-grade at the curve site 4B. This pressure (2 psi) is consistent with those pressures measured at Station KSC-2.

## 4.3.2 Analytical Correlation with Pressure Data

In Section 5 both numerical and analytical methods of predicting roadbed pressure distributions are described. Some empirical equations had been derived for railroad geometries and loads and are described by Talbot's and the Japanese National Railway formulas listed in Section 5.1. These empirical equations must be treated with some care, however, because they are inferred from railroad configurations and may

TABLE 4.9

Variation in Top of Subgrade Pressure and Tie/Ballast Interface Pressure Under Rail Seat

## Top of Subgrade Pressure (psi)

### Tangent

| Vehicle | 30 mph Avg. | 30 mph Max | 50 mph Avg. | 50 mph Max |
|---|---|---|---|---|
| R-42 Crush | 4.2 | 5.3 | 3.7 | 5.3 |
| R-42 Light | 3.1 | 4.3 | 3.1 | 3.4 |
| MBTA Crush | 2.1 | 2.4 | 2.1 | 2.4 |

### Curve

| Vehicle | 30 mph Avg. | 30 mph Max | 50 mph Avg. | 50 mph Max |
|---|---|---|---|---|
| R-42 Crush | 1.2 | 1.6 | 0.60 | 0.80 |
| R-42 Light | 0.77 | 0.83 | 0.55 | 0.83 |
| MBTA Crush | 0.33 | 0.37 | 0.11 | 0.17 |

## Tie/Ballast Interface Pressure (psi)

### Tangent

| Vehicle | 30 mph Avg. | 30 mph Max | 50 mph Avg. | 50 mph Max |
|---|---|---|---|---|
| R-42 Crush | 20 | 25 | 17 | 20 |
| R-42 Light | 14 | 17 | 13 | 15 |
| MBTA Crush | 7 | 8 | 7 | 8 |

### Curve

| Vehicle | 30 mph Avg. | 30 mph Max | 50 mph Avg. | 50 mph Max |
|---|---|---|---|---|
| R-42 Crush | 5 | 7 | 3 | 4 |
| R-42 Light | 4 | 5 | 3 | 4 |
| MBTA Crush | 1.5 | 2.2 | 1 | 2 |

not identify the variations necessary to describe transit track geometries and transit vehicle loads. Section 5.1 also lists two analytical formulas based on the physics of an assumed _elastic_ half-space. These equations assume constant elastic properties throughout a half-space (infinite plane and infinite depth) and are derived for singular point loads or in their integrally distributed circular load form, (Boussinesq and Love's equations respectively, see Section 5.1.5.4). In addition there are several numerical computer codes that have been developed to predict track system response, and two of these, ILLITRACK and MULTA, are discussed in Section 5.2. Some basic calculations have been made with these codes (Tables 5.1c and 5.2), and the predictions from the most representative models will be compared to each other, to the four equations listed above, and to the experimental results of Section 4.3.1.

Only the worst case loading will be considered here, and this consists of the crush loaded R-42 vehicle at either velocity along the tangent section of track. Tables 5.1a and 5.2 describe the models that were used for ILLITRACK and MULTA and Section 5.1.5.4 gives the four equations as discussed above. The wheel load that is used in all of these predictive analyses is 16 kips. This load is consistent with all of the ILLITRACK and MULTA predictive runs made before and after the test program at the TTT and is consistent with the maximum expected wheel loads predicted in Section 4.1.

Figure 4.8 shows a comparison of these six predictive formulations with the maximum measured pressures in the tangent roadbed (see Figure 4.4). For both the ILLITRACK and the MULTA predictions, the new soil model (as given in Tables 5.1a and 5.2 and discussed in Section 4.6) is used. All comparisons are being made for a depth of eighteen inches which corresponds to the top of the subgrade.

All of the analytical and empirical formulations overpredict the subgrade pressure. (It should be noted that no "factors of safety" were introduced into these equations.) Section 5.1 indicates a preference for Love's Equation to predict top of subgrade design pressures, but this overpredicts the maximum experimentally recorded pressure by eighty-four percent. ILLITRACK with its nonlinear ballast and subgrade

85
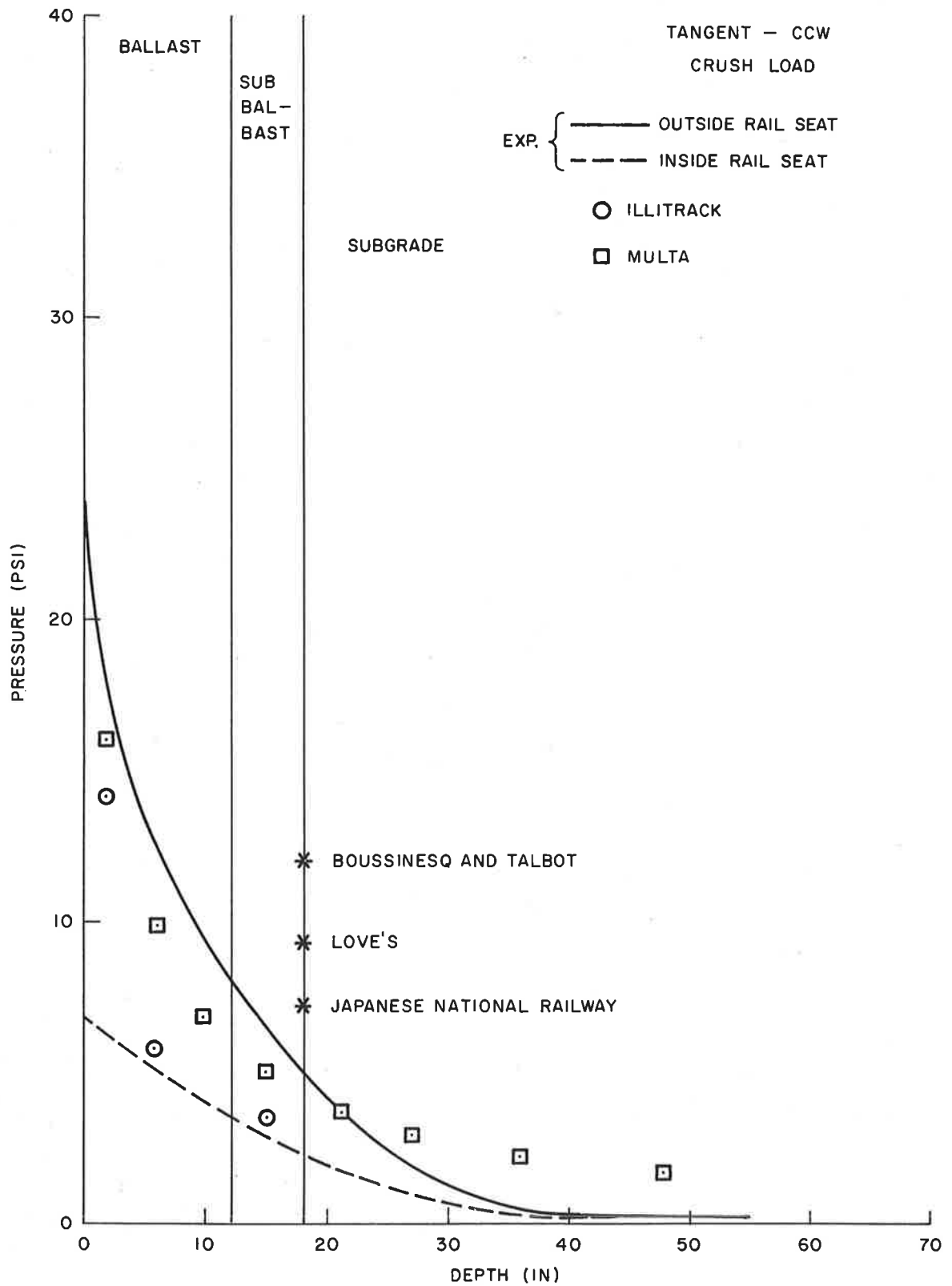
FIGURE 4.8. PREDICTIVE MODELS COMPARED WITH R-42
VEHICLE EXPERIMENTALLY MEASURED ROADBED
PRESSURES, TANGENT SECTION

model appears to give the most accurate predictions of the UMTA transit test road bed response. The differences between ILLITRACK and MULTA are most readily attributed to differences between linear and nonlinear soil models, and the differences with the analytical Boussinesq and Love's equations are due to the applied load distribution description and to the lack of homogeneity in the ballasted roadbed. The differences in the predictions of the two empirical formulas must be attributed to a change in track geometry and vehicle loads which were not incorporated in the original empirical study.

Figures 4.4a and 4.5a include the pressure predictions of ILLITRACK and MULTA next to the composite maximum measured experimental pressures. These numbers show the consistencies of the predictions and also show the dispersion that must be present in experiments of this type or in assumed two dimensional static analyses such as ILLITRACK and MULTA.

4.4  BALLAST AND SUBGRADE STRAINS AND DISPLACEMENTS

The ballast strains were measured with the use of Bison inductive coils as described in Section 3. The measurement of the change in the magnetic field between independent coils in the ballast gives an indication of relative displacement and therefore the relative strain between the two locations is quantified. The primary reason for the utilization of Bison coils for ballast strain measurements was for comparison with similiar Bison coils installed at the old instrumentation stations TTC-4A and TTC-4B. The Bison coils have a highly nonlinear response and therefore an accurate initial coil location must be established in order to use these instruments for strain measurements. The instrumentation sites 4A and 4B were installed seven years prior to these experiments, and because the Bison coils at 4A and 4B were not monitored during that time, it became apparent that no accurate information could be obtained from the soil strain measurements at the old instrumentation stations. This situation leads to the conclusion that the following soil strain data must be analyzed with good engineering judgement. Fortunately, data obtained from the nearby FAST test facility is available (Reference 4.1), and some comparisons are made here to judge the validity of the measured ballast strain data at the TTT.

Table 4.10 shows a representative sample of maximum strains and deflections measured along the tangent and curve transit track sites. Additionally, a sample of strains and deflections was taken from Reference 4.1 for a 15 kip wheel load and this is shown with the transit tangent data. The transit data appear to be consistent within itself, and the values appear to be twice as great as the data measured at the FAST facility. However, the ballast and ties were different at the FAST facility, so these numbers can only be used as a relative indication of measurement accuracy.

It is interesting to note that there are no design procedures based upon ballast strain or subgrade deflection; instead roadbed designs are based upon predicted ballast and subgrade pressure levels. All of the strains and deflections measured in the transit experiment appeared to be completely elastic; however, these are single pass data resulting from experiments conducted over a relatively short period of time (three weeks). Strain and deflection are much more useful as long term indications of roadbed settlement and compaction rates, rates that are measured in millions of gross vehicle tons passing over a particular site. One million gross tons is the equivalent of more than 8300 R-42 vehicles passing over the test site, which could not be accomplished in a short term experiment.

The strains and deflections that were measured at the transit curve and tangent sites do not show any unusual deformations occurring during a vehicle passage. These measurements could serve as a benchmark if, in the future, strain and deflection measurements are monitored periodi- cally. The results of these additional data would be an indication of the "aging" of the test sites. Thus, future soil stress and tie bending moment measurements could be compared with those presented in Sections 4.2 and 4.3.

## 4.5 RAIL FASTENER LOADS

The use of concrete ties in the transit roadbed system requires a special fastener design for securing the rail to the concrete tie. There are many fastener designs available for this purpose, but at the

TABLE 4.10

Ballast Strains and Subgrade Deflections

(Typical Maximum Values at KSC-1 and KSC-2)

| | R-42 Crush | R-42 Light | MBTA Crush | FAST* 15 KIP Load |
|---|---|---|---|---|
| TANGENT | | | | |
| Ballast Strain (%) | 1.3 | 1.0 | 0.7 | 0.5 |
| Subballast Strain (%) | 0.22 | 0.11 | 0.02 | .06 |
| Subgrade Deflection (in) | .021 | .016 | .014 | .02 |
| | | | | |
| CURVE | | | | |
| Ballast Strain (%) | 0.80 | 0.60 | 0.29 | |
| Subballast Strain (%) | 0.21 | 0.15 | 0.09 | |
| Subgrade Deflection (in) | .045 | - | - | |

*Taken from Reference 4.1 for similiar track construction.

TTT in test section IV only the Flexiclip fastener was installed. Initially it was anticipated that an indication of rail seat load could be obtained by the appropriate instrumentation of the fastener clip. This measurement technique proved to be unfeasible, but four clips were instrumented for strain detection at both the tangent and curve sites, see Section 3.5.2.

The instrumented clips were all attached to the "modified" ties installed at KSC-1 and KSC-2 for tie-ballast interface pressure measurements (T+9 and C-14, respectively), see Figures 3.10 and 3.11. The strain gages were each instrumented with two sets of temperature compensating strain gages as indicated in Figure 3.9. The clip-rail-tie system is bolted into place with a prescribed torque which places the clip into a state of initial strain. These initial strains were measured and the additional dynamic strains were measured during the passage of the various test vehicles. The total stress level (combination of initial stress plus dynamic stress) is compared to the yield stress of 150000 psi for the SAE 1095 spring steel used in the clips. This comparison will indicate the nearness to single cycle failure (material yielding) that the clips are exposed to by vehicle loading. Additionally a comparison of dynamic alternating stress is made with the initial preload stress to identify the likelihood of fastener clip fatigue failure due to the loadings of multiple vehicle passages.

Table 4.11 summarizes the experimental data for the three vehicle configurations: R-42 crush and light loaded and the MBTA vehicle. All the clips, both those at tangent and curve sites, were taken together and both vehicle velocities were used in assembling Table 4.11. The average stress due to the torqued bolt is 68500 psi while the yield stress for this material is approximately 150000 psi. The alternating stress levels are similiar for both R-42 loading conditions but are distinctly lower for the MBTA vehicle. The maximum peak values, as compared to the average peak values experienced during the passage of a single test vehicle, are due to the wheel flats discussed in earlier sections. The examination of the susceptibility of SAE 1095 steel to fatigue, based upon notched specimens (to account for the bolt hole),

90

TABLE 4.11

FASTENER CLIP STRESS

Alternating Peak Stress Levels

(KSI)

| | Positive | | Negative | |
|---|---|---|---|---|
| | Avg | Max | Avg | Max |
| R-42 Crush | 1.6 | 3.8 | 2.8 | 5.7 |
| R-42 Light | 1.3 | 4.4 | 2.3 | 4.9 |
| MBTA Crush | 1.1 | 3.0 | 0.5 | 2.5 |

Average Pre-load stress (due to bolt torque) 68.5 KSI

Yield stress                                       150.0 KSI

Average life for mean stress at 68.5 KSI, alternating stress at 10KSI and notched condition is in excess of $10^7$ cycles.

shows that for the measured mean and alternating stress levels fatigue failure is not a major problem.  It is estimated that for the bending fatigue (ignoring bolt slippage and geometry changes), this clip should be able to withstand a minimum of ten million load cycles.  It is highly unlikely that a transit system could subject a clip to more than three quarters of a million load cycles in any given operating year.

It should be pointed out that this experimental study did not examine the fatigue failure of the attachment bolt or the susceptibility of the bolt to pull free of the concrete tie.  Additionally, changes in track geometry were not addressed, and the stress levels induced in the fastener clip by track perturbations should be examined.

## 4.6  ROADBED MATERIAL EVALUATION

A major criterion for the analysis of a track system is an accurate representation of the components of that system.  In Section 5.1 the standard design practices for determining rail stress, and tie bending moments depend upon knowing the stiffness of the "elastic foundation" or the properties of the ballast, subballast and subgrade.  In Section 5.2, in order to utilize the predictive capabilities of the ILLITRACK and MULTA computer codes, it is necessary to know the stress-strain constitutive relation of the various components of the transit roadbed.

For the analyses conducted in this program a basic reliance was made upon ballast, subballast and subgrade data collected and analyzed by other agencies (see References 5.18 and 5.19) for the same or similar material along the FAST Track at the TTT.  The data contained in References 5.18 and 5.19 were used to represent the ballast and sub-ballast properties; however, an additional study was undertaken to ascertain the subgrade properties at the tangent site of the TTT. Appendix E gives a description of the sampling techniques used to obtain soil specimens and a description of the triaxial tests performed on these specimens.

During the experimental process, outlined in Table 3.1, continual monitoring of the roadbed temperature, density and moisture content was performed in order to be able to utilize and compare data that was

collected over a two month span of time. Table 4.12 summarizes the temperature profile that was measured during each of the experiments, at both the tangent and curve sites. Eight thermocouples were used at each site and the temperature profile was monitored each minute during the tests. Table 4.12 shows the depthwise location of the thermocouples (see Figures 3.9 and 3.10 for a planar location description) and it contains the average temperatures, standard deviations, and absolute high and low temperatures based on data at both sites during the entire three week testing period.

The subgrade temperature data is based on the information recorded by the lower six thermocouples during the entire program, whereas the ballast statistics only include data collected from thermocouple number seven at the tie-ballast interface. The subgrade temperature was almost constant during this test period whereas the ballast temperature varied widely during the early to mid fall test period and the 12 noon to 8 pm daily test window.

The moisture and density profile was sampled at each test site several times during the experimental program. A NIC-5 Nuclear Moisture Density Meter with a NIC-10 Depth Probe was utilized for the sampling procedure. The profiles were basically identical at both the tangent and curve sites (about one-half mile apart). The profiles had two distinct regions with a break point at about one foot below the top of the subgrade. The first foot of the subgrade had a constant 100 pcf wet density with a variable moisture content of 7 to 16% as the depth increased to one foot. At the one foot point to four feet below top of subgrade, the soil was fairly constant having a wet density of 102 pcf, a dry density of 81 pcf and a moisture content of twenty-five percent.

This soil temperature, density and moisture data was used by the University of Colorado (Prof. Ko and Mr. Kim) to perform accurately the designated triaxial tests upon the subgrade soil samples (see Appendix E). The soil samples ranged in density from 123 to 137 pcf and the moisture levels had to be adjusted to conform to the field measured moisture content. A triaxial test procedure was designed based on information

93

TABLE 4.12

ROADBED TEMPERATURE DISTRIBUTION

| Thermocouple Number | Depth (in) | Location |
|:---:|:---:|:---|
| 7 | 0 | Bottom of Tie |
| 6 | 12 | Ballast/Subballast Interface |
| 5 | 18 | Subballast/Subgrade Interface |
| 4 | 24 | Recompacted Subgrade |
| 3 | 30 | Recompacted Subgrade |
| 2 | 36 | Recompacted Subgrade |
| 1 | 42 | Recompacted Subgrade |
| 0 | 54 | Untreated Subgrade |

Subgrade Temperature (Thermocouples 0-5)

| | | | |
|:---|:---|:---|:---|
| Average | 71.8°F | High | 73.7°F |
| Std. Dev. | 1.3°F | Low | 64.8°F |

Bottom of Tie Temperature (Thermocouple 7)

| | | | |
|:---|:---|:---|:---|
| Average | 76.9°F | High | 86.2°F |
| Std. Dev. | 5.9°F | Low | 64.9°F |

contained in reports by the Army Waterways Experimental Station, (Reference 4.4). The test, as detailed in Appendix E, consists of six different stress paths. Two of these paths (those with equal increments of axial and lateral stresses) were used for recompactions and for measuring the change in bulk modulus of the sample. Two other stress paths (a constant lateral stress and an increasing axial stress) are standard test paths that demonstrate the effects of static vertical loads on the soil. The last two stress paths include increases first in lateral pressure and secondly an increase in vertical stress. These stress paths are used to represent the approach of a wheel in a dynamic loading sequence, see Reference 4.4.

There are distinct differences measured in the soil response as the different stress paths are followed. The "dynamic" stress path allows for a relaxation of the soil and a loss of some of the accummulated plastic response of the soil, built up from previous stress paths. In order to have a statistically sufficient number of data points an appropriate combination of stress path data was taken from the two soil samples that represented the first one foot of recompacted subgrade to determine the soil properties listed in Tables 5.1a and 5.2 and summarized as follows:

Initial Elastic Modulus            4000 psi
Poisson's Ratio ($\gamma$)            0.22
Resitient Modulus vs. Stress Invarient      $E_R = 504\ \theta^{0.86}$

These soil properties, as calculated from the results of two tri-axial samples, each subjected to six stress paths, is by no means conclusive or final. There were enough differences in initial sample density compared to field measured density to question the soil sampling procedure and the ultimate effects it had on the soil properties. Additionally the soil samples were tested only over a small stress range, never approaching soil "failure" and there were only two samples from each of only three depths. It is recommended that further, more intensive and more extensive soil research be carried out both to measure the basic properties of the soil along the test site and to ascertain the effects a dynamic loading pattern have upon the soil properties.

# 5.  TRANSIT TRACK DESIGN STANDARDS

Design standards for transit systems do not formally appear in the transit industry literature.  The railroad industry has, over an extensive period of time, assembled common design guidelines (Reference 5.1), but the transit industry has relied upon these railroad guidelines with modifications based upon transit experience for their design procedures. Prause, et al (Reference 5.2), assessed some of the design tools and criteria for transit systems in the early 70's, and this has been expanded upon in Section 5.1 by reviewing transit design history and examining a basic transit design example (see Appendix A).

Most of the design tools that are used by both the rail and transit industries are either applications of analytical elasticity solutions or tables compiled from empirical data.  Recently the railroad industry and the FRA have had some numerical computer analyses developed for the loads and deflections predictions of roadbed designs.  In Section 5.2, two of these codes, ILLITRACK and MULTA, are compared and examined for their applicability to transit track design.

The primary components of an at-grade tie ballast track structure are the rail, fasteners, tie plates, ties, ballast, subballast and subgrade.  The key track parameters used in the design of this type of track construction are the size (weight) of rail, type of tie/fastener combination (size and material), tie spacing, depth of ballast and depth of subballast.  The type of subgrade, local yearly weather conditions, weight and speed of track vehicles, vehicle traffic patterns, availability and cost of materials, and maintenance practices are usually known to the designer and influence the selection of the key track design parameters based on deflections and stresses within the track structure, experience, and the economics of both initial construction costs and maintenance costs.

An important function of these track components is to distribute the vehicle induced forces through the track structure and into the subgrade soil without exceeding the allowables set forth for each component.  However, many of these components have other requirements that must be considered in the design, such as electrical conductivity, drainage, track stability, material availability and economics.

## 5.1  CURRENT DESIGN TECHNIQUES

### 5.1.1  Evolution of Design Technology

For some time after the development of the steam locomotive, little engineering analysis of the track structure was attempted. However, in the latter part of the 19th century efforts in Germany, Great Britain and the United States were made to analyze the stresses in the system.  Until 1875, crude assumptions had been made in order to derive expressions for rail stress.  The period from 1875 to 1915 saw the introduction of the "Winkler Beam" solution, first as a continuous beam on discrete rigid supports and then as an infinite beam supported on discrete elastic foundations.  A final analysis compared the discrete elastic support with a continuous elastic support medium and found good comparison for the two methods.

However, general acceptance of this method did not emerge for years, even after exhaustive tests, in 1937, proved the method to be valid. Once the rail stress procedure had been accepted, the determination of stresses in other components followed.  Just as the rail analysis had been a long time evolving, so was the analysis for the subgrade response. Techniques ranged from early tests, in which a single tie was loaded and deflection measured, to current methods, wherein a length of track is loaded and deflections are measured.  Early experiments ignored the fact that subgrade response is a non-linear function of the loaded area and that true deflection measurement must include rail stiffness, as well as other components of the track structure and subgrade, with test loaded lengths similar to those for which the predictions are meant.

This, then, brings us to the present, with research continuing in several areas of rail structure stress analysis.  Among them are track-train dynamics for continuous welded rail and jointed tracks, track buckling for continuous welded rail, and dynamic testing of a track constructed with perturbations simulating existing conditions found in most jointed rail trackage in the United States and elsewhere.  Studies are continuing in other areas as well, with special interest in rail lateral stability.

Much work is needed in the areas of dynamic loadings and lateral loadings, and while effects have been observed, the causes of inconsistent results in these areas remain uncertain.

5.1.2  Routine Design Procedures

It is safe to assume that experience and standard practice dictate much of track design in this country.  Member sizes are more a method of uniform convention, within each rail company, than anything else (although there are notable exceptions to this practice).  Often, these standard sizes are based on component availability (such as crossties).  Other sizes (such as rails and tie plates) are a function of considerations other than stress related, and some considerations are discussed in various sections of this report.  Transit track design seems to be similar to that of railroad design.

Perhaps the AREA will reduce the complex formulae of the researchers to practical design equations in their specifications.  Some of the recent work has been appearing in the AREA Journals.  In the past, minor code changes have been "tested" in Journal exposure before their final inclusion into the specifications.

This is not to condemn the practice in use, for there is no better method than using the knowledge gained from years and years of experience, by the railroads, as to what does and does not perform.  Maintenance practice among domestic Class I railroads amounts to replacement, annually, of some 5,000 miles of track, including rail, ties, tie plates, joint bars and spikes.  Given the present economic situation, one must conclude that the selection of replacements is based upon performance and not upon whim.

5.1.3  AREA Specifications

The American Railway Engineering Association (AREA), in its Manual for Railway Engineering (Reference 5.1), has recognized the basic principles of design for subgrades.  Chapter I of the manual deals with the appropriate investigation of soils along a proposed route, and refers to

conventional geotechnical methods for design. While recommended procedures are suggested, no practical design formulae appear in this section. An approach to allowable subgrade stress is given in Chapter 22, "Economics of Railway Construction and Maintenance", wherein a value of 20 psi is suggested without regard to soil type. Corrective measures (stabilization methods) for weak subsoils are also outlined.

Material specifications are found in the manual for all track components as well as for ballast and subballast. Extensive material specifications and testing methods are spelled out in the manual. Stress formulae are given in the manual in Chapter 22.

Since there is no binding obligation on the part of the railroads to follow the manual, it serves as a guide only. Some of the railroads choose to design and analyze by their own criteria while the majority follow the AREA Manual recommendations without much individual engineering effort.

5.1.4  Special Considerations in Track Selection

In Section 5.1.2, it was mentioned that considerations, other than those of optimum design for stress, often dictate size selections. Maintenance practice, economics and standard parts approach play an important role in the selection of rail size, tie plate size, ties and rail hardware. An example of such decision making might involve a railroad whose jointed rail construction, while adequate for strength, has shown poor performance as far as joint settlement goes. A decision to increase maintenance (tamping) against a decision to spend more money on heavier rail tie plates and joint bars to match might take place. While the reason for poor joint performance may be traced back to a non-rail structural inadequacy, the decision is based upon economics. Of course, this decision is not different from those made in most other industries, but the practice found to be economical along one piece of track may dictate use of the same construction along the rest of the system. Standardization of track components, which also has obvious benefits, would reinforce that decision.

100

Of major importance in the selection of rail size is the life of rails in curved track. Selection of rail size is often dictated by a reduction in maintenance (i.e. replacement of curve worn rail) through the use of heavier rails than those required for stress.

Elimination of joints, through the use of continuous welded rail (CWR) was adopted largely due to the fact that it eliminated much of the maintenance expenditure in track.

5.1.5  <u>Application of Accepted Principles</u>

As previously indicated, some acceptable formulae have been developed for investigation of stresses in the track structure and substructure. These design relationships for the various track components are presented in the following subsections. The use of these design relationships are also demonstrated in the design example given in Appendix A.

5.1.5.1  Rail Response – By examination of Figure 3.1a, q is defined as the reaction of the continuous elastic support medium (or similarly the discrete support element divided by the space between discrete supports) to a concentrated load P on the rail. Variation of q along the continuous beam is not known; however, its magnitude is a function of the deflection.

$$q = ky \tag{1}$$

where k is the spring constant of the elastic support and
y is deflection.

AREA uses a k value of 2000 psi for 7" x 9" x 8'-6" ties spaced at 20". Other values can be computed by the formula $k = 128 A_b/S$ where $A_b$ is the bearing area of tie and S is the spacing.

The differential equation for the elastic curve of any beam on a continuous (or effectively continuous) elastic foundation is given by

$$EId^4y/dx^4 = ky \tag{2}$$

101
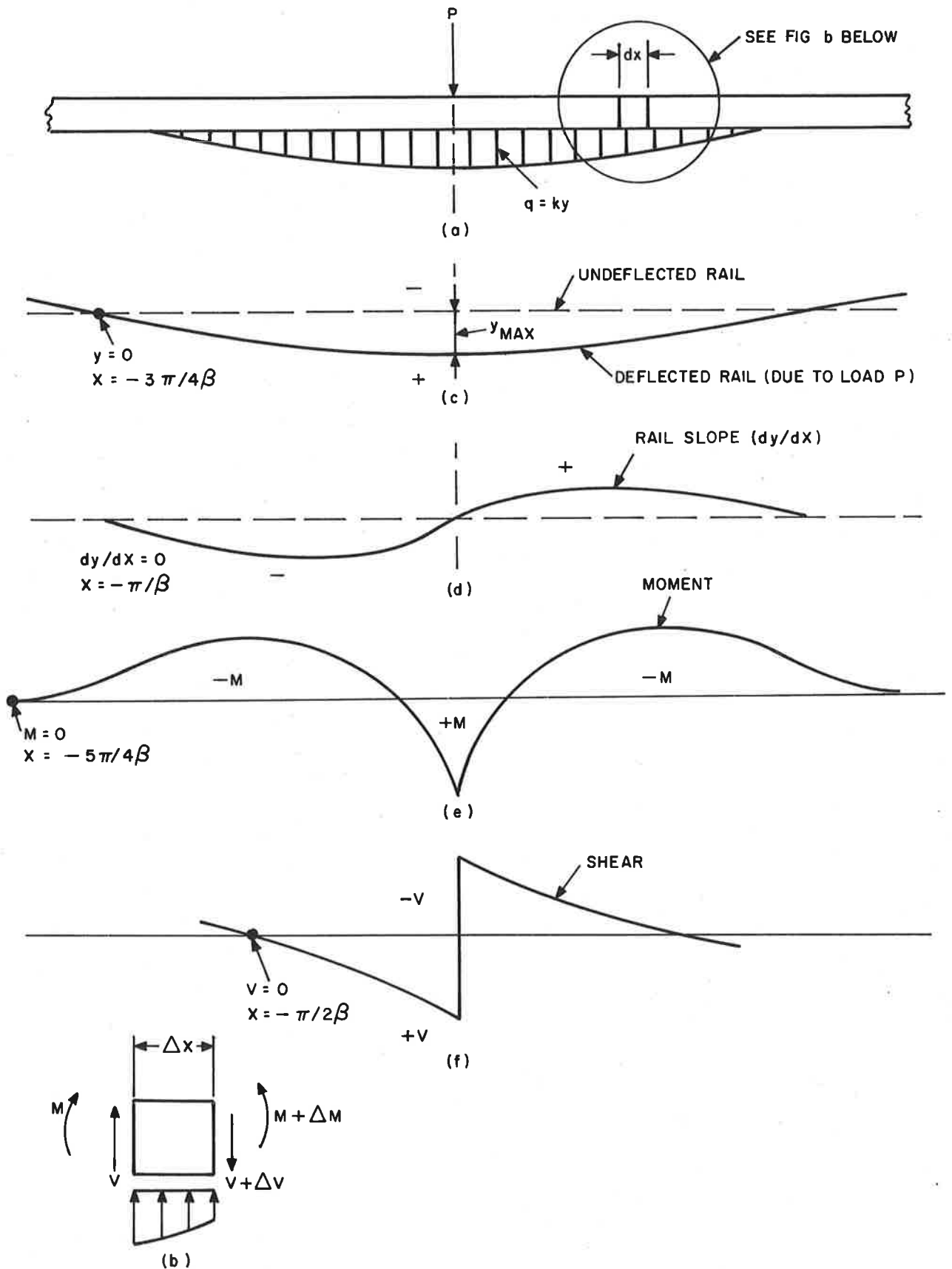
FIGURE 5.1. CONTINUOUS RAIL ON AN ELASTIC FOUNDATION

From the solution of this fourth order differential equation, the deflection for any positive value of x is given by

$$y = (P\beta/2k)e^{-\beta x} (Cos\beta x + Sin\beta x) \qquad (3)$$

where $\beta = \sqrt[4]{k/4EI}$

E = elastic modulus of rail

I = moment of inertia of rail

The moment and shear equations for the rail are as follows:

$$M = (Pe^{-\beta x}/4\beta) (Cos\beta x - Sin\beta x) \qquad (4)$$

$$V = - (Pe^{-\beta x}/2) Cos\beta x \qquad (5)$$

5.1.5.2 Tie Stress - Prediction of tie stress under tie plates is based upon half the total track or one rail reaction (for tangent track) as determined from the subgrade response diagram (Figure 5.1a) which can be solved by the methods just discussed.

While bearing stress can be predicted with relative ease, bending and shearing stresses within the ties are another matter. The distribution of the reaction across the tie is a function of the maintenance practice as much as anything else. Figure 5.2 demonstrates the extremes that can be encountered from a theoretical response to load (Figure 5.2a) to extremes encountered in operating track systems.

Conditions indicated in Figure 5.2b are those recommended by AREA. Conditions shown in Figure 5.2c, while worse than normal conditions, forms a limiting case of poor maintenance practice. Application of simple statics will yield the maximum design results. Some conservative design practices have been carried out for the "end-bound" and "center-bound" conditions (per Figures 5.2d and 5.2e) to simulate the worst possible conditions.

AREA approach to tie design is predicated on the establishment of an effective bearing length of tie given in the following expression:

$$L = \ell-60 \left\{ 1- \frac{0.018 (\ell-60)}{t^{0.75}} \right\} \qquad (6)$$

103
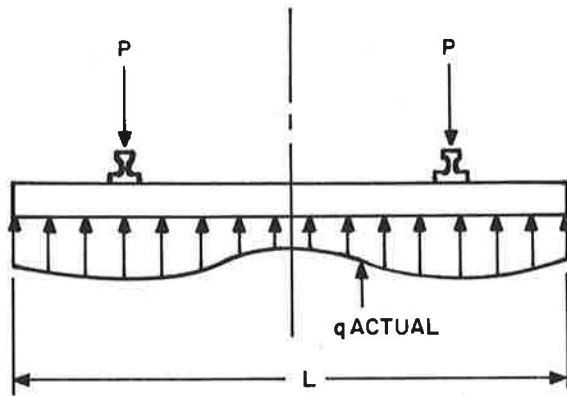
a) ACTUAL DISTRIBUTION
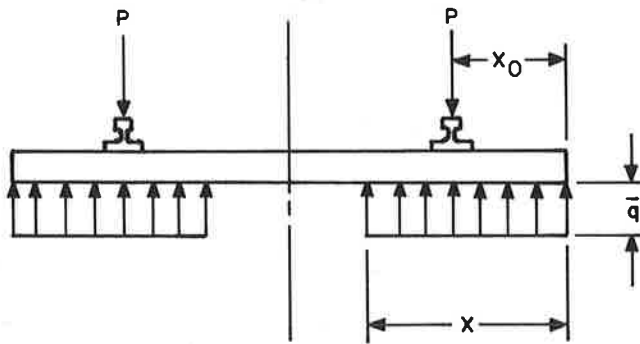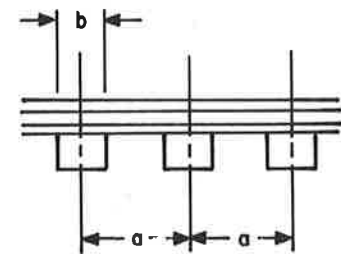
b) ASSUMED DISTRIBUTION

$P$ = RAIL SEAT REACTION
$\bar{q}$ = EQUIVALENT PRESSURE

$$\bar{q} : \frac{P}{X}$$

$$M_1 = \frac{q X_0^2}{2}$$

$$V_1 = q \bar{X}_0$$

$X_0$ USUALLY = L/6
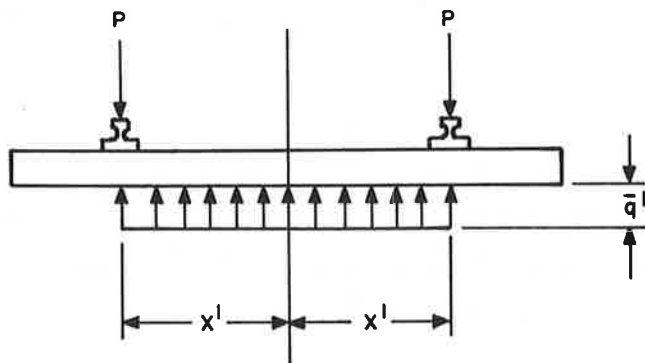
c) ASSUMED DISTRIBUTION

$P$ = RAIL SEAT REACTION
$\bar{q}^l$ = EQUIVALENT PRESSURE

$$\bar{q}^l = \frac{P}{2x^l}$$

$$M_2 = \frac{\bar{q}^l x^{l\,2}}{8}$$

$$V_2 = \bar{q}^l x^l$$

FIGURE 5.2.   PRESSURE DISTRIBUTIONS FOR CROSSTIES

104

P = RAIL SEAT REACTION
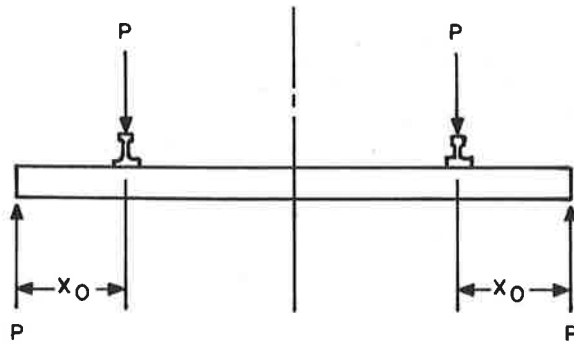
$$M_1 = P \cdot X_0$$
$$V_1 = P$$
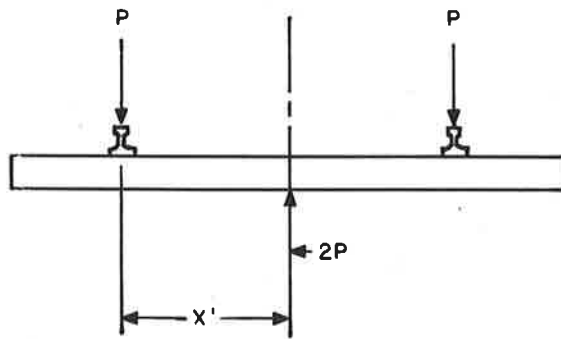
d)   "END−BOUND" CONDITION

P = RAIL SEAT REACTION

$$M_2 = P \cdot X'$$
$$V_2 = P$$

e)   "CENTER−BOUND" CONDITION

FIGURE 5.2.   (Continued)

DESIGN CONDITIONS FOR EXTREMES

where L = x (from Figure 3.2b)

ℓ = tie length in inches

t = tie depth in inches

Solution of this equation for normal size wood ties results in a L value in the range of one third of ℓ (or x is about one third of ℓ as shown in Figure 5.2b).

AREA suggests that x becomes ℓ/2 for concrete ties without any explanation. A comparison of relative flexural rigidities of concrete ties and wood ties for a given depth of tie is in the order of from four or five to one. The more rigid concrete tie would tend to deform less under load and would approach the condition of an infinitely rigid beam and a complete uniform reaction across the full length assuming continuous ballast support.

Recommended amplification of the elastically determined design tie load is then doubled to account for other factors. (See Section 5.1.5.3 for a discussion of load multipliers.)

5.1.5.3 Ballast Stress – Continuing research into the dynamic load/ strain relationship of ballast is in a state of relative infancy. For decades, the assumption was made that the ballast represented a uniform elastic type of support to the tie, whereas in fact it appears to be a random discrete series of bearing points.

The relationship between permanent strain and load cycles has been studied, but the problem of dynamic loading (impact stress) at high speed has not been properly researched.

Distribution of stresses from the bottom of tie level to the top of subgrade level is routinely handled in the AREA. Specifications by assuming a stress pyramid comprised of a lateral base width equal to the length of tie plus the depth of ballast plus the depth of fill and a longitudinal base width of three feet plus the depth of ballast and fill, but not more than the axle spacing.

106

This specification is used to compute the static load intensity on a buried structure (e.g. box culvert, etc.):

$$\delta_v = \frac{P}{(\ell_t + d)\ (z)}$$ (7)

where  $P$ = axle load

  $\ell_t$ = tie length

  $d$ = depth of soil and ballast

  $z$ = the lesser of $3' + d$ or axle spacing

  $\delta_v$ = vertical static pressure on buried surface

Dynamic load contribution is assumed to vary linearly from a maximum of 40%, where base of rail is in contact with the surface, to 0% where base of rail is 10 feet above the surface.  No reference to a variation with velocity is made.  It is assumed that the values, therefore, are for speeds of 40 mph or more, to be consistent with other sections in the manual.

In determining ballast pressures, AREA recommends a limiting value of stress as 65 psi applied by the tie.  Since measured loads under ties have been found to be frequently 1.66 times and infrequently found to be as much as 2.7 times the elastic theory load, a design value of twice the elastic theory tie load is recommended in determination of ballast stress.  AREA notes the reasons for the measured amplification factors are related to items such as play between rail and tie plate, non-uniform tamping of ties and general variations in roadbed firmness.

5.1.5.4  Distribution of Stress to Subgrade – While AREA endorses a 20 psi limit to applied subgrade stress, four equations are furnished to compute the required ballast depth to accomplish this limiting stress of 20 psi.  No explanation is offered in AREA as to which formula produces the most reasonable value.  These equations are presented below:

Talbot Equation $$P_s = \frac{16.8 P_b}{h^{1.25}}$$ (8)

Japanese National Railways $$P_s = \frac{50\ P_b}{10 + h^{1.35}}$$ (9)
(h in centimeters)

Boussinesq Equation $$P_s = \frac{3q_o}{2\pi h^2} \qquad (10)$$

Love's Equation $$P_s = P_b \left\{ 1 - \left(\frac{1}{1 + (r/h)^2}\right)^{1.5} \right\} \quad (11)$$

Where $P_s$ = 20 psi = pressure at top of subgrade

$P_b$ = intensity of pressure applied to ballast
= $q_o/A_b$

$q_o$ = twice the rail seat load

$A_b$ = effective tie bearing area (see Section 5.1.5.2 and next page)

$h$ = required depth of ballast under tie (inches except as noted above)

$r$ = radius of a circle whose area is equal to $A_b$

Solutions of these formulae to suit AREA limits yield the following values of ballast depth. ($P_b$ taken = 65 psi).

| Equation | h |
|---|---|
| Talbot | 24.5" |
| J.N.R.    (41.4 cm) | 16.3" |
| Boussinesq | 20.2"[*] |
| Love | 17.4"[*] |

[*]Based upon an assumed bearing length of 33 inches and a tie width of 8".

Talbot's Equation results in a fairly deep ballast section.  If sub-ballast is included as part of the required "h" value, then the resulting section is still deeper by (six inches more or less) than the majority of existing main line track sections.  The Japanese National Railways result is predicated upon narrow gage track, as reported by G.P. Raymond (Reference 5.3), and should not be used in its present form for standard gage track.  The Boussinesq and related Love Equations are applications of theoretical soil mechanics principles.

Since one classical method of investigation of sub-surface stress distribution is analysis by the Boussinesq equation, the use of this method has found acceptance within the railroad industry.  Vertical

stress can be estimated by this method since the distribution is practically independent of the physical properties of the soil. This is not the case of other components of stress as indicated below:

$$\delta_v = \frac{3Q}{2\pi z^2} \left\{ \frac{1}{1 + (r/z)^2} \right\}^{5/2} \quad \text{Boussinesq Equation} \tag{12}$$

where  Q = total point load applied

 $\delta_v$ = normal or vertical stress resulting at a point due to load

 r&z = are dimensions shown in Figure 5.3.

While the Boussinesq Equation gives a reasonable estimate of vertical pressure at a point due to a surface load Q located a horizontal distance r and a vertical distance z from the point, its associated method, the Newmark Influence Chart, relates the total vertical pressure at a point (or points) due to several loads that can be assumed to form a uniformly distributed load.

Ballast depths and the stress distribution to the top of the sub-grade have been evaluated by first determining an effective bearing area of the tie. As indicated in Section 5.1.5.2, repeated tests seem to indicate that on a reasonably well maintained track, in which there is no "center-bound" or "end-bound" condition, the bearing length under each rail seat is close to one third of the tie length:

For the usual condition of wood ties:

 $A_b \cong (L/3)b$ = Bearing area

where L = total tie length (standard = 102")

 b = tie width inches

for standard 7" x 9" x 8'-6" tie

 $A_b = (102/3)9 = 306 \text{ in}^2$.

Love's Equation, an extension of the Boussinesq theory, is used to predict pressure exerted onto the subgrade by distribution through the ballast and sub-ballast layer and is given previously in Equation 11.
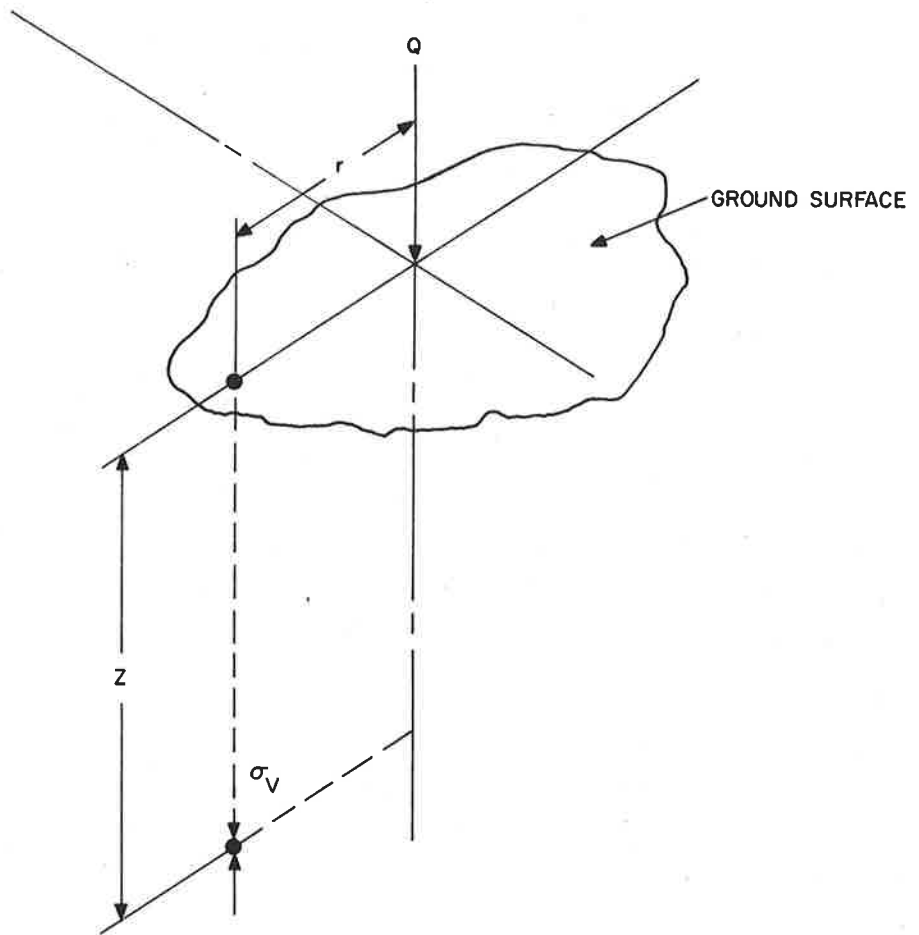
FIGURE 5.3.   VERTICAL PRESSURE GEOMETRY

Standard practice for both railroad and rapid transit is usually about 12 inches of ballast with some sub-ballast. Rule of thumb procedure is to reduce the stress applied to the subgrade, from the dynamic wheel loads, to 60 percent of the presumptive "safe" bearing value. This is comparable to the AREA value of 20 psi using the multiplier of 2 times the elastically determined dynamic tie load: 60% x 65 psi ÷ 2 = 19.5 psi. It is anticipated that the 40 percent cushion will cover effects from track irregularities and uneven tie bearing conditions, etc.

For typical domestic railroads, subgrade stress levels range from 20 to 35 psi where 12 inches of ballast alone is used and range from 12 to 18 psi where 12 inches of ballast with 6" of sub-ballast is used to carry E80 loads on a subgrade (load from locomotive E80) whose response value $k_r$ (see Equation 1) ranges from 1000 psi to 4000 psi respectively. Computed stresses from the dynamic wheel loads are elastically distributed, but are not doubled (as used in the previous examples of ballast depth equations).

Some of the more common conditions presented by Clarke (Reference 5.4) are shown below:

| Soil Description | Safe Brg. Press. | Design Brg. Press. |
|---|---|---|
| Alluvial soil | <10 psi | <6 psi |
| Uncompacted embankment | 10-15 psi | 7-9 psi |
| Soft clay, wet or loose sand | 16-20 psi | 10-12 psi |
| Dry gravel | 31-40 psi | 19-24 psi |
| Compacted soils | <41 psi | <25 psi |

Clarke assumes that the design pressure should be sixty percent of the safe bearing pressure. Based upon Clarke's values, and E80 loading, some soil classifications may not meet the design criteria without more subballast. The minimum value of k assumed as 1000 for this analysis may be high for some of these lesser strength soils. Values of top of subgrade pressure increase with increasing values of k.

5.1.5.5 Dynamics - Earlier discussions mentioned the fact that research in dynamic loads is continuing.  It is a recognized fact that there are many factors influencing the intensities due to dynamics.  Flat spots on wheels, rail imperfections, rail joints, horizontal and vertical misalignment of rails, vehicle unsprung mass vs. sprung mass ratios and track structure stiffness are but a few of the factors that make modeling this problem extremely complex.

In spite of this, there are several formulae that are generally accepted that account for dynamic multipliers of static loads.  Among them is a factor adopted by the AAR (Association of American Railroads):

$$K = 33V/100D \tag{13}$$

where
$V$ = velocity in miles per hour

$D$ = driven wheel diameter in inches

$K$ = impact factor expressed as a decimal

More recent investigations have produced more complex results. German and French engineers have been using a dynamic coefficient that does not vary linearly with velocity.  Figure 3.4 is a plot of the variation of dynamic multiplier, $K$, with velocity, $V$.  Curve "a" is from the French and German method, while curve "b" is from the AAR (Equation 13).

Some studies, such as those conducted in Japan, have determined wide ranges of variation in K values for different vehicle weights and suspension systems.  It is felt that the complexity of this interaction demands more research.

Faced with a need to estimate dynamic effects now, the design engineer must settle for the AAR version for conventional railroad track.  Perhaps the use of Curve a in Figure 5.4 is more fitting for rapid transit design as the axle loads of domestic transit equipment are closer to much of the European standard rail equipment than to domestic standard rail equipment.  Also, the use of CWR eliminates the high impact found at joints as determined in Equation 13.
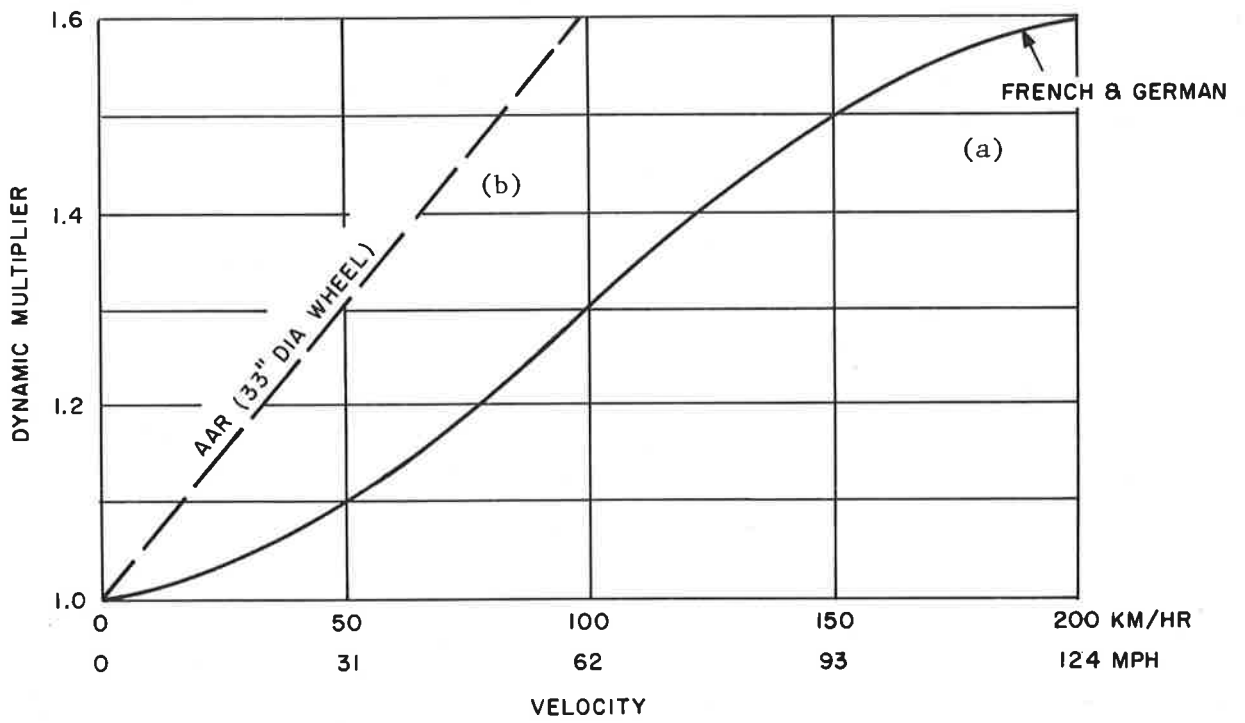
FIGURE 5.4. RAIL IMPACT LOADING VERSUS VELOCITY

113

5.1.5.6  Lateral Forces and Rail Buckling – Continuing research into lateral forces and rail stability is aimed at defining the reasons for observed conditions, and is of particular importance with continuous welded rail (CWR) installation.  Several items become critical in CWR installations, and these can be categorized as follows:

- (a)  track geometry
- (b)  thermal stress
- (c)  braking, traction and other vehicle induced forces.

a.    Track Geometry

In the absence of vehicle loading, geometrically induced forces become temperature dependent and are discussed in the next subsection. With vehicle loads considered, a variety of horizontal forces are applied to the rail.

There is, first, the so-called "hunting" or tracking forces exerted when the trucks skew slightly from an alignment that is tangent to the track.  This skew or angle of attack, when in the order of one degree, can cause a lateral force in the rail equal to the maximum adhesion force.  For usual dry rail conditions, the lateral adhesion force can be as high as 25 to 35 percent of the vertical wheel loads.

The lateral force caused by deficient superelevation for a given line speed can be derived from the formula for centrifugal force.

$$F = WV^2/gR \tag{14}$$

where    $F$ = centrifugal force

$W$ = weight of vehicle

$V$ = velocity of vehicle (ft./sec)

$R$ = radius of curvature in feet

$g$ = acceleration of gravity 32.16 ft/sec$^2$

To offset the force $F$, the outer rail is raised (superelevated) so that the lateral rail force is balanced at a selected velocity as determined below (see Figure 5.5 for nomenclature)

$$\text{Tan}\theta = E/B = F/W = WV^2/WgR = V^2/gR$$

$$E = BV^2/gR$$
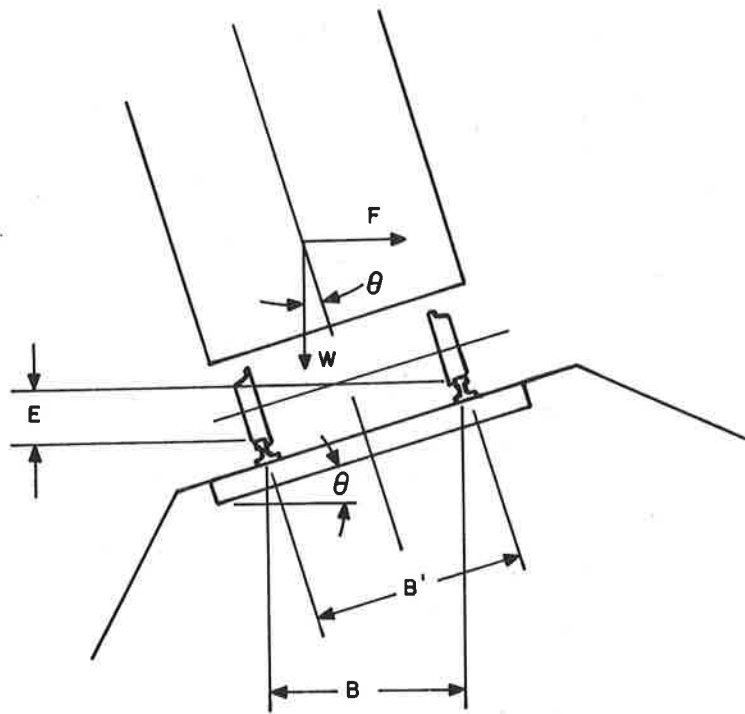
FOR SMALL VALUES OF $\theta$, $B' \cong B$

FIGURE 5.5.   DEFINITION OF TERMS — SUPERELEVATION

115

This latter formula is the AREA formula for equilibrium condition superelevation. By rearrangement,

$$V^2 = EgR/B$$

Whereby substitution of this expression into the expression for F yields

$$F = EW/B$$

Let the amount of elevation required for equilibrium conditions be denoted by E and the actual elevation by $E_a$, the actual velocity by $V_a$. Then the deficient amount of superelevation is:

$$\Delta E = (E - E_a)$$

and the unbalanced lateral force, $F_u$, due to insufficient superelevation or overspeed become:

$$F_u = W \, (\Delta E)/B$$

$$F_u = W \, (V^2 - V_a^2)/gR \qquad (15)$$

Finally, lateral loading of the rail can result from wheel forces in track with horizontal misalignment or tight gage conditions. These forces are not easily expressed in a formula due to the dependency on both the shape and severity of the defect.

b.   Thermal Stress

The potential for problems with CWR is generally one of thermally induced buckling, the chance of which can be increased greatly by the passage of trains, poor maintenance and installation procedures. Adequate coverage of the latter two topics would require a separate study. Superficially, any procedure that reduces the friction between ties and ballast, or lessens the effective lateral resistance of the track or lessens the weight of the ties or rails enhances the chance of buckling. Examples of the above would be tamping track, especially on a hot day; removal of the ballast shoulder; reducing the weight on rails by letting ties become unfastened.

Similarly to the last cause mentioned, the passage of wheel loads, as shown earlier (see Figure 5.1c) causes negative rail deflection ahead or behind (depending on axle spacing). Negative deflection actually means rail lift-off, a situation that is reducing both the lateral and vertical resistance to buckling. It becomes obvious, that heavy ties (such as concrete ties) tend to reduce the detrimental effects of rail lift-off.

An additional cause for concern is the installation of CWR in a temperature environment that is either too hot or too cold. Failure of the track under these circumstances can be thermal buckling or rail pull-apart.

Although many tests have been conducted for determination of safe conditions (track stability) of CWR, A.D. Kerr's (Reference 5.5) investigation of these models has pointed out the shortcomings of such analyses. While much of the work has been based upon forced solutions, wherein the derived equations are forced to agree with test model results (or the reverse) by limiting or incorrect assumptions, one phenomenon emerged from the tests of actual track sections that raises some concern for marginally stable CWR installation. From limited tests, where thermal stress was applied to test sections of ballasted track, it was noted that application of an increase in rail temperature from ambient conditions to a level $T_1$ (just less than the temperature necessary to cause buckling ($T_{cr}$) could not be repeated without inducing buckling at a temperature less than $T_1$. Temperature $T_1$, having been defined as that temperature at which a certain lateral displacement would occur without buckling, seems to be subject to some variation similar to a fatigue condition in a structural member subjected to large changes in stress due to load passages.

Within the past year Dr. Arnold D. Kerr has developed a more precise model for lateral track buckling (Reference 5.6).

Track geometry can also contribute to lateral movement under thermal stress. Consider the cold weather condition for CWR in a sharp curve.

117

The inside curve component of the rail tensile stress can be shown to be approximated by the expression:

$$F_i = N \, T \, (\text{Sin}\theta) \tag{16}$$

Where $F_i$ = inward force

$N$ = induced rail tensile force per 1°F temp. change (=0.0000065AE)

$T$ = temperature change

$\theta$ = central angle of curve for 1 foot of arc

$A$ = cross sectional area of rail

$E$ = modulus of elasticity of rail

For small values of $\theta$, $\text{Sin}\theta$ approaches $\theta$ in radians or $\text{Sin}\theta = 1/R$, where R is the radius of the curve. If the lateral resistance of the track structure is known, then the limiting radius can be determined that does not produce an $F_i$ greater than the lateral resistance with some margin of safety. Of course, the inward force $F_i$ for cold weather becomes an outward force $F_o$ in hot weather and a similar analysis can be made. These conditions, again, can be aggrevated by the same conditions outlined at the start of this subsection.

Once again, due to the vast complexity involved in prediction of track buckling, further complicated by the conditions described in the preceding sections, and because no universally accepted and proven mathematical model has yet been made, good engineering judgement and experience has become the best available design aids. Some parameters have been evaluated, such as the field measurement of lateral resistance of a particular piece of track. If a certain minimum value of required resistance is known to have been adequate, through experience, its value becomes a basis for use under similar track conditions.

c. Braking, Traction and Other Vehicle Induced Forces

Section 5.1.5.6a addressed the lateral force produced by truck "hunting", superelevation deficiency or overspeed generation of lateral rail head loading and lateral loads caused by track alignment deficiency. Of concern in this subsection are the miscellaneous forces causing rail stresses that enhance the chances of rail buckling.

Application of train brakes under normal conditions can cause some lateral (nosing) force as well as a longitudinal (axial) rail load. Since both of these forces can decrease the margin of safety against track buckling, they are of concern.

As a limit, braking longitudinal force can reach the adhesion limit of the wheel-rail interface; a value of 25 percent (or higher) of the wheel loads, under unusual conditions, might be applied. Nosing or lateral loading is not easily defined. AREA has recommended that, on bridges, a value of 25 percent of the heaviest design axle load be used. Traction force is effectively similar to braking (except opposite in direction and without the nosing force) in magnitude.

Experience has shown that there is concern for stress build-up due to longitudinal flow in rails. Both vertical geometry and train direction cause this phenomenon. Flow is particularly evident in single direction operation of track wherein a residual stress is built up from constant traffic in one direction, and most noticeably at the sag areas of steep grade vertical curves, where, through braking or tractive forces, the rail is being "dragged" or pushed downhill.

Again, this effect is difficult to express as any percentage of gross tonnage, or the like, due to variables involved. However, knowledge of its existence and the fact that it can contribute to buckling can temper design decisions.

5.1.5.7 Allowable Rail Stress - Common practice is to limit the design stress to a percentage of the yield stress by applying factors to account for the various loads being applied to the rail. G.M. Magee, of the AAR Research Center, developed the following relationship:

$$\delta = \frac{(\delta_y - \delta_t)}{(1+K_l)\ (1+K_w)\ (1+K_u)\ (1+K_c)} \tag{17}$$

where  $\delta_y$ = yield stress of rail 60,000 to 70,000 psi

$\delta_t$ = thermal stress CWR - usually 20,000 psi

$K_l$ = lateral bending factor = 0.20±

$K_w$ = rail wear factor = 0.15±

$K_u$ = unbalanced superelevation factor = 0.15$\pm$

$K_c$ = track condition factor = 0.25

$\delta$ = allowable bending stress about x axis

$$\delta = \frac{(\delta_y - 20000)}{(1.20)\ (1.15)\ (1.15)\ (1.25)} = 0.504\ (\delta_y - 20000)$$

For $\delta_y$ = 70000 psi then $\delta$ = 25000 psi.

## 5.1.6 Transit Track Design

Recent designs have retained standard rail and rail components for many of the rapid transit systems now under construction. It has been shown in this section that for reasons of economics (component standardization) and also for stability (against track buckling), the use of heavy rails and ties in standard ballasted track construction is justified.

The great temptation, in transit design, is to question the use of standard rails if one looks into design from the aspects of stress alone. Yet, the earlier discussion clearly indicates the need to consider a host of other factors. Among these, and particularly for the usual transit alignment, is the curve wear on rails. Since sharp curves are generally required in most transit systems, this parameter may be the most important of all. Therefore, a reduction of rail weight, using available standard rails, might involve only a small initial savings while generating a large maintenance cost.

## 5.1.7 Future Studies

One possible change might be to depart from standard rails, to produce a rail with a large head while trimming some of the base. Determination of rail fasteners, tie plates and other components to allow a decrease in the base would have to be made along with a cost study of any special order parts as well as special order rails.

Reduction of weight in track might be fine for use in tunnels, where there is little concern for buckling of the track. On surface lines, however, any reduction of gravity load must be measured against the increased tendancy of buckling. Increasing use of concrete ties is noticed in both the transit and railroad industries. Benefits to be

gained by their use can be in both maintenance and in design. Since the concrete tie weight is considerably greater than wood ties (for any reasonable tie spacing) a gain in offsetting buckling forces (where there is concern for buckling) has been realized. Potentially, there may be more reason to change rail sections due to both the increase in gravity load of the ties plus the fact that fastenings for rail-to-concrete tie can be (and are) more rigid (torsionally rigid) which promotes lateral strength against buckling, rail overturning, gauge widening and other undesirable results.

## 5.2 CURRENT NUMERICAL MODELS

Section 5.1.5 provides a discussion of current railroad and transit design practices based on AREA recommendations. The designer that is guided by the AREA methods is using empirical or classical elasticity equations to analyze the pressure distributions in the ballast and subgrade. These design equations are discussed further in References 5.1, 5.2, 5.7, and 5.8, based on their limitations and applicability. Many of these equations have been correlated with railroad data (References 5.7 and 5.8) but the load levels and tie spacing are significantly different from those used in rapid transit system; thus, the unqualified use of these equations for rapid transit design might be questioned.

With the availability of high speed computers the Federal Railroad Administration has sponsored the development of several numerical analyses for determining the load distribution in cross tie-ballast track systems. Two of these computer programs, ILLITRACK and MULTA (References 5.9 and 5.10), have been evaluated in this study. Both programs were used for a preliminary analysis of the transit roadbed pressure distribution in order to determine a calibration range for the experimental pressure transducers. After the experimental data base was obtained from the TTT (see Sections 3 and 4), a correlation study was performed with both ILLITRACK and MULTA.

An excellent discussion of these two computer models and other available numerical analyses is contained in References 5.2, 5.7, 5.11, 5.12, and 5.13. These studies examine both ILLITRACK and MULTA based on a wide variety of track material and geometric configurations, and

attempt to evaluate the magnitude of various parametric effects. The use of these analyses in this study was to determine their usefulness for rapid transit design. All of the studies referenced above have examined these codes for only railroad configurations (wood ties, close tie spacing, deep ballast, heavy loads, and fine grained soils), and their predictive capabilities for concrete ties, wide tie spacing, shallow ballast, transit loads and sandy subgrade soil were unknown. In the following subsections each computer code will be evaluated based on model assembly and applicability. Section 4 discusses in further detail the correlation of the numerical predictions with the experimental data base.

5.2.1 ILLITRACK

The University of Illinois was contracted in the 1970's by the FRA to develop an analytical model of railroad track support systems. The work of Robnett, et al (Reference 5.14) evolved into the ILLITRACK computer code (Reference 5.9), a quasi-three-dimensional finite element model. This model utilizes a longitudinal two-dimensional analysis to establish load distribution along the track, followed by a transverse two-dimensional analysis of a selected tie to determine particular ballast and subgrade response. A pseudo-plane strain formulation is used to couple the two two-dimensional analyses into an approximate three-dimensional load dissipation description. The pseudo-plane-strain method (Reference 5.15) allows the finite elements to increase in thickness as the depth into the roadbed increases to account for realistic pressure dissipation, as shown in Figure 5.6. However this requires the user to estimate a dissipation factor $\phi$ for the soil and an assumed bearing length, L, for the tie. These parameters are essential in calculating the actual pressure dissipation with depth in the roadbed material. For this analysis, after some investigation and discussion (References 5.11, 5.16, and 5.17), a standard value was chosen for both of these distribution parameters in the present study.

L = EFFECTIVE BEARING LENGTH
    OF TIE
W = WIDTH OF TIE
t = THICKNESS OF ELEMENT IN PLANE
    STRAIN ANALYSIS
t' = THICKNESS OF ELEMENT IN
    PSEUDO-PLANE STRAIN
    ANALYSIS
$\phi$ = ANGLE OF DISTRIBUTION

a) TRANSVERSE ANALYSIS

b) LONGITUDINAL ANALYSIS
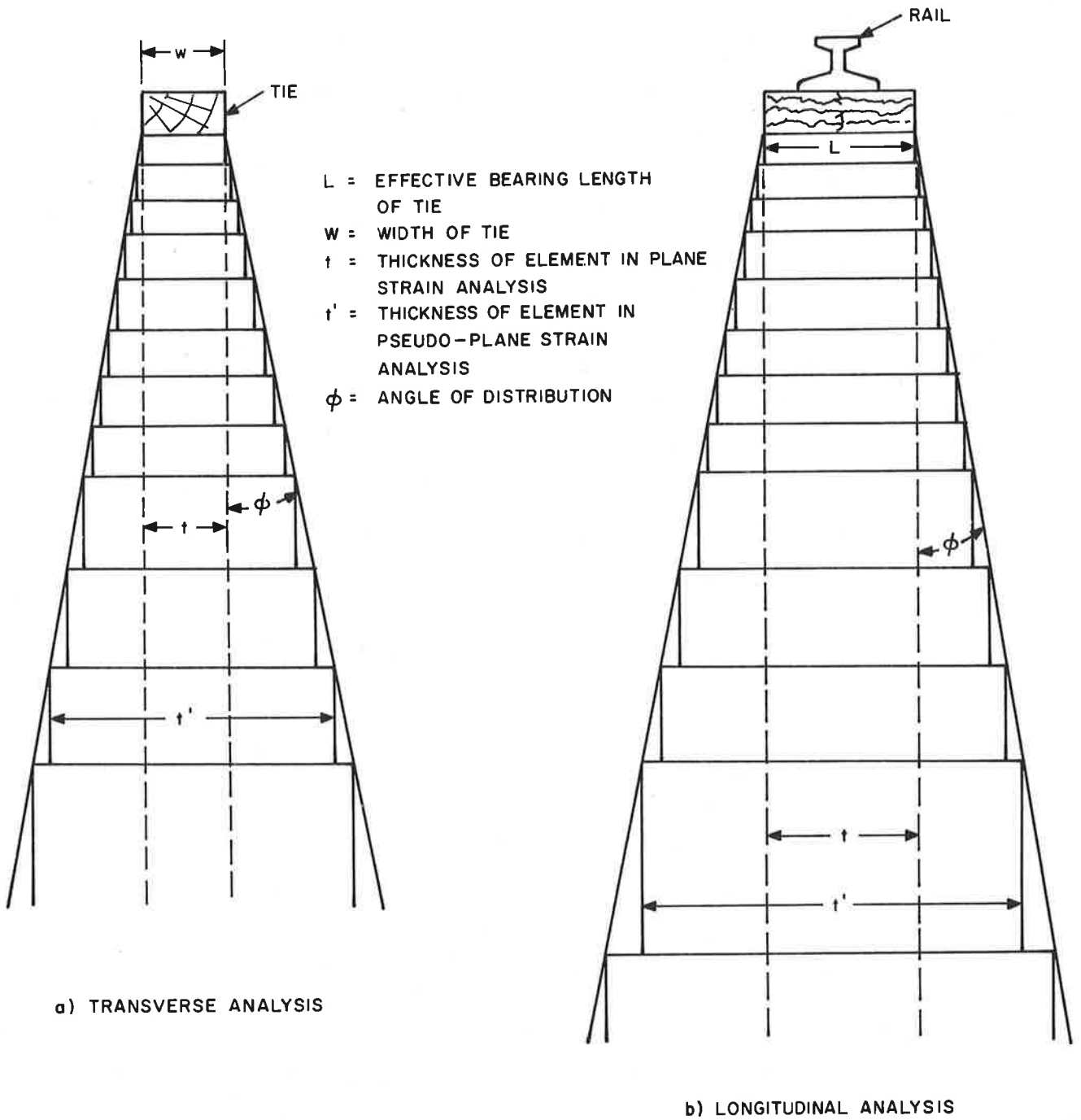
*OBTAINED FROM REFERENCE 5.9

FIGURE 5.6.*    PSEUDO-PLANE STRAIN APPROXIMATION

The original ILLITRACK work (References 5.9, 5.13, 5.15) uses a dispersion angle, $\phi$, equal to ten degrees. However the work of Chang and the discussions with Thompson (References 5.11, 5.16) led to the use of 35 degrees for $\phi$ for sandy soils. Final calculations using the ILLITRACK model show that for the UMTA test site a variation of $\phi$ from $25°-45°$ produces only a two percent change in tie settlement and a ten percent change in top of subgrade pressure predictions. For the value of L, the bearing length, the standard AREA representation of L for a concrete tie was used as $\ell/2$ where $\ell$ equals the total tie length. If the L normally associated with a wooden tie is used (30 inches) and compared to $L=\ell/2$ (54 inches) the ballast and subgrade surface pressures are altered by as much as eighty percent or approximately as much as the ratio of bearing lengths. The confirmation of using $L=\ell/2$ for the Gerwick RT-7 Mark 38 concrete ties is given in Section 5 which shows that the ballast and subgrade pressures are associated more closely with the $L=\ell/2$ bearing length tie description.

The ILLITRACK computer code allows the user the option to choose a nonlinear material description of the roadbed ballast and subgrade. For the ballast and subballast used on the TTT, material models that were empirically formulated for similar material on the FAST track at TTC were utilized. The basic nonlinear material model for the ballast and subballast was taken from triaxial test results given in Reference 3.11 as:

Ballast: $E_r = 7735 \, (\theta)^{0.51}$, $\nu = 0.35$

Subballast: $E_r = 2182 \, (\theta)^{0.69}$, $\nu = 0.40$

where $E_r$ = Resilient Modulus = $\dfrac{\text{Deviator Stress}}{\text{Recoverable Axial Strain}}$

$\theta$ = First Stress Invarient = $\sigma_1 + \sigma_2 + \sigma_3$ = Sum of Principal Stresses

$\nu$ = Poisson's Ratio

The effect of variation in ballast properties was studied by changing the resilient modulus as follows:

$$E_r = 10200 \, (\theta)^{0.5}$$
$$E_r = 5000 \, (\theta)^{0.6}$$

This variation was similar to those indicated in References 5.18 and 5.19, and resulted in only a one percent change in predicted rail seat load, a two percent change in ballast deflection and a maximum seven percent change in ballast and subgrade pressures. There was no provision in this contract to perform triaxial tests on the actual ballast and subballast so the material properties of the similar FAST ballast and subballast were adopted for the entire ILLITRACK study.

One of the thrusts of this study was to examine the response of the roadbed subgrade soil to transit vehicle induced forces. This effort included a sampling of the soil and the performance of a small series of triaxial tests (see Section 4) to determine the subgrade nonlinear material properties. Preliminary use of the ILLITRACK program necessitated the utilization of data from the TTC FAST track located approximately one-half mile from the UMTA test site. The basic soil properties from References 5.11 and 5.19 are:

$$E_r = 523 \ (\theta)^{1.08}, \ \nu = 0.45, \ E = 5000 \ \text{psi}$$

where E is the initial Young's modulus.

Seismic tests performed by TTC in 1971 show an initial E = 38000 psi and $\nu = 0.35$. ILLITRACK was excercised with the above values and E = 20000, $\nu = 0.35$ and the predicted responses varied by less than five percent for rail seat load and pressure distribution. The nonlinear resilient response curve was then varied as follows;

$$E_r = 260(\theta)^{1.50}$$
$$E_r = 1000(\theta)^{0.75}$$

There were twenty-five percent variations in predicted response. This demonstrates the importance of accurate material models. The subgrade model determined after the current triaxial soil tests is:

$$E_r = 504(\theta)^{0.86}, \ \nu = 0.22, \ E = 4000$$

and the predictions are discussed in Section 5.

The ILLITRACK computer code is structured to handle three types of numerical solution procedures and two methods of combining the longitudinal and transverse response predictions. The nonlinear analysis techniques include: additive incremental loading, equal incremental

loading, and an iterative loading technique. The equal incremental loading technique sums up the deformations at the end of each load step to obtain the cumulative deformation pattern and then solves for the stresses and strains. This method was tried for the sandy soil subgrade and no solution convergence was perceived for trials of 3, 4, or 6 steps in the solution. The additive incremental solution resolves the problem at the end of each step with an additional load and after the final step performs a single iteration with the new moduli values to determine the stress and deformation state. This method showed reasonable convergence for either 3 or 6 steps. However, discussions with Dr. Thompson (Reference 5.16) indicated that no previous work had been performed with granular subgrade material (sandy soil) using the ILLITRACK program. The recommendation from Dr. Thompson was to use the iterative solution which applies the full load at once and then performs an assigned number of iterations. This technique worked well and showed excellent convergence for either 4 or 6 iterations and became the solution method used throughout this study.

There are two means by which the predictions from the longitudinal analysis can be used to start the transverse analysis. The tie deflection can be input to the transverse analysis as an initial deflection or the rail seat load can be input as an assumed force. For fine grained soils the initial displacement method has been checked by the authors of ILLITRACK and shows reasonable convergence. However, for granular soils (sandy) the initial displacement method is too stiff and unreasonably large tie reaction forces are calculated in the transverse analysis. Therefore, (Reference 5.16), the initial force method is recommended for sandy soil, using the rail seat load calculated in the longitudinal analysis to start the transverse analysis.

Tables 5.1a, b and c give a summary of the main ILLITRACK prediction calculations performed during this study. Table 5.1a presents a description of the input parameters that are needed to use ILLITRACK (Reference 5.9), and gives a symbol table for the variables that will be compared in Tables 5.1b and c.

126

## TABLE 5.1a

### Key to ILLITRACK Analyses

**Solution Types**

A.I.  =  Additive Incremental

E.I.  =  Equal Step Incremental

I.T.  =  Iterative

I.D.  =  Initial Displacement

F.  =  Initial Force

**Failure Criterion**

$(\sigma_1/\sigma_3)_{max}$  =  10.0

$\sigma_{3_{min}}$  =  0.0 psi

$\tau_{subgrade}$  =  25.0 psi

**Failure Moduli**

Ballast = Subballast = 4000 psi
Subgrade = 100 psi

**Material Models**

All Subballast:  $E_r = 2182\theta^{0.60}$, E = 20000, $\nu$ = 0.4

Ballast:  B1:  $E_r = 7735\theta^{0.51}$, E = 30000, $\nu$ = 0.35

B2:  $E_r = 10200\theta^{0.51}$, E = 20000, $\nu$ = 0.4

B3:  $E_r = 5000\theta^{0.60}$, E = 20000, $\nu$ = 0.4

Subgrade:  SG1:  $E_r = 523\theta^{1.08}$,  E = 5000,  $\nu$ = 0.45

SG2:  $E_r = 523\theta^{1.08}$,  E = 20000, $\nu$ = 0.35

SG3:  $E_r = 260\theta^{1.5}$,  E = 5000,  $\nu$ = 0.45

SG4:  $E_r = 1000\theta^{0.75}$,  E = 5000,  $\nu$ = 0.45

SG5:  $E_r = 504\theta^{0.86}$,  E = 4000,  $\nu$ = 0.22

Tie:  T1:  Width = 10 in., I = 500, E = 5000000, $\nu$ = 0.0

T2:  Width = 11 in., I = 202, E = 4600000, $\nu$ = 0.0

T3:  Width = 11 in., I = 202, E = 4600000, $\nu$ = 0.3

### Basic ILLITRACK Parameters

Tie Spacing = 30 in.
Tie Length = 108 in.
Rail Gauge = 56.5 in.
Rail Size = 119 lb., E = 30000000, I = 71.4
Ballast Depth = 12 in.
Subballast Depth = 6 in.
Subgrade Depth = 258 in.
Applied Load = Two 16000 lb static wheel loads
Load Position = 55 in. and 137 in. from model center line
$\phi$ = Angle of Dispersion  
B.L. = Bearing Length   } Varied in Tables 5.1b and c.

127

TABLE 5.1b

ILLITRACK - Longitudinal - Tangent

| Solution Type/Steps | φ (deg) | B.L. (in.) | Tie | Ballast | Subgrade | Failure Inclusion | Rail Sent Load (lbs) | Tie Defl. (in.) | Pressure (psi) 2" / 6" / 15" / 21" |
|---|---|---|---|---|---|---|---|---|---|
| EI/ 3 | 35 | 30 | T1 | B1 | SG1 | No | 8256 | 0.230 | 20.8/12.7/ 5.9/ 4.6 |
| EI/ 4 | 35 | 30 | T1 | B1 | SG1 | No | 8676 | 0.125 | 23.2/14.1/ 6.5/ 4.8 |
| EI/ 6 | 35 | 30 | T1 | B1 | SG1 | No | 9932 | 0.024 | 27.3/18.4/ 9.5/ 6.2 |
| AI/ 3 | 35 | 30 | T1 | B1 | SG1 | No | 8347 | 0.160 | 22.9/13.4/ 6.0/ 4.6 |
| AI/ 6 | 35 | 30 | T1 | B1 | SG1 | No | 8686 | 0.164 | 24.2/16.3/ 6.9/ 4.9 |
| AI/ 3 | 35 | 30 | T1 | B1 | SG1 | Yes | 8074 | 0.175 | 17.2/12.4/ 9.3/ 5.2 |
| AI/ 3 | 10 | 18 | T1 | B1 | SG1 | No | 8218 | 0.151 | 36.9/24.0/13.3/10.6 |
| IT/ 3 | 35 | 30 | T1 | B1 | SG1 | No | 8611 | 0.162 | 21.9/13.6/ 6.3/ 4.8 |
| IT/ 6 | 35 | 30 | T1 | B1 | SG1 | No | 8799 | 0.165 | 24.9/16.9/ 7.2/ 5.1 |
| IT/ 4 | 35 | 54 | T1 | B1 | SG1 | No | 8733 | 0.163 | 13.7/ 9.0/ 4.2/ 3.4 |
| IT/ 4 | 35 | 54 | T2 | B1 | SG1 | No | 8816 | 0.162 | 12.4/ 8.7/ 4.2/ 3.3 |
| IT/ 4 | 35 | 30 | T1/90 in. | B1 | SG1 | No | 8665 | 0.164 | 24.1/14.8/ 6.6/ 4.9 |
| IT/ 4 | 35 | 54 | T3 | B1 | SG1 | No | 8816 | 0.162 | 12.4/ 8.7/ 4.2/ 3.4 |
| IT/ 4 | 25 | 54 | T2 | B1 | SG1 | No | 8794 | 0.159 | 12.4/ 8.9/ 4.5/ 3.7 |
| IT/ 4 | 45 | 54 | T2 | B1 | SG1 | No | 8766 | 0.165 | 12.4/ 8.3/ 3.8/ 2.9 |
| IT/ 4 | 35 | 54 | T2 Tie Spacing=27" | B1 | SG1 | No | 8310 | 0.148 | 11.8/ 7.6/ 4.0/ 3.3 |
| IT/ 4 | 35 | 54 | T2 | B2 | SG1 | No | 8813 | 0.160 | 12.6/ 8.7/ 4.0/ 3.3 |
| IT/ 4 | 35 | 54 | T2 | B3 | SG1 | No | 8889 | 0.165 | 12.6/ 9.3/ 4.5/ 3.5 |
| IT/ 4 | 35 | 54 | T2 | B1 | SG2 | No | 8744 | 0.247 | 12.8/ 8.3/ 3.9/ 3.5 |
| IT/ 4 | 35 | 54 | T2 | B1 | SG3 | No | 9647 | 0.276 | 14.3/11.1/ 5.2/ 3.9 |
| IT/ 4 | 35 | 54 | T2 | B1 | SG4 | No | 8729 | 0.092 | 11.0/ 7.7/ 4.1/ 3.3 |
| IT/ 4 | 35 | 54 | T2 | B1 | SG1 | Yes | 8353 | 0.171 | 13.1/ 6.7/ 4.4/ 3.3 |
| IT/ 4 | 35 | 54 | T2 | B1 | SG5 | No | 8132 | 0.367 | 9.5/ 6.5/ 3.5/ 2.8 |
| IT/ 4 | 35 | 54 | T2 | B1 | SG5 | Yes | 6966 | 0.79 | 10.4/ 5.1/ 2.3/ 4.6 |

TABLE 5.1c

ILLITRACK – Transverse – Tangent

| Solution Type/Steps | Loading | φ | Tie | Ballast | Subgrade | Failure Inclusion | Tie Reaction (lbs) | Tie Defl. (in.) | Pressure (Rail Seat) 2" | 6" | 15" | 21" |
|---|---|---|---|---|---|---|---|---|---|---|---|---|
| EI/ 3 | ID | 35 | T1 | B1 | SG1 | No | 14682 | 0.1 | 34.2 | – | – | – |
| EI/ [4] | ID | 35 | T1 | B1 | SG1 | No | 7111 | 0.1 | 14.9 | – | – | – |
| EI/ [6] | ID | 35 | T1 | B1 | SG1 | No | 1539 | 0.1 | 3.3 | – | – | – |
| AI/ 3 | ID | 35 | T1 | B1 | SG1 | No | 109317 | [0.160] | 285.0 | – | – | – |
| AI/ 6 | ID | 35 | T1 | B1 | SG1 | No | 3251 | 0.1 | 6.6 | – | – | – |
| AI/ 3 | ID | 35 | T1 | B1 | SG1 | [Yes] | 151576 | [0.177] | 453.0 | – | – | – |
| AI/ 3 | ID | [18] | T1 | B1 | SG1 | No | 48125 | [0.150] | 103.0 | – | – | – |
| IT/ 3 | ID | 35 | T1 | B1 | SG1 | No | 71065 | 0.1 | 101.6 | – | – | – |
| IT/ [6] | ID | 35 | T1 | B1 | SG1 | No | 103558 | 0.1 | 312.0 | – | – | – |
| IT/ 4 | [F] | 35 | T1 | B1 | SG1 | No | 8627 | 0.081 | 15.2 | 9.5 | 5.3 | 3.9 |
| IT/ 4 | F | 35 | T1 | B1 | SG1 | No | [8745] | 0.080 | 15.5 | 9.7 | 5.4 | 4.0 |
| IT/ 4 | F | 35 | [T2] | B1 | SG1 | No | 8823 | 0.085 | 19.1 | 11.8 | 6.1 | 4.4 |
| IT/ 4 | F | 35 | [T3] | B1 | SG1 | No | 8823 | 0.085 | 19.1 | 11.8 | 6.1 | 4.4 |
| IT/ 4 | F | [25] | T2 | B1 | SG1 | No | 8800 | 0.083 | 18.9 | 12.3 | 7.6 | 5.7 |
| IT/ 4 | F | [45] | T2 | B1 | SG1 | No | 8774 | 0.086 | 19.1 | 10.3 | 4.8 | 3.3 |
| IT/ 4 | F | 35 | T2 Spacing=27" | B1 | SG1 | No | 8318 | 0.085 | 17.7 | 11.0 | 5.7 | 4.1 |
| IT/ 4 | F | 35 | T2 | B1 | [SG5] | No | 8141 | 0.316 | 16.1 | 9.9 | 5.1 | 3.7 |
| IT/ 4 | F | 35 | T2 | B1 | [SG5] | [Yes] | 6969 | 0.405 | 13.8 | 9.2 | 5.5 | 4.3 |

129

Table 5.1b summarizes the longitudinal ILLITRACK runs, and Table 5.1c summarizes the transverse ILLITRACK runs. Note that a boxed in parameter signifies the variable that is being observed during the particular run. It is evident from both tables that the equal step incremental solution has not converged. The additive incremental and the iterative solution appear to be similar; however, the iterative solution technique was selected for most of the study. Tie T1 was the initial prototype model for comparisons and pre-experiment predictions, whereas tie T2 is geometrically similiar to the Gerwick RT-7 tie on the TTT. It should be noted that there are very slight differences in rail seat load, displacement and pressure prediction for these two tie models.

The bearing length variance shows large differences in pressure dissipation and distribution as mentioned earlier. The 54 inch bearing length is more consistent with the general industry perception of a concrete tie. The tie spacing variation from 30 inches to 27 inches shows a consistent deformation change. The 27 inch spacing is typical of the TTT curved sections and the gentle curve (3820 foot radius) allows the section to be treated as a tangent by ILLITRACK without much loss of modeling accuracy.

The greatest response variation is related to changes in subgrade material model. The range of material models SG2, SG3 and SG4 show significant response changes with changes in the resilient modulus curve. Changes in the initial Young's modulus and Poisson's ratio have negligible influence on the pressure distribution. Models SG1 and SG5 will be compared to the experimental data in Section 4 of this report.

5.2.2 MULTA

The MULTA computer code (Reference 5.10) is a combination of two computer codes: BURMISTER and LOADS AND COMBINATIONS. BURMISTER uses Burmister's multi-layer elastic theory to represent the ballast and soil layers (Figure 5.7). The LOADS AND COMBINATIONS code is a matrix

130

UNIFORMLY—LOADED SEGMENT OF TIE

EQUIVALENT UNIFORMLY—LOADED CIRCULAR AREA

LAYER PROPERTIES = $E_1$ , $\nu_1$        $h_1$

$E_2$ , $\nu_2$        $h_2$

$E_i$ , $\nu_i$        $h_i$

HALF SPACE : DEPTH = $\infty$
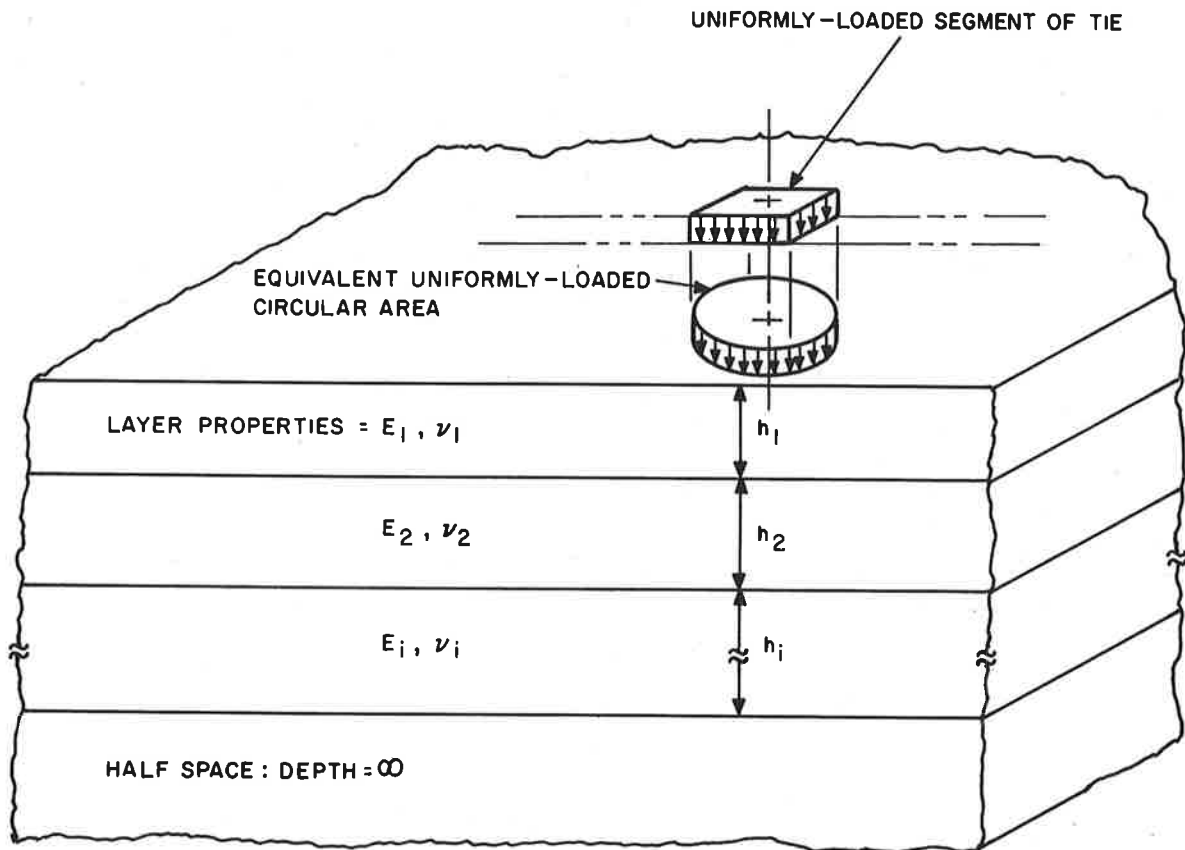
*OBTAINED FROM REFERENCE 5.10

FIGURE 5.7.*   SCHEMATIC DIAGRAM OF BURMISTER MODEL

structural analysis model which solves for the tie/ballast reactions using the method of consistent deformation; a schematic representation is given in Figure 5.8.

MULTA, unlike ILLITRACK, is a completely linear elastic solution analysis, with the roadbed represented by a maximum of three elastic layers (ballast, subballast, and semi-infinite subgrade), Reference 5.20. The user only has a choice of Young's modulus and Poisson's ratio for the description of the roadbed material. Table 5.2 shows the range of examples that were exercised through the MULTA code, and it should be noted that there is a one to one correspondence between the MULTA model and the ILLITRACK models in Table 5.1

Table 5.2 demonstrates that changes in the elastic material properties of the roadbed do not have as significant an effect on the resultant load distribution as did a corresponding change in the nonlinear material description of ILLITRACK. The subgrade model varied Young's modulus (E) from 37000 to 4000 with only a fifty percent change in top of subgrade pressure. The high value of E (37000) was determined from low stress level seismic tests (performed at TTT in 1971), and the low value of E (4000) was determined from KSC triaxial test data. It is reasonable to assume that the high value of E corresponds to the initial tangent modulus of the soil and that the low value of E corresponds to the secant modulus over the triaxial test range (10 psi difference in axial load, see Section 4). In light of this information it is more reasonable to use the predictions from soil models SG2 and SG3 (Table 5.2) to analyze the roadbed response of the TTT. Further comparisons of MULTA with the experimental data were presented in Section 4 of this report.
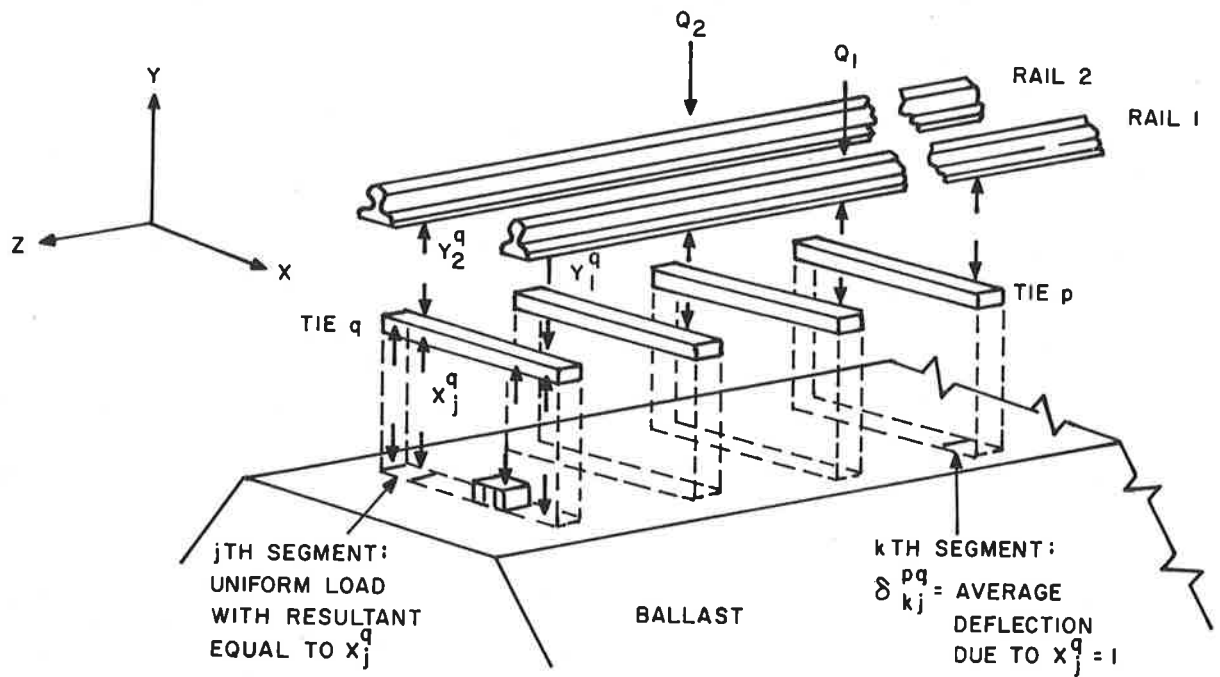
$^*$OBTAINED FROM REFERENCE 5.10

FIGURE 5.8.$^*$    SCHEMATIC DIAGRAM OF LAC CODE

TABLE 5.2

MULTA Analysis

|  | E (psi) | $\nu$ |
|---|---|---|
| All Ballast: | 30000 | 0.35 |
| All Subballast: | 20000 | 0.40 |
| Subgrade:  SG1 | 37000 | 0.365 |
|  SG2 | 5000 | 0.45 |
|  SG3 | 4000 | 0.22 |

Tie:    T1  10" x 108", cross section 100 $in^2$, I = 500, E = 5000000

T2  11" x 108", cross section  77 $in^2$, I = 202, E = 4600000

Rail:    cross section 11.65 $in^2$, E = 30000000, I = 71.4

Load:    One wheel 16000 lb symmetric about tie and rail
pressures show superposition of two wheel loads

| Tie | Subgrade | Rail Seat Load (lbs) | Tie Deflection (in) | Roadbed Pressures (psi) 0"/ 6"/15" |
|---|---|---|---|---|
| T1 | SG1 | 9837 | 0.012 | 18.2/9.2/6.7 |
| T2 | SG2 | 8467 | 0.041 | 14.2/6.0/3.7 |
| T3 | SG3 | 8391 | 0.048 | 14.1/5.8/3.4 |

# 6. TRANSIT TRACK DESIGN EVALUATION

## 6.1 TRANSIT VS RAILROAD DESIGN PARAMETERS

Since the concensus of industry clearly indicates that rapid
transit design philosophy is the railroad's foster child, a quick glance
at the similarities and differences is in order to understand how and
why things are as they are. Many parameters, in fact, show marked
differences and, at face value, may serve to stimulate questions as to
why rapid transit track construction resembles, closely, that of the
railroads.

Operationally, transit headways can vary from as little as 2 minutes
during peak periods to 30 minutes in the off peak hours with some
lighter service late at night (or all night on some systems). Frequency
of service on railroad freight and commuter lines varies tremendously
but 5 to 10 minute headways in heavy commuter rail territory is reason-
able during peaks with freight and commuter service often in the range
of 1/2 to 1 hour during off peak times. Commuter traffic rarely extends
late into the night, although freight is often hauled day and night. It
is important to note that, due to the relative infrequency of railroad
traffic as compared to that of transit, some very important differences
in both design and maintenance practice result. Some of these differences,
however, tend to impact on the results of other design considerations,
and these points are discussed later on.

Just as there are large differences in operations, so are there
large differences in loadings. A review of the major heavy rail transit
systems indicate that, on the average, axle loads vary from 20,000 to
27,000 lbs. Extremes in equipment show a low gross weight of 16,000 lbs
per axle to a high of about 35,000 lbs per axle, in the United States.
Railroad loads, governed by freight traffic, typically run 65,000 lbs
per axle and some roads operate even heavier axles. There is a ratio
of about 2 to 1 for axle loads, when comparing an average railroad
against an average transit axle.

Differences in grade and curvature can also be significant. While typical mainline railroads usually have maximum grades in the 1% range (although there are several exceptions in hilly country) and maximum curvature of 6 to 8 degrees, typical transit systems have grades of up to 5% maximum and curves of 25 to 30 degrees especially in the older systems. Curves found off the main lines of railroads (in yards, terminals, and on side tracks) are often sharper (up to 20 degrees or more) as are transit curves.

There are other differences in operating conditions that impose different design and maintenance restraints. One of these involves mixed service on railroads where high speed passenger trains and slow, heavy tonnage freights operate over the same trackage. Because of the differences in operating speeds, compensation for centrifugal force on curves (super-elevation) must be a compromise or, as is generally done, set for freight while passenger trains are run above the "balanced" or "equilibrium" speed of these curves. Aside from infrequent, slow speed operations (due to peak period jams or maintenance trains), all traffic moves close to or at design speeds which thus allows superelevation to be set for the balanced condition, where curvature permits. Sharp curves limit use of superelevation to (about) six inches out of concern for the stopped train condition.

Rail wear concerns are related to operating characteristics, such as the curve speed situation. Other factors influencing rail wear include braking and traction characteristics of equipment. Again, the railroad and transit equipment differ substantially. Braking characteristics of transit equipment allows for quicker stops than railroad equipment and all wheels (generally) of transit vehicles are powered as contrasted with locomotive, only, powered wheels of railroads.

The impact of these and other parameters is discussed in the next subsection of this report.

6.2  DEGREE OF CONSERVATISM IN TRACK DESIGN

As indicated previously, a comparison of typical gross axle loads between railroad and transit equipment will show railroad loads to be

in the range of 200% of the transit loads. Logically, then, the question
asked is why are the track structures so much alike, even down to
details? While this question is an obvious one, its answer is not so
obvious.

Several criteria influence the selection of track components,
and they are briefly outlined in the following paragraphs.

a)    Rail Stress and Deflection

In most instances, deflection criteria controls the design as
the recommended maximum value (0.25 in) is attained with rail
bending stress at about 85 to 90% of the allowable stress. Relaxation
of the deflection limit could result in a theoretical reduction in
rail size needed to suit stress criteria. However, an increase in
rail deflection is almost certain to cause an increase in track
deterioration. It is unlikely that possible small savings in rail
weight could outgain the losses of increased maintenance costs.

b)    Tie Size and Spacing

Track modulus, which is a measure of stiffness of the track
structure and, therefore, has a direct bearing upon track deflection,
can be altered by tie size and spacing selection. The stiffer the
track structure becomes, the smaller track deflection is (and a
corresponding decrease in rail stress results). A comparison of
various tie size, spacing, and rail combinations can be made in
order to select the most economical one. By increasing tie size or
by decreasing tie spacing (or by both) it may be possible to
decrease rail size. In Appendix F a series of possible component
combinations was analyzed for two rapid transit car loadings and
the material costs were computed. Certain general rules and guide-
lines were extracted from the results of the calculations, and
these are discussed in Section 6.4 of this report. In the cal-
culations of Appendix F, wood ties were used primarily because of
the abundance of data available on their use.

c) Ballast Depth

There is little doubt that increasing ballast depth will increase track stiffness, but there is no universally accepted convenient formula and little has been done in the field to measure changes in stiffness by changing ballast depth. Because this parameter can effect other component selections (just as tie size and spacing can effect rail selection), it needs to be better understood. Use of this method to increase track modulus (stiffness) may well be the most economical way.

Other considerations which impact upon ballast depth include the provision of sufficient depth to permit free drainage of water from the ties and sufficient depth to allow tie tamping. Another depth consideration is the depth which is sufficient to prevent contamination of ballast from fine soils below, although recent use of geocloths (filter fabrics) have proven to be very effective at keeping the ballast clean and free draining.

d) Vehicle Selection

There is evidence of the need to make transit vehicles compatible with the track structure stiffness that exists in the field. Extreme cases of accelerated rail wear on curves have been noted where some of the newer transit equipment, utilizing stiff trucks for improved ride quality, is operating over a rigid track structure. Rail wear rates, in such instances, have been far greater than predicted for these relatively light axle loads. Braking rates of transit vehicles are high, and evidence of rail "corrugations" at station approaches is linked to these sudden decelerations. Rail corrugation is another form of rail wear that is causing concern. Curve worn and corrugated rail is a problem common to both railroads and transit, but braking wear (corrugation) is associated with only the transit systems.

e)    Traction Power

       Traction power requirements, for the modern transit system,
can impact the rail size selection.  Since the running rails are
used as negative returns for power, the designer must provide a
system that is economical from both the structural and electrical
aspects.  By increasing the running rail size, it may be possible
to reduce or eliminate other high cost items.  Power substations
may be spaced farther apart, and the use of expensive supplementary
returns (large cables acting along with the rails as a power return)
may not be required if a larger rail size is used.  In close headway,
close station, and heavy load systems the use of 75 lb rail, satisfying
the stress and deflection criteria, may not otherwise be an economical
choice.

f)    Maintenance and Operating Policies

       Component selection is heavily influenced by maintenance and
operating department concerns.  Since transit systems typically
have very close headways, as discussed in Section 6.1, major
maintenance projects, such as rail replacement, can disrupt the
system.  Accordingly, the maintenance and operations staff tend to
resist a minimal design and insist on durability at the expense of
initial cost.  Truly, their concerns are valid and their input for
design criteria is important.

g)    Component Availability

       While 75 pound rail may satisfy stress and deflection criteria
for a given system design, there remains the problem of availability.
Since this rail is no longer routinely produced in this country, it
would take a large volume to rekindle any market interest in pro-
duction.  Both cost and long lead time penalties could be anti-
cipated in ordering this rail.  Light rails are available from
other countries, but along with rail the need for compatible rail
hardware would have to be satisfied in foreign markets also.

       In an earlier discussion, it was suggested that transit design is
based upon design principals of the railroad industry.  With one hundred

years (plus) experience behind them, it is understandable how both the designers and manufacturers of track components are depended upon to furnish the needs of both industries. During the development of the railroad industry, an engineering organization was formed to formulate guidelines and specifications. The American Railway Engineering Association (AREA) remains the major source of technical design information for the railroad industry today. Much of the material has also been adapted to rapid transit use, especially in design, for there has not as yet emerged an equivalent design code strictly for transit.

Many of the standards adopted in railroad practice, have been used on transit construction. Among these are, as mentioned before, track components and construction standards. An example of the later is the use of 12 inches of ballast under the tie when, for stress purposes, less would suffice. Retention of standard gauge railroad track (on most of the existing systems) is another adopted standard.

And while there is this obvious railroad influence, recent trends indicate somewhat of a change. On one newer system, a wider (than standard) gauge was adopted. There are other differences that have evolved due to basic differences in the two industries. Restraining rail use on transit curves is one example. Because of the extremely sharp curves found on transit systems, the need to provide derailment protection and to prevent excessive wear to rail was satisfied by use of the restraining rail. Since main line, high speed railroad curves are much flatter than those of transit systems, a similar need is not present on railroads. More extensive use of guard rails is also found in transit, due to safety concerns for passenger-carrying equipment, operating through sharp radius turnouts and on steep grades. Although the first uses of concrete ties in the United States were in railroad installations, with only a few exceptions these were fairly small, trial installations. The transit industry, on the other hand, has expanded their use to many of the newer systems or extensions of existing systems. Transit systems have also adopted the use of direct fixation track in tunnel construction while there are no known similar uses of this on domestic railroads.

6.3  MAINTENANCE PRACTICE

Maintenance practices of transit properties vary from those of railroads due to several factors, some of which have already been mentioned but are discussed further in this section.

a)  Headways

One of the most influential factors in determining maintenance methods is the schedule gap between trains.  As noted earlier, railroads have relatively large periods of time between trains and also can often detour (single track) around areas undergoing repairs.  Transit systems generally do not have the day time schedule gaps nor the system and schedule flexibility for single tracking.  Major maintenance must be done very late at night or at the expense of a shut-down (in some cases), and minor work needed during the day must generally be done by hand (without on-track equipment, etc.).

b)  Impact on Design

Due to the limitations just discussed, it becomes incumbent upon the designers to eliminate frequent maintenance.  Thus, for example, the use of 75 lb rail in a sharp tunnel curve (which satisfies stress and deflection criteria) might need to be replaced due to rail wear in such a short period of time that the initial savings (over heat-treated, i.e., high strength, rail of the same size or even a larger sized rail) might be more than overcome by excessive maintenance expense.

c)  Maintenance Practice

Railroads have been developing maintenance equipment for years, and the sophistication is quite impressive.  In transit maintenance, usage of mechanized equipment is much less than that of railroads, especially in maintaining conventional track in tight tunnels. It is more difficult to maintain the transit system, and this fact, again, discourages any minimum designs.

141

On the at-grade portions of transit systems use of deep ballast sections is similarly justified as it will not become "fouled" and in need of work as quickly as a shallow section. Deeper sections will also lessen the decay of wood ties by promoting drainage of water away from ties and preventing siltation of ballast up to the tie level.

Industry standards are beginning to influence transit maintenance levels just as they have been forcing the railroads, in recent years, to change their practice. The Federal Railroad Administration inspects and enforces certain track standards that must be maintained by the railroads in order to continue operations at posted speed. Minimum standards exist for both the condition of components and the track surface and line for a given allowable operating speed, and the railroads are spending more to maintain their tracks or are having to reduce operating speeds to meet FRA requirements. The equivalent transit requirements are outlined in recommendations of APTA (American Public Transit Association), but there is no enforcement of these criteria.

# 7. CONCLUSIONS AND RECOMMENDATIONS

Throughout the sections of this report many conclusions and recommendations are discussed in detail. For a full understanding of the results of this study these sections should be carefully examined by the reader. In this section, however, only the more significant conclusions and recommendations are delineated. It should be noted that the experiment performed in this pilot study for the definition of the vehicle induced load environment was limited in scope in that various track configurations, soil conditions, track irregularities, transit vehicles and wheel irregularities were not included. Thus, many conclusions set forth are primarily based on the results from this pilot study and should be considered as statements of trends.

The general conclusions are as follows:

1. Measured pressures are well within the design maximum at both the top of ballast and top of the subgrade. Current AREA recommended design formulas did not predict the pressure distribution through the ballast and subgrade accurately.

2. The measured tie bending moments were similar for all the instrumented ties and were all within the design maximum.

3. Stresses in the fastener clips were well below yield, and the alternating incremental stress during the passage of the vehicle should not produce a fatigue failure in the fastener clip.

4. Significant increases in the wheel/rail loads were observed from wheel flats. These increases were also apparent in the measured load environment of all track components.

5. From measured wheel to rail loads a design factor can be determined as the load that is exceeded only five percent of the time with a ninety-five percent level of confidence. This determines a load that due to its expected presence will have a significant influence on the life of the track system.

143

6.  Maximum vertical and lateral wheel loads showed insignificant dependence upon vehicle velocity for the configurations tested.  Lateral wheel loads varied by a factor of three between the tangent and the curve sites, but the vertical wheel loads were constant between the two sites.

7.  Roadbed strains were elastic and small for these vehicle configurations.

8.  Analytical computer code comparisons with the experimental data resulted in fair agreement in the definition of the load environment.  It should be noted that for these transit vehicles the nonlinear soil behavior was not significant.

9.  Instrumentation from the old sites, installed in 1972, yielded very limited data for comparison with new site data.

10. The embedment of pressure gages in the bottom of a concrete tie and the insertion of encapulated pressure gages in the ballast proved to be sucessful measurement techniques. Additionally it is not necessary to measure pressures within the subgrade in future studies.  It is essential to measure pressures at the tie/ballast interface, within the ballast and at the top of the subgrade to ascertain the vehicle induced load effects upon the track roadbed.

11. Soil properties depend upon the stress paths to which the soil is subjected.  It is necessary to determine accurately soil properties and to determine the dynamic wheel rolling effects upon cumulative soil behavior.  These data are essential for the development of accurate analytical prediction methods.

12. Although it was shown that significant conservatism exists in transit design for at-grade ballasted track structures on the basis of stress criteria, the transit industry feels that potential savings in construction cost through a more optimal design would be overshadowed by an increase in the maintenance costs.

144

13. The definition of the load environment for the various track components not only is important for design purposes, but this information can also be used to reduce maintenance problems.

14. As track modulus ($k_r$) increases, rail stress and track deflection decrease while dynamic rail seat load increases.

15. Increasing rail size to offset weak track modulus requires a large increase in rail weight for a small gain in lowering track deflection and rail stress.

16. Change in tie size or tie spacing (or both) is an effective method of increasing track modulus.

17. Increasing ballast depth may well be the best means of increasing track modulus although more research is needed to derive the relationship between ballast depth and track modulus (see Section 6.2.6).

18. Rail bending stress will rarely (if ever) control the design, for normal tie size and spacing, unless the allowable track deflection is greater than 0.25 inch.

19. Increasing rail size without increasing tie size and/or decreasing tie spacing tends towards an unstable track structure (thermally induced buckling).

20. Concrete ties, due to their weight, resist thermal buckling. While it is theoretically possible to space these ties considerably farther apart than 30 inches, excessive wear (abrasion) occurs on the bottom of ties (probably due to rotation associated with rail bending).

21. for the usual wheelset configurations, the "end car" case (i.e., two axles) produces greater rail bending stress and deflection than four axle load condition found between cars.

The recommendations fall into two categories: those made relative to further research that could be extracted from the present experimental site at the UMTA transit test track at TTC and those made to expand the

145

determination of vehicle induced load environment to other track configurations. Specific recommendations covering both categories are as follows:

1. Tests should be performed on the UMTA transit test track at Pueblo to determine the effect on the load environment caused by track perturbations, wheel flats and further roadbed compaction of the instrumented sites.

2. Track instrumentation for the accurate measurement of rail seat loads and fastener load environment needs to be developed for use on any track configuration either at the TTT or on transit properties. The present instrumented site could serve as an excellent place to check-out and evaluate such new instrumentation.

3. Development of improved design methods should be considered using the analytical computer codes and present and future experimental results.

4. Testing techniques and portable instrumentation packages should be developed that are suitable for the testing of various track configurations on transit properties.

5. The definition of load environment in transit track systems should be extended to other track configurations, such as direct fixation concrete slab construction.

6. Onboard vehicle measurement systems should be developed and tested to measure the influence of transit vehicle truck configurations upon the structural integrity of transit track systems.

7. Life cycle loads should be examined experimentally and analytically to determine the distribution of component loads and the transfer of load between components during a track life cycle. This load definition will aid in determining the cause of maintenance problems and lead to a better overall system design.

# 8. REFERENCES

4.1     Yoo, T-S, Selig, E.T., "Field Observations of Ballast and Sub-
        grade Deformations in Track - FAST", Prepared for Transportation
        Research Board Meeting at DOT-TSC, Cambridge, Mass., January 1979.

4.2     Winter, G., Nilson, A.H., DESIGN OF CONCRETE STRUCTURES, Eighth
        Edition, McGraw-Hill, New York, N.Y., 1972, 615 p.

4.3     Hanna, A.N., "Laboratory Evaluation of Concrete Ties and
        Fastenings for Transit Use", UMTA-MA-06-0100-79-8, March 1979.

4.4     Ledbetter, R.H., "General Deformation (Elastic and Inelastic)
        and Stress Distribution Theory in Soils", Soils and Pavements
        Laboratory, U.S. Army Engineer Waterways Experiment Station,
        Vicksburg, Miss., TS-S-77-10, September 1977.

5.1     Manual for Railway Engineering, American Railway Engineering
        Association, Chicago, Illinois, March 1978.

5.2     Prause, R.H., Meacham, H.C., et al, "Assessment of Design
        Tools and Criteria for Urban Rail Truck Structures, Volume I.
        At-Grade Tie Ballast Track," UMTA-MA-06-0025-74-3, April 1974.

5.3     Raymond, G.P., "Design for Railroad Ballast and Subgrade Support",
        A.S.C.E. Journal of the Geotechnical Engineering Division,
        January 1978.

5.4     Clarke, "Truck Loading Fundamentals - 3", the Railway Gazette,
        pg. 159, February, 1953.

5.5     Kerr, A.D., Unpublished research on Federal Contracts Nos.
        DOT-FR-40017 and DOT-FR-10019.

5.6     Kerr, A.D., "Thermal Buckling of Straight Tracks; Fundamentals,
        Analyses, and Preventative Measures", FRA/ORD-78/49.

5.7     So, W., Martin, G.C., et al., "Mathematical Models for Track
        Structures", Association of American Railroads, R-262,
        April, 1977.

5.8     Prause, R.H., Harrison, H.D., Kennedy, J.C., Arnlund, R.C..
        "An Analytical and Experimental Evaluation of Concrete Cross-
        Tie and Fastener Loads", FRA/ORD-77/71, Interim Report,
        December, 1977.

5.9     Tayabji, S.D., Thompson, M.R., "Finite Element Analysis of a
        Railway Track Support System", FRA-ORD-76-257, July 1976.

5.10    Kenneth, J.C., Prause, R.H., "The MULTA Computer Program for Linear Analysis of Railway Track Structures - User's Manual", FRA/ORD-78/Interim Report, November 1978.

5.11    Chang, C.S., Adegoke, C.W., Selig, E.T., "A Study of Analytical Models for Track Support Systems", Prepared for Transportation Research Board Annual Meeting, DOT-TSC Cambridge, Mass., January 1979.

5.12    Raad, L., Thompson, M.R., "Discussion of Chang, Adegoke, and Selig's Paper at Transportation Research Board Annual Meeting - January 1979", Dept. of Civil Engineering, University of Illinois at Urbana - Champaign, Janaury 1979.

5.13    Tayabji, S.D. and Thompson, M.R., "Track Support Systems Parameter Study", FRA-ORD-76-256, July 1976.

5.14    Robnett, Q.L., et al., "Development of a Structural Model and Materials Evaluation Procedures", FRA-ORD-76-255, 1976.

5.15    Tayabki, S.D., "Considerations in the Analysis of Conventional Railway Track Support Systems", Ph.D. Thesis, Department of Civil Engineering, University of Illinois at Urbana - Champaign, 1976.

5.16    Private Communication with Prof. Marshall R. Thompson, Department of Civil Engineering, University of Illinois at Urbana - Champaign.

5.17    Private Communication with Clement W. Adegoke at University of Massachusetts, Amherst, Massachusetts.

5.18    Knutson, R.M., Thompson, M.R., Mullin, T., Tayabji, S.D., "Material Evaluation Study", FRA-ORD-77-02, January 1977.

5.19    Thompson, M.R., "Ballast and Subgrade Materials Evaluation at FAST", FRA-ORD-77/32, Interim Report, December 1977.

5.20    Private Communication with James C. Kennedy at Battelle - Columbus Laboratories, Columbus, Ohio.

6.1     Dyer, T.K., Hale, W.K., Ingalls, F.A., Whelan, R.B., "Rail Transit System Cost Study", UMTA-MA-06-0025-76-3, March 1977.

APPENDIX A

TRANSIT TRACK DESIGN EXAMPLE

In this appendix a design problem is worked out for demonstration
purposes in accordance with AREA guidelines for a heavy rapid rail line.
These example calculations consider stress and deflection analysis
without concern for any traction power or maintenance costs. Following
the design example is an example of rail wear computed by two methods.
Both the AREA method which may not predict rail wear for transit systems
as well as it does for railroad, and the Couard method, which some
designers feel is closer to the truth for transit, have been presented.
The Couard method includes the effects of gradient and speed in its rail
wear formula. Since transit grades are quite variable, the inclusion of
these effects was found necessary, while in the AREA method these effects
are less important due to the narrow range of grades.

Finally, an approximation for predicting track structure stability
against thermally induced buckling is presented. A base case, which is
known to be valid, is used to compare tie dead loads against rail cross
sectional area to form the approximation.

Basic Design Example
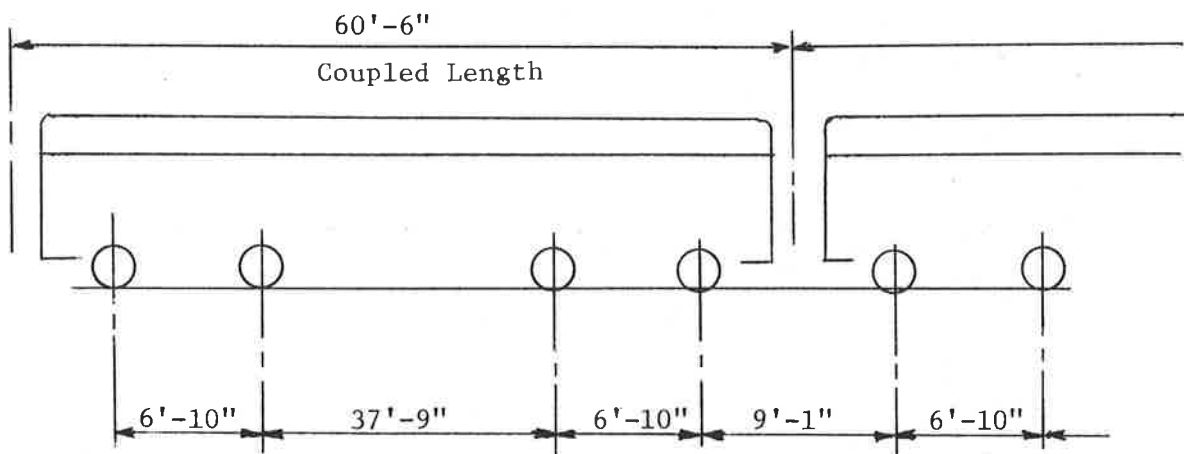
Using the current AREA design criteria (per Chapter 22 of
Reference 3.1) limiting tie spacing is determined for 100 lb rail with
6"x7"x8'-0" tie and proposed operating speeds of 60 mph (scheme "a") or
70 mph (scheme "b").  Also, rail bending stress, deflection and ballast
depth are determined.

Equipment parameters include the following:

1. Wheel diameter:  34"
2. Gross crush load of vehicle:  121,600 lbs
3. Multiple car trains

(A) Maximum wheel load (static)

$$P_w = 121,600/8 = 15,200 \text{ lbs @ 0 mph}$$

(B) Impact factor

$$I = 33 \ V/100 \ D = \text{Impact Factor}$$
$$V_a = 60 \text{ mph}$$
$$V_b = 70 \text{ mph}$$
$$D = 34" \text{ dia.}$$
$$I_a = 33 \times 60/100 \times 34 = 0.5823$$
$$I_b = 33 \times 70/100 \times 34 = 0.6794$$

(C) Dynamic wheel loads

$$P_{w_a}^1 = 1.5823 \times 15,200 = 24,050 \text{ lbs @ 60 mph}$$
$$P_{w_b}^1 = 1.6794 \times 15,200 = 25,530 \text{ lbs @ 70 mph}$$

(D) Tie parameters

(1) $L = (\ell-60) \left\{ 1 - \dfrac{0.018 \ (\ell-60)}{t^{0.75}} \right\}$

$L$ = tie effective bearing length - inches
$\ell$ = tie (total) length - inches
$t$ = tie depth - inches
tie dimensions = 6"x7"x8'-0"

$$L = (96-60) \left\{ 1 - \dfrac{0.018 \ (96-60)}{6^{0.75}} \right\} = 29.915 \text{ in.}$$

150

(2)  $A_b = L \times b$

   $A_b$ = effective tie bearing area - in$^2$
   b = tie (base) width - inches
   $A_b$ = 29.91 x 7 = 209.40 in$^2$

(3)  $M_t = w x_o^2/2 = S_t F_b$

   $M_t$ = tie bending moment
   w = unit load per foot of tie bearing length L lbs/ft
   $x_o$ = distance from rail seat to tie end-feet
   $S_t$ = tie section modulus - in$^2$
   $F_b$ = tie allowable bending stress (1100 psi usually)
   $P_d$ = dynamic rail seat load = w L

$S_t = 6^2 \times 7/6 = 42.0$ in$^3$

$M_t$ capacity = 42.0 x 1100 = 46,200 in-1b = 3850 ft-1b

Determine maximum rail seat load allowed on this tie

   $x_o = (\ell-60)/2 = (96-60)/2 = 18" = 1.50'$
   $w = P_d/L$
   $M_t = P_d x_o^2/2L$
   $P_d = M_{tcap} \times 2L/x_o^2 = 3850 \times 2 \times (29.91/12)/1.50^2 = 8530$ lbs (max.)

(E)  "Track Modulus"  $k_r$

   Using AREA base case 7"x9"x8'-6" ties @ 20" o.c., $k_r^1$ = 2000 psi

   $A_b^1 = 311.60$ in$^2$

   $k_r = \dfrac{s^1 \times A_b}{s \times A_b^1} k_r^1$

   $k_r$ = track modulus - psi
   $s^1$ = base case tie spacing = 20"
   s = particular case tie spacing - inches
   $A_b$ = particular base tie effective bearing area (209.40 in$^2$)
   $A_b^1$ = base case tie effective bearing area (311.60 in$^2$)
   $k_r^1$ = base case track modulus value = 2000 psi

   $k_r = \dfrac{20 \times 209.40}{s \times 311.60} \times 2000 = (26,880/s)$

For reasonable values of s (tie spacing)

| s | Values of $k_r$ for Computations |
|---|---|
| 20" | 1340 psi |
| 22" | 1220 psi |
| 24" | 1120 psi |
| 26" | 1030 psi |
| 28" | 960 psi |
| 30" | 900 psi |

Scheme "a"

Determine maximum tie spacing for given tie (6"x7"x8'-0") with 100 lb rail for a maximum track speed of 60 mph.

Scheme "b"

Same as scheme "a" except maximum track speed is 70 mph.

A.R.E.A. requirements or recommendations:

1.  maximum rail bending stress = 25,000 psi ($F_y$ = 70,000 psi)

2.  maximum allowable track deflection = 0.25"

3.  dynamic impact on ties to be 100% (for all speeds)

4.  maximum subgrade stress (ballast/subgrade interface) = 20 psi

5.  maximum tie/ballast stress = 65 psi

(I) Rail bending stress

100 lb RE rail $I_x$ = 49.0 in$^4$, $S_x$ min = 15.17 in$^3$

$$M = P_w^1 = e^{-\beta x}/r\beta \ (\cos \beta x - \sin \beta x)$$

$P_w^1$ = dynamic wheel load – lbs

e = base of natural logs

$\beta = (k_r/4EI)^{1/4}$

E = rail modulus of elasticity $30 \times 10^6$ psi

I = rail moment of inertia

x = location of wheel load from point at which moment is desired – inches
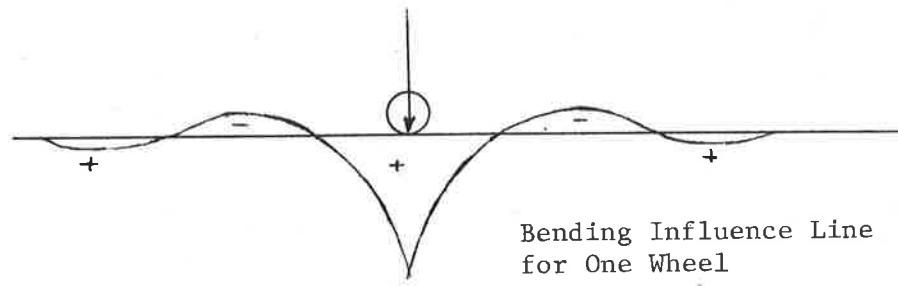
Bending Influence Line
for One Wheel

From wheel configuration:



82"    109"    82"

Point of
Ref. for
Calculations

x = 141"    x = 109"    x = 0    x = 82
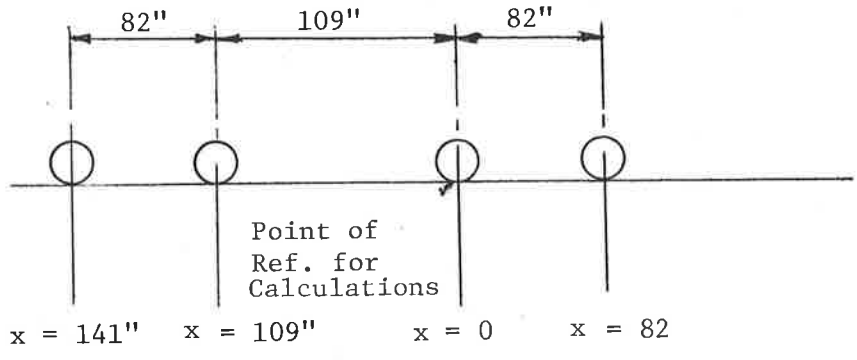
(II) Track deflection

$$y_d = \beta P_w^1 / 2k_r \; e^{-\beta x}(\cos\beta x + \sin\beta x)$$

$y_d$ = deflection in inches due to dynamic wheel loads

(III)  Tie rail seat load

$$P_d = 2y_s s k_r$$

$P_d$ = dynamic rail seat load

$y_s$ = track deflection under static wheel loads

$$= y_d P_w / P_w^1$$

s = tie spacing – inches

2 = AREA dynamic multiplier (Impact = 100% for all speeds)

(IV)  Required ballast depth (Love's Equation)

$$P_s = P_b \left\{ 1 - \left( \frac{1}{1 + r^2/h^2} \right)^{3/2} \right\}$$

$P_s$ = allowable ballast pressure (20 psi)

$P_b$ = actual ballast pressure = $(P_d/A_b)$ psi

153

$r$ = radius of circle whose area = $A$ = $\sqrt{A_b/\pi}$

$h$ = required ballast depth for $p_s \leq 20$ psi

by rearrangement:

$$h = r \sqrt{\frac{-(1 - P_s/P_b)^{2/3}}{-1 + (1-P_s/P_b)^{2/3}}}$$

Scheme "a" values

For V = 60 mph, $P_w^1$ = 24,050, $P_w$ = 15,200, Ix rail = 49.0 in$^4$, $S_x$ = 15.17 in$^3$

Try ties @ 24" o.c.

(I)  Rail bending

$\beta = (k_r/4EI)^{1/4} = (1120/4 \times 30 \times 10^6 \times 49)^{1/4} = 0.020891$

$M = P_w^1 e^{-\beta x}/4\beta \; (\text{Cos}\beta x - \text{Sin}\beta x)$

Determine which condition maximizes bending - 2 wheels (i.e. end car condition) or 4 wheels (between car conditions)

2 - wheels x = 0, 82

    x = 0 M = 287,803 in-lb

    x = 82" M = $\underline{-58,728 \text{ in-lb}}$

    $\sum M$ =  229,075 in-lb

4 - wheels x = 0, 82,109,191

    $\sum M$ = 229,075 in-lb

    x = 109"      -41,620

    x = 191"      $\underline{475}$

                  187,930 in-lb

                    M max = end car 2 wheels = 229,075 in-lb

Rail bending stress:

$f_b = M/S_x = 229,075/15.17 = 15,100$ psi $<25,000$ psi

(II) Deflection

$$y_d = \beta P_w^1/2k_r \; e^{-\beta}x(\text{Cos}\beta x + \text{Sin}\beta x)$$

2 wheels x = 0, 82

    x = 0 $y_d$ = 0.2243"

    x = 82 $y_d$ = $\underline{0.0343"}$

$\sum y_d$ =          0.2586" > 0.250" (Maximum)

$$x = 109 \quad 0.0026$$
$$x = 191 \quad \underline{-0.0059}$$
$$0.2553'' \qquad y_d \text{ is excessive} > 0.25''$$

Try 22" tie spacing

$$k_r = 1220$$
$$\beta = (1220/4 \times 30 \times 10^6 \times 49.0)^{1/4} = 0.021343$$

(I)  Bending

$$x = 0 \quad M = 281,715 \text{ in-lb}$$
$$x = 82 \quad M = \underline{-56,895}$$
$$\sum M = 224,820 \text{ in-lb}, \quad f_b = 14,820 \text{ psi}$$

(II)  Deflection

$$x = 0 \quad y_d = 0.2104''$$
$$x = 82 \quad y_d = \underline{0.0294''}$$
$$0.2398'' < 0.25'' \text{ (Max)}$$

$$y_s = y_d \times P_w/P_w^1 = 0.2398 \times 15,200/24,050 = 0.1516''$$

(III)  Dynamic rail seat load

$$P_d = 2sy_s k_r$$
$$P_d = 22 \times 0.1516 \times 2 \times 1220 = 8138 \text{ lb} < 8530 \text{ lb}$$
Contact stress @ bottom of tie
$$P_d = P_d/A_b = 8138/209.40 = 38.86 \text{ psi} < 65 \text{ psi}$$

(IV)  Ballast depth required

$$r = \sqrt{A_b/\pi} = \sqrt{209.40/\pi} = 8.164 \text{ in}$$

$$P_d = P_d/A_b = 38.86 \text{ psi}$$
$$P_s = 20 \text{ psi per AREA allowable}$$

$$h = 8.164 \sqrt{\frac{-(1-20/38.86)^{2/3}}{-1+(1-20/28.86)}2/3} = 10.37''$$

Scheme "b" values

For $V = 70$ mph, $P_w^1 = 25,530$, $P_w = 15,200$, $I_x = 49.0$, $S_x = 15.17$

Try 22" Spacing

$k_r = 1220$

$\beta = 0.021343$

$x = 0.82$

(I)   Bending

$M = 299,050 - 60,396 = 238,654$ in-lb

$f_b = 15,732$ psi

(II)  Deflection

$y_d = 0.2233 + 0.0313 = 0.2546 \quad 0.25"$

$y_s = 0.2546 \times 15,200/25,530 = 0.1516$

(III) Dynamic rail seat

$P_d = 22 \times 0.1516 \times 2 \times 1220 = 8138$ lb

$P_b = 38.86$ psi

(IV)  Ballast depth

Same as before $= 10.37$ in

Transit Rail Wear

Compute traffic densities of the system

1.  Peak 2 hour period twice daily
    with 2 min. headways for 1 hour
    and 5 min. headways for 1 hour
    number of trains = 2 @ (60/2 + 60/5) =          84 trains

2.  Off peak service
    5AM to 7AM headways @ 15 mins              8 trains
    9AM to 4PM headways @ 10 mins             42 trains
    6PM to 9PM headways @ 10 mins             18 trains
    9PM to 1AM headways @ 15 mins             16 trains
                    Total volume daily =    168 trains/day

156

3.  Saturday & Sunday (Holidays)

    5AM to 1AM headway avg @ 30 mins         40 trains

Annual volume of trains

    (365-114)(168) + 114(40) = 46,728 trains/annum

Gross tonnage (daily)

    Peak periods 4 cars @ 100,000 lb x 84 trains/2000 = 16,800
    Off peak     2 cars @ 80,000    x 84 trains/2000 = <u>6,720</u>
                                         23,520 tons

        (Sat, Sun, Holidays)
    Avg. 2 cars @ 80,000 x 40 trains/2000         3,200 tons

Annual Gross Tons

    (365-114)(23,520) + 114(3,200) = 6,268,320 or 6.3 Million Gross Tons

## Tangent Track Rail Life - AREA Method

$$T = KWD^{0.565} \quad \text{(for 3/16" = 0.1875" wear)}$$

    $K = 0.545$ in the absence of actual data
    $W$ = wgt. of rail (75,100,115)
    $D$ = traffic density (millions of gross tons/year) 6.3 MGT/yr.

75 lb rail
    $T = 0.545 \times 75 \times 6.3^{0.565} = 115.6$ million gross tons
100 lb rail
    $T = 0.545 \times 100 \times 6.3^{0.565} = 154.2$ million gross tons
115 lb rail
    $T = 0.545 \times 115 \times 6.3^{0.565} = 177.3$ million gross tons

For 10 degree curves: allow 3/8" max. headwear (0.375")
    Unlubricated curve factor = 0.10
    Lubricated curve factor   = 0.37

Unlubricated 10° curve - Rail Life

    RL (75 lb rail) = 11.6 MGT x 0.375/0.1875 ÷ 6.3 MGT/yr = 3.7 yrs
    RL (100 lb rail) = 15.4 MGT x 0.375/0.1875 ÷ 6.3 MGT/yr = 4.9 yrs
    RL (115 lb rail) = 17.7 MGT x 0.375/0.1875 ÷ 6.3 MGT/yr = 5.6 yrs

Lubricated 10° curve - Rail Life

$$RL\ (75) = 0.37 \times 115.6\ MGT \times 0.375/0.1875 \div 6.3\ MGT/yr = 13.6\ yrs$$
$$RL\ (75) = 0.37 \times 154.6\ MGT \times 0.375/0.1875 \div 6.3\ MGT/yr = 18.1\ yrs$$
$$RL\ (100) = 0.37 \times 177.3\ MGT \times 0.375/0.1875 \div 6.3\ MGT/yr = 20.8\ yrs$$

## Tangent Track Rail Wear - Couard Method

$$W_{vt} = r_w(1+0.23g^{1.7})\ 5 \times 10^{-6}\ BV + 0.0025$$

$W_{vt}$ = vertical headwear - inches (0.375" allowable)

g = track gradient - percent (use 1%)

B = traffic density - MGT/yr. (6.3 MGT/yr)

V = track speed - mph (70 mph)

$r_w$ = ratio head widths of 140 lb rail to rail x

(a) 75 lb rail  w = 2 15/32"  $r_w$ = 1.215

$$W_{vt} = 1.215(1+0.23 \times 1.0)\ 5 \times 10^{-6} \times 6.3 \times 70 + 0.0025" = 0.0058"/yr$$
$$RL = 0.375"/0.0058 = 64.6\ yrs$$

(b) 100 lb rail  w = 2 11/16  $r_w$ = 1.116

$$W_{vt} = 1.116(1.23) \times 5 \times 10^{-6} \times 6.3 \times 70 + 0.0025 = 0.0055"$$
$$RL = 0.375/0.0055 = 68.2\ yrs$$

(c) 115 lb rail  w = 2 23/32  $r_w$ = 1.103

$$W_{vt} - 1.103(1.23) \times 5 \times 10^{-6} \times 6.3 \times 70 + 0.0025 = 0.0055"$$
$$RL = 0.375/0.0055 = 68.2\ yrs$$

## Curved Track Rail Wear - Vertical

$$W_{vc} = 1.1r_w\ (1+0.1U + 0.23g^{1.7})\ 5 \times 10^{-6}\ BV + 0.0025$$

U = Unbalanced superelevation - Inches (use 3 in)

V = 35 mph 10° curve with 6" superelevation

(a) 75 lb rail

$$W_{vc} = 1.1 \times 1.215(1+0.3 + 0.23)\ 5 \times 10^{-6} \times 6.3 \times 35 + 0.0025 = 0.0048"/$$
$$RL = 0.375/0.0048 = 78.9\ yrs.$$

(b) 100 lb rail

$$W_{vc} = 1.1 \times 1.116(1.53)5 \times 10^{-6} \times 6.3 \times 35 + 0.0025 = 0.0046"/yr$$
$$RL = 0.375/0.0046 = 81.5\ yrs$$

(c)  115 lb rail

$$W_{vc} = 1.1 \times 1.103(1.53)5 \times 10^{-6} \times 6.3 \times 35 + 0.0025 = 0.0046''/\text{yr}$$
$$RL = 0.375/0.0046 = 81.5 \text{ yrs.}$$

## Curved Track Rail Wear – Side

$$W_s = r_h \ (1.6 \ D_c)(1+0.1U+0.23g^{1.7}) \ 5 \times 10^{-6} \ BV + 0.0025$$

$W_s$ = Side wear in head – inches (3/8" allowable)

$r_h$ = ratio head depth of 140 lb rail: rail x

$D_c$ = degree of curve = 10°

(a)  75 lb rail  h = 1 21/32   $r_h$ = 1.245

$$W_s = 1.451(24.48) \ 5 \times 10^{-6} \times 6.3 \times 35 + 0.0025 = 0.0361''/\text{yr}$$
$$RL = 0.375/0.0361 = 10.4 \text{ yrs.}$$

(b)  100 lb rail  h = 1 21/32   $r_h$ = 1.245

$$W_S = 1.245(24.48) \ 5 \times 10^{-6} \times 6.3 \times 35 + 0.0025 = 0.0361''/\text{yr}$$
$$RL = 0.375/0.0361 = 10.4 \text{ yrs.}$$

(c)  115 lb rail  h = 1 11/16"  $r_h$ = 1.222

$$W_S = 1.222(24.48) \ 5 \times 10^{-6} \times 6.3 \times 35 + 0.0025 = 0.0355$$
$$RL = 0.375/0.0355 = 10.6 \text{ yrs.}$$

Side head wear controls in this case

(a)   75 lb rail   RL =  9.0 yrs
(b)  100 lb rail   RL = 10.4 yrs
(c)  115 lb rail   RL = 10.6 yrs

## Track Stability Against Vertical Lift and Buckling

Approximation by comparison of dead load vs rail cross section
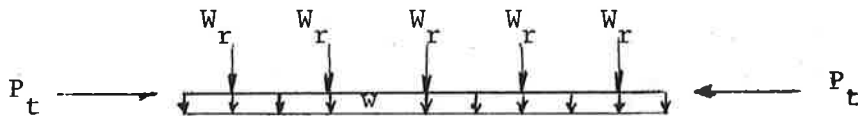
$W_t$ = weight of tie, tie plate, spikes, etc.

$w$ = weight of rail

$P_t$ = thermal load in rail due to a temperature increase of $\Delta T$

Since $P_t$ is proportional to $A_x$ of rail, assume that a known stable track structure, consisting of 115 lb rail with 7"x9"x8'-0" ties @ 24" o.c., can be used to predict stability of other combinations of rail and ties. Rail weight will be ignored in this comparison.

$$(A_{x1}/A_x) \times V_t = V_{t1}$$

where $V_{t1}$ = tie volume per foot of track required to prevent vertical buckling stability

$V_t$ = tie volume of base case (i.e. 7"x9"x8'-0" @ 24" o.c.)

= 1.75 cu.ft/c.f. track

$A_{y1}$ = rail cross section $in^2$

$A_y$ = rail cross section $in^2$ base case

$W$ = rail weight

$$V_{t1} = W_1 \times V_t / W = 0.0152\ W_1\ ft^3/ft.track$$

Therefore, assume track stability is adequate when:

$$V_t \geq 0.0152\ W_1\ per\ foot\ of\ track$$

From the approximation for stability derived, determine the stability of all combination of rail and tie used in this report.

| Tie Size | Tie Volume for Various Tie Spacings cu.ft/L.F. | | | | | |
|---|---|---|---|---|---|---|
| | 20" | 22" | 24" | 26" | 28" | 30" |
| 6"x7"x8'-0" | 1.40 | 1.27 | 1.17 | 1.08 | 1.00 | 0.93 |
| 6"x8"x8'-0" | 1.60 | 1.45 | 1.33 | 1.23 | 1.14 | 1.07 |
| 6"x8"x8'-6" | 1.70 | 1.55 | 1.42 | 1.31 | 1.21 | 1.13 |
| 7"x8"x8'-0" | 1.87 | 1.70 | 1.56 | 1.44 | 1.33 | 1.24 |
| 7"x8"x8'-6" | 1.98 | 1.80 | 1.65 | 1.53 | 1.42 | 1.32 |
| 7"x9"x8'-0" | 2.10 | 1.91 | 1.75 | 1.62 | 1.50 | 1.40 |
| 7"x9"x8'-6" | 2.23 | 2.03 | 1.86 | 1.72 | 1.59 | 1.49 |

| | | | |
|---|---|---|---|
| 115 lb rail | $V_t \geqq 0.0152 \times 115 = 1.75$ | | |
| 100 lb rail | $V_t \geqq 0.0152 \times 100 = 1.52$ | | |
| 75 lb rail | $V_t \geqq 0.0152 \times 75 = 1.14$ | | |

| Tie Size | Maximum Tie Spacings vs Rail Weight (30" maximum spacing) | | |
|---|---|---|---|
| | 75 lb | 100 lb | 115 lb |
| 6"x7"x8'-0" | 24" | * | * |
| 6"x8"x8'-0" | 28" | 20" | * |
| 6"x8"x8'-6" | 30" | 22" | * |
| 7"x8"x8'-0" | 30" | 24" | 20" |
| 7"x8"x8'-6" | 30" | 26" | 22" |
| 7"x9"x8'-0" | 30" | 26" | 24" |
| 7"x9"x8'-6" | 30" | 28" | 24" |

*Maximum spacing is less than 20", so not recommended

APPENDIX B

CROSSTIE LOAD CALIBRATION TESTS

## Introduction

Kaman Sciences Corporation (KSC) instrumented rails, concrete crossties and ballast at two locations on the Transit Track at the Transportation Test Center near Pueblo, Colorado. Thirteen crossties at each location were to be strain gaged to determine bending moments due to vehicle loading. One of these thirteen ties at each location is recessed in five places on the bottom surface to accept pressure transducers. It is required to determine the load/strain (sensitivity) relationships for these ties and the effect, if any, of the bottom surface recesses by testing a limited sample. The imbedded pressure transducers are also to be calibrated in place to account for effects of installation and sealing on the output characteristics.

## Objective

Load/strain relationships are determined for three loading conditions on each of four crosstie specimens and the load/output (sensitivity) for five imbedded pressure gages in each of two crosstie specimens as defined herein.

## Test Specimens

Four concrete crosstie specimens as defined in Figure B-1 were provided by KSC. Two crossties had five recesses machined in the bottom surface in which pressure gages and cover plates have been installed (not shown in Figure B-1). Weight of each crosstie is approximately 700 pounds.

## Instrumentation

Each crosstie incorporates five strain gages in the locations shown in Figures B-2 and B-3. Two crossties also include five imbedded pressure gages and sealed cover plates. All necessary cabling, conditioning and readout equipment for these transducers were provided by KSC. Dial gages (3 total) were employed in the midspan bending tests to measure deflections at the point load application and at each support.

PLAN

INSERTS ON ₵

9' – 0"

₵"

5' – 10 1/8"

SLOPE 1:40

10 1/4"

B
₵ SYMM

ELEVATION

AT ₵ OF RAIL SEAT

10 1/4"

A

8 3/8"

RAIL SEAT SECTION

1 1/4"

10 1/4"

7 3/4"

40

1 1/4"

3/4" X 2 3/4"
STAINLESS STEEL
INSERTS

SECTION B

9 7/8"

11"

2 3/8"

6"

SECTION A

5/8"

7 3/4"

6–3/8" STRANDS

1 1/2"

1 1/2"

8 3/8"
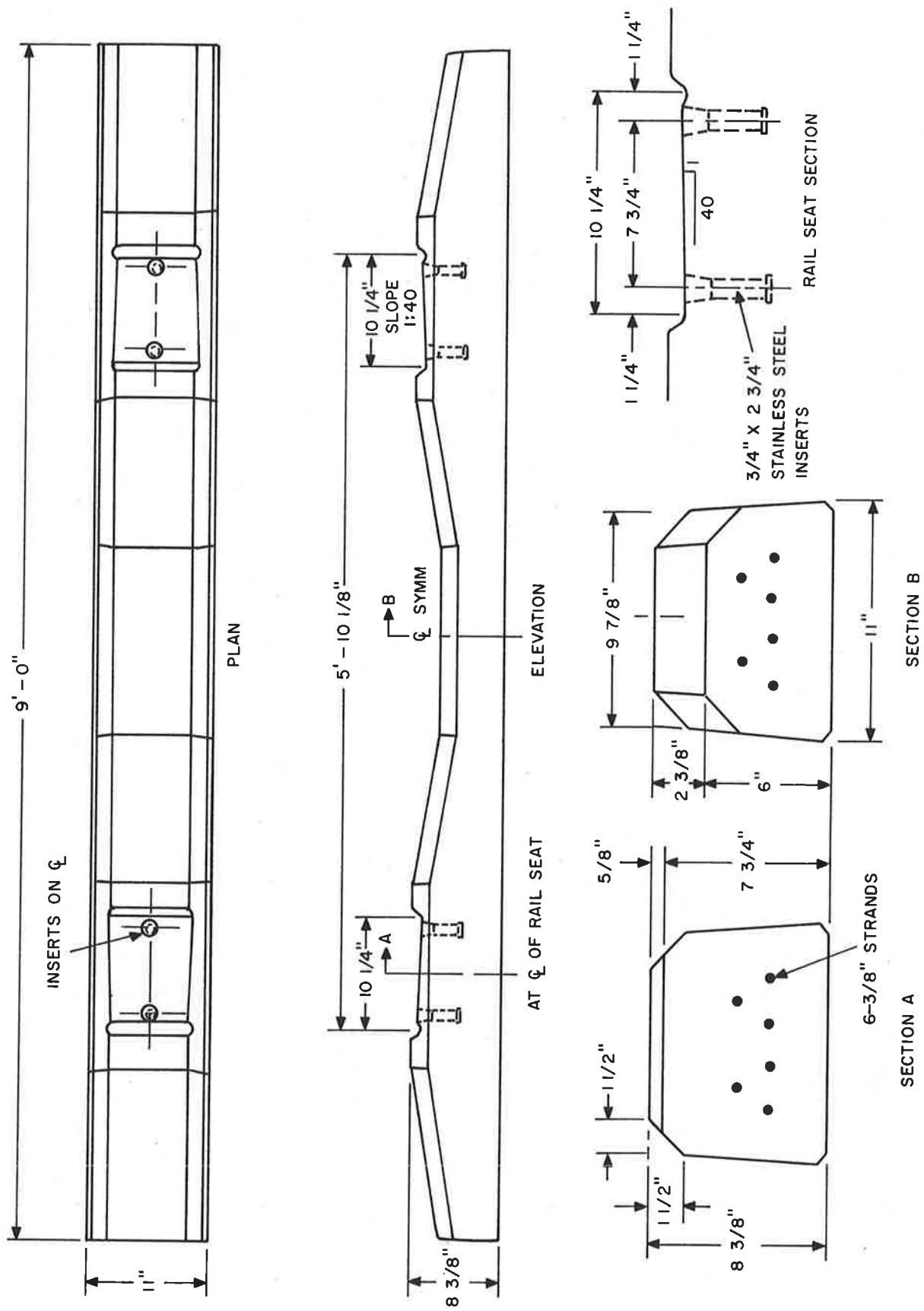
FIGURE B–1. CONCRETE CROSSTIE CONFIGURATION – GERWICK RT–7 MARK 38
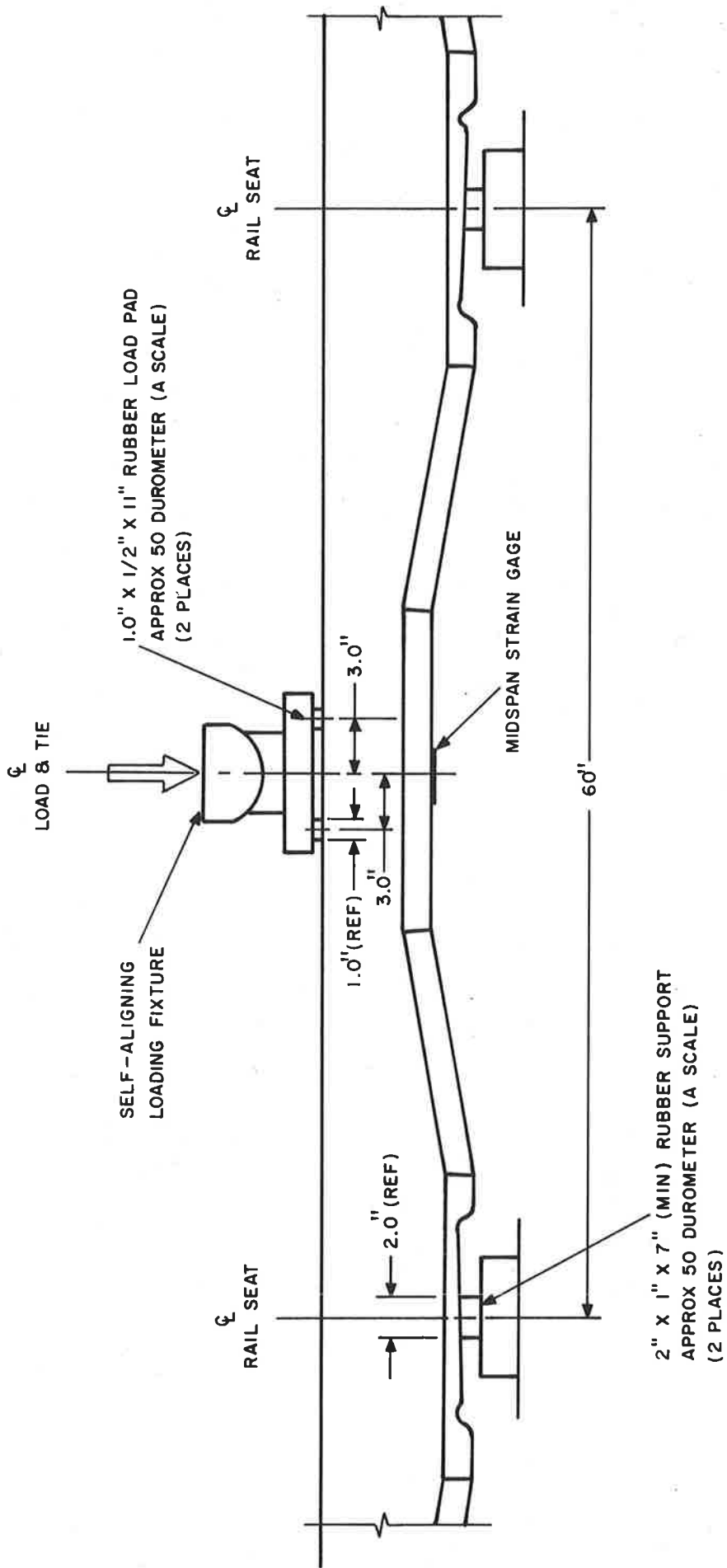
FIGURE B-2. CROSSTIE MIDSPAN BENDING TEST SET-UP

165

I" X I/2" X 7" (MIN) RUBBER LOAD PAD
APPROX 50 DUROMETER (A SCALE)
(2 PLACES)

$\mathcal{C}$
LOAD & RAIL SEAT

SELF ALIGNING LOADING FIXTURE

MIDSPAN STRAIN GAGE

1.0"(REF)

2 1/4 "

2 1/4"

2.0"(REF)

16.0"

16.0"

RAIL SEAT STRAIN GAGE (4 PLACES)

≈ 24 "

2" X I" X II" RUBBER SUPPORT
APPROX 50 DUROMETER (A SCALE)
(2 PLACES)

60"

"A"

"B" RAIL SEAT "C"

$\mathcal{C}$

$\mathcal{C}$
RAIL SEAT

CONSTANT LOAD
(OR FORCE)≈
1/2 TIE WEIGHT

W
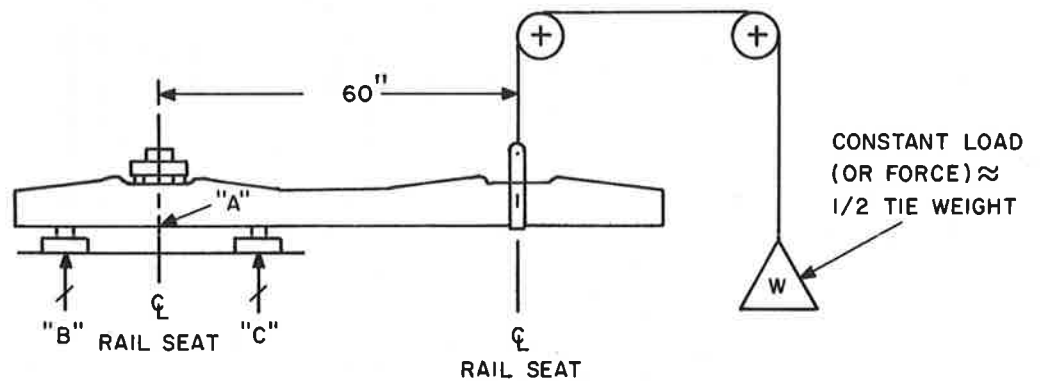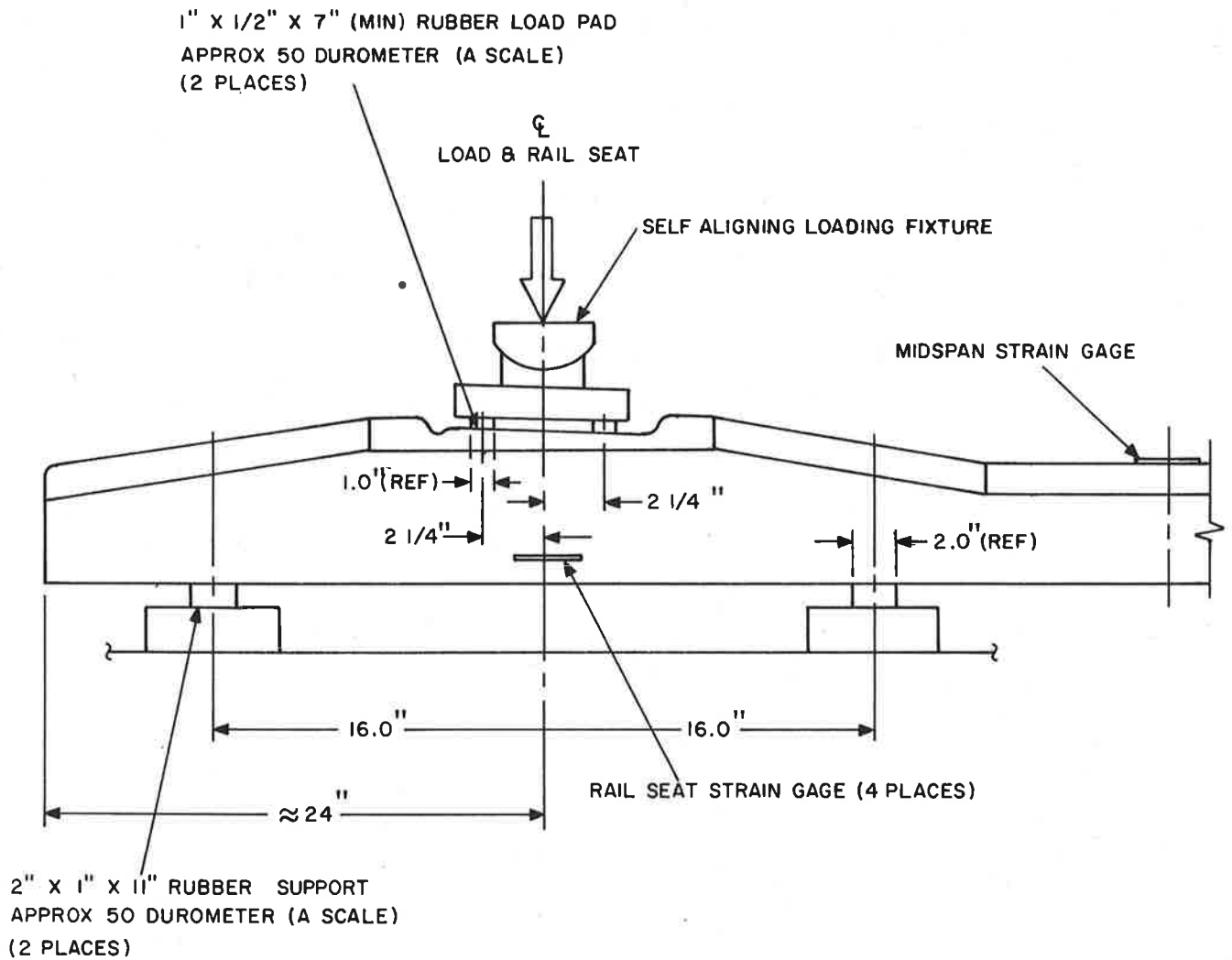
FIGURE B-3.    RAIL SEAT BENDING TEST SET-UP AND CROSSTIE
FREE END SUPPORT SCHEMATIC

166

Test Conditions and Procedures

Three separate loading conditions were performed on each crosstie specimen as defined below.

Condition I: Test set-up for the midspan bending test is shown in Figure B-2. Each crosstie was inverted and supported on rubber supports as specified in Figure B-2 located at the rail seat centerlines. Loading is applied at the crosstie centerline at midspan through rubber pads as specified in Figure B-2 using a self-aligning loading fixture to compensate for bottom surface misalignments and irregularities. Dial gages are positioned to measure crosstie deflections at the point of load application (midspan) and at each reaction point (rail seat centerlines). The loading range was from zero to 5000 pounds and returned to zero in 1000 pound increments. The load was held approximately five minutes at each increment to allow for strain gage data acquisition and assessment.

Condition II: Test set-up for the rail seat bending test is shown in Figure B-3. Each crosstie was supported at the end marked "OUTER" on rubber supports as specified in Figure B-3 located symmetrically about the rail seat centerline. The load axis passes through the intersection of the crosstie and rail seat centerlines. Loading was applied through rubber pads as specified in Figure A-2 using a self-aligning loading fixture to compensate for the rail seat angle of tilt. The loading was varied from zero to 11,000 pounds and returned to zero in 1000 pound increments. The load was held approximately five minutes at each increment to allow for strain gage data acquisition and assessment.

During testing, the opposite end of the crosstie (marked "INNER") was supported by a constant force device as illustrated schematically in Figure B-3. This device was capable of maintaining a constant force during loading

167

(and thus provide equal reactions at "B" and "C") while
the supported end experiences vertical motions resulting
from crosstie bending deformations and deflection of
the rubber support pads.  The midspan strain gage was
monitored during the loading and unloading cycles to
assure the support load remains constant.  This load is
nominally equal to one-half the tie weight (or approxi-
mately 350 pounds) and varies somewhat with each crosstie.
The proper magnitude was achieved prior to each test by
temporarily supporting the test end on a narrow fulcrum
at "C" and varying the load until the crosstie is horizontal.

Condition III: The test set-up and procedures for this condition are
identical to those of Condition II with the "INNER" and
"OUTER" ends of the crosstie interchanged.

The following loading condition was performed on each of the two
crossties containing imbedded pressure gages.

Condition IV:  Each crosstie was inverted and positioned so that load
can be applied in turn to each of the sealed plates
covering the imbedded pressure gages.  The crosstie was
supported approximately perpendicular to the load appli-
cation axis in a manner that minimizes bending.  The
loading was applied using a self-aligning loading fixture
to minimize eccentricity and a flat disc to effect proper
distribution.  The loading varied from zero to 3000 pounds
and returned to zero in 500 pound increments after first
cycling from zero to 3000 pounds one or more times to
assure free operation of the cover plates.  The load was
held approximately one minute at each increment to allow
for data acquisition.

## Data Recording and Accuracy

At each load increment, strain indications for all gages were
recorded.  The loading accuracy was $\pm 2\%$ of the indicated value at each
increment.

## APPENDIX C

## CALIBRATION LOADING TEST PLAN FOR L/V RAIL CIRCUITS
## AND INSTRUMENTED CROSSTIES

### Introduction

Two segments of the transit track at the Transportation Test Center (TTC) have been instrumented with various types of transducers to measure forces induced during the passage of transit vehicles. Locations and descriptions of these instrumented segments are given in Figure C-1. Kaman Sciences Corporation (KSC) installed ten (10) additional lateral/vertical (L/V) wheel-rail load measurement circuits on the outside rail of the transit track oval at TTC in the vicinity of Wayside Stations 4A and KSC-1. The locations of all the L/V rail circuits at 4A and KSC-1 are shown in Figure 4.24. Prior to acquisition of test data, it was necessary that certain of these transducers be calibrated by application of known vertical and lateral loads to the rails at several stations. This appendix defines the sequence and procedures for application of these calibration loads.

All loading are applied using the hydraulic system on the "54 Calibration Car" which is capable of simultaneous application of vertical and lateral loadings of 40,000 and 20,000 pounds, respectively, to each rail at a single station.

### Loading Sequence

Locations and descriptions of the two instrumented track segments to be calibrated are given in Figures C-1 and 4.24. Calibration of transducers was accomplished at each track segment in the order specified in Table C-1.

### Loading Procedures

Calibration loadings were applied equally to both rails at the locations specified in Table C-1. The loading was held at each increment a sufficient time to enable recording of all required data. Applied
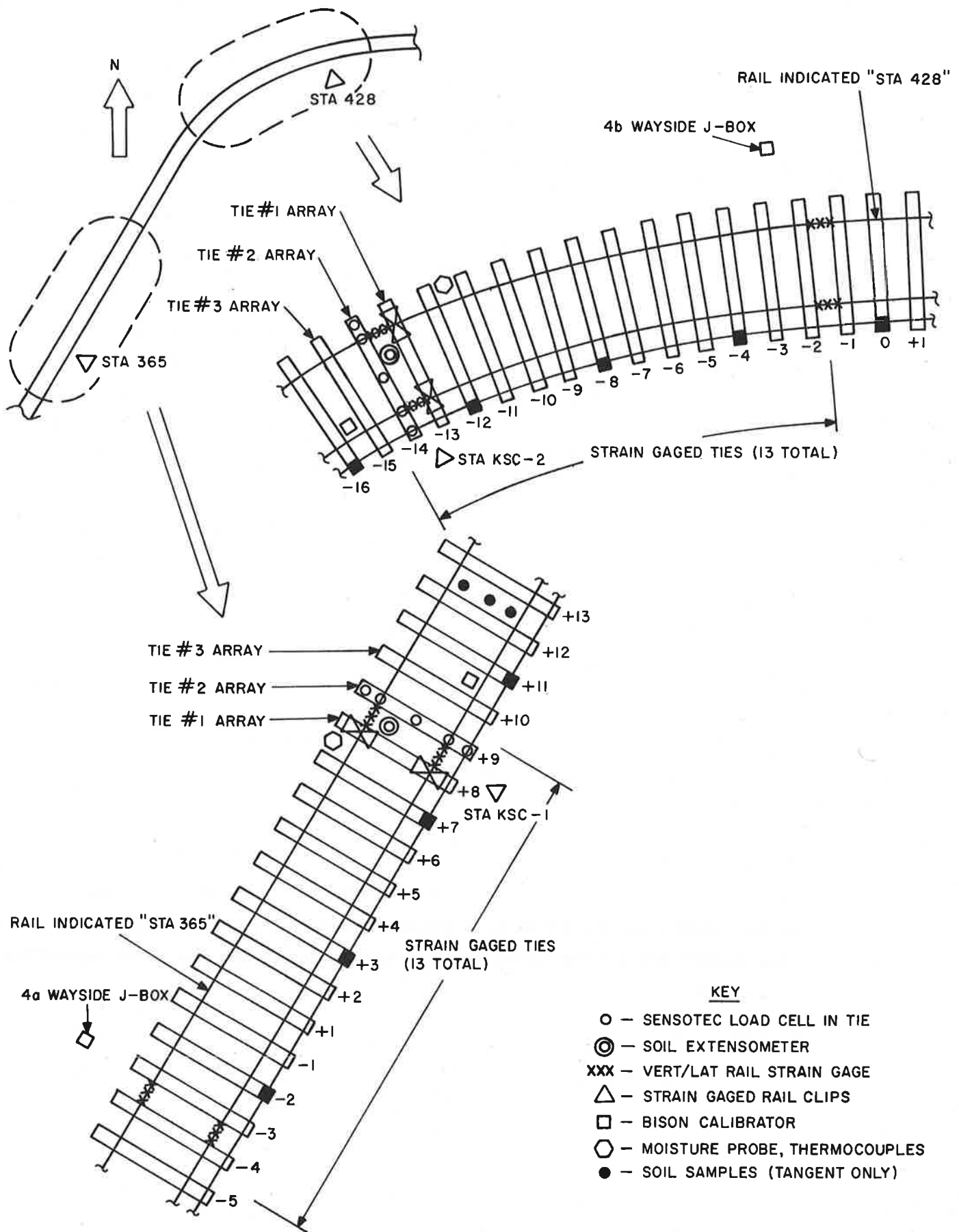
FIGURE C-1. TRANSIT TRACK INSTRUMENTED SEGMENTS

170

loading agreed with the values specified within the following limits of accuracy.

| Specified Loading | Accuracy |
|---|---|
| 0 - 1000 pounds | $\pm$ 100 pounds |
| 1000 - 5000 pounds | $\pm$ 200 pounds |
| > 5000 pounds | $\pm$ 500 pounds |

Load magnitudes were recorded to an accuracy of one percent.

Detail specifications of the loading conditions and the transducers to be monitored at each loading sequence are given below.

L/V rail circuits (Sequence numbers 1 and 2). The loading was applied incrementally at each of the four L/V rail circuit locations as specified in Table C-2. Rail circuit data were recorded at each load increment. In addition, strain indications from the instrumented rail clips were recorded at each load increment during sequence number 2.

Tie #1 array (Sequence number 3). Vertical loading was applied incrementally from zero to 20,000 pounds and returned to zero in 5,000 pound increments. Lateral load was nominally zero. Strain indications from the four instrumented tie clips and the five crosstie-mounted strain gages in addition to output from the Sensotec gage immediately beneath the crosstie at the outside rail were recorded at each load increment.

Tie #2 array (Sequence number 4). Vertical loading was applied incrementally from zero to 20,000 pounds and returned to zero in 5,000 pound increments. Lateral load was nominally zero. Strain indications from the five crosstie-mounted strain gages and outputs from the five integral Sensotec gages were recorded at each load increment.

Strain gaged ties (Sequence numbers 5 through 15). Vertical loading was applied incrementally from zero to 20,000 pounds and returned to zero in 5,000 pound increments. Lateral load was nominally zero. Strain indications from the three crosstie-mounted strain gages were recorded at each load increment.

<u>Additional L/V rail circuits</u> (Sequence 16). The calibration loadings were applied equally to both rails at the locations specified in Figure C-2. The loading was applied incrementally at each of the ten L/V rail circuit locations according to the sequence specified in Table C-2. The loading was held at each increment a sufficient time to enable recording of all required data.

## TABLE C-1

### Loading Sequence - Transit Track Transducer Calibration

| Sequence Number | Item Description | Crosstie Number | |
|---|---|---|---|
| | | Curved Segment | Tangent Segment |
| 1 | Station 4b, 4a L/V rail circuits | Between 428-2 and 428-3 | Between 365-3 and 365-4 |
| 2 | Station KSC-2, KSC-1 L/V rail circuits plus instrumented rail clips | Between 428-13 and 428-14 | Between 365+8 and 365+9 |
| 3 | Tie #1 array (including instrumented rail clips) | 428-13 | 365+8 |
| 4 | Tie #2 array (including integral Sensotec gages) | 428-14 | 365+9 |
| 5 | Strain gaged tie | 428-12 | 365+7 |
| 6 | "        "        " | 428-11 | 365+6 |
| 7 | "        "        " | 428-10 | 365+5 |
| 8 | "        "        " | 428-9 | 365+4 |
| 9 | "        "        " | 428-8 | 365+3 |
| 10 | "        "        " | 428-7 | 365+2 |
| 11 | "        "        " | 428-6 | 365+1 |
| 12 | "        "        " | 428-5 | 365-1 |
| 13 | "        "        " | 428-4 | 365-2 |
| 14 | "        "        " | 428-3 | 365-3 |
| 15 | "        "        " | 428-2 | 365-4 |
| 16 | Vicinity of KSC-1, 4a L/V rail circuits | | Between 365+9 and 365-26 |

## TABLE C-2

## Rail Circuit Loading Sequence

| Load (kips) | | Comments |
|---|---|---|
| Vertical | Lateral | |
| 0 | 0 | Initial zero calibration |
| 20 | 0 | Vertical load |
| 20 | 2.5 | Combined L/V |
| 20 | 5.0 | Combined L/V |
| 20 | 7.5 | Combined L/V |
| 20 | 10.0 | Combined L/V |
| 20 | 7.5 | Combined L/V |
| 20 | 5.0 | Combined L/V |
| 20 | 2.5 | Combined L/V |
| 20 | 0 | Vertical load |
| 0 | 0 | Record zero shift, re-zero as necessary |
| 15 | 0 | Vertical load |
| 15 | 2.5 | Combined L/V |
| 15 | 5.0 | Combined L/V |
| 15 | 7.5 | Combined L/V |
| 15 | 5.0 | Combined L/V |
| 15 | 2.5 | Combined L/V |
| 15 | 0 | Vertical load |
| 0 | 0 | Record zero shift, re-zero as necessary |
| 10 | 0 | Vertical load |
| 10 | 1.25 | Combined L/V |
| 10 | 2.5 | Combined L/V |
| 10 | 3.75 | Combined L/V |
| 10 | 5.0 | Combined L/V |
| 10 | 3.75 | Combined L/V |
| 10 | 2.5 | Combined L/V |
| 10 | 1.25 | Combined L/V |
| 10 | 0 | Vertical load |
| 0 | 0 | Record zero shift, re-zero as necessary |
| 5 | 0 | Vertical load |
| 5 | 1.25 | Combined L/V |
| 5 | 2.5 | Combined L/V |
| 5 | 1.25 | Combined L/V |
| 5 | 0 | Vertical load |
| 0 | 0 | Record zero shift, re-zero as necessary |
| 0 | .5 | Lateral load |
| 0 | 1.0 | Lateral load |
| 0 | .5 | Lateral load |
| 0 | 0 | Record final zero shift |

APPENDIX D

DATA COLLECTION TEST PLAN

## Introduction and Background

During initial construction, several areas of the transit track at the Transportation Test Center (TTC) were instrumented with transducers to measure such parameters as strain, pressure, temperature, soil extension and soil moisture. More recently, Kaman Sciences Corporation (KSC), with the assistance of the TTC and TTC O&M Contractor, has installed additional instrumentation arrays at two locations, each adjacent to one of the original instrumentation sites.

This appendix defines the procedures employed for vehicle ballasting and weighing, for additional pre-test calibration of specified track structure and roadbed instrumentation using the R42 and MBTA Blue Line transit vehicles, and for the required data passes over the instrumented areas for the acquisition of data.

## Objective

The objective of these tests is to determine vehicle-induced forces in transit track structure by measuring and recording data from transducers located on the rails and crossties and in the ballast, subballast and subgrade soil.

## Test Specimens

The test specimens consist of two areas of instrumented track structure, one in tangent and one in curved track, in the transit oval at the TTC. Test vehicles consist of the TTC R42 transit vehicles (both crush loaded and light) and the MBTA Blue Line transit vehicles (crush loaded only).

## Instrumentation

The TTC No. 408 Data Van was used for signal conditioning and data acquisition.

175

Test Procedures

Pre-test transducer calibration and test data acquisition passes
were performed with the R42 and MBTA Blue Line transit vehicles in
accordance with the following matrix. All activities with the R42
vehicles will be completed prior to calibration and testing with the
MBTA vehicles. The following procedures shall be employed, as applicable
for both test vehicle types.

| Vehicle/Configuration | Data Acquisition | Pre-test Calibration |
|---|---|---|
| R42/crush loaded | Table D-1 | Table D-2 |
| R42/light | Table D-1 | – |
| MBTA/crush loaded | Table D-3 | Table D-4 |

A.  Vehicle Ballasting

Prior to all pre-test calibrations and crush loaded data acquisition
passes, each transit vehicle pair was ballasted to the crush load
configuration. The ballast was adjusted within each transit vehicle
to equalize the weight at the two trucks.

B.  Calibration

Prior to crush loaded data acquisition passes, various transducers
at each test area were subjected to static calibration as specified
in Table D-2 (R42) or Table D-4 (MBTA). While proceeding in a
counter-clockwise direction around the transit track oval, the lead
wheelset of the front truck of the leading vehicle was positioned,
in turn, over each location specified in Table D-2 or D-4 and
illustrated in Figure C-1. The indicated instrumentation was
monitored for operation during the final approach. At each
location, a period of three (3) minutes was allowed for soil
stabilization prior to recording the static calibration values on
tape.

The pre-test vehicle calibration of the additional ten (10) wheel-
rail load measurement circuits, plus eight (8) others installed
initially at 4A and KSC-1 is delineated. Starting at KSC-1, each

176

of the L/V wheel-rail load measurement circuits identified below was calibrated using the crush loaded R42 vehicles.

    4 channels at Station KSC-1
    4 channels at Station 4A
    2 channels between ties 365+6 and 365+5
    2 channels between ties 365+3 and 365+2
    2 channels between ties 365-6 and 365-7
    2 channels between ties 365-8 and 365-9
    2 channels between ties 365-11 and 365-12
    2 channels between ties 365-14 and 365-15
    2 channels between ties 365-19 and 365-20
    2 channels between ties 365-22 and 365-23
    2 channels between ties 365-25 and 365-26

A Bendix connector receptable (PTO7SE-14-18S) was installed on the outer rail end of an adjacent crosstie for each lateral and vertical wheel-rail load measurement circuit utilizing pin connection data provided by the TTC O&M Contractor.

The zero balance was established for all L/V circuits at the particular location and the step calibrations recorded for each channel with the R42 vehicles at least fifty (50) feet removed. Then, while proceeding in a counter-clockwise direction around the transit track oval, the lead wheelset of the front truck of the leading vehicle was positioned over the midpoint of each L/V circuit. The circuit was monitored and the outputs recorded during the final twenty (20) feet of wheelset approach. The wheelset was parked over the L/V circuit for a period of at least one (1) minute prior to recording the final calibration load on tape. O-graph plots were obtained of the step calibration, approach and final calibration load activities. This procedure was repeated for each of the twelve (12) L/V measurements. The R42 vehicles were backed away (clockwise direction) for obtaining zero balances of all L/V circuits.

C.   Data Passes

Vehicle passes for data acquisition were made as specified in Table D-1 (R42) or Table D-3 (MBTA). The number of passes indicated was based upon the inability to acquire data simultaneously from Stations KSC-1 and 4A (and from Stations KSC-2 and 4B). The R42

crush loaded passes preceded the light configuration passes at each test area. Time was allowed between data passes to obtain sufficient O-graph plots to assure transducer function. Pre-test data passes were made with each vehicle prior to actual data passes for each change in loading and/or tests area for the purpose of final instrumentation checkout.

Procedures are also defined for subsequent data passes of the crush loaded R42 transit vehicles wherein data will be acquired from all eighteen (18) wheel-rail load measurement circuits, crosstie mounted strain gages in ties 365+5 through 365+9, and five (5) crosstie mounted Sensotec pressure gages in tie 365+9. Six (6) passes of the crush loaded R42 transit vehilces were made for the acquisition of data, three (3) at 50 miles per hour and three (3) at 30 miles per hour. All passes were made in a counter-clockwise direction with the transit vehicles proceeding around the entire oval between passes to assure random wheel positioning. In addition to the L/V wheel-rail measurements, data from the following transducers were acquired during each pass.

Crosstie strain gages:
    5 channels on tie 365+9
    5 channels on tie 365+8
    3 channels on tie 365+7
    3 channels on tie 365+6
    3 channels on tie 365+5

Interfacing connectors were installed in the KSC-1 junction box. These are full-bridge, 350 ohm/arm gage installations. (Total channels = 19)

Tie mounted Sensotec pressure transducers in crosstie 365+9. Interfacing connectors were installed in the KSC-1 junction box. (Total channels = 5)

Zero balances were established for all channels and step calibrations recorded prior to each data pass. Sufficient pre-test data passes were performed at 50 miles per hour to assure proper operation of transducers and instrumentation. A step calibration for each channel was recorded prior to each data pass.

## Task Definition

KSC:

    1)    Monitor test set-up calibration, and data passes

    2)    Reduce all data from FM tapes

TTC O&M Contractor:

    1)    Configure TTC No. 408 data van and interface instrumentation transducers

    2)    Ballast transit vehicles in accordance with this procedure

    3)    Perform pre-test calibration and checkout

    4)    Direct operations of transit vehicles

    5)    Acquire data in accordance with this procedure

    6)    Provide KSC with O-graph plots of all calibration and test data

    7)    Provide KSC with original and one (1) duplicate of each FM data tape

TABLE D-1

Data Pass Test Matrix - R42 Vehicles

| Event Number | Loading Condition | Velocity (mph) | Direction | Recording Station |
|---|---|---|---|---|
| 1a | Crush | 30 | CCW | KSC-2 |
| 1b | Crush | 30 | CCW | KSC-2 |
| 2 | Crush | 30 | CW | KSC-2 |
| 3 | Crush | 30 | CCW | 4b |
| 4a | Crush | 50 | CCW | KSC-2 |
| 4b | Crush | 50 | CCW | KSC-2 |
| 5 | Crush | 50* | CW | KSC-2 |
| 6 | Crush | 50 | CCW | 4b |
| 7a | Light | 30 | CCW | KSC-2 |
| 7b | Light | 30 | CCW | KSC-2 |
| 8 | Light | 30 | CW | KSC-2 |
| 9 | Light | 30 | CCW | 4b |
| 10a | Light | 50 | CCW | KSC-2 |
| 10b | Light | 50 | CCW | KSC-2 |
| 11 | Light | 50* | CW | KSC-2 |
| 12 | Light | 50 | CCW | 4b |
| 13a | Crush | 30 | CCW | KSC-1 |
| 13b | Crush | 30 | CCW | KSC-1 |
| 14 | Crush | 30 | CW | KSC-1 |
| 15 | Crush | 30 | CCW | 4a |
| 16a | Crush | 50 | CCW | KSC-1 |
| 16b | Crush | 50 | CCW | KSC-1 |
| 17 | Crush | 50* | CW | KSC-1 |
| 18 | Crush | 50 | CCW | 4a |
| 19a | Light | 30 | CCW | KSC-1 |
| 19b | Light | 30 | CCW | KSC-1 |
| 20 | Light | 30 | CW | KSC-1 |
| 21 | Light | 30 | CCW | 4a |
| 22a | Light | 50 | CCW | KSC-1 |
| 22b | Light | 50 | CCW | KSC-1 |
| 23 | Light | 50* | CW | KSC-1 |
| 24 | Light | 50 | CCW | 4a |

\* If 50 mph in clockwise direction is not possible, use maximum velocity
obtained in Sequence 5 for Sequences 11, 17 and 23.

TABLE D-2

R42 Transit Vehicle Calibration of Instrumentation

| Location of Leading Wheelset (Crosstie Number) | Instrumentation Read |
|---|---|
| 428-2 | Tie strain gages |
| Between 428-2 & 428-3 | L/V rail circuits at Station 4b |
| 428-3 | Tie strain gages |
| 428-4 | Tie strain gages |
| 428-5 | Tie strain gages |
| 428-6 | Tie strain gages |
| 428-7 | Tie strain gages |
| 428-8 | Tie strain gages |
| 428-9 | Tie strain gages |
| 428-10 | Tie strain gages |
| 428-11 | Tie strain gages |
| 428-12 | Tie strain gages |
| 428-13 | Tie strain gages, rail clips, imbedded transducers |
| Between 428-13 & 428-14 | L/V rail circuits at Station KSC-2 |
| 428-14 | Tie strain gages, integral load cells, imbedded transducers |
| 428-15 | Imbedded transducers |
| 365+10 | Imbedded transducers |
| 365+9 | Tie strain gages, integral load cells, imbedded transducers |
| Between 365+9 & 365+8 | L/V rail circuits at Station KSC-1 |
| 365+8 | Tie strain gages, rail clips, imbedded instrumentation |
| 365+7 | Tie strain gages |
| 365+6 | Tie strain gages |
| 365+5 | Tie strain gages |
| 365+4 | Tie strain gages |
| 365+3 | Tie strain gages |
| 365+2 | Tie strain gages |
| 365+1 | Tie strain gages |
| 365-1 | Tie strain gages |
| 365-2 | Tie strain gages |
| 365-3 | Tie strain gages |
| Between 365-3 & 365-4 | L/V rail circuits at Station 4a |
| 365-4 | Tie strain gages |

TABLE D-3

Data Pass Test Matrix - MBTA Vehicles

| Event Number | Loading Condition | Velocity (mph) | Direction | Recording Station |
|---|---|---|---|---|
| 1a | Crush | 30 | CCW | KSC-2 |
| 1b | Crush | 30 | CCW | KSC-2 |
| 2 | Crush | 30 | CW | KSC-2 |
| 3 | Crush | 30 | CCW | 4b |
| 4a | Crush | 50 | CCW | KSC-2 |
| 4b | Crush | 50 | CCW | KSC-2 |
| 5 | Crush | 50 | CW | KSC-2 |
| 6 | Crush | 50 | CCW | 4b |
|  |  |  |  |  |
| 13a | Crush | 30 | CCW | KSC-1 |
| 13b | Crush | 30 | CCW | KSC-1 |
| 14 | Crush | 30 | CW | KSC-1 |
| 15 | Crush | 30 | CCW | 4a |
| 16a | Crush | 50 | CCW | KSC-1 |
| 16b | Crush | 50 | CCW | KSC-1 |
| 17 | Crush | 50 | CW | KSC-1 |
| 18 | Crush | 50 | CCW | 4a |

TABLE D-4

MBTA Transit Vehicle Calibration of Instrumentation

| Location of Leading Wheelset (Crosstie Number) | Instrumentation Read |
|---|---|
| 428-2 | Tie strain gages |
| Between 428-2 & 428-3 | L/V rail circuits at Station 4b |
| 428-3 | Tie strain gages |
| 428-13 | Tie strain gages, rail clips, imbedded transducers |
| Between 428-13 & 428-14 | L/V rail circuits at Station KSC-2 |
| 428-14 | Tie strain gages, integral load cells, imbedded transducers |
| 365+9 | Tie strain gages, integral load cells, imbedded transducers |
| Between 365+9 & 365+8 | L/V rail circuits at Station KSC-1 |
| 365+8 | Tie strain gages, rail clips, imbedded instrumentation |
| 365-3 | Tie strain gages |
| Between 365-3 & 365-4 | L/V rail circuits at Station 4a |
| 365-4 | Tie strain gages |

# APPENDIX E

## SOIL SAMPLE TESTING PROCEDURE

### Introduction

Soil samples taken from the subgrade of the transit track at the Transportation Test Center were analyzed to determine various physical properties. These values are, in turn, used as input data in computer analyses to characterize the soil behavior in the transit track structure at TTC. This appendix contains procedures employed in the acquisition and testing of the soil samples.

A total of three (3) segmented soil samples, each five (5) feet in combined length were obtained from the subgrade between crossties 365+12 and 365+13 adjacent to the KSC-1/4A tangent test area. The location and subsurface orientations are shown in Figure E-1. At each location, the sample was obtained by driving three (3) 2.120 inch inside diameter, 24 inch long, carbon steel tubes to successively greater depths as shown in Figure E-2. Each tube contains a sample of soil approximately 20 inches in length.

Triaxial tests were performed to define the response of representative samples from the Transportation Test Center under various loading and unloading stress paths, in order to form a data base for soil characterization to be used in computer analysis of the transit track structure.

### Soil Samples and Equipment

The following samples given in Table E-1 were successfully selected and prepared for the testing.

Table E-1

Sample Location

|  | | Specimen Location | |
| --- | --- | --- | --- |
| Test Sample No. | | Tube No. | Depth, (in.) |
| 1 | | G 28 | D +5 |
| 2 | | G 28 | D +30 |
| 3 | | G 28 | D +55 |
| 4 | | G 38 1/2 | D +5 |
| 5 | | G 38 1/2 | D +30 |
| 6 | | G 14 | D +30 |
| 7 | | G 14 | D +55 |

*Test No. 2 results may not be reliable due to
misalignment of the ram detected during the test.

185

BALLAST 12"

SUBBALLAST 6"

RECOMPACTED SUBGRADE

UNTREATED SUBGRADE

SAMPLE LENGTH = 5'- 0"

CRIB
₵

STA 365 +16    +15    +14    +13    +12    +11    +10    +9         ₵ 3RD RAIL
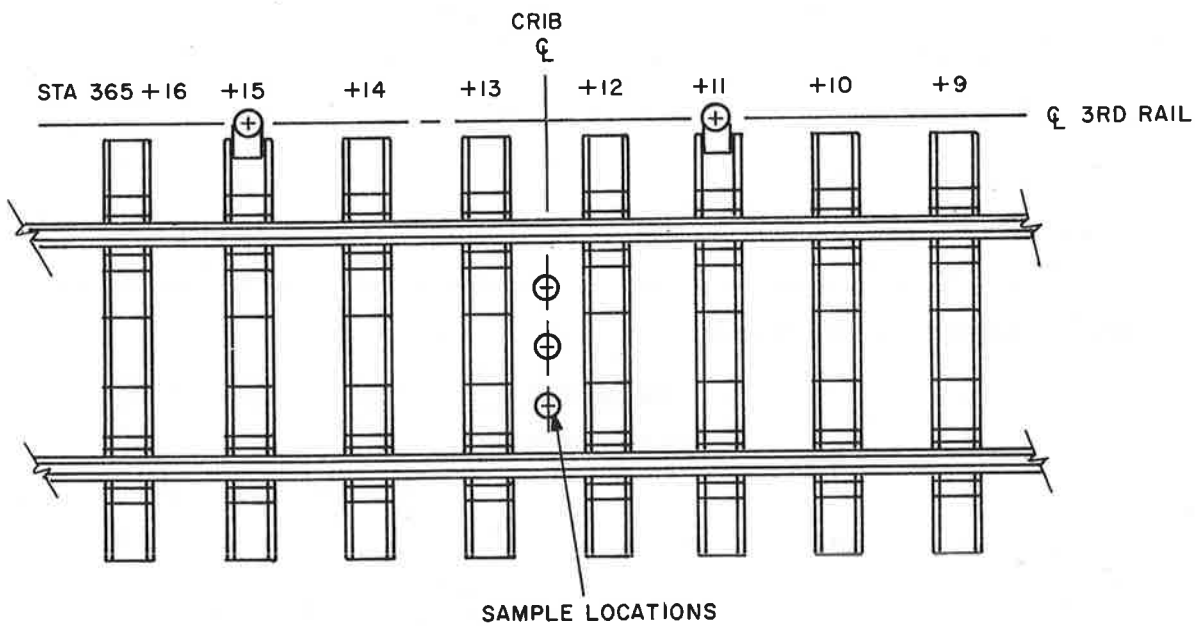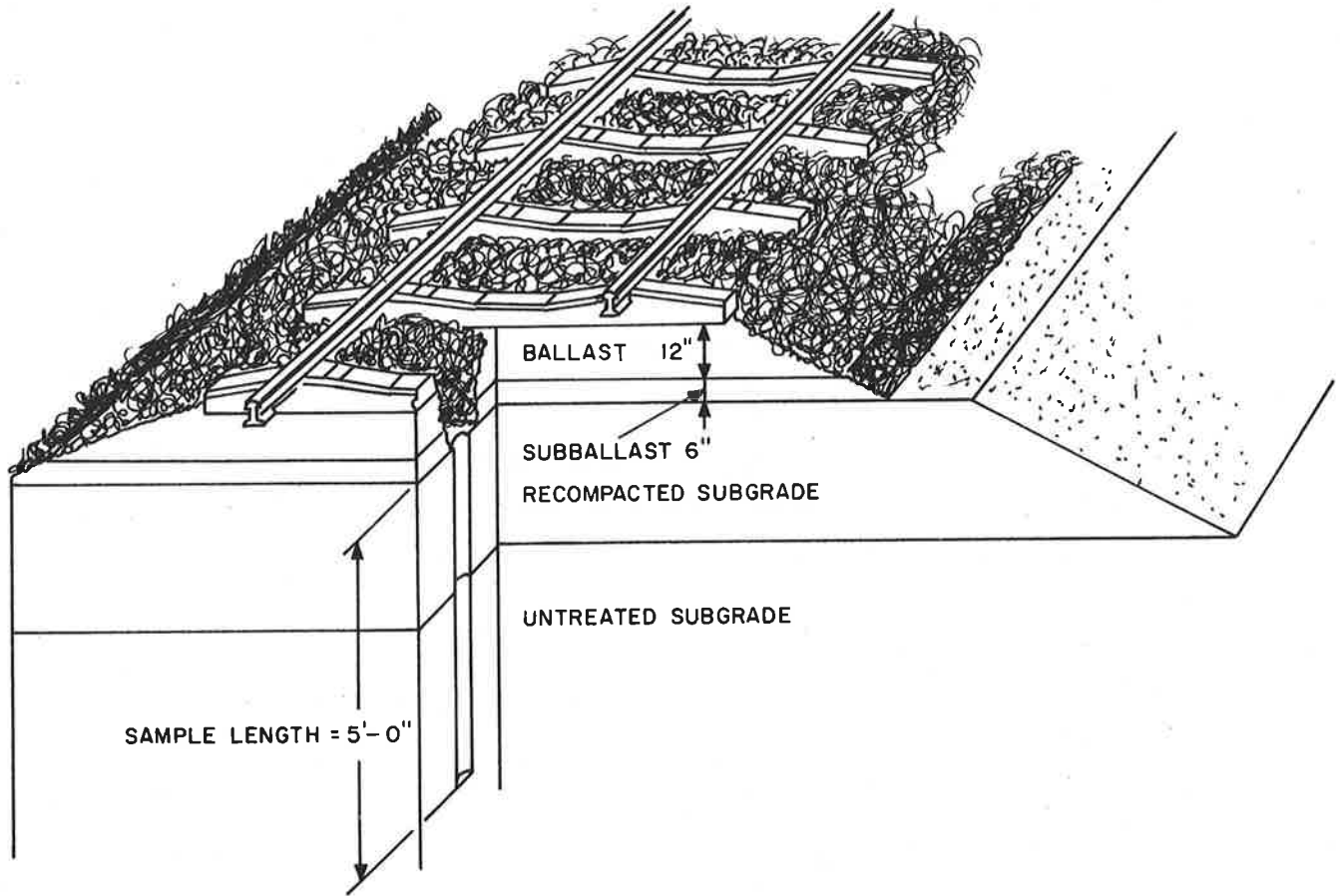
SAMPLE LOCATIONS

FIGURE E-1.   SOIL SAMPLE LOCATION AND SUBSURFACE ORIENTATION –
TTC TRANSIT TRACK

SUBBALLAST/SUBGRADE INTERFACE

20

13 1/3

40

13 1/3

6 2/3

60

PREFERRED AREA FOR SELECTION OF
SOIL TEST SPECIMAN

6 2/3
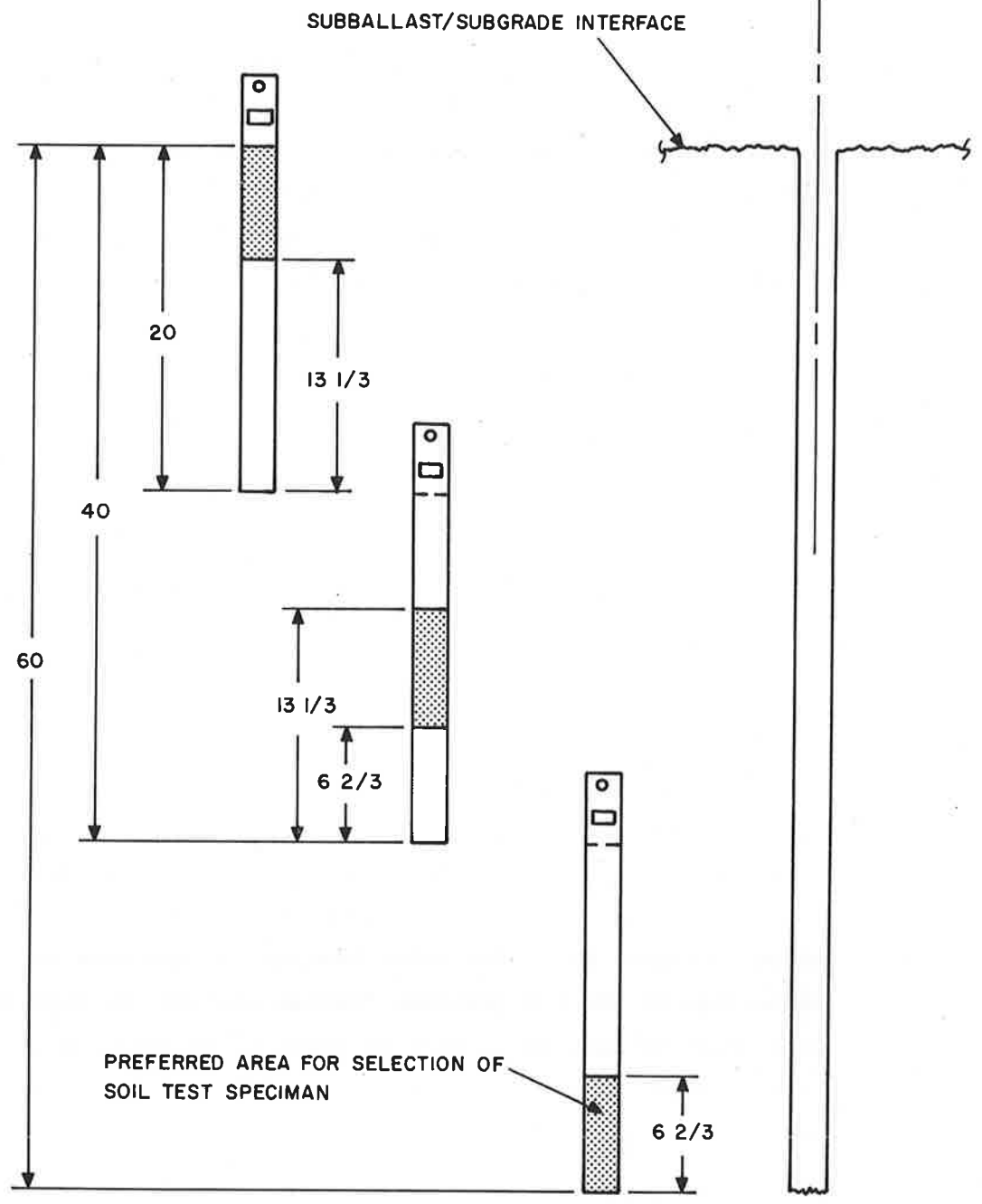
ALL DIMENSIONS IN INCHES

FIGURE E-2.   LOCATION OF SOIL SAMPLES

These samples were extruded from the tubes in which they were cored from the ground by first splitting the tube longitudinally. This step was necessitated by the fact that rusting had developed between the soil and the tube and it was very difficult to extrude the soil directly from the intact tube. About six inches of the soil were extruded each time and the most representative segment was selected to be trimmed down to the correct size for testing. A 1.4 in. diameter by 3.2 in. nominal height specimen was trimmed from the selected section by means of a wire saw. The unit weight of the specimen was determined and recorded. A typical specimen thus prepared is shown in Figure E-3.

## Test Procedures

Specimens were tested as shown schematically in Figure E-4. The test apparatus is capable of applying and maintaining vertical (piston) pressure ($\sigma_1$) and horizontal (fluid) pressure ($\sigma_3$). A latex rubber sleeve, 0.012 in. thick, was stretched over the specimen mounted on the lower pedestal of the triaxial cell. Two cantilevers were mounted on the base of the triaxial cell, serving as feeler gages to measure the lateral deformation of the test specimen as shown in Figure E-5. These aluminum cantilevers were instrumented with strain gages whose response was monitored by a digital voltmeter. When the triaxial test cell was assembled and mounted on the test frame, a proving ring was attached to the axial loading ram for measuring the deviator load, while a dial gage was mounted to the frame to measure axial deformation as shown in Figure E-6. The axial loading ram was modified to make a rigid connection to the top specimen loading platten, so that an extension load could be applied to soil in order to go into the triaxial extension stress state. The proving ring was calibrated for both compression and tension modes of operation.

## Test Conditions

All tests were carried out along the stress paths shown in Figure E-7. The six-step loading sequence for each specimen is shown in Table E-2.
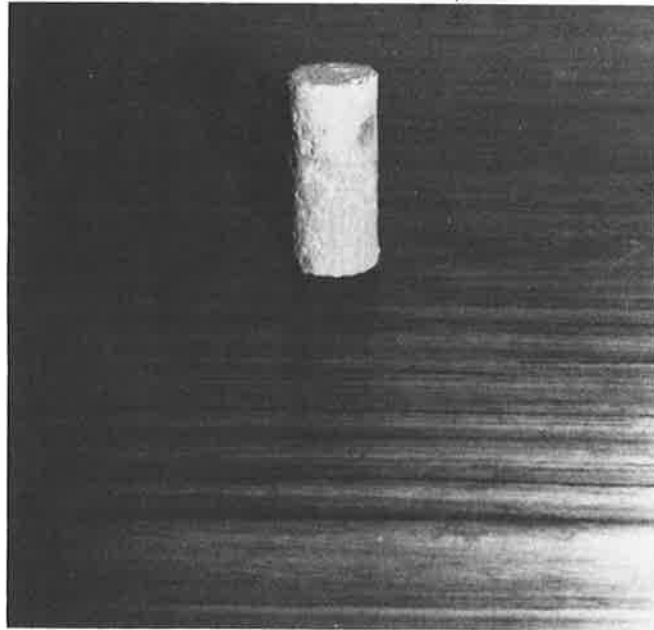
FIGURE E-3.   TYPICAL SOIL SPECIMEN
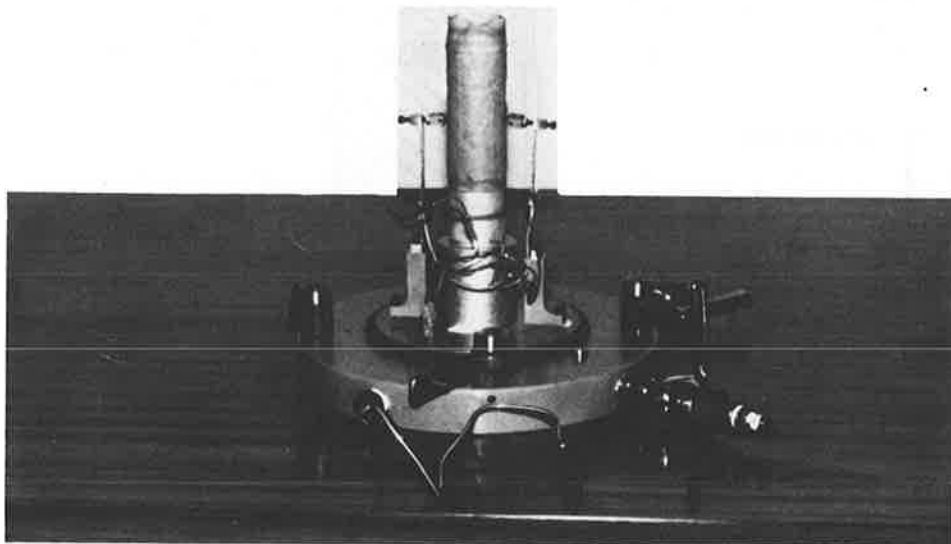


FIGURE E-5.   SOIL SAMPLE IN RUBBER MEMBRANE WITH LATERAL
DEFORMATION CANTILEVERS MOUNTED

189
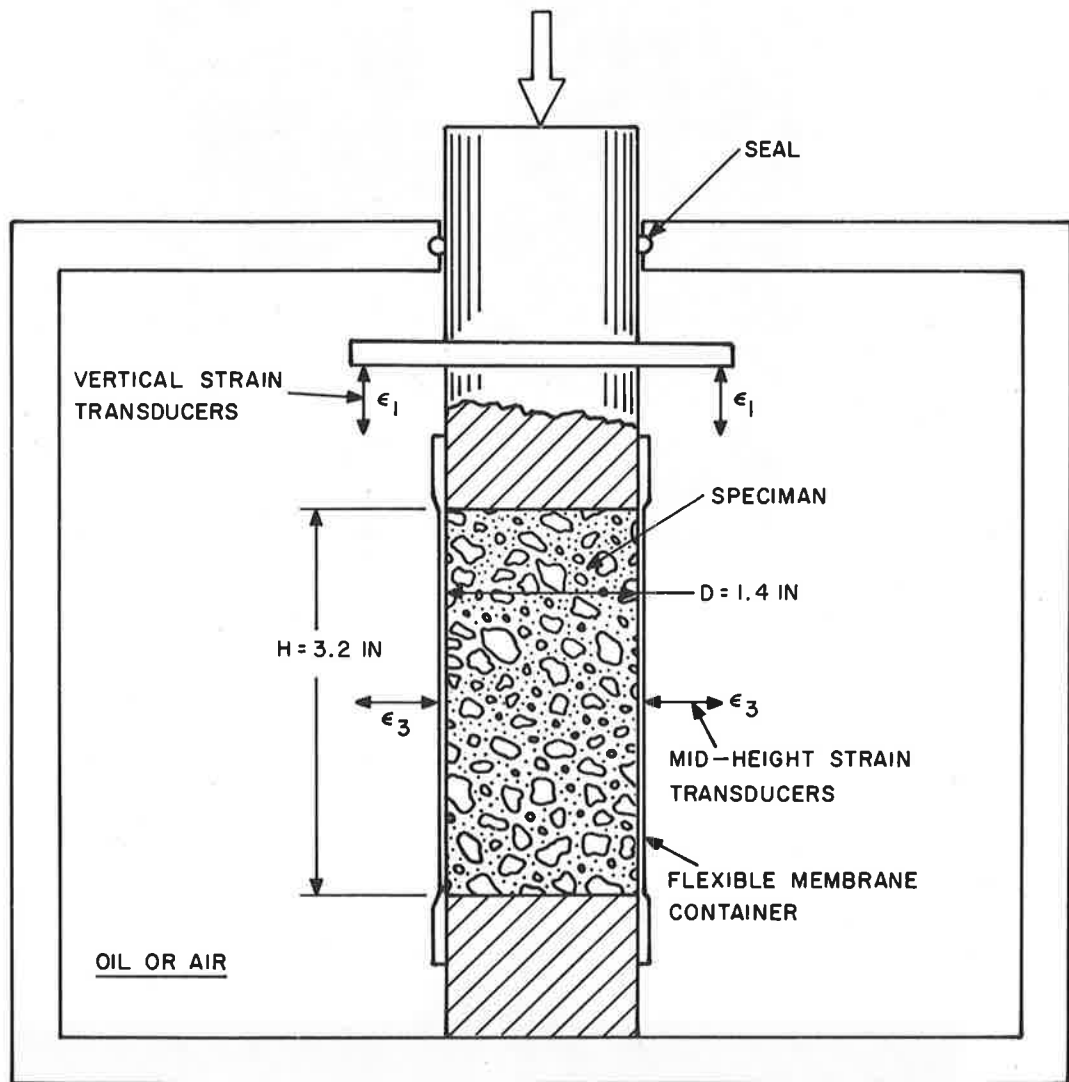
FIGURE E-4, SOIL SAMPLE TEST SCHEMATIC

190
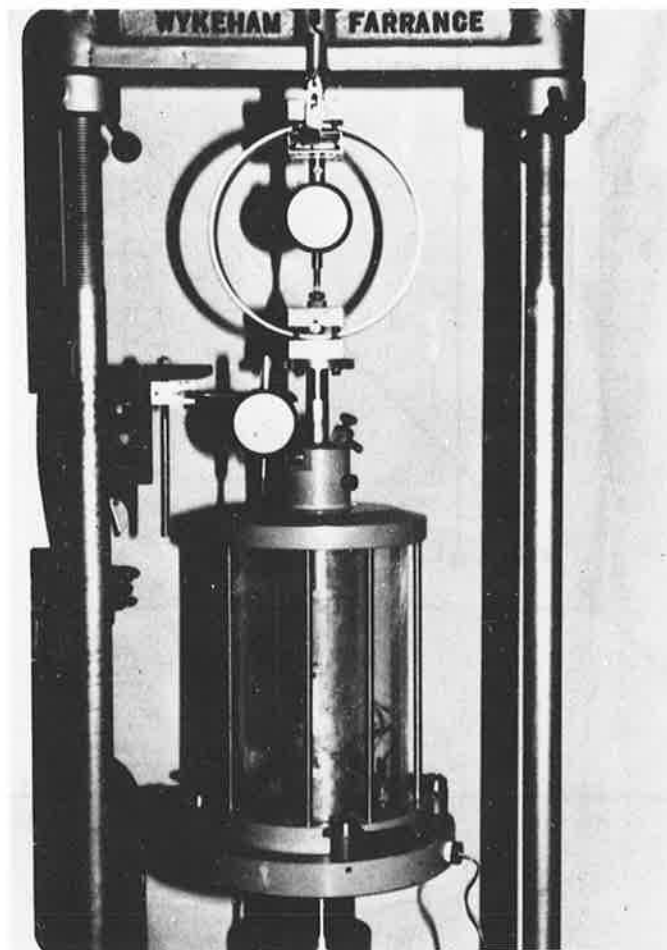
FIGURE E-6.   TRIAXIAL CELL WITH PROVING RING AND
AXIAL DEFORMATION DIAL GAGE
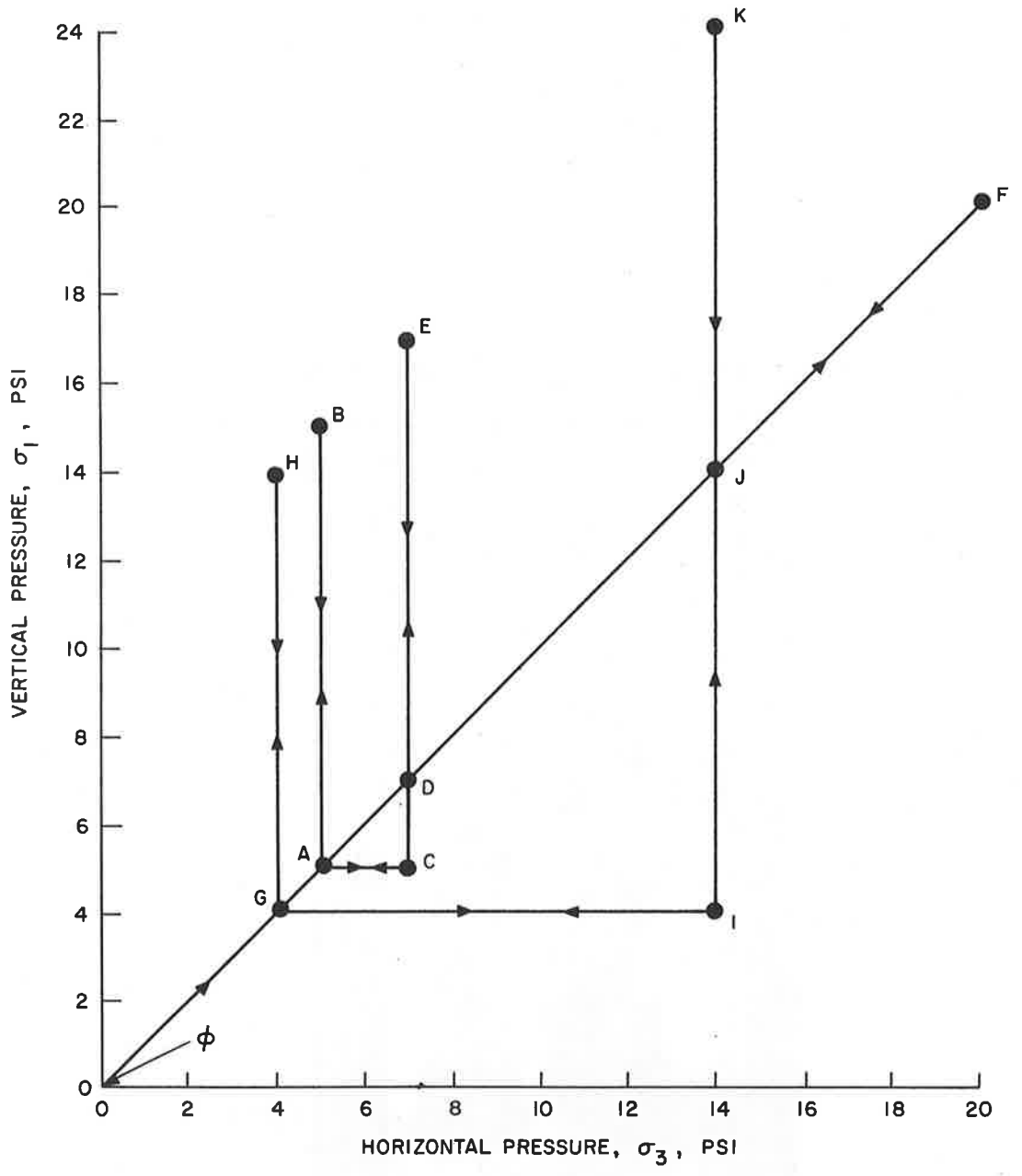
FIGURE E-7.   LOADING PATHS FOR SOIL TESTS

Table E-2

Loading Sequence

| Step | Loading Sequence |
|------|------------------|
| 1 | $\phi \to A \to B \to A$ |
| 2 | $A \to C \to D \to E \to D \to C \to A$ |
| 3 | $A \to F \to G$ |
| 4 | $G \to H \to G$ |
| 5 | $G \to I \to J \to K \to J \to I \to G$ |
| 6 | $G \to F \to \phi$ |

The values of vertical pressure $(\sigma_1)$ and horizontal pressure $(\sigma_3)$ corresponding to sequence codes $\phi$ and A through K are given in Table E-3. In this sequence of loading, either $\sigma_1$ and $\sigma_3$ is held constant while the other is varied, or both $\sigma_1$ and $\sigma_3$ are varied simultaneously by equal amounts.

Readings were taken along each step at 1 psi loading increment of either the vertical stress, $\sigma_1$, or the horizontal stress, $\sigma_3$. The readings on the proving ring were corrected for the uplift force on the ram due to the cell pressure. The axial deformation readings were corrected for the compression of the proving ring.

Although a total of six tests were indicated, a seventh test was carried out to complete the required test program due to the possible inaccuracy in the data in test no. 2 due to misalignment of the loading ram detected during the test.

The data collected for these seven tests include the raw data, i.e., proving ring readings, dial gage reading and the output readout from the digital voltmeter. In addition, the reduced and corrected stress data, $\sigma_1$ and $\sigma_3$, and corresponding strain data, $\varepsilon_1$ and $\varepsilon_3$, were also determined.

PRESSURE VALUES ASSOCIATED WITH LOADING PATHS

| Test Sequence Codes | Vertical Pressure $\sigma_1$ (psi) | Horizontal Pressure $\sigma_3$ (psi) | $q^* = \sigma_1 - \sigma_3$ (psi) | $p^* = (\sigma_1 - 2\sigma_3)/3$ (psi) |
|---|---|---|---|---|
| $\phi$ | 0 | 0 | 0 | 0 |
| A | 5 | 5 | 0 | 5 |
| B | 15 | 5 | 10 | 8.33 |
| C | 5 | 7 | -2 | 6.5 |
| D | 7 | 7 | 0 | 7 |
| E | 17 | 7 | 10 | 10.33 |
| F | 20 | 20 | 0 | 20 |
| G | 4 | 4 | 0 | 4 |
| H | 14 | 4 | 10 | 7.33 |
| I | 4 | 14 | -10 | 10.67 |
| J | 14 | 14 | 0 | 14 |
| K | 24 | 14 | 10 | 17.33 |

* For reference only.

APPENDIX F

TRACK DESIGN PARAMETRIC CALCULATIONS

This appendix presents calculations and summaries that were pro-
duced to demonstrate which combinations of materials, using AREA
criteria, would satisfy stress and deflection requirements. No account
was taken for any other criteria, such as electrical, maintenance, etc.,
in this work. Results of these calculations are summarized in Tables F-1
through F-5. Ballast depth was also assumed not to impact on track
modulus values even though there is definitely an impact. Base case
AREA track modulus (which makes no mention of rail size or ballast
depth) was used to compute all other values of modulus for various tie
sizes and spacings.

A plot of computed values, in accordance with the AREA method is
found in Figure F-2. Base value suggested by the AREA is 2000 psi
modulus for 7"x9"x9'-6" ties spaced at 20" on centers. It is assumed
that, while not specified, 12" of ballast under the tie is also a base
value. However, without a relationship to define what impact variable
ballast depth has upon track modulus, it was assumed to be unimportant
in calculating allowable ballast depths for various tie and rail com-
binations. Only the specified allowable 20 psi pressure at the bottom
of ballast was used to determine ballast depth.

Ballast depth formulas, presented in the AREA, are four in number.
Of these four only the so-called Love's Equation and the Boussinesq
Equation have any theoretical basis and the other two produce unrealistic
results. One of these two, the Japanese National Railways Equation is
for narrow gauge track and should not be used on standard guage track.
Talbot's Equation produces very conservative results when comparing
actual track in service to values derived from this equation. Since the
third equation is the Boussinesq Equation, for a point load, it is not
as good as the integrated version, Love's Equation. Love's Equation
assumes a uniformly loaded circular area, at the bottom of tie, equal to
the ties computed bearing area. Even this approach has a short coming
as the overlapping effects from adjacent rail seat loads are not considered.

VEHICLE CONFIGURATIONS



$P_w$ = 12,000 lbs. "crush loaded" — 28" dia.

"Red Line" MBTA Car



$P_w$ = 15,200 lbs. "crush loaded" — 34" dia.

NYCTA R42 Type Car
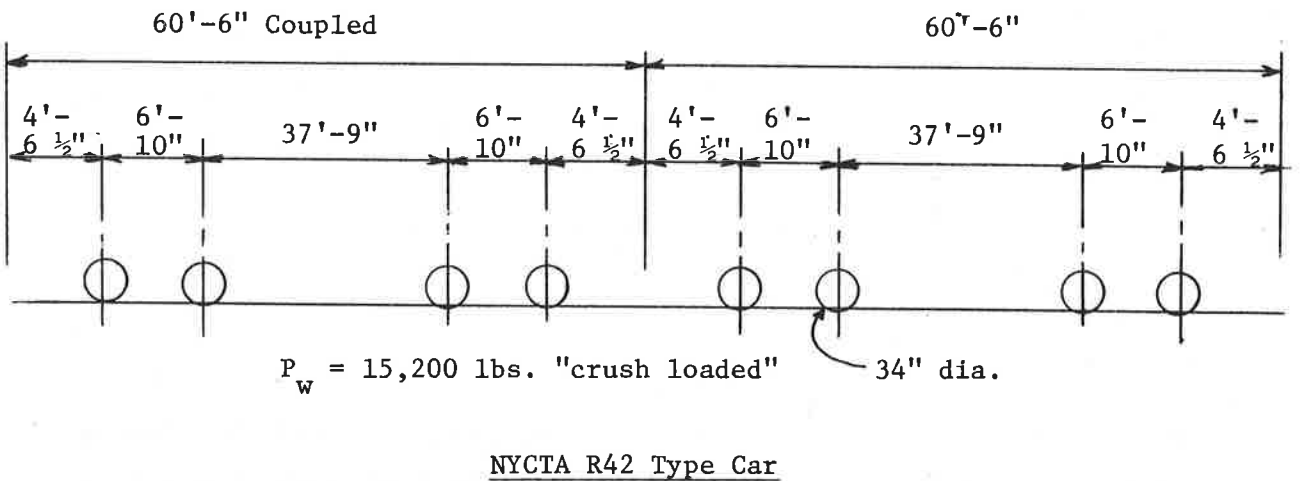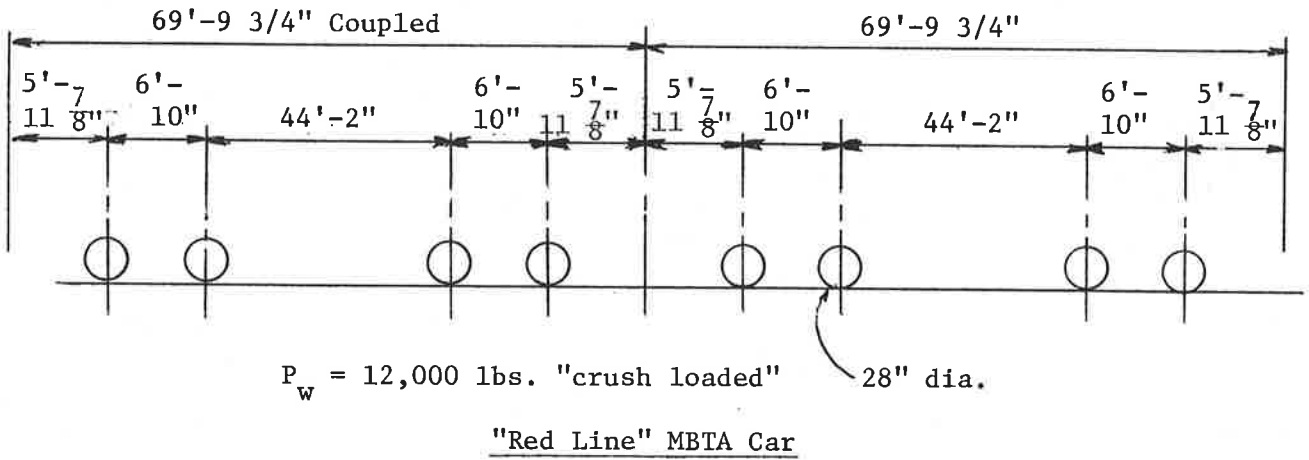
Dynamic Wheel Loads

| Red Line Car | | R42 Car | |
|---|---|---|---|
| @ 50 mph | 19,070 lbs | @ 50 mph | 22,580 lbs |
| @ 60 mph | 20,485 lbs | @ 60 mph | 24,050 lbs |
| @ 70 mph | 21,900 lbs | @ 70 mph | 25,530 lbs |
| @ 0 mph | 12,000 lbs | @ 0 mph | 15,200 lbs |

TABLE F-1

WORKABLE TIE SELECTIONS FOR 75 LB RAIL - MBTA RED LINE CARS

| Rail and Tie Description | Limiting *Criteria & Speed for Various Tie Spacing | | | | | |
|---|---|---|---|---|---|---|
| | 20" | 22" | 24" | 26" | 28" | 30" |
| 75 lb Rail 6"x7"x8'-0" Ties | 70 mph | 70 mph (Rail Defl.) | 60 mph (Rail Defl.) | **50 mph (Rail Defl.) | - | - |
| 75 lb Rail 6"x8"x8'-0" Ties | 70 mph | 70 mph | 70 mph | 70 mph (Rail Defl.) | 60 mph (Rail Defl.) | **50 mph (Rail Defl.) |
| 75 lb Rail 6"x8"x8'-6" Ties | 70 mph | 70 mph | 70 mph (Tie Stress) | - | - | - |
| 75 lb Rail 7"x8"x8'-0" Ties | 70 mph | 70 mph | 70 mph | 70 mph (Rail Defl.) | 60 mph (Rail Defl.) | 50 mph (Rail Defl.) |
| 75 lb Rail 7"x8"x8'-6" Ties | 70 mph | 70 mph | 70 mph | 70 mph | 70 mph | 70 mph (Rail Defl.) |
| 75 lb Rail 7"x9"x8'-0" Ties | 70 mph | 70 mph | 70 mph | 70 mph | 70 mph | 70 mph (Rail Defl.) |
| 75 lb Rail 7"x9"x8'-6" Ties | 70 mph | 70 mph | 70 mph | 70 mph | 70 mph | 70 mph |

These results are for:

1. well maintained track - no "center bound" tie conditions
2. MBTA Red Line Cars (96,000 lbs gross "crush load" wheel load @ 12000 lbs - static)
3. Subgrade response derived from AREA base case
4. Operating speeds above 70 mph & below 50 mph not considered

**Note: This combination may be unstable (thermal vert. buckling)
*Note: Limiting criteria is shown for item closest to allowable value only when near to allowable value

197

## TABLE F-2

### WORKABLE TIE SELECTIONS FOR 75 LB RAIL - NYCTA R-42 CARS

| Rail and Tie Description | Limiting *Criteria & Speed for Various Tie Spacing | | | | | |
|---|---|---|---|---|---|---|
| | 20" | 22" | 24" | 26" | • 28" | 30" |
| 75 lb Rail 6"x7"x8'-0" Ties | 60 mph (Rail Defl.) | 50 mph (Rail Defl.) | – | – | – | – |
| 75 lb Rail 6"x8"x8'-0" Ties | 70 mph | 70 mph | 60 mph (Rail Defl.) | – | – | – |
| 75 lb Rail 6"x8"x8'-6" Ties | 70 mph (Tie Stress) | – | – | – | – | – |
| 75 lb Rail 7"x8"x8'-0" Ties | 70 mph | 70 mph (Rail Defl.) | 60 mph (Rail Defl.) | 50 mph (Rail Defl.) | – | – |
| 75 lb Rail 7"x8"x8'-6" Ties | 70 mph | 70 mph | 70 mph | 60 mph (Rail Defl.) | 50 mph (Rail Defl.) | – |
| 75 lb Rail 7"x9"x8'-0" Ties | 70 mph | 70 mph | 70 mph (Rail Defl.) | 60 mph (Rail Defl.) | 50 mph (Rail Defl.) | – |
| 75 lb Rail 7"x9"x8'-6" Ties | 70 mph | 70 mph | 70 mph | 70 mph | 70 mph | 60 mph |

These results are for:

1. well maintained track – no "center bound" tie conditions
2. New York City Transit Authority R42 Cars (crush load $P_w$ = 15,200 lbs static)
3. Subgrade response derived from AREA base case
4. Operating speeds above 70 mph & below 50 mph not considered

*Note: Limiting criteria is shown for item closest to allowable value only when near to allowable value

198

## TRACK COMPONENT COMBINATIONS FOR 75 LB RAIL

| Tie Dimensions ($A_b$) | Tie Spacing (in) | Red Line Car Loading | | | NYCTA R42 Car Loading | | |
|---|---|---|---|---|---|---|---|
| | | Track Speed (mph) | Dynamic Rail Seat (lb) | Ballast Depth (in) | Track Speed (mph) | Dynamic Rail Seat (lb) | Ballast Depth (in) |
| 6"x7"x8'-0" | 20 | – | – | – | 60 | 8,259 | 10.52 |
| (209.40) | 22 | 70 | 7,092 | 9.05 | 50 | 8,983 | 11.33 |
| | 24 | 60 | 7,640 | 9.77 | – | – | – |
| | 26 | 50 | 8,182 | 10.43 | – | – | – |
| 6"x8"x8'-0" | 22 | – | – | – | 70 | 9,169 | 10.95 |
| (239.32) | 24 | – | – | – | 60 | 9,867 | 11.70 |
| | 26 | 70 | 8,342 | 9.97 | – | – | – |
| | 28 | 60 | 8,891 | 10.63 | – | – | – |
| | 30 | 50 | 9,427 | 11.23 | – | – | – |
| 6"x8"x8'-6" | 20 | 70 | 6,806 | 6.80 | 70 | 8,755 | 9.80 |
| (269.74) | 22 | – | – | – | – | – | – |
| | 24 | 70 | 7,431 | 8.69 | – | – | – |
| 7"x8"x8'-0" | 22 | – | – | – | 70 | 10,402 | 12.15 |
| (244.63) | 24 | – | – | – | 60 | 9,904 | 11.64 |
| | 26 | 70 | 8,372 | 9.89 | 50 | 10,601 | 12.35 |
| | 28 | 60 | 8,913 | 10.55 | – | – | – |
| | 30 | 50 | 9,469 | 11.17 | – | – | – |
| 7"x8"x8'-6" | 24 | – | – | – | 70 | 10,085 | 11.21 |
| (276.97) | 26 | 70 | 8,528 | 9.33 | 60 | 10,797 | 11.97 |
| | 28 | 70 | 9,080 | 10.05 | 50 | 11,500 | 12.66 |
| | 30 | 70 | 9,625 | 10.70 | | | |
| 7"x9"x8'-0" | 24 | | | | 70 | 10,078 | 11.24 |
| (275.21) | 26 | | | | 60 | 10,790 | 11.99 |
| | 28 | | | | 50 | 11,491 | 12.68 |
| | 30 | 70 | 9,625 | 10.73 | | | |
| 7"x9"x8'-6" | 28 | | | | 70 | 11,032 | 11.57 |
| (311.60) | 30 | 70 | 9,797 | 10.15 | 60 | 12,412 | 12.95 |

Notes:
Subgrade stress = 20 psi
Ballast depth via Love's Formula
Dynamic rail seat load = 2 x static
For a "well maintained railroad"

# TABLE F-4

## TRACK COMPONENT COMBINATIONS FOR 100 LB RAIL

| Tie Dimensions | Tie Spacing (in) | Red Line Car Loading | | | NYCTA R42 Car Loading | | |
|---|---|---|---|---|---|---|---|
| | | Track Speed (mph) | Dynamic Rail Seat (lb) | Ballast Depth (in) | Track Speed (mph) | Dynamic Rail Seat (lb) | Ballast Depth (in) |
| 6"x7"x8'-0" | 20 | | | | | | |
| | 22 | | | | 70 | 8,138 | 10.38 |
| | 24 | | | | 50 | 8,149 | 10.39 |
| | 26 | 70 | 7,445 | 9.52 | | | |
| | 28 | 60 | 7,951 | 10.15 | | | |
| | 30 | 50 | 8,456 | 10.74 | | | |
| 6"x8"x8'-0" | 24 | | | | 70 | 8,926 | 10.67 |
| | 26 | | | | 60 | 9,579 | 11.39 |
| | 28 | 70 | 8,070 | 9.63 | | | |
| | 30 | 60 | 8,576 | 10.26 | | | |
| 6"x8"x8'-6" | 20 | | | | 70 | 7,716 | 8.36 |
| | 22 | | | | | | |
| | 24 | | | | | | |
| | 26 | | | | | | |
| | 28 | 70 | 8,187 | 9.05 | | | |
| 7"x8"x8'-0" | 24 | | | | 70 | 8,954 | 10.59 |
| | 26 | | | | 60 | 9,608 | 11.32 |
| | 28 | | | | 50 | 8,149 | 9.61 |
| | 30 | 70 | 8,606 | 10.18 | | | |
| 7"x8"x8'-6" | 26 | | | | | | |
| | 28 | | | | 70 | 10,405 | 11.56 |
| | 30 | 70 | 8,725 | 9.60 | 60 | 11,052 | 12.22 |
| 7"x9"x8'-0" | 28 | | | | 70 | 10,400 | 11.59 |
| | 30 | 70 | 8,725 | 9.64 | 60 | 11,052 | 12.26 |
| 7"x9"x8'-6" | 30 | 70 | 8,842 | 8.89 | 70 | 11,212 | 11.76 |

Notes:
    Subgrade stress = 20 psi
    Ballast depth per Love's Equation
    Dynamic rail seat load $P_d$ = 2 x static
    For "well maintained railroad"

TABLE F-5

TRACK COMPONENT COMBINATIONS FOR 115 LB RAIL

| Tie Dimensions | Tie Spacing (in) | Red Line Car Loading | | | NYCTA R42 Car Loading | | |
|---|---|---|---|---|---|---|---|
| | | Track Speed (mph) | Dynamic Rail Seat (lb) | Ballast Depth (in) | Track Speed (mph) | Dynamic Rail Seat (lb) | Ballast Depth (in) |
| 6"x7"x8'-0" | 24 | – | – | – | 70 | 8,494 | 10.79 |
| | 26 | 70 | 7,196 | 9.19 | – | – | – |
| | 28 | 60 | 7,698 | 9.83 | – | – | – |
| | 30 | 50 | 8,176 | 10.42 | – | – | – |
| 6"x8"x8'-0" | 28 | – | – | – | 70 | 9,886 | 11.72 |
| | 30 | 70 | 8,293 | 9.91 | – | – | – |
| 6"x8"x8'-6" | 22 | – | – | – | 70 | 8,103 | 8.93 |
| | 24 | – | – | – | – | – | – |
| | 26 | – | – | – | – | – | – |
| | 28 | 70 | 7,916 | 8.66 | – | – | – |
| 7"x8"x8'-0" | 26 | – | – | – | – | – | – |
| | 28 | – | – | – | – | – | – |
| | 30 | 70 | 8,322 | 9.83 | 70 | 10,540 | 12.29 |
| 7"x8"x8'-6" | 30 | 70 | 8,432 | 9.20 | 70 | 10,684 | 11.85 |
| 7"x9"x8'-0" | 30 | 70 | 8,432 | 9.25 | 70 | 10,684 | 11.88 |
| 7"x9"x8'-6" | 30 | 70 | 8,547 | 8.45 | 70 | 10,829 | 11.35 |

Notes:
1. Ballast depth determined by Love's equation (a Boussinesq derivative) using allowable subgrade stress = 20 psi per AREA
2. Values are for a "well maintained railroad"
3. When ties are limiting (i.e. when $P_d$ applied $\cong$ $P_d$ allowable or "dynamic rail seat value" $\cong$ allowable) no greater spacing of ties at reduced speed is allowed. This is because an impact factor of 100% is applied to the static rail seat load at any speed to compute the dynamic rail seat load $P_d$.
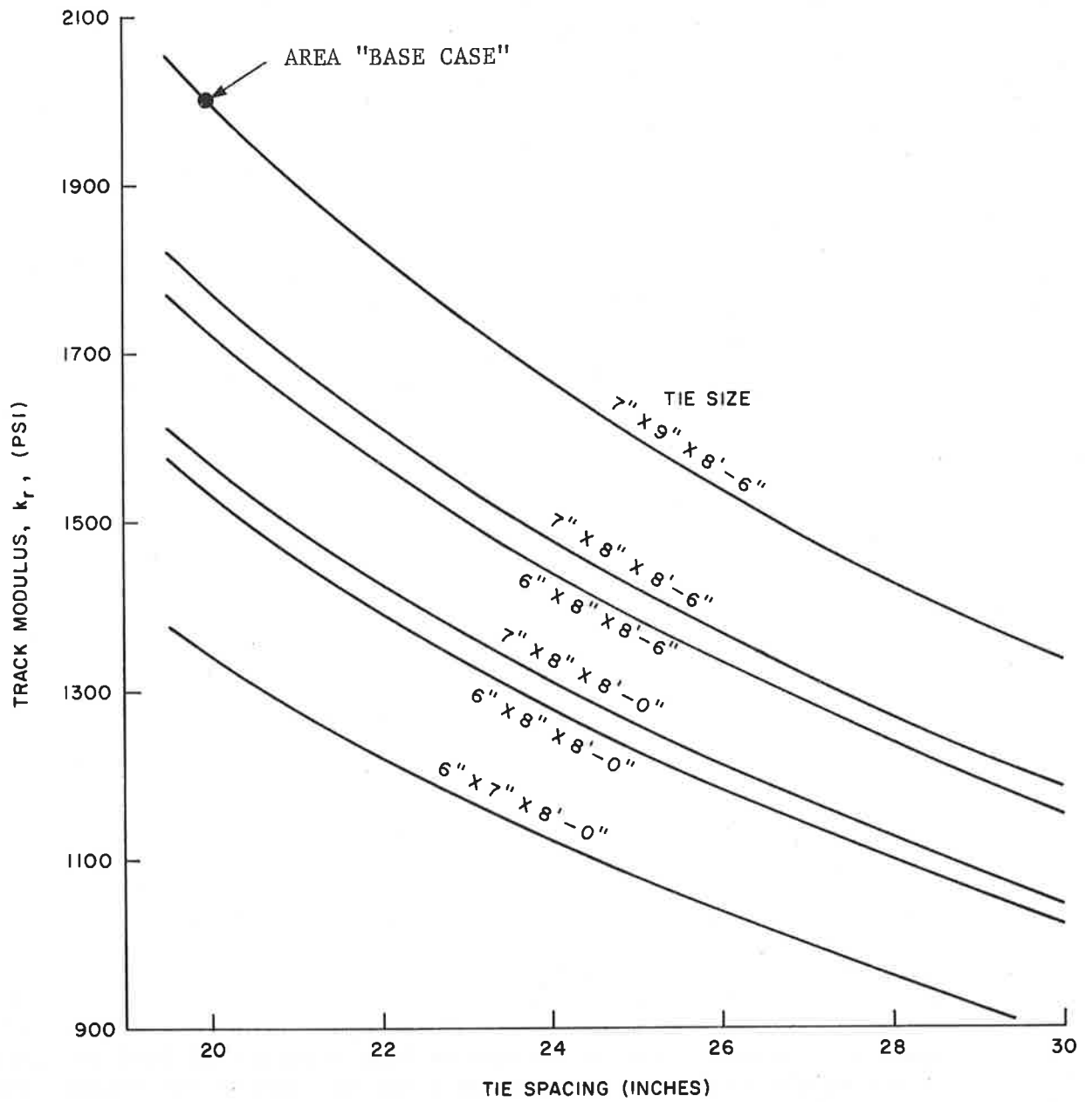
FIGURE F-2.   TRACK MODULUS PER RAIL VERSUS TIE SPACING

Further integration of Boussinesq Equations could be done to include the overlapping effects and also as an approach to incorporating ballast depth into the track modulus formula.

Selection of the two transit cars, from the heavy rail group, was made to involve a typical car (MBTA Red Line car) and one of the heavier cars (NYCTA R42 car) for contrast. Light rail vehicles are substantially lighter and would produce lighter (theoretical) designs than the rapid rail class vehicles chosen.

Material cost comparisons for various component combinations were also prepared. Since labor and equipment costs can vary so markedly from job-to-job and contractor-to-contractor, it was decided to compare material costs only. This is a valid comparison, for the labor and equipment costs in a given situation would tend to remain fairly constant from combination to combination. Costs presented cover only the running rails, ties, rail hardware, and ballast, and do not provide any third rail or catenary power costs.

A quick analysis of concrete tie designs and a cost comparison with wood tie designs are also found in the appendix. This is followed by some back-up data and calculations used in the Life-Cycle Cost analysis found in Section 6.4.
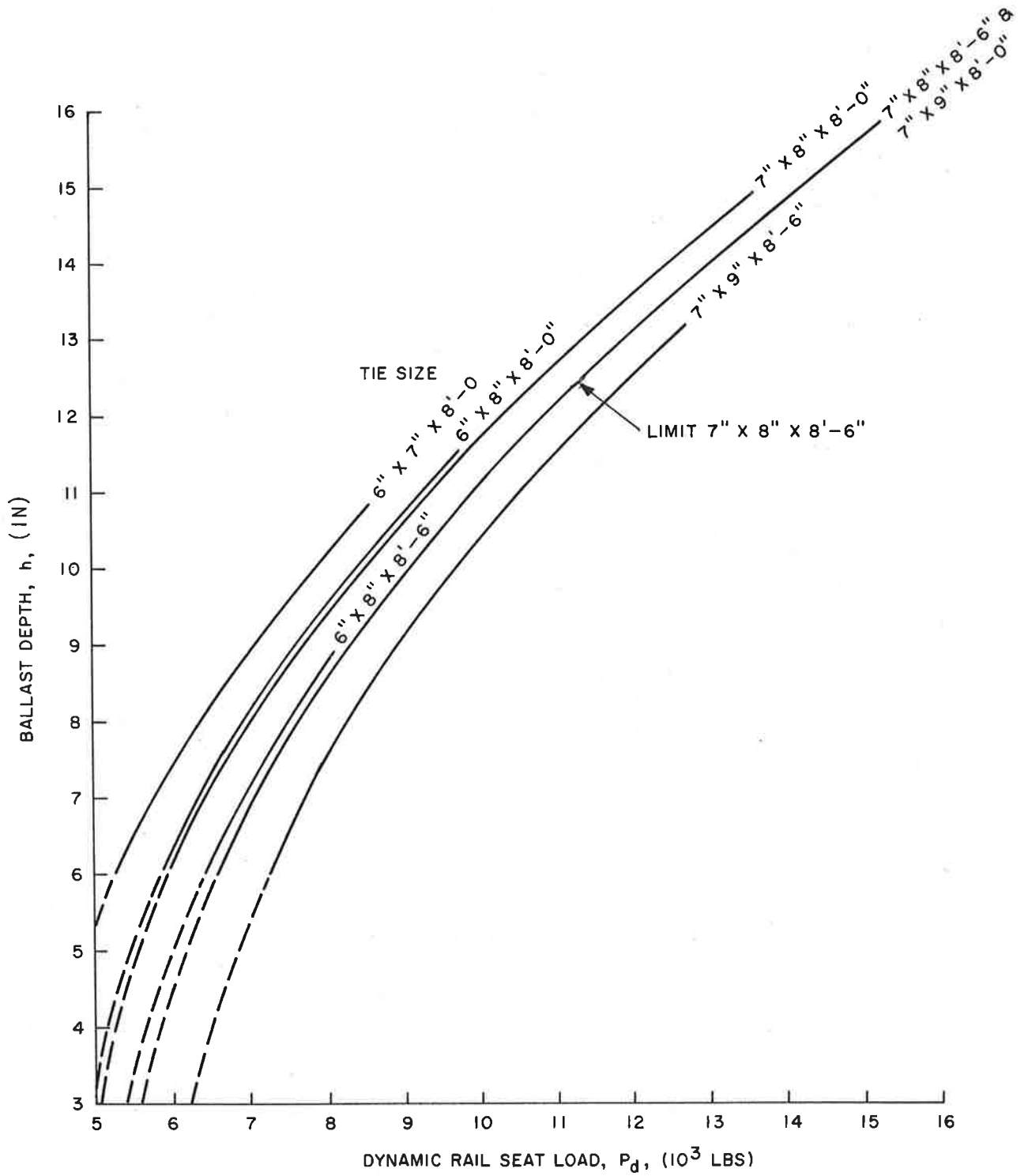
FIGURE F-3.   BALLAST DEPTH VERSUS DYNAMIC RAIL SEAT LOAD

## TABLE F-6

## BEARING LENGTHS OF TIES & BEARING AREAS

| Tie Designat. | AREA Size | Tie Dimensions | L Bearing Length | $A_b$ Bearing Area | $L/\ell$ |
|---------------|-----------|----------------|------------------|--------------------|--------|
| 2   | 2 | 6"x7"x8'-0" | 29.91 | 209.40 | 0.31 |
| 3-A | 3 | 6"x8"x8'-0" | 29.91 | 239.32 | 0.31 |
| 3-B | 3 | 6"x8"x8'-6" | 33.72 | 269.74 | 0.33 |
| 4-A | 4 | 7"x8"x8'-0" | 30.58 | 244.63 | 0.32 |
| 4-B | 4 | 7"x8"x8'-6" | 34.62 | 276.97 | 0.34 |
| 5-A | 5 | 7"x9"x8'-0" | 30.58 | 275.21 | 0.32 |
| 5-B | 5 | 7"x9"x8'-6" | 34.62 | 311.60 | 0.34 |

TABLE F-7

VALUES OF TRACK MODULUS ($k_r$) FOR VARIOUS TIE LENGTHS,
WIDTHS, DEPTHS AND SPACINGS

| Tie Designat. | AREA Size | Tie Dimensions | Values of $k_r$ for Various Tie Spacings | | | | | |
|---|---|---|---|---|---|---|---|---|
| | | | 19½" | 22" | 24" | 26" | 28" | 30" |
| 2 | 2 | 6x7x8'-0 | 1379 | 1222 | 1120 | 1034 | 960 | 896 |
| 3-A | 3 | 6x8x8'-0 | 1575 | 1396 | 1280 | 1182 | 1097 | 1024 |
| 3-B | 3 | 6x8x8'-6 | 1776 | 1574 | 1443 | 1332 | 1237 | 1154 |
| 4-A | 4 | 7x8x8'-0 | 1610 | 1427 | 1309 | 1208 | 1122 | 1047 |
| 4-B | 4 | 7x8x8'-6 | 1823 | 1616 | 1481 | 1368 | 1270 | 1185 |
| 5-A | 5 | 7x9x8'-0 | 1812 | 1606 | 1473 | 1359 | 1262 | 1178 |
| 5-B | 5 | 7x9x8'-6 | 2051 | 1818 | 1667 | 1538 | 1429 | 1333 |
| AREA Base Case | | 7x9x8'-6 | $k_r$ for 20" spacing = 2000 | | | | | |

TABLE F-8

MINIMUM BALLAST DEPTH FOR UNIFORM SUBGRADE REACTION
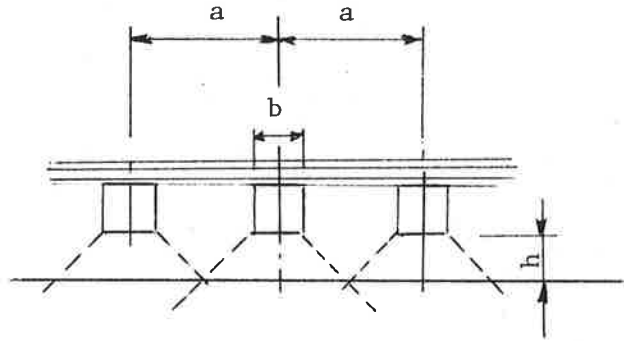


| Width of Tie b (in) | Values of "h" min. for Tie Spacings "a" (in) | | | | | |
|---|---|---|---|---|---|---|
| | 20 | 22 | 24 | 26 | 28 | 30 |
| 7 | 6.5 | 7.5 | 8.5 | 9.5 | 10.5 | 11.5 |
| 8 | 6.0 | 7.0 | 8.0 | 9.0 | 10.0 | 11.0 |
| 9 | 5.5 | 6.5 | 7.5 | 8.5 | 9.5 | 10.5 |
| *12 | - | - | - | - | - | 9.0 |

*Concrete Tie - 30" maximum spacing is good for all rail sizes used in this example.

207

TABLE F-9

MATERIAL COST FOR SINGLE TRACK MILE (1980 COSTS)

(Rail, Ties, Ballast, Anchors, Spikes & Tie Plates)
(No Catenary or Third Rail Materials Included)

Red Line Car System

| Design Speed (mph) | Tie Spacing (in) | Rail Size | Tie Size | (1) Ballast Depth (in) | (2) Per Mile Quantities | | | (3) Cost Per Mile-Track Mat'l. |
|---|---|---|---|---|---|---|---|---|
| | | | | | Rail (tons) | Ties (Number) | Ballast (tons) | |
| 70 | 22 | 75 | 6"x7"x8'-0" | 9 | 132 | 2880 | 4423 | $180,200 |
| 60 | 24 | 75 | 6"x7"x8'-0" | 10 | 132 | 2640 | 4840 | 176,000 |
| 50 | *26 | 75 | 6"x7"x8'-0" | 10 | 132 | 2437 | 4868 | 170,300 |
| 70 | 26 | 75 | 6"x8"x8'-0" | 10 | 132 | 2437 | 4820 | 175,500 |
| 60 | 28 | 75 | 6"x8"x8'-0" | 11 | 132 | 2263 | 5234 | 172,700 |
| 50 | *30 | 75 | 6"x8"x8'-0" | 11 | 132 | 2112 | 5263 | 168,200 |
| 70 | 24 | 75 | 6"x8"x8'-6" | 9 | 132 | 2640 | 4575 | 183,200 |
| 70 | 26 | 75 | 7"x8"x8'-0" | 10 | 132 | 2437 | 5146 | 184,900 |
| 60 | 28 | 75 | 7"x8"x8'-0" | 11 | 132 | 2263 | 5577 | 181,700 |
| 50 | 30 | 75 | 7"x8"x8'-0" | 11 | 132 | 2112 | 5605 | 176,700 |
| 70 | 30 | 75 | 7"x8"x8'-6" | 11 | 132 | 2112 | 5818 | 180,900 |
| 70 | 30 | 75 | 7"x9"x8'-0" | 11 | 132 | 2112 | 5556 | 182,000 |
| 70 | 30 | 75 | 7"x9"x8'-0" | 10 | 132 | 2112 | 5354 | 183,800 |
| 70 | *26 | 100 | 6"x7"x8'-0" | 10 | 176 | 2437 | 4868 | 194,200 |
| 60 | *28 | 100 | 6"x7"x8'-0" | 10 | 176 | 2263 | 4893 | 189,200 |
| 50 | *30 | 100 | 6"x7"x8'-0" | 11 | 176 | 2112 | 5305 | 187,400 |
| 70 | *28 | 100 | 6"x8"x8'-0" | 10 | 176 | 2263 | 4848 | 194,000 |
| 60 | *30 | 100 | 6"x8"x8'-0" | 10 | 176 | 2112 | 4872 | 189,400 |
| 70 | *28 | 100 | 6"x8"x8'-6" | 9 | 176 | 2262 | 4640 | 195,200 |
| 70 | *30 | 100 | 7"x8"x8'-0" | 10 | 176 | 2112 | 5206 | 197,900 |
| 70 | *30 | 100 | 7"x8"8x'-6" | 10 | 176 | 2112 | 5406 | 201,900 |
| 70 | *30 | 100 | 7"x9"x8'-0" | 10 | 176 | 2112 | 5157 | 203,100 |
| 70 | *30 | 100 | 7"x9"x8'-6" | 9 | 176 | 2112 | 4950 | 204,900 |
| 70 | *26 | 115 | 6"x7"x8'-0" | 9 | 202.4 | 2437 | 4485 | 206,500 |
| 60 | *28 | 115 | 6"x7"x8'-0" | 10 | 202.4 | 2263 | 4893 | 203,900 |
| 50 | *30 | 115 | 6"x7"x8'-0" | 10 | 202.4 | 2112 | 4914 | 199,500 |
| 70 | *30 | 115 | 6"x8"x8'-0" | 10 | 202.4 | 2112 | 4872 | 204,000 |
| 70 | *28 | 115 | 6"x8"x8'-6" | 9 | 202.4 | 2263 | 4640 | 209,900 |
| 70 | *30 | 115 | 7"x8"x8'-0" | 10 | 202.4 | 2112 | 5026 | 212,500 |
| 70 | *30 | 115 | 7"x8"x8'-6" | 9 | 202.4 | 2112 | 5002 | 214,000 |
| 70 | *30 | 115 | 7"x9"x8'-0" | 9 | 202.4 | 2112 | 4766 | 215,200 |
| 70 | "30 | 115 | 7"x9"x8'-6" | 8 | 202.4 | 2112 | 4553 | 216,900 |

208

TABLE F-9 (Concluded)

NYCTA R-42 Car System

| Design Speed (mph) | Tie Spacing (in) | Rail Size | Tie Size | (1) Ballast Depth (in) | (2) Per Mile Quantities | | | (3) Cost Per Mile-Track Mat'l. |
|---|---|---|---|---|---|---|---|---|
| | | | | | Rail (tons) | Ties (Number) | Ballast (tons) | |
| 60 | 20 | 75 | 6"x7"x8'-0" | 11 | 132 | 3168 | 5157 | $193,400 |
| 50 | 22 | 75 | 6"x7"x8'-0" | 11 | 132 | 2880 | 5197 | 185,300 |
| 70 | 22 | 75 | 6"x8"x8'-0" | 11 | 132 | 2880 | 5140 | 191,400 |
| 60 | 24 | 75 | 6"x8"x8'-0" | 12 | 132 | 2640 | 5577 | 186,700 |
| 70 | 20 | 75 | 6"x8"x8'-6" | 10 | 132 | 3168 | 4882 | 202,300 |
| 70 | 22 | 75 | 7"x8"x8'-0" | 12 | 132 | 2880 | 5868 | 204,800 |
| 60 | 24 | 75 | 7"x8"x8'-0" | 12 | 132 | 2640 | 5913 | 196,800 |
| 50 | 26 | 75 | 7"x8"x8'-0" | 12 | 132 | 2437 | 5951 | 190,100 |
| 70 | 24 | 75 | 7"x8"x8'-6" | 11 | 132 | 2640 | 5713 | 199,000 |
| 60 | 26 | 75 | 7"x8"x8'-6" | 12 | 132 | 2437 | 6173 | 194,800 |
| 50 | 28 | 75 | 7"x8"x8'-6" | 13 | 132 | 2263 | 6635 | 191,600 |
| 70 | 24 | 75 | 7"x9"x8'-0" | 11 | 132 | 2640 | 5445 | 200,700 |
| 60 | 26 | 75 | 7"x9"x8'-0" | 12 | 132 | 2437 | 5894 | 196,200 |
| 50 | 38 | 75 | 7"x9"x8'-0" | 13 | 132 | 2263 | 6345 | 192,700 |
| 70 | 28 | 75 | 7"x9"x8'-6" | 12 | 132 | 2263 | 6152 | 194,800 |
| 60 | 30 | 75 | 7"x9"x8'-6" | 13 | 132 | 2112 | 6613 | 192,000 |
| 70 | *22 | 100 | 6"x7"x8'-0" | 10 | 176 | 2880 | 4806 | 206,800 |
| 50 | *24 | 100 | 6"x7"x8'-0" | 10 | 176 | 2640 | 4840 | 200,000 |
| 70 | *24 | 100 | 6"x8"x8'-0" | 11 | 176 | 2640 | 5178 | 208,100 |
| 60 | *26 | 100 | 6"x8"x8'-0" | 11 | 176 | 2437 | 5211 | 201,900 |
| 70 | 20 | 100 | 6"x8"x8'-6" | 8 | 176 | 3168 | 4097 | 221,400 |
| 70 | 24 | 100 | 7"x8"x8'-0" | 11 | 176 | 2640 | 5507 | 218,200 |
| 60 | *26 | 100 | 7"x8"x8'-0" | 11 | 176 | 2437 | 5545 | 211,400 |
| 50 | *28 | 100 | 7"x8"x8'-0" | 10 | 176 | 2263 | 5178 | 202,900 |
| 70 | *28 | 100 | 7"x8"x8'-6" | 12 | 176 | 2263 | 6208 | 212,600 |
| 60 | *30 | 100 | 7"x8"x8'-6" | 12 | 176 | 2112 | 6238 | 207,300 |
| 70 | *28 | 100 | 7"x9"x8'-0" | 12 | 176 | 2263 | 5931 | 213,800 |
| 60 | *30 | 100 | 7"x9"x8'-0" | 12 | 176 | 2112 | 5962 | 208,300 |
| 70 | *30 | 100 | 7"x9"x8'-6" | 12 | 176 | 2112 | 6185 | 212,900 |
| 70 | *24 | 115 | 6"x7"x8'-0" | 11 | 202.4 | 2640 | 5231 | 217,400 |
| 70 | *28 | 115 | 6"x8"x8'-0" | 12 | 202.4 | 2263 | 5637 | 213,900 |
| 70 | *22 | 115 | 6"x8"x8'-6" | 9 | 202.4 | 2880 | 4535 | 229,800 |
| 70 | *30 | 115 | 7"x8"x8'-0" | 12 | 202.4 | 2112 | 6012 | 217,800 |
| 70 | *30 | 115 | 7"x8"x8'-6" | 12 | 202.4 | 2112 | 6238 | 222,000 |
| 70 | *30 | 115 | 7"x9"x8'-0" | 12 | 202.4 | 2112 | 5962 | 223,000 |
| 70 | *30 | 115 | 7"x9"x8'-6" | 11 | 202.4 | 2112 | 5766 | 224,800 |

Notes
 * These combinations may be unstable (thermally induced buckling)
(1) Ballast depths rounded to nearest inch
(2) Quantities are rounded to nearest integer (except as denoted otherwise)
    and are for single track.
(3) Costs rounded to nearest $100.
Certain designs, for which costs have been computed, feature ties at 30" spacing.
Thirty inches was set as a maximum, for requirements other than rail, tie, ballast
or subgrade stress (as analyzed in this study). By the criteria used here, a
spacing in excess of 30" would have been possible and thus the per mile material
costs are not economical for these certain combinations.

TABLE F-10

RED LINE CAR SYSTEM

Gross Wgt. (Crush Loaded) 96,000 lbs.

| Design Speed (mph) | Rail Size (lbs) | Ties (Wood) Dimensions | Spacing (in) | Ballast Depth (in) | Cost per Mile Track Mat'l. | Track Deflection (in) | Notes (see below) |
|---|---|---|---|---|---|---|---|
| 70 | 75 | 6"x7"x8'-0" | 22 | 9 | $180,200 | 0.24 | (1) |
| | | 6"x8"x8'-0" | 26 | 10 | 175,500 | 0.25 | (1) |
| | | 6"x8"x8'-6" | 24 | 9 | 183,200 | 0.21 | (2) |
| | | 7"x8"x8'-0" | 26 | 10 | 184,400 | 0.24 | (1) |
| | | 7"x8"x8'-6" | 30 | 11 | 180,900 | 0.25 | (1) |
| | | 7"x9"x8'-0" | 30 | 11 | 182,000 | 0.25 | (1) |
| | | 7"x9"x8'-6" | 30 | 10 | 183,800 | 0.22 | (3) |
| 70 | 100 | 6"x7"x8'-0" | – | – | – | – | (5) |
| | | 6"x8"x8'-0" | 20 | 6 | 212,100 | 0.18 | (4) |
| | | 6"x8"x8'-6" | 22 | 7 | 209,800 | 0.17 | (4) |
| | | 7"x8"x8'-0" | 24 | 8 | 210,500 | 0.21 | (4) |
| | | 7"x8"x8'-6" | 26 | 9 | 210,600 | 0.20 | (4) |
| | | 7"x9"x8'-0" | 26 | 9 | 212,300 | 0.20 | (4) |
| | | 7"x9"x8'-6" | 28 | 10 | 213,100 | 0.19 | (4) |
| 70 | 115 | 6"x7"x8'-0" | – | – | – | – | (5) |
| | | 6"x8"x8'-0" | – | – | – | – | (5) |
| | | 6"x8"x8'-6" | – | – | – | – | (5) |
| | | 7"x8"x8'-0" | 20 | 6 | 238,600 | 0.17 | (4) |
| | | 7"x8"x8'-6" | 22 | 7 | 236,000 | 0.16 | (4) |
| | | 7"x9"x8'-0" | 24 | 8 | 232,000 | 0.18 | (4) |
| | | 7"x9"x9'-6" | 24 | 8 | 237,000 | 0.16 | (4) |

Notes:
(1)   Rail deflection controls design, therefore optimum tie spacing used
(2)   Tie bending stress controls
(3)   Tie spacing limited by 30" max. criteria (not by stress criteria)
(4)   Tie spacing reduced to satisfy stability requirements
(5)   Tie spacing not practical to satisfy stability requirements (i.e. < 20")

TABLE F-11

NYCTA R-42 Car System

Gross Wgt. (Crush Loaded) 121,600 lbs.

| Design Speed (mph) | Rail Size (lbs) | Ties (Wood) Dimensions | Spacing (in) | Ballast Depth (in) | Cost per Mile Track Mat'l. | Track Deflection (in) | Notes |
|---|---|---|---|---|---|---|---|
| 70 | 75 | 6"x7"x8'-0" | - | - | - | - | (6) |
| | | 6"x8"x8'-0" | 22 | 11 | $191,400 | 0.25 | (1) |
| | | 6"x8"x8'-6" | 20 | 10 | 202,300 | 0.21 | (2) |
| | | 7"x8"x8'-0" | 22 | 12 | 204,800 | 0.25 | (1) |
| | | 7"x8"x8'-6" | 24 | 11 | 199,000 | 0.21 | (2) |
| | | 7"x9"x8'-0" | 24 | 11 | 200,700 | 0.24 | (1) |
| | | 7"x9"x8'-6" | 28 | 12 | 194,800 | 0.23 | (1) |
| 70 | 100 | 6"x7"x8'-0" | - | - | - | - | (5) |
| | | 6"x8"x8'-0" | 20 | 9 | 219,300 | 0.21 | (4) |
| | | 6"x8"x8'-6" | 20 | 8 | 221,400 | 0.19 | (2) |
| | | 7"x8"x8'-0" | 24 | 11 | 218,200 | 0.24 | (1) |
| | | 7"x8"x8'-6" | 26 | 11 | 215,900 | 0.23 | (4) |
| | | 7"x9"x8'-0" | 26 | 11 | 217,400 | 0.23 | (4) |
| | | 7"x9"x8'-6" | 28 | 11 | 215,800 | 0.22 | (4) |
| 70 | 115 | 6"x7"x8'-0" | - | - | - | - | (5) |
| | | 6"x8"x8'-0" | - | - | - | - | (5) |
| | | 6"x8"x8'-6" | - | - | - | - | (5) |
| | | 7"x8"x8'-0" | 20 | 9 | 245,900 | 0.20 | (4) |
| | | 7"x8"x8'-6" | 22 | 9 | 241,100 | 0.19 | (4) |
| | | 7"x9"x8'-0" | 24 | 10 | 237,000 | 0.21 | (4) |
| | | 7"x9"x9'-6" | 24 | 9 | 239,500 | 0.19 | (4) |

Notes:
(1)    Rail deflection controls design, therefore optimum tie spacing used
(2)    Tie bending stress controls
(3)    Tie spacing limited by 30" max. criteria (not by stress criteria)
(4)    Tie spacing reduced to satisfy stability requirements
(5)    Tie spacing not practical to satisfy stability requirements
(6)    Max. speed with this tie @ 20 "o.c." 60 mph

## TABLE F-12

### VOLUME (cu.ft.) OF TIES PER MILE
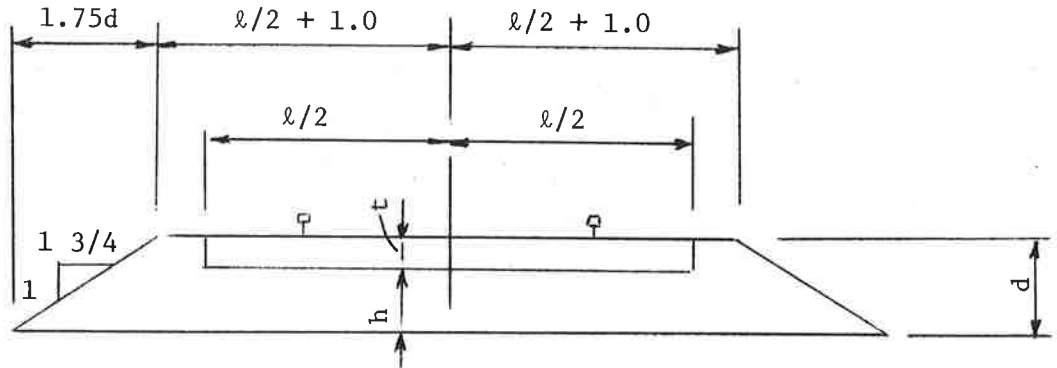


tie volume = $\ell$ x t x b

a = spacing of ties     Vol. ballast

d = h + t (ft.)     Per mile = 5280 d ($\ell$ + 2 + 1.75d) - Vol. ties

### Tie Spacing - Volume of Ties

| Tie Size | 20" | 22" | 24" | 26" | 28" | 30" |
|---|---|---|---|---|---|---|
| 6"x7"x8'-0" | 7,392 | 6,720 | 6,160 | 5,686 | 5,280 | 4,928 |
| 6"x8"x8'-0" | 8,448 | 7,680 | 7,040 | 6,499 | 6,035 | 5,632 |
| 6"x8"x8'-6" | 8,976 | 8,160 | 7,480 | 6,905 | 6,412 | 5,984 |
| 7"x8"x8'-0" | 9,856 | 8,960 | 8,213 | 7,582 | 7,040 | 6,571 |
| 7"x8"x8'-6" | 10,472 | 9,520 | 8,727 | 8,056 | 7,480 | 6,981 |
| 7"x9"x8'-0" | 11,088 | 10,080 | 9,240 | 8,530 | 7,921 | 7,392 |
| 7"x9"x8'-6" | 11,781 | 10,710 | 9,816 | 9,063 | 8,416 | 7,854 |

No. of ties per mile

| | | | | |
|---|---|---|---|---|
| @ 20" | 3168 | | @ 26" | 2437 |
| @ 22" | 2880 | | @ 28" | 2263 |
| @ 24" | 2640 | | @ 30" | 2112 |

TABLE F-13

SUMMARY OF INCREMENTAL COST PER MILE
FOR VARIOUS SINGLE TRACK COMPONENT CHANGES

### (A) Rail - Increase Weight of Rail (1980 Costs)

| Change | Incremental Cost per Mile |
|---|---|
| 75 lb to 90 lb | $13,600 |
| 90 lb to 100 lb | 9,100 |
| 100 lb to 115 lb | 13,600 |

### (B) Ties - Decrease Tie Spacing (1980 Costs)

| Change | Incremental Cost per Mile* 6"x8"x8'-0" | Incremental Cost per Mile* 7"x9"x8'-6" |
|---|---|---|
| 30" to 28" | $4800 | $ 5900 |
| 28" to 26" | 5500 | 6800 |
| 26" to 24" | 6400 | 7900 |
| 24" to 22" | 7600 | 9300 |
| 22" to 20" | 9100 | 11200 |

*Average value for all wgts. of rail (75, 90, 100, 115) used

### (C) Ballast - Increase Depth (1980 Costs)

| Change | Incremental Cost per Mile 8'-0" Ties | Incremental Cost per Mile 8'-6" Ties |
|---|---|---|
| 6" to 8" | $4900 | $5100 |
| 8" to 10" | 5100 | 5300 |
| 10" to 12" | 5300 | 5500 |
| 12" to 14" | 5500 | 5700 |

213

TABLE F-14

CAPITAL MATERIAL COST COMPARISON

REPRESENTATIVE WOOD TIE VS CONCRETE TIE COMBINATIONS

(R-42 Equipment Load Designs)

| Design Speed (mph) | Rail Size (lbs) | Ties Description | Spacing (in) | Ballast Depth (in) | Track Deflection (in) | Cost per Mile Track Mat'l. | Notes |
|---|---|---|---|---|---|---|---|
| 70 | 75 | 6"x8"x8'-0" wood | 22 | 11 | 0.24 | $191,400 | (a) |
| 70 | 75 | 7"x9"x9'-0" wood | 24 | 11 | 0.25 | 200,700 | (a) |
| 70 | 75 | 9"x12"x8'-0" Concrete | 30 | 12 | 0.09 | 225,600 | (b) |
| 70 | 100 | 6"x8"x8'-0" wood | 20 | 9 | 0.21 | 219,300 | (c) |
| 70 | 100 | 7"x9"x8'-0" wood | 26 | 11 | 0.22 | 215,800 | (c) |
| 70 | 100 | 9"x12"x8'-0" Concrete | 30 | 12 | 0.08 | 248,300 | (b) |
| 70 | 115 | 7"x9"x8'-0" wood | 24 | 10 | 0.31 | 237,000 | (c) |
| 70 | 115 | 9"x12"x8'-0" Concrete | 30 | 12 | 0.07 | 261,900 | (b) |

Notes

(a)  Rail deflection controls design (tie spacing is optimum)

(b)  Concrete tie minimum 12" ballast to be used (theoretically shallower depth may be possible)

(c)  Tie spacing reduced to satisfy stability requirements.

# TABLE F-15

## LIFE-CYCLE COST COMPARISON

1. Compare system A with system B on a Life-Cycle basis assuming interest rate to be 0%

   "A" = 75 lb rail with 6"x8"x8'-0" ties @ 20" o.c. & 12" ballast
   "B" = 115 lb rail with 7"x9"x8'-0" ties @ 24" o.c. & 12" ballast

| | | "A" | "B" |
|---|---|---|---|
| (A) | Capital Costs | | |
| | (1) Material | $203,000 | $242,000 |
| | (2) Labor & Equipment | 130,000 | 140,000 |
| | Subtotal | $333,000 | $382,000 |
| (B) | Maintenance Costs – Mat'l Replacement | | |
| | *Rail Mat'l. | $ 68,000 | $104,000 |
| | Rail Installation | 70,000 | 71,000 |
| | **Tie Mat'l | 63,000 | 82,000 |
| | Tie Installation | 106,000 | 104,000 |
| | OTM | 48,000 | 47,000 |
| | Subtotal | $355,000 | $408,000 |
| (C) | Maintenance Costs – Surfacing | 174,000 | 171,000 |
| | Total | $862,000 | $961,000 |

Annual Cost

"A" 75 lb rail with 6"x8" ties @ 22" o.c.
   Rail Life = 40.7 yrs (base)
   Annual Cost = 862,000/40.7 = $21,200

"B" 115 lb rail with 7"x9" ties @ 24" o.c.
   Rail Life = 48.4 years (base)
   Annual Cost = $961,000/48.4 = $19,900

## TABLE F-16

### CAPITAL COSTS PER MILE SINGLE TRACK

|  | "A" | "B" |
|---|---|---|
| **(a) Material** | | |
| Rail | 132 tons @ $515 = $67,980 | 202.4 tons @ 515 = $104,236 |
| Ties | 3168 ea @ $18 = 57,024 | 2640 ea @ 23.63 = 62,370 |
| Ballast | 5492 tons @ 6.50 = 35,701 | 5851 tons @ 6.50 = 38,032 |
| OTM | 3168 ties @ 13.25 = <u>41,976</u> | 2640 @ 14.25 = <u>37,620</u> |
|  | 202,681 | 242,258 |
| Subtotal – Material | $203,000 | $242,000 |
| **(b) Labor & Equip.** | 130,000 | 140,000 |

**(c) Mat'l. replacement**

| | "A" | "B" |
|---|---|---|
| Tie life | 33.3 yrs [1] | 37.0 yrs [1] |
| Rail life | 40.7 yrs | 48.4 yrs |
| Ties replaced | 40.7/33.3 x 2880 = 3520 ea. | 48.4/37 = 2640=3453 ea. |
| Rail replaced | 40.7/40.7 x 132 = 132 tons | 202.4 tons |
| O.T.M. | 125%x$38,160 = $48,000/mile | 125%x37,620 = $47,000 |
| Tie labor | $30/ea | $30/ea |
| Rail labor | $530/ton | $350/ton |

**(d) Resurfacing**

| | "A" | "B" |
|---|---|---|
| | @ 7 yrs. | @ 8 1/2 yrs. |
| Costs | 40.7/7 x 30000=$174,000 | 48.4/8.5 x 30000 =$170,800 |

Notes: (1) based upon 70% tangent & 30% curves (avg. = 3°)

## APPENDIX G

## REPORT OF NEW TECHNOLOGY

The work performed under this contract, while leading to no new inventions, has led to two innovative concepts involving the measurements of pressures under concrete ties and in the ballast. The former involves recessing the pressure gage and ballast bearing plates directing into the bottom of the concrete tie so that the enlarged bearing plate is flush with the bottom concrete surface. The latter involves the encapsulation of the pressure gage between enlarged flat circular bearing plates to distribute the nearly point loadings from the surrounding ballast to the diaphragm of the pressure gage.